

# Subcellular metabolic regulation of plant cold acclimation

**Dissertation**

zur Erlangung des naturwissenschaftlichen Doktorgrades

„Doctor rerum naturalium“ (Dr. rer. nat.)



an der Fakultät für Biologie  
der Ludwig-Maximilians-Universität München

vorgelegt von

**Anastasia Kitashova**

München 2024



Diese Dissertation wurde angefertigt  
unter Leitung von Prof. Dr. Thomas Nägele  
im Bereich Evolutionäre Zellbiologie der Pflanzen  
der Fakultät für Biologie  
an der Ludwig-Maximilians-Universität München

Erstgutachter: Prof. Dr. Thomas Nägele

Zweitgutachter: Prof. Dr. Hans-Henning Kunz

Tag der Abgabe: 11.11.2024

Tag der mündlichen Prüfung: 28.01.2025



## ***Eigenständigkeitserklärung***

Hiermit versichere ich an Eides statt, dass die vorliegende Dissertation mit dem Titel

**Subcellular metabolic regulation of plant cold acclimation**

---

von mir selbstständig verfasst wurde und dass keine anderen als die angegebenen Quellen und Hilfsmittel benutzt wurden. Die Stellen der Arbeit, die anderen Werken dem Wortlaut oder dem Sinne nach entnommen sind, wurden in jedem Fall unter Angabe der Quellen (einschließlich des World Wide Web und anderer elektronischer Text- und Datensammlungen) kenntlich gemacht. Weiterhin wurden alle Teile der Arbeit, die mit Hilfe von Werkzeugen der künstlichen Intelligenz de novo generiert wurden, durch Fußnote/Anmerkung an den entsprechenden Stellen kenntlich gemacht und die verwendeten Werkzeuge der künstlichen Intelligenz gelistet. Die genutzten Prompts befinden sich im Anhang. Diese Erklärung gilt für alle in der Arbeit enthaltenen Texte, Graphiken, Zeichnungen, Kartenskizzen und bildliche Darstellungen.

**Neuried, 31.10.2024**

---

(Ort / Datum)

**Anastasia Kitashova**

---

(Vor und Nachname in Druckbuchstaben)

**Anastasia Kitashova**

---

(Unterschrift)

## ***Affidavit***

Herewith I certify under oath that I wrote the accompanying Dissertation myself.

Title: **Subcellular metabolic regulation of plant cold acclimation**

---

In the thesis no other sources and aids have been used than those indicated. The passages of the thesis that are taken in wording or meaning from other sources have been marked with an indication of the sources (including the World Wide Web and other electronic text and data collections). Furthermore, all parts of the thesis that were de novo generated with the help of artificial intelligence tools were identified by footnotes/annotations at the appropriate places and the artificial intelligence tools used were listed. The prompts used were listed in the appendix. This statement applies to all text, graphics, drawings, sketch maps, and pictorial representations contained in the Work.

**Neuried, 31.10.2024**

---

(Location/date)

**Anastasia Kitashova**

---

(First and last name in block letters)

**Anastasia Kitashova**

---

(Signature)



## **Erklärung** **Declaration**

Hiermit erkläre ich, \*  
Hereby I declare

dass die Dissertation nicht ganz oder in wesentlichen Teilen einer anderen  
Prüfungskommission vorgelegt worden ist.  
*that this work, complete or in parts, has not yet been submitted to another  
examination institution*

dass ich mich anderweitig einer Doktorprüfung ohne Erfolg **nicht**  
unterzogen habe.  
*that I did **not** undergo another doctoral examination without success*

dass ich mich mit Erfolg der Doktorprüfung im Hauptfach  
*that I successfully completed a doctoral examination in the main subject*

und in den Nebenfächern  
*and in the minor subjects*

bei der Fakultät für \_\_\_\_\_  
*at the faculty of*

der \_\_\_\_\_  
*at*  
(Hochschule/University)

unterzogen habe.

dass ich ohne Erfolg versucht habe, eine Dissertation einzureichen oder mich  
der Doktorprüfung zu unterziehen.  
*that I submitted a thesis or did undergo a doctoral examination without success*

Neuried, 31.10.2024  
Ort, Datum/place, date

Anastasia Kitashova  
Unterschrift/signature

\*) Nichtzutreffendes streichen/  
*delete where not applicable*





### **3 Table of contents**

1	Statutory declaration and statement.....	5
2	Declaration on former attempts of a doctorate.....	7
3	Table of contents.....	9
4	List of abbreviations .....	11
5	List of publications and declaration of contribution to the publications .....	13
6	Summary .....	15
7	Zusammenfassung.....	17
8	Introduction.....	19
9	Results.....	29
10	Discussion .....	105
11	Conclusion and outlook.....	113
12	References .....	115
13	Acknowledgements .....	127
14	Curriculum vitae.....	131



## 4 List of abbreviations

Table 1. List of abbreviations used in the following work.

<b>Abbreviation</b>	<b>Full meaning</b>
AGPase	ADP-glucose pyrophosphorylase
ANS	Anthocyanidin synthase
ATP	Adenosine triphosphate
BAM3	$\beta$ -amylase 3
CBBC	Calvin Benson Bassham cycle
CHUP1	CHLOROPLAST UNUSUAL POSITIONING 1
CHS	Chalcone synthase
CHI	Chalcone isomerase
DFR	Dihydroflavonol 4-reductase
F3H	Flavanone 3-hydroxylase
F6P	Fructose 6-phosphate
F <sub>v</sub> /F <sub>m</sub>	Maximum quantum yield of Photosystem II efficiency
FBA	Flux balance analysis
FOLD1	Mitochondrial bifunctional 5,10-methylene-THF dehydrogenase/5,10-methenyl-THF cyclohydrolase
FRCK	Fructokinase
FUM2	Cytosolic fumarase
G6P	Glucose 6-phosphate
GC-MS	Gas chromatography–mass spectrometry
GLCK	Glucokinase
KAC 1 and 2	Kinesin CDKA1 Associated 1 And 2
LC-MS	Liquid Chromatography–Mass Spectrometry
NADPH	Nicotinamide Adenine Dinucleotide Phosphate
ODE	Ordinary Differential Equation
P <sub>i</sub>	Orthophosphate
PGM	Phosphoglucomutase
ROS	Reactive oxygen species
RuBisCO	Ribulose-1,5-bisphosphate carboxylase/oxygenase
SHM1	Mitochondrial serine hydroxymethyltransferase
SnRK1	Sucrose non-fermenting related kinase 1
SPS	Sucrose-phosphate synthase
SUT4	Sucrose transporter 4
pSUT	Plastidial sugar transporter
TCA	Tricarboxylic acid (cycle)
THF	Tetrahydrofolate
UDP-GT	Glucuronosyltransferase

#### 4. List of abbreviations

---

## 5 List of publications and declaration of contribution to the publications

This dissertation is based on four publications, to three of which the doctoral candidate contributed as the first author, and to the fourth as a co-author. The following sections detail the specific contributions to each of these works.

### Publication 1

**Kitashova A**, Schneider K, Fürtauer L, Schröder L, Scheibenbogen T, Fürtauer S, Nägele T (2021) Impaired chloroplast positioning affects photosynthetic capacity and regulation of the central carbohydrate metabolism during cold acclimation. *Photosynthesis Research* 147: 49–60

**AK** performed experiments, KS performed microscopy, LF, LS, TS, SF and TN supported experimental analysis. **AK** and TN analysed data and wrote the manuscript. TN conceived the study.

### Publication 2

**Kitashova A**, Adler SO, Richter AS, Eberlein S, Dziubek D, Klipp E, Nägele T (2023) Limitation of sucrose biosynthesis shapes carbon partitioning during plant cold acclimation. *Plant, Cell & Environment* 46: 464–478

**AK** performed experiments, statistics, mathematical modelling and wrote the paper. SOA and EK performed modelling, ASR performed qPCR analysis, TN performed statistics, mathematical modelling and wrote the paper. EK and TN conceived the study.

### Publication 3

Adler SO, **Kitashova A**, Bulović A, Nägele T, Klipp E (2024) Plant cold acclimation and its impact on sensitivity of carbohydrate metabolism. *bioRxiv preprint* 2024.06.04.597423

## 5. List of publications and declaration of contribution to the publications

---

SOA performed mathematical modelling and wrote the manuscript, **AK** performed experiments, TN wrote the manuscript, EK wrote the manuscript. EK and TN conceived the study.

### Publication 4

**Kitashova A**, Lehmann M, Schwenkert S, Münch M, Leister D, Nägele T (2024) Insights into physiological roles of flavonoids in plant cold acclimation. *The Plant Journal* in print, available online <https://doi.org/10.1111/tpj.17097>

**AK** performed fractionation experiments, statistical analysis and data evaluation, and wrote the paper. ML performed metabolomics analyses, MM performed quantification of flavonoids, SS and DL performed, supervised, and conceived proteomics analyses; TN conceived the study, performed statistics and data evaluation and wrote the paper.

Doctoral candidate:

Anastasia Kitashova

---

Supervisor:

Thomas Nägele

---

### **6 Summary**

In many plant species, exposure to low but non-freezing temperatures induces a multigenic process termed cold acclimation which ultimately increases freezing tolerance. Extensive research over the last decades revealed key processes of cold acclimation, comprising, e.g., the accumulation of carbohydrates, amino acids, polyamines, and specialised metabolites. For many metabolic pathways, however, it remains elusive how they are regulated at low temperature, and how this results in a stabilised photosynthetic performance. The high degree of compartmentalisation of plant cells together with complex system dynamics of metabolic networks are main reasons for ambiguity of current cold acclimation models. To overcome some of these limitations, this dissertation combined plant physiological experiments with subcellular high-throughput analysis of proteomes and metabolomes to feed and optimise mathematical models of plant cold acclimation.

In the first study, the impact of chloroplast positioning on primary carbohydrate metabolism and photosynthetic efficiency was analysed during cold acclimation. It was demonstrated that, although chloroplast relocation under high light intensities can affect photosynthetic efficiency, the plasticity of sucrose metabolism is essential for buffering the effects of impaired chloroplast relocation during cold acclimation. In the second study, it was shown that sucrose biosynthesis plays a central role in allocating carbon fluxes between pathways of primary and specialised metabolism. Using a kinetic modelling approach, organic acids were identified as an additional carbon sink to mitigate limitations in starch and flavonoid metabolism during cold exposure. In the third study, hexose phosphates, which are substrate for sucrose biosynthesis, were identified as the most sensitive metabolite pools during cold acclimation which indicates a central regulatory interface of diverse metabolic pathways. Finally, subcellular metabolomics and proteomics analysis indicated that flavonoids are involved in the regulation of photorespiration during the initial period of cold acclimation. This significantly promotes the current understanding of metabolic cold acclimation in plants and highlights the importance of compartment-specific analysis of metabolism.





# 7 Zusammenfassung

Bei vielen Pflanzen löst die Einwirkung niedriger Temperaturen über dem Gefrierpunkt den komplexen Prozess der Kälteakklimatisierung aus. Umfangreiche Studien der vergangenen Jahrzehnte haben wichtige Prozesse der Kälteakklimatisierung aufgedeckt, zu denen unter anderem auch die Akkumulation von Kohlenhydraten, Aminosäuren, Polyaminen und spezialisierten Stoffwechselprodukten gehört. Jedoch ist bei vielen der involvierten Stoffwechselwegen noch unklar, wie sie bei niedrigen Temperaturen reguliert werden, und wie dies zur Stabilisierung von Photosynthese beiträgt. Die Kompartimentierung von Pflanzenzellen sowie die komplexe Systemdynamik der Stoffwechselnetzwerke sind Hauptgründe für die Mehrdeutigkeit aktueller Modelle zur Kälteakklimatisierung. Um einige dieser Einschränkungen zu überwinden, wurden in der vorliegenden Dissertation physiologische Experimente mit subzellulären Hochdurchsatzanalysen kombiniert, um mathematische Modelle der Kälteakklimatisierung von Pflanzen zu optimieren.

In einer ersten Studie wurde der Einfluss der Chloroplastenpositionierung auf den Kohlenhydratstoffwechsel sowie die Effizienz der Photosynthese während der Kälteakklimatisierung analysiert. Es konnte gezeigt werden, dass die Chloroplastenpositionierung unter hoher Lichtintensität die photosynthetische Effizienz beeinflusst. Zudem wurde gezeigt, dass die Plastizität des Saccharosestoffwechsels entscheidend dazu beiträgt, die Auswirkungen einer beeinträchtigten Chloroplastenpositionierung während der Kälteakklimatisierung zu begrenzen. In einer zweiten Studie wurde gezeigt, dass die Saccharosebiosynthese eine zentrale Rolle bei der Verteilung intrazellulärer Kohlenstoffflüsse spielt. Mit Hilfe eines kinetischen Modells wurden organische Säuren als eine wichtige zusätzliche Kohlenstoffsänke identifiziert, die Limitationen im Stärke- und Flavonoidstoffwechsel während der Kälteexposition ausgleichen konnte. In einer dritten Studie wurden Hexosephosphate, die Substrate für die Saccharosebiosynthese darstellen, als regulatorisch sensitive Stoffwechselintermediate während der Kälteakklimatisierung identifiziert, was auf eine zentrale regulatorische Schnittstelle verschiedener Stoffwechselwege hinweist. Schließlich zeigten Analysen subzellulärer Metabolit- und Proteinprofile, dass Flavonoide an der Regulation der Photorespiration während der Kälteakklimatisierung beteiligt sind. Zusammenfassend konnte damit gezeigt werden, dass die kompartimentspezifische Analyse des pflanzlichen

## 7. Zusammenfassung

---

Stoffwechsels einen wichtigen Beitrag zum Verständnis des Prozesses der Kälteakklimatisierung liefert.

# 8 Introduction

Plant metabolism comprises a broad number of metabolic compounds that are dynamically synthesised, degraded, and interconverted by enzymatic reactions within a subcellular metabolic network. A tight regulation of this network enables adjustment and adaptation of plant metabolism to a changing environment. Among environmental stressors, fluctuating temperature causes diverse responses in plants, affecting gene expression, protein homeostasis and metabolite dynamics (Thomashow 2001; Wahid et al. 2007; Fürtauer et al. 2019). The increased frequency of warm and cold extremes due to global warming underscores the need to understand both the basic physiology of plant responses and the molecular mechanisms that underline decreased plant fitness due to global warming (Johnson et al. 2018).

Plant cold acclimation is a complex, multifaceted, and multigenic process, that has been extensively studied, revealing several key regulatory responses on various molecular levels (Chinnusamy et al. 2006; Guy et al. 2008; Thomashow 2010). For instance, ribosomes have been identified as central hubs for maintaining protein homeostasis under thermodynamically unfavourable conditions (Garcia-Molina et al. 2020). The Calvin Benson Bassham cycle (CBBC) and the photosynthetic machinery (photosystems I and II, and the electron transport chain) interact closely, primarily through the exchange of  $\text{NADP}^+/\text{NADPH}$  and  $\text{ATP}/\text{P}_i$ . In cold-exposed plants, photosynthetic activity was found to be associated with a reduced consumption of photosynthetically generated reducing power, leading to an increased reduction state of the chloroplast stroma, which is reflected in elevated NADP-MDH activity and a higher  $\text{ATP}/\text{NADPH}$  ratio (Savitch et al. 2001). Additionally, metabolic cold acclimation is not a straightforward process: even within the first four days of cold exposure, metabolic adjustments show a temporal distribution across early, intermediate, and late stages of cold stress (Kaplan et al. 2004).

Therefore, during cold acclimation, it becomes vital for plants to regulate and stabilise metabolism to prevent an imbalance between photochemistry and biochemistry, mitigate reactive oxygen species (ROS) formation, avoid photoinhibition, and prevent tissue damage (Huner et al. 1998). Carbohydrates, which are the direct products of photosynthetic  $\text{CO}_2$  assimilation, are substrates for various metabolic pathways, for example, for carboxylic acid

metabolism, lipid biosynthesis, amino acid and protein production (Stitt et al. 2010). Moreover, carbohydrates serve as precursors for a diverse group of specialised compounds, which are synthesised through the shikimate and arogenate pathways (Maeda and Dudareva 2012; Wang et al. 2020). These specialised metabolites are crucial for protecting plants against various environmental stresses, both biotic and abiotic (see e.g. (Di Ferdinando et al. 2012; Erb and Kliebenstein 2020)).

### **8.1 Regulation of plant metabolism during cold acclimation**

Sugar phosphates are the products of the CBBC, which serve as a branching point in plant metabolism. These metabolites act as substrates for multiple pathways including biosynthesis of sucrose, transitory starch, glycolysis, organic acids, amino acids, and specialised metabolites. The entry of hexose phosphates into the oxidative pentose phosphate pathway provides additional reduction power, which can be used in various anabolic reactions (Landi et al. 2021). However, under low temperature, balance between light absorption and energy consumption by the CBBC is affected and requires significant adjustment of plant metabolism (Huner et al. 1998). Consequently, enzymes involved in the CBBC and sucrose metabolism need to be tightly regulated during cold acclimation to accommodate metabolic limitation (Savitch et al. 1997; Strand et al. 1999). The interplay between photosynthesis and sucrose metabolism is facilitated by the continuous exchange of triose phosphates and orthophosphate ( $P_i$ ) via the triose phosphate/phosphate translocator (Flügge and Heldt 1984). Sucrose biosynthesis in the cytosol involves fructose 6-phosphate (F6P) and UDP-glucose, and is catalysed by sucrose-phosphate synthase (SPS) and sucrose-phosphate phosphatase (Ruan 2014). Activity of SPS, which catalyses the rate-limiting reaction in sucrose biosynthesis, is regulated by protein phosphorylation, enhanced by glucose 6-phosphate (G6P), and inhibited by  $P_i$  (Huber and Huber 1996).

The regulation of sucrose metabolism during cold acclimation is crucial for establishing the metabolic homeostasis and ensuring optimal carbon utilisation. Sucrose transport between cytosol, vacuole, and chloroplasts is catalysed by sucrose transporter SUT4 and plastidial sugar transporter (pSUT) transporters, respectively, which have been shown to significantly contribute to plant cold acclimation and freezing tolerance (Endler et al. 2006; Patzke et al. 2019). The regulation of SPS is essential during cold acclimation to prevent limitations in the

triose phosphate/phosphate exchange between the cytosol and chloroplasts, which could lead to restriction in ATP biosynthesis (Nägele et al. 2012). Invertase enzymes catalyse sucrose hydrolysis and are found in plastids, cytosol, vacuole, mitochondria, and the cell wall (Lee and Sturm 1996; Sturm 1999; Sherson et al. 2003; Xiang et al. 2011; Xiang and Van den Ende 2013). The hydrolytic breakdown of sucrose into hexoses by invertases, followed by their ATP-dependent re-phosphorylation by glucokinase and fructokinase enzymes, initially appears to form a futile sucrose cycle. However, previous studies have shown that this cycle plays a crucial role in the sensitive metabolic regulation of central carbohydrate metabolism (Geigenberger and Stitt 1991; Gonzali et al. 2001; Fürtauer and Nägele 2016; Aguilera-Alvarado and Sánchez-Nieto 2017). Also, the tight regulation of the sucrose cycle during cold exposure was hypothesised to be crucial for cold acclimation and stabilisation of photosynthesis. Recent evidence highlights the importance of vacuolar sucrose cleavage in stabilising photosynthesis upon cold exposure (Weizmann et al. 2018), while elevated rates of sucrose transport across the chloroplast membrane have been linked to cold tolerance (Nägele and Heyer 2013). Furthermore, the transport of sucrose into the vacuole represents a significant regulatory point during cold acclimation (Nägele 2022). In addition to sucrose, other carbohydrates, such as hexoses and raffinose, show increased amounts in cold, which positively correlate with enhanced freezing tolerance (Sasaki et al. 1996; Wanner and Junttila 1999; Klotke et al. 2004; Korn et al. 2008). However, not only increased absolute amounts, but also the subcellular distribution of soluble sugars and raffinose was shown to be associated with cold tolerance (Knaupp et al. 2011; Nägele and Heyer 2013; Hoermiller et al. 2017).

Another critical aspect of cold acclimation involves the metabolism and mobilisation of transitory starch. Starch, synthesised in the chloroplast through a sequential enzymatic reaction mediated by phosphoglucose isomerase, phosphoglucomutase (PGM), and ADP-glucose pyrophosphorylase (AGPase), together with starch synthases and (de-)branching enzymes, serves as a significant energy reserve. During the night, starch is degraded by amylases and phosphorylases, ensuring the availability of carbon for other essential pathways (Smith 2012). The degradation of starch yields maltose and glucose, which is important during initial cold acclimation, as it provides a necessary carbon source for soluble sugars. These sugars, as was discussed above, are crucial for establishing a new metabolic

homeostasis during cold acclimation (Sicher 2011; Seydel et al. 2022). The importance of starch degradation for cold acclimation is further indicated by studies showing that the deficiency in  $\alpha$ -glucan water dikinase activity, which impairs starch degradation, results in reduced freezing tolerance after one day of cold exposure (Yano et al. 2005). The enzyme  $\beta$ -amylase 3 (BAM3) is significantly involved in starch degradation during cold acclimation (Sicher 2011; Monroe et al. 2014). Notably, reduced BAM3 activity has been linked to increased sensitivity of photosystem II, directly associating starch metabolism with photosynthetic efficiency (Kaplan and Guy 2005). Consequently, efficient starch mobilisation through BAM3 activity seems to enhance a plant's capability to cope with low temperatures (Nagler et al. 2015). Furthermore, impaired carbon flux in starch metabolism was discussed to significantly influence subcellular amino acid metabolism, which might contribute to reduced freezing tolerance in the starch deficient plastidial *pgm1* mutant of *Arabidopsis* (Hoermiller et al. 2017, 2022). This suggests a regulatory crosstalk between carbohydrate and amino acid metabolism. Additionally, starch degradation has been linked to plastidial malate metabolism (Liu et al. 2024), suggesting an underlying regulatory connection between primary carbohydrate and organic acid metabolism. Finally, cytosolic fumarase 2 (FUM2) mutants were found to have altered amount of starch during cold exposure, which further suggests that a highly interconnected metabolic network is involved in metabolic cold acclimation (Dyson et al. 2016).

The multicompartmental pathway of photorespiration, which starts with the oxygenation of ribulose-1,5-bisphosphate by RuBisCO resulting in 2-phosphoglycolate, plays a crucial role in maintaining the metabolic stability upon environmental perturbations (for an overview, see e.g., Eisenhut et al. 2019). This pathway contributes to balancing reducing equivalents between chloroplasts, mitochondria and peroxisomes, which prevents photooxidation under abiotic stress (Voss et al. 2013). For example, the reaction of serine hydroxymethyltransferase (SHM1), which interconverts glycine to serine in mitochondria, is associated with the response to high light and salt stress and mitigating ROS generation and oxidative damage (Moreno et al. 2005). Photorespiration potentially contributes to the antioxidative defence system during cold acclimation, as it was shown in rice by elevated catalase activity (Guo et al. 2006). The photorespiratory pathway also comprises the conversion of glutamate and glyoxylate to 2-oxoglutarate and glycine, which directly links

photorespiration with amino acid metabolism (Igarashi et al. 2006). This linkage may be critical for cold acclimation, as amino acid content significantly changes upon cold exposure, with a notable increase in proline, glutamine, and asparagine. Simultaneously, less abundant amino acids are incorporated into proteins, contributing to the induction of protein synthesis (Hildebrandt 2018). The localisation of proline to the cytosol plays a crucial role in cold response, emphasising the importance of not only the total amino acid content but also their subcellular distribution (Hoermiller et al. 2022).

Photorespiration is also linked to other pathways, such as tetrahydrofolate (THF) and methionine metabolism, connecting carbon, nitrogen, and sulphur metabolism. THF metabolism plays an important role in many metabolic processes and comprises reactions located in chloroplasts, mitochondria, cytosol and the vacuole (Gorelova et al. 2019). The initial steps of its biosynthesis involve interconversion of chorismate, which is produced by the shikimate pathway, into para-aminobenzoic acid, a precursor for THF (Tohge and R. Fernie 2017). In mitochondria, SHM1 connects THF-metabolism and photorespiration, mediating the interconversion of glycine to serine and 5,10-methylen-THF to THF (Moreno et al. 2005). Moreover, 5-formyl THF has been suggested to inhibit SHM1, further indicating a regulatory connection between photorespiration and THF metabolism (Collakova et al. 2008).

### **8.2 Flavonoid metabolism**

Flavonoids play a crucial role in plant response to low temperature by acting as antioxidants, helping to mitigate oxidative damage (Janská et al. 2010; Agati et al. 2012). Furthermore, the enzymes involved in flavonoid metabolism are significantly activated upon cold exposure (Bittner et al. 2020). This highlights the importance of the integration of flavonoids in the broad metabolic response to cold, as flavonoid precursors are directly linked to photosynthesis and carbohydrate metabolism through the plastidial shikimate pathway (Herrmann and Weaver 1999; Rippert et al. 2009). The shikimate pathway yields phenylalanine, which is then transported to the cytosol, where flavonoids are synthesised and allocated to different cellular compartments, for example, vacuole and endoplasmic reticulum (for an overview see e.g., Pucker and Selmar 2022).

## 8. Introduction

---

The core biosynthetic pathway of flavonoids involves the enzymes chalcone synthase (CHS), chalcone isomerase (CHI), flavanone 3-hydroxylase (F3H), dihydroflavonol 4-reductase (DFR), and anthocyanidin synthase (ANS; Figure 1). These enzymes are associated with the endoplasmic reticulum membrane, forming a metabolon with complex interaction dynamics that facilitate efficient production of flavonoids (Burbulis and Winkel-Shirley 1999; Crosby et al. 2011). CHS catalyses the first step in flavonoid biosynthesis, generating chalcone, which serves as a substrate for downstream enzymes to produce various flavonoid compounds (B. Austin and P. Noel 2003). F3H, a 2-oxoglutarate-dependent dioxygenase, is a key enzyme in the biosynthesis of flavanols and subsequently anthocyanins from naringenin (Owens et al. 2008). Additionally, the complex interactions between enzymes in the early flavonoid biosynthesis pathway enable the possibility of bypassing missing reactions. F3H interacts closely with CHS and flavonol synthase (FLS), which, in turn, interacts with DFR. Mutation in the F3H enzyme allows for the biosynthesis of flavanols via flavonoid 3-hydroxylase (F'3H) and DFR. Furthermore, Schilbert and colleagues demonstrated that *f3h* mutants, despite the blockage in the pathway, can still accumulate quercetin, a compound downstream of the F3H-catalysed step (Schilbert et al. 2024) (Figure 1).

The proposed function of anthocyanins as osmoprotectants in cold conditions suggests potential mechanisms for their role in plant stress responses (Chalker-Scott 1999). In *Arabidopsis*, flavonoid accumulation has been correlated with enhanced freezing tolerance, implying a physiological role in cold acclimation (Schulz et al. 2015, 2016). Despite the strong evidence indicating that flavonoids are important and beneficial during cold acclimation, their specific physiological functions and the mechanism behind the precise coordination of carbohydrate and specialised metabolism remains unclear. Further research is needed to elucidate how flavonoid biosynthesis is integrated into the broader metabolic network, contributing to plant resilience in cold environments.



## 8. Introduction

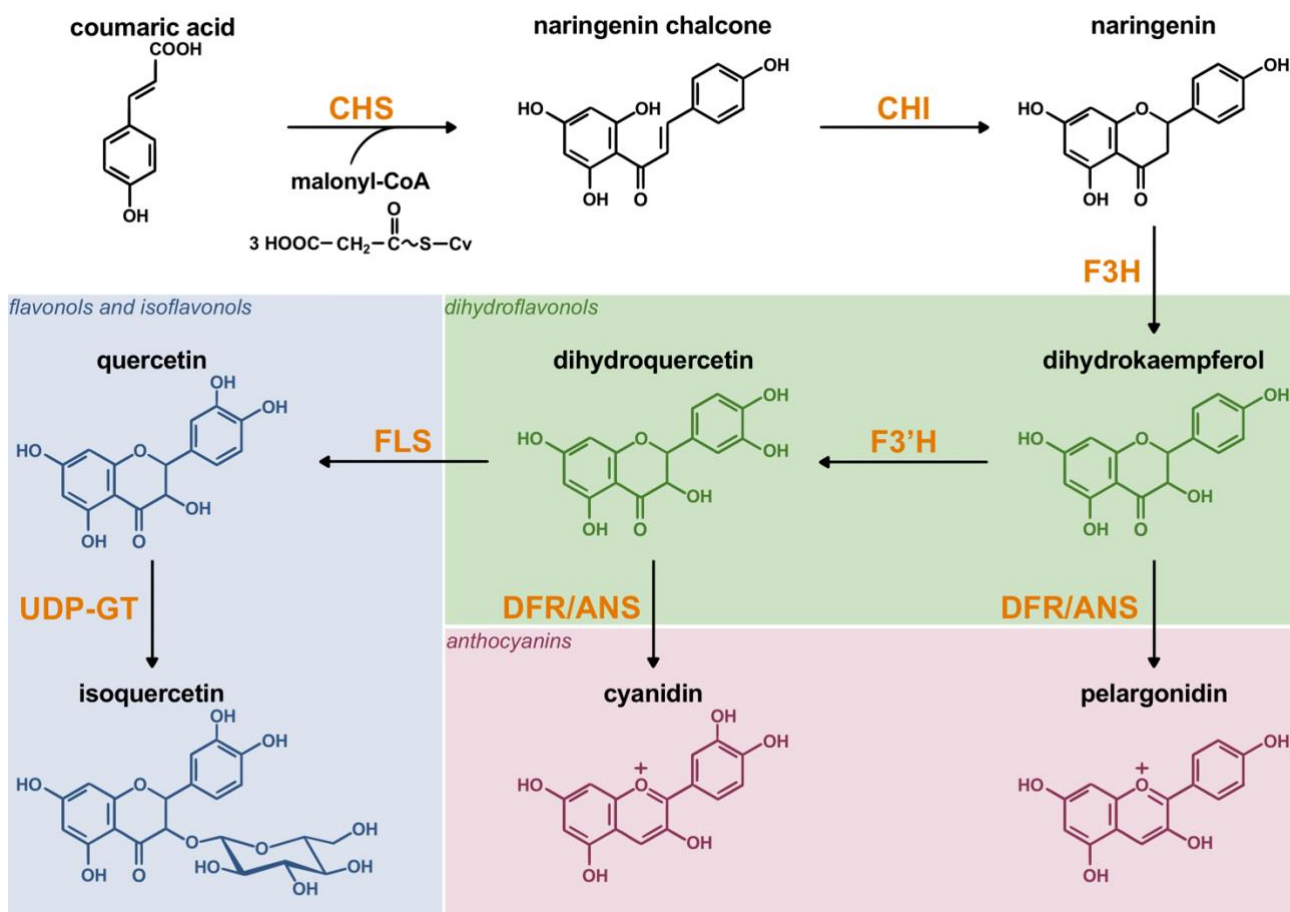


**Figure 1. Flavonoid biosynthesis pathway.** The core pathway of flavonoid biosynthesis is shown, highlighting key intermediate compounds and potential modifications (not exhaustive). Enzymes involved in the pathway are indicated in orange: CHS – chalcone synthase; CHI – chalcone isomerase; F3H – flavanone 3-hydroxylase; F3'H – flavonoid 3-hydroxylase; FLS – flavonol synthase; DFR – dihydroflavonol 4-reductase; ANS – anthocyanidin synthase; UDP-GT – glucuronosyltransferase.

### 8.3 Chloroplast positioning in a dynamic environment

Positioning of chloroplast within a cell has been shown to significantly affect photosynthetic efficiency and biomass accumulation (Gotoh et al. 2018). Adequate and sufficient light energy capture by photosynthetic machinery in chloroplasts is also crucial for stabilising photosynthesis during cold acclimation (Wanner and Juntila 1999; Flügge et al. 2016). Efficient light capture by the photosynthetic machinery under stress conditions and the establishing of a new metabolic homeostasis cannot be achieved without proper chloroplast positioning. The dynamic relocation of chloroplasts in response to various light stimuli has been extensively characterised (Wada 2013; Figure 2). For instance, under strong light exposure, chloroplasts relocate to the cell's anticlinal walls to minimise photodamage

(Kasahara et al. 2002). Throughout diurnal dynamics of light during day, chloroplast avoidance positioning correlates with the midday depression of photosynthesis in sorghum leaves (Maai et al. 2020). Similarly, at low temperature, where enzymatic processes are slower due to thermodynamic constraints (van't Hoff 1884), optimal chloroplast positioning might become critical to prevent photodamage. Studies on the liverworts *Marchantia polymorpha* and the fern *Adiantum capillus-veneris* have shown that chloroplasts relocate to the anticlinal walls when exposed to low temperatures (Kodama et al. 2008; Ogasawara et al. 2013), thereby protecting chloroplast integrity under cold stress conditions.

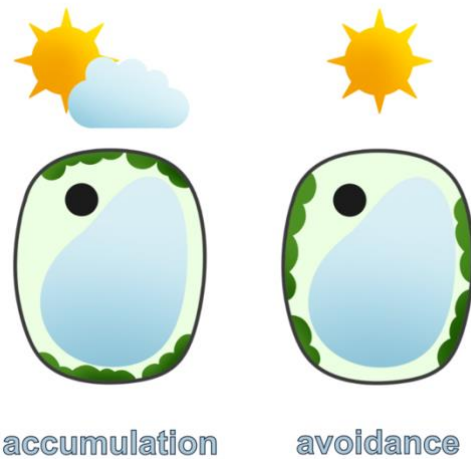


**Figure 2. Chloroplast positioning under various light conditions.** Left panel illustrates accumulation response, i.e., accumulation of chloroplasts at periclinal cell walls under low light. Right panel illustrates avoidance response, i.e., accumulation of chloroplasts at anticlinal cell walls in the response to highlight.

The CHLOROPLAST UNUSUAL POSITIONING 1 (CHUP1) protein has been identified as an essential factor for binding chloroplasts to the plasma membrane (Kasahara et al. 2002). Functioning as a nucleator in polymerisation of chloroplast associated actin filaments, CHUP1 mediates the chloroplast movement within a cell (Schmidt von Braun and Schleiff 2008; Kong et al. 2024). CHUP1 forms a complex with kinesin-like proteins Kinesin CDKA1 Associated 1 and 2 (KAC 1 and 2), as well as THRUMIN 1, receiving signals from photoreceptors such as phototropin 1 and 2 or the FLAVIN-BINDING, KELCH REPEAT, F-BOX 1 (Suetsugu and Wada 2020; Yuan et al. 2023).

While the chloroplast positioning is seemingly crucial for acclimation of plants to environmental stimuli by influencing absorption of light energy, the understanding of cold-induced chloroplast movement in *Arabidopsis* and its effects on acclimation processes remains limited. Considering the complex metabolic responses during cold acclimation, plausible that there is a regulatory connection between chloroplast positioning and the regulation of central carbohydrate metabolism, such as sucrose metabolism, which is closely linked to photosynthetic acclimation (Strand et al. 2003).

### **8.4 Aims of the thesis**

Although regulation of photosynthesis, primary metabolism and chloroplast positioning have been shown to play an important role for plant cold acclimation before, an integrated understanding of these processes is missing. Additionally, while the cold-induced accumulation of flavonoids has been reported earlier, the role of flavonoids during metabolic cold acclimation is not well understood. To improve the understanding of these processes, this thesis explored the significance of chloroplast positioning in photosynthesis and carbohydrate metabolism under cold and varying light conditions. By focusing on the effects of chloroplast distribution, it unveiled its direct effects on photosynthesis and sucrose metabolism under low temperature.

Further, the allocation of carbon between carbohydrate and specialised metabolic pathways was quantified during cold acclimation. Development and validation of a mathematical model could reveal regulatory interactions between metabolism of carbohydrates, flavonoids, and carboxylic acids. Finally, this thesis focuses on the role of flavonoids in cold acclimation. Using subcellular metabolomics and proteomics, this research uncovers a crucial link between photorespiration, amino acid metabolism, and flavonoid biosynthesis through THF metabolism (Figure 3). The findings highlight the importance of flavonoid biosynthesis for maintaining cellular protein amount under low temperature.

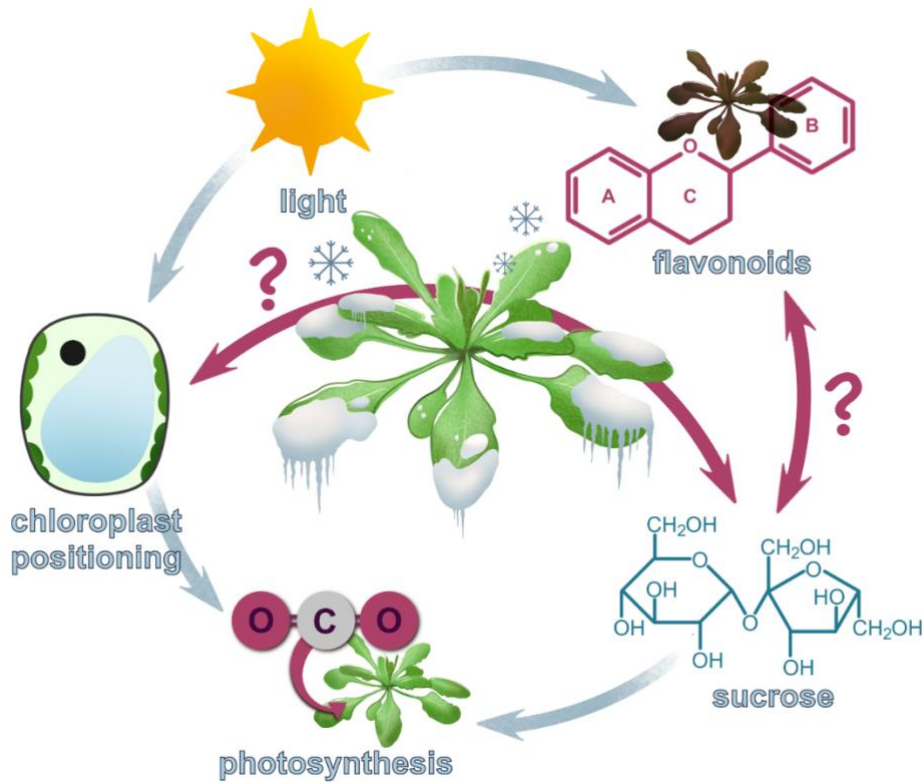


**Figure 3. Hypothesised regulatory links between plant metabolism and chloroplast positioning during plant cold acclimation.** Blue arrows represent established regulatory links, and pink arrows represent missing information on regulatory connections during cold acclimation.

## 9 Results

As this cumulative dissertation is based on four publications (see "4 List of publications and declaration of contribution to the publications" section), the results are presented below as journal articles and are available as open access on the respective journal websites.

### 9.1 Publication 1: Impaired chloroplast positioning affects photosynthetic capacity and regulation of the central carbohydrate metabolism during cold acclimation

**Kitashova A**, Schneider K, Fürtauer L, Schröder L, Scheibenbogen T, Fürtauer S, Nägele T (2021) Impaired chloroplast positioning affects photosynthetic capacity and regulation of the central carbohydrate metabolism during cold acclimation. *Photosynthesis Research* 147: 49–60

Supplementary material is available at:

<https://link.springer.com/article/10.1007/s11120-020-00795-y>



# Impaired chloroplast positioning affects photosynthetic capacity and regulation of the central carbohydrate metabolism during cold acclimation

Anastasia Kitashova<sup>1</sup> · Katja Schneider<sup>2</sup> · Lisa Fürtauer<sup>1</sup> · Laura Schröder<sup>1</sup> · Tim Scheibenbogen<sup>1</sup> · Siegfried Fürtauer<sup>1,3</sup> · Thomas Nägele<sup>1</sup>

Received: 8 May 2020 / Accepted: 6 November 2020 / Published online: 19 November 2020  
© The Author(s) 2020

## Abstract

Photosynthesis and carbohydrate metabolism of higher plants need to be tightly regulated to prevent tissue damage during environmental changes. The intracellular position of chloroplasts changes due to a changing light regime. Chloroplast avoidance and accumulation response under high and low light, respectively, are well known phenomena, and deficiency of chloroplast movement has been shown to result in photodamage and reduced biomass accumulation. Yet, effects of chloroplast positioning on underlying metabolic regulation are less well understood. Here, we analysed photosynthesis together with metabolites and enzyme activities of the central carbohydrate metabolism during cold acclimation of the *chloroplast unusual positioning 1 (chup1)* mutant of *Arabidopsis thaliana*. We compared cold acclimation under ambient and low light and found that maximum quantum yield of PSII was significantly lower in *chup1* than in Col-0 under both conditions. Our findings indicated that net CO<sub>2</sub> assimilation in *chup1* is rather limited by biochemistry than by photochemistry. Further, cold-induced dynamics of sucrose phosphate synthase differed significantly between both genotypes. Together with a reduced rate of sucrose cycling derived from kinetic model simulations our study provides evidence for a central role of chloroplast positioning for photosynthetic and metabolic acclimation to low temperature.

**Keywords** Cold acclimation · Chloroplast positioning · Photosynthesis · *Arabidopsis thaliana* · Carbohydrate metabolism · Hexose phosphates · Hexokinase · Kinetic modelling

## Introduction

Tight regulation and balance of photosynthetic primary and secondary reactions are a prerequisite for efficient CO<sub>2</sub> fixation, biomass accumulation and stress tolerance of higher plants. Particularly under changing environmental

conditions, stabilization of this balance is essential for prevention of tissue damage due to cytotoxic accumulation of reactive oxygen species (ROS). Intracellular distribution of chloroplasts changes in response to changing light intensity. Chloroplast movement plays an important role in protection of photosynthetic machinery against high light intensities and increases photosynthetic efficiency under low light (Wada 2013). Typically, high light induces an avoidance response where chloroplasts are located at the side-walls of palisade cells to minimize light absorption. Under low light, chloroplasts re-distribute to the upper and lower side of the cells to maximize light absorption (accumulation response; schematic overview in (Wada 2013)).

The cytoplasmic protein CHLORPLAST UNUSUAL POSITIONING 1 (CHUP1) localizes to the chloroplast surface, contains an actin binding domain and has been shown to be essential for chloroplast movement (Oikawa et al. 2003, 2008). It was demonstrated that CHUP1 interacts with actin, independent of its filamentation status, and

---

**Electronic supplementary material** The online version of this article (<https://doi.org/10.1007/s11120-020-00795-y>) contains supplementary material, which is available to authorized users.

---

✉ Thomas Nägele  
thomas.naegle@lmu.de

- <sup>1</sup> Department Biology I, Plant Evolutionary Cell Biology, LMU München, 82152 Planegg-Martinsried, Germany
- <sup>2</sup> Department Biology I, Plant Development, LMU München, 82152 Planegg-Martinsried, Germany
- <sup>3</sup> Fraunhofer Institute for Process Engineering and Packaging IVV, 85354 Freising, Germany

further binds to profilin which is an actin modifying protein (Schmidt von Braun and Schleiff 2008). On gene expression level, no alteration of other components involved in chloroplast positioning was observed in a *CHUP1* deletion mutant (Schmidt von Braun and Schleiff 2008). From their gene expression data, the authors concluded that the observed genetic effect rather resulted from altered positioning of chloroplasts and peroxisomes, which was shown to be coupled before (Oikawa et al. 2003), than from alteration of genes encoding for components of light perception and chloroplast movement. Under short-day growth conditions, i.e. 8 h light phase, *chup1* plants displayed reduced photosynthesis and biomass accumulation over a wide range of light intensities, i.e. 50–300  $\mu\text{mol m}^{-2} \text{s}^{-1}$  (Gotoh et al. 2018). In their study, Gotoh and co-workers compared different mutants affected in chloroplast positioning and finally concluded that trade-offs of biomass production and photo-protection are essentially driven by chloroplast movement under changing growth light.

With decreasing temperature, changes in light intensity become an increasing challenge for plants. During the multigenic process of cold acclimation, which is induced by exposure of higher plants to low but non-freezing temperature, numerous molecular and physiological processes are adjusted to enhance freezing tolerance and to minimize cellular and tissue damage, e.g. caused by ROS production (Dreyer and Dietz 2018; Levitt 1980; Xin and Browse 2000). Cold acclimation plays an important role in ecology and evolution of many plant species of the temperate zone due to the significant impact of low temperature on their range boundaries (Hoffmann 2002). It affects gene expression, translational, post-translational and metabolic regulation (Bahrani et al. 2019; Fürtauer et al. 2019; Liu et al. 2019; Wang et al. 2017). Further, composition and activation state of the photosynthetic apparatus is adjusted within a process termed photosynthetic acclimation, in which, however, many of the involved molecular mechanisms still remain elusive (Herrmann et al. 2019). Low temperature is generally accompanied by a reduced membrane fluidity which affects, e.g., the repair cycle of the D1 protein (Aro et al. 1990). Additionally, low temperature significantly affects enzyme activities of the Calvin-Benson cycle which needs to be counteracted during cold stress response and acclimation to prevent imbalance between primary and secondary photosynthetic reactions (Khanal et al. 2017). Absorption of excessive sunlight by the light-harvesting complex leads to ROS generation which damages the photosystems, particularly PSII, and finally leads to photoinhibition (Gururani Mayank et al. 2015). Yet, while particularly under low temperature excessive light is harmful for plants, a combination of low temperature and light is essential for enhancing freezing tolerance in *Arabidopsis thaliana* (Wanner and Junttila 1999).

Comparing temperature effects on photosynthesis in natural *Arabidopsis* accessions previously revealed that limitation of photosynthesis by triose-phosphate utilization was less under low temperature than under high temperature comparing low vs. high irradiance (Pons 2012). Together with many other studies, this observation clearly emphasizes the essential role of tight regulation of photosynthesis and carbohydrate metabolism. Sucrose (Suc) metabolism is well known to play a central role in photosynthetic acclimation (Herrmann et al. 2019; Nägele et al. 2012; Stitt et al. 2010; Strand et al. 2003). In the light, photosynthetic  $\text{CO}_2$  fixation results in triose phosphates which are substrate for starch biosynthesis in the chloroplast and Suc biosynthesis in the cytosol. Key regulators of Suc biosynthesis are cytosolic fructose-1,6-bisphosphatase (cFBPase) and sucrose phosphate synthase (SPS) (Strand et al. 2000). Suc is the central transport sugar in many plant species, represents an osmotically active solute and is involved in sugar signalling (Ruan 2014). Supportingly, recent findings suggest that Suc export from the chloroplast into the cytosol is involved in cold acclimation and is required for development of maximal freezing tolerance (Patzke et al. 2019). Also, in our own studies we demonstrated that Suc compartmentation and invertase-driven cleavage in cytosol and vacuole significantly affect cold stress response and stabilization of photosynthesis (Nägele and Heyer 2013; Weiszmann et al. 2018).

In the present study we aimed to reveal the effect of defective chloroplast positioning on photosynthesis and regulation of carbohydrate metabolism during cold acclimation under ambient and low light in *Arabidopsis thaliana*.

## Materials and methods

### Plant material and growth conditions

Plants of *Arabidopsis thaliana* accession Col-0 and the homozygous *chup1* T-DNA insertion line SALK\_129128C (locus At3g25690; validated by PCR) were grown on a 1:1 mixture of GS90 soil and vermiculite in a climate chamber under short-day conditions (8 h/16 h light/dark; 100  $\mu\text{mol m}^{-2} \text{s}^{-1}$ ; 22 °C/16 °C; 60% relative humidity). After 6 weeks, plants were transferred to the greenhouse and grown under long day conditions (16 h/8 h light/dark, 100  $\mu\text{mol m}^{-2} \text{s}^{-1}$ ). After 5 days in the greenhouse, plants were either (i) sampled at midday, i.e. after 8 h in the light, or (ii) transferred to a cold room for cold acclimation at 4 °C under long day conditions (16 h/8 h light/dark), with either PAR 100  $\mu\text{mol m}^{-2} \text{s}^{-1}$  (samples ambient light/low temperature, AL/LT) or PAR 20  $\mu\text{mol m}^{-2} \text{s}^{-1}$  (samples low light/low temperature, LL/LT). After 7 days at 4 °C, plants were sampled at midday after 8 h in the light. One sample consisted of 3 leaf rosettes which were immediately frozen

in liquid nitrogen and stored at  $-80\text{ }^{\circ}\text{C}$  until further use. For photosynthesis measurements, plants were grown with the same protocol.

### Net photosynthesis and chlorophyll fluorescence measurements

Maximum quantum yield of PSII (Fv/Fm) was determined after 15 min of dark adaptation by supplying a saturating light pulse. Dynamics of quantum efficiency of PSII ( $\Phi\text{PSII}$ ), electron transport rate (ETR), photochemical (qP), non-photochemical quenching (qN) and rates of net  $\text{CO}_2$  assimilation, i.e. net photosynthesis (NPS), were determined within light response curves by stepwise increase of photosynthetically active radiation (PAR) from 0 to  $1200\text{ }\mu\text{mol m}^{-2}\text{ s}^{-1}$  in 5 min intervals. Additionally, all parameters were recorded within  $\text{CO}_2$  response curves where  $\text{CO}_2$  concentration was stepwise increased from 50 to 1200 ppm under constant PAR intensity of  $1200\text{ }\mu\text{mol m}^{-2}\text{ s}^{-1}$ . All measurements were performed using a WALZ® GFS-3000FL system equipped with measurement head 3010-S and Arabidopsis chamber 3010-A (Heinz Walz GmbH, Effeltrich, Germany, <https://www.walz.com/>). NPS and chlorophyll fluorescence parameters of control plants were determined at ambient temperature ( $22\text{ }^{\circ}\text{C}$ ), parameters of AL/LT and LL/LT plants were determined at  $4\text{ }^{\circ}\text{C}$ .

### Quantification of amount of starch, soluble carbohydrates and hexose phosphates

Starch amount was determined as described previously with slight modification (Nägele et al. 2012).  $400\text{ }\mu\text{l}$  of 80% EtOH were added to ground plant material and incubated at  $80\text{ }^{\circ}\text{C}$  for 30 min. After centrifugation, the supernatant was transferred into a new tube and extraction was repeated. Supernatants (80% EtOH) were pooled, dried in a desiccator and used for quantification of soluble carbohydrates. Starch containing pellets were incubated with  $500\text{ }\mu\text{l}$  0.5 N NaOH at  $95\text{ }^{\circ}\text{C}$  for 60 min before slight acidification with  $500\text{ }\mu\text{l}$  1 M  $\text{CH}_3\text{COOH}$ . The starch hydrolysate was digested with amyloglucosidase for 2 h at  $55\text{ }^{\circ}\text{C}$ . Glucose content, derived from starch digestion, was photometrically determined by a glucose oxidase/peroxidase/o-dianisidine reaction at 540 nm.

Soluble sugars, i.e. glucose, fructose and sucrose, were determined from dried EtOH extracts. Sucrose was quantified using an anthrone assay after incubation with 30% KOH at  $95\text{ }^{\circ}\text{C}$ . For the assay, anthrone was dissolved in 14.6 M  $\text{H}_2\text{SO}_4$  (0.14% w/v), incubated with the samples for 30 min at  $40\text{ }^{\circ}\text{C}$  before absorbance was determined at 620 nm.

Glucose amount was determined using a coupled hexokinase/glucose 6-phosphate dehydrogenase assay resulting in  $\text{NADPH} + \text{H}^+$  which was determined photometrically

at 340 nm. For fructose quantification, phosphoglucosomerase was added to the reaction mixture after glucose determination.

Glucose 6-phosphate (G6P) and fructose 6-phosphate (F6P) were extracted and photometrically quantified using enzyme cycling-based assays as described earlier (Gibon et al. 2002). In brief, hexose phosphates were extracted using trichloroacetic acid (TCA) in diethyl ether (16% w/v), washed with 16% (w/v) TCA in 5 mM EGTA and neutralised with 5 M KOH/1 M triethanolamine. Enzymatic reactions catalysed the equimolar interconversion of G6P and F6P into  $\text{NADPH} + \text{H}^+$  which was finally detected photometrically from slopes of a cyclic reaction yielding a formazan dye from thiazolyl blue (MTT) at 570 nm.

### Quantification of enzyme activities

Activity of all enzymes was determined under substrate saturation ( $v_{\text{max}}$ ).

Activity of sucrose phosphate synthase (SPS) was determined using the anthrone assay as described earlier (Nägele et al. 2012). Frozen leaf tissue was suspended in extraction buffer containing 50 mM HEPES–KOH (pH 7.5), 10 mM  $\text{MgCl}_2$ , 1 mM EDTA, 2.5 mM DTT, 10% (v/v) glycerine and 0.1% (v/v) Triton-X-100. After incubation on ice, extracts were incubated for 30 min at  $25\text{ }^{\circ}\text{C}$  with reaction buffer containing 50 mM HEPES–KOH (pH 7.5), 15 mM  $\text{MgCl}_2$ , 2.5 mM DTT, 35 mM UDP-glucose, 35 mM F6P and 140 mM G6P. Reactions were stopped by adding 30% KOH and heating the samples to  $95\text{ }^{\circ}\text{C}$ . Sucrose was determined photometrically after incubation with anthrone in  $\text{H}_2\text{SO}_4$  as described above and blanks (stopped before reaction) were subtracted.

Glucokinase and fructokinase activities were determined photometrically at 340 nm recording the slopes of  $\text{NADP}^+$  reduction to  $\text{NADPH} + \text{H}^+$  (Wiese et al. 1999). In brief, frozen leaf tissue was suspended in extraction buffer containing 50 mM Tris–HCl (pH 8.0), 0.5 mM  $\text{MgCl}_2$ , 1 mM EDTA, 1 mM DTT and 1% (v/v) Triton-X-100. Following incubation on ice, reaction was started with a reaction buffer containing 100 mM HEPES–KOH (pH 7.5), 10 mM  $\text{MgCl}_2$ , 2 mM ATP, 1 mM NADP, 0.5U G6PDH and either 5 mM glucose for glucokinase measurement or 5 mM fructose and 0.5U PGI for fructokinase measurement.

Neutral (nInv), acidic (aInv) and cell wall-bound (cwInv) invertase activities were determined as described before with slight modifications (Nägele et al. 2010). Frozen leaf tissue was homogenized in extraction buffer containing 50 mM HEPES–KOH (pH 7.5), 5 mM  $\text{MgCl}_2$ , 2 mM EDTA, 1 mM phenylmethylsulfonylfluoride (PMSF), 1 mM DTT, 10% (v/v) glycerine and 0.1% (v/v) Triton-X-100. After incubation on ice, samples were centrifuged at  $4\text{ }^{\circ}\text{C}$  and supernatants were transferred to a new tube. Pellets contained



cell wall-bound invertase and were re-suspended in extraction buffer. Soluble, i.e. nInv and aInv, invertase activities were determined from supernatants, cwInv activity was determined from resuspended pellets. Activity of nInv was determined using a reaction buffer with pH 7.5 (20 mM HEPES–KOH, 100 mM sucrose), aInv and cwInv activities were determined at pH 4.7 (20 mM sodium acetate, 100 mM sucrose). After incubation of extract with reaction buffers reactions were stopped at 95 °C and glucose built from invertase reactions was photometrically determined by a glucose oxidase/peroxidase/o-dianisidine assay at 540 nm.

Activity of glucose 6-phosphate dehydrogenase (G6PDH) under substrate saturation was determined as reported earlier (Fahrendorf et al. 1995) with slight modification. Ground plant material was suspended in extraction buffer consisting of 0.05 M Tris HCl (pH 8.0), 0.3 M NaCl, 0.1 mM benzamidine, 0.1 mM PMSF, 1 mM DTT and 0.1% (v/v) Triton-X-100. A low concentration of 1 mM DTT was used due to the previous observation of a potential reduction of G6PDH activity in mature spinach leaves and barley primary leaves by 10 mM DTT (Johnson 1972). After incubation on ice and centrifugation at 4 °C, supernatants were incubated with assay buffer containing 0.1 M Tris HCl (pH 8.0) and 0.4 mM NADP. After pre-incubation at 30 °C for 10 min, G6P was added and reduction of NADP<sup>+</sup> by G6PDH was measured photometrically at 340 nm at 30 °C for 10 min.

Phosphoglucose isomerase (PGI) extraction and activity quantification under substrate saturation was based on previously described methods with slight modification (Kunz et al. 2014). Ground plant material was suspended in extraction buffer containing 0.05 M Tris HCl (pH 8.0), 0.5 mM MgCl<sub>2</sub>, 1 mM EDTA, 2.5 mM DTT and 1% (v/v) Triton-X-100. The suspension was incubated on ice, followed by centrifugation at 4 °C. PGI activity was estimated from supernatants in a coupled reaction with G6PDH by photometrically measuring reduction of NADP<sup>+</sup> at 340 nm. For this, supernatants were incubated with assay buffer consisting of 100 mM HEPES–KOH (pH 7.5) and 10 mM MgCl<sub>2</sub>. After addition of 2 µl of 100 mM NADP and 1 U G6PDH, the solution was pre-incubated at 30 °C for 10 min. The reaction was initiated by addition of 20 µl of 50 mM F6P (or 20 µl of ddH<sub>2</sub>O for blanks), followed by recording absorbance at 340 nm at 30 °C for 10 min. The linear range of recorded kinetic was interpolated and the slope was used to calculate maximal activity of PGI.

### Sample preparation and sectioning for microscopy analysis

Primary leaves of *Arabidopsis thaliana*, Col-0 and *chup1*, were cut into 1 mm square pieces and fixed in fixation buffer (75 mM sodium cacodylate, 2 mM MgCl<sub>2</sub>, pH 7) substituted with 2.5% (v/v) glutaraldehyde for 2 days at 4 °C. The

leave pieces were washed three times at room temperature using fixation buffer and post-fixed with 1% (w/v) osmium tetroxide for 2 h. Subsequent to washing with fixation buffer and water, the samples were stained *en bloc* with 1% (w/v) uranyl acetate in 20% (v/v) acetone for 30 min. Samples were dehydrated in a series of graded acetone and embedded in Spurr's resin. Samples were either ultra-thin sectioned (thickness, 60 nm) for TEM (transmission electron microscope) analysis or semi-thin sectioned (thickness, 2 µm) for LM (light microscope) analysis. For sectioning a diamond knife was used on a Reichert Ultracut-E ultramicrotome. Ultra-thin sections were mounted on collodium-coated copper grids, post-stained with lead citrate (80 mM, pH 13) and examined with an EM 912 transmission electron microscope (Zeiss, Oberkochen, Germany) equipped with an integrated OMEGA energy filter operated in the zero-loss mode at 80 kV. Images were acquired using a 2 k × 2 k slow-scan CCD camera (Tröndle Restlichtverstärkersysteme, Moorenweis, Germany). Semi-thin sections mounted on glass slides and examined using a Zeiss Axiophot light microscope. Images were acquired using a SPOT insight 2 MP CCD color digital camera.

### Statistics and mathematical modelling

For statistical data evaluation we used the free software environment R Version 3.6.1 (<https://www.r-project.org/>) (R Core Team 2019) and RStudio Version 1.2.5019 (<https://rstudio.com/>) (RStudio Team 2019). Statistics comprised analysis of variance (ANOVA) and Tukey's honestly significant difference post-hoc test. Mathematical modelling was performed in MATLAB® R2019b ([www.mathworks.com](http://www.mathworks.com)) with the toolbox *IQM Tools* developed by IntiQuan (<https://www.intiquan.com/>). Ordinary differential equations (ODEs), enzyme kinetic equations and kinetic parameter values are provided in the supplements (Supplementary Table IV–VI). Rates of net photosynthesis ('rNPS') were derived from interpolation of photosynthesis measurements, i.e. net CO<sub>2</sub> assimilation rates (interpolation model:  $f(x) = a \cdot \exp(b \cdot x) + c \cdot \exp(d \cdot x)$ ). For simulation of sucrose cleavage rates, experimentally quantified invertase activities of nInv, aInv and cwInv were summed up (model parameter 'vmax\_inv'). Rates of net starch synthesis ('rStarch') were estimated from the amount measured after 8 h in the light (i.e. amount/8 h). For simulation at low temperature (AL/LT and LL/LT), quantified v<sub>max</sub> values were temperature corrected to 4 °C applying the van't Hoff rule (Eq. 1) with a Q<sub>10</sub> factor of 2.5 (Reyes et al. 2008).

$$Q_{10} = (R_2/R_1)^{\frac{10K}{(T_2-T_1)}} \quad (1)$$

Ranges of kinetic parameters which were not experimentally quantified in the present study, i.e.  $K_M$  and  $K_i$  values,

were derived from our previous studies and further literature (Fürtauer and Nägele 2016; Nägele et al. 2010, 2012; Scharte et al. 2009; Schnarrenberger and Oeser 1974; Weiszmann et al. 2018).

## Results

### The CHUP1 mutation significantly affects maximum quantum yield of PSII under low temperature and rates of net CO<sub>2</sub> fixation under high light

Affected chloroplast positioning in *chup1* (see Supplementary Figures S1 and S2) had significant effects on photosynthesis both under ambient and low temperature. While Fv/Fm did not differ between *chup1* and Col-0 under control conditions, it was lower in *chup1* than in Col-0 at 4 °C under both ambient and low light (Fig. 1; AL/LT:  $p = 0.07$ ; LL/LT:  $p < 0.05$ , ANOVA). Interestingly, in both genotypes Fv/Fm was significantly higher under LL/LT ( $> 0.82$ ) than under control ( $\sim 0.815$ ) conditions ( $p < 0.001$ , ANOVA). In summary, maximum quantum yield of PSII did not differ between both genotypes under control conditions but was lower in *chup1* than in Col-0 after 7 days at 4 °C under both low ( $20 \mu\text{mol m}^{-2} \text{s}^{-1}$ ) and ambient light ( $100 \mu\text{mol m}^{-2} \text{s}^{-1}$ ).

Rates of net CO<sub>2</sub> assimilation were recorded together with chlorophyll fluorescence parameters within light response curves and CO<sub>2</sub> response curves (Fig. 2, Supplementary Figures S3 and S4). Analysis of variance (ANOVA) revealed a highly significant condition effect ( $p < 0.001$ ) on net CO<sub>2</sub> fixation rates of both genotypes separating control vs. AL/LT and control vs. LL/LT across a wide range of PAR

intensity and CO<sub>2</sub> concentration (Fig. 2a–d). No significance was observed between AL/LT and LL/LT neither in light response curves nor in CO<sub>2</sub> response curves. Further, under high PAR intensity, i.e.  $1200 \mu\text{mol m}^{-2} \text{s}^{-1}$ , and at ambient temperature (22 °C) *chup1* had a significantly lower net CO<sub>2</sub> fixation rate than Col-0 ( $p < 0.001$ , ANOVA; a summary of all ANOVA results is provided in the supplements, Supplementary Tables I–III). Local polynomial regression under control conditions (green lines in Fig. 2) indicated that net CO<sub>2</sub> assimilation rates of *chup1* were near to saturation at  $1200 \mu\text{mol m}^{-2} \text{s}^{-1}$  (Fig. 2b) which was not observed for Col-0 (Fig. 2a). Under high CO<sub>2</sub> concentration, i.e. 900 and 1200 ppm, and high irradiance ( $1200 \mu\text{mol m}^{-2} \text{s}^{-1}$ ), net CO<sub>2</sub> assimilation rates did not significantly differ between Col-0 and *chup1* (Fig. 2c, d). Instead, Col-0 had significantly higher CO<sub>2</sub> fixation rates than *chup1* at 200 ppm and 400 ppm (ANOVA,  $p < 0.01$ ). After 7d at 4 °C, CO<sub>2</sub> assimilation rates were found to neither differ between genotypes nor between light conditions within a genotype, i.e. AL/LT and LL/LT.

Light and CO<sub>2</sub> response curves of chlorophyll fluorescence parameters were recorded together with net CO<sub>2</sub> assimilation rates (Supplementary Figures S3 and S4) revealing no significant difference between Col-0 and *chup1* (Supplementary Table 1). Yet, only in Col-0 qN was significantly higher under control than under low temperature at high PAR intensity, i.e.  $1200 \mu\text{mol m}^{-2} \text{s}^{-1}$  (ANOVA,  $p < 0.05$ ; Supplementary Figure 3G).

### Low temperature induced accumulation of hexose phosphates is significantly affected in *chup1*

Quantification of central carbohydrates revealed similar amounts of starch and sucrose in Col-0 and *chup1* under all tested conditions (Fig. 3). Compared to control condition, in both genotypes, starch increased significantly  $\sim$  tenfold under AL/LT (ANOVA,  $p < 0.001$ ) and decreased significantly to a level  $\sim 0.5 \mu\text{mol gFW}^{-1}$  under LL/LT (ANOVA,  $p < 0.05$ ; Fig. 3a, b). Similarly, sucrose increased significantly  $\sim 2.5$ -fold under AL/LT (ANOVA,  $p < 0.001$ ) while no significant change was observed under LL/LT neither for Col-0 nor for *chup1* (Fig. 3c, d). Although it is difficult to estimate biological variance from 5 biological replicates, our data indicated a slightly higher variance of starch and sucrose amount in *chup1* than in Col-0, particularly under control and AL/LT. Next, we quantified dynamics of free hexoses, i.e. glucose and fructose, and of their phosphorylation products, G6P and F6P (Fig. 4). In both genotypes, glucose and fructose significantly increased under AL/LT ( $p < 0.001$ ) and significantly dropped under LL/LT ( $p < 0.05$ ) compared to the amount under control conditions (Fig. 4a–d). Neither amount of glucose nor fructose significantly differed between Col-0 and *chup1*

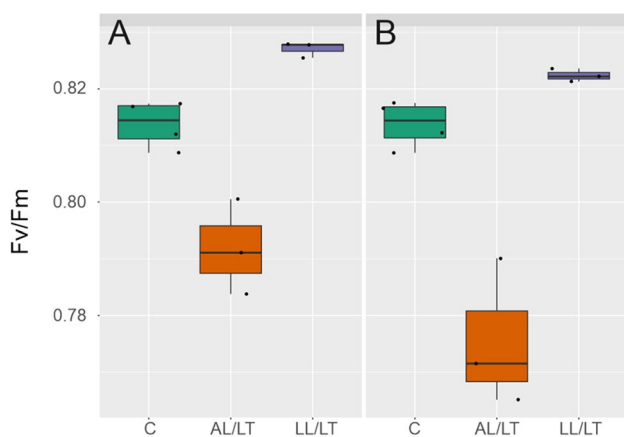
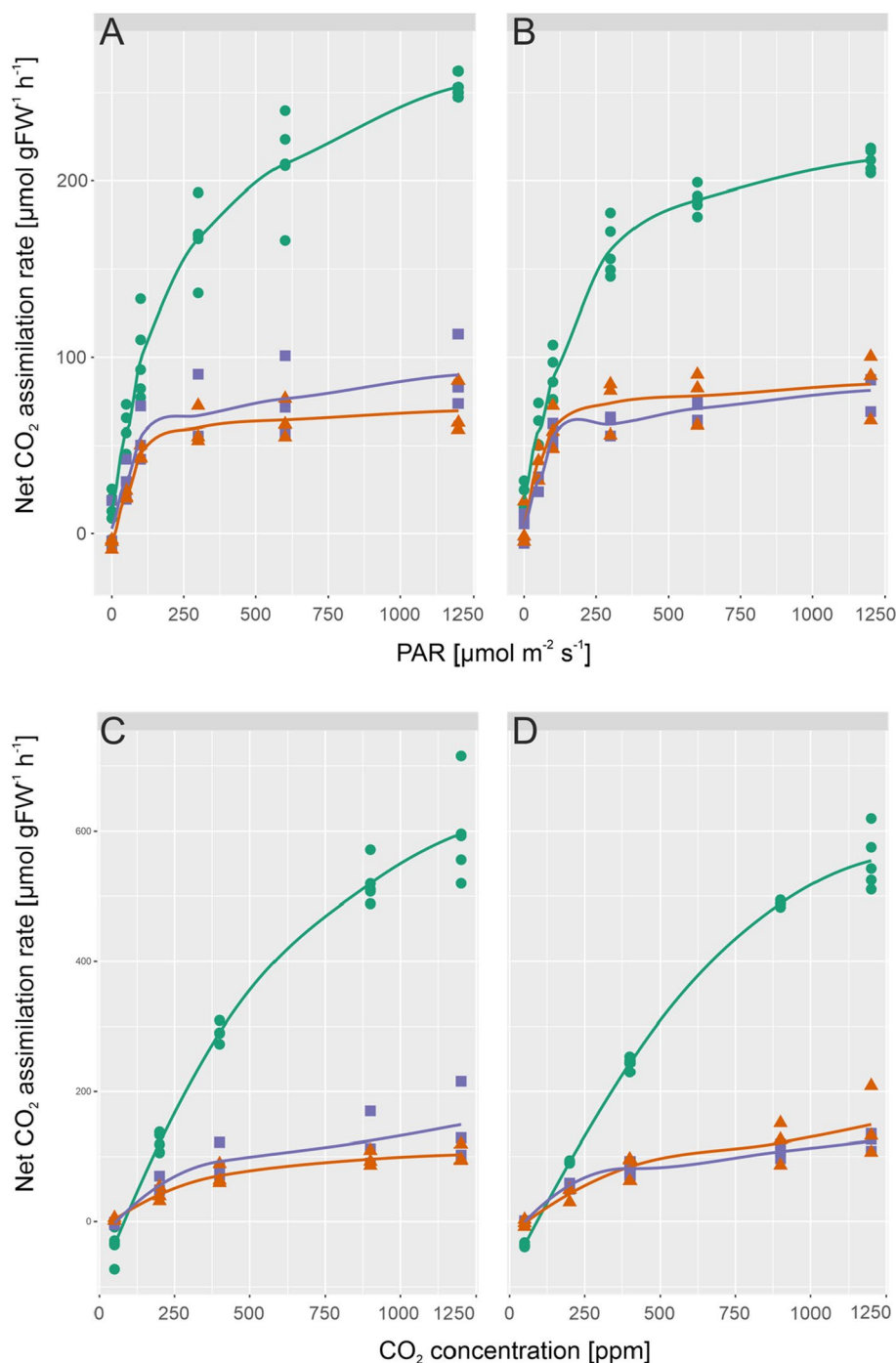


**Fig. 1** Maximum quantum yield of PSII in Col-0 and *chup1*. **a** Fv/Fm in Col-0 and **b** in *chup1* under control (green box,  $100 \mu\text{mol m}^{-2} \text{s}^{-1}$ , 22 °C), ambient light/low temperature (orange box, AL/LT,  $100 \mu\text{mol m}^{-2} \text{s}^{-1}$ ) and low light/low temperature (purple box, LL/LT,  $20 \mu\text{mol m}^{-2} \text{s}^{-1}$ ). In addition to coloured box-and-whisker plots single measurements are indicated by black dots

**Fig. 2** Rates of net CO<sub>2</sub> assimilation in Col-0 and *chup1* as a function of irradiance and CO<sub>2</sub> concentration. **a** Rates of net CO<sub>2</sub> assimilation in Col-0 under control (green circles), AL/LT (orange triangles) and LL/LT (purple squares) as a function of PAR, **b** rates of net CO<sub>2</sub> assimilation in *chup1* under control (green circles), AL/LT (orange triangles) and LL/LT (purple squares) as a function of PAR, **c** rates of net CO<sub>2</sub> assimilation in Col-0 under control (green circles), AL/LT (orange triangles) and LL/LT (purple squares) as a function of CO<sub>2</sub> concentration, **d** rates of net CO<sub>2</sub> assimilation in *chup1* under control (green circles), AL/LT (orange triangles) and LL/LT (purple squares) as a function of CO<sub>2</sub> concentration. Symbols represent measurements of independent biological replicates ( $n \geq 3$ ). Lines represent a local polynomial regression. Measurements of control samples were performed at 22 °C, measurements of AL/LT and LL/LT at 4 °C. An overview of significances revealed by ANOVA is provided in the supplements (Supplementary Tables I and II)



under any tested condition. In contrast, dynamics of G6P and F6P revealed significant genotype-effects under low temperature (Fig. 4e–h). While G6P amounts significantly increased ~ threefold in both genotypes under AL/LT, only in Col-0 we observed a significant difference between G6P amount under AL/LT and LL/LT (Fig. 4e, f). In *chup1*, G6P amount was similar in LL/LT and AL/LT (Fig. 4f). Also, dynamics of F6P amount significantly differed between Col-0 and *chup1* where already under control

conditions a reduced amount was observed in *chup1* ( $p = 0.06$ , ANOVA). Under AL/LT, amount of F6P significantly increased ~ threefold in *chup1* while no change was observed in Col-0 (Fig. 4g, h). Only under LL/LT, F6P amount increased ~ 1.5-fold in Col-0 ( $p < 0.001$ ). In summary, sucrose/starch ratios and free hexose amounts were similar in both genotypes while hexose phosphates significantly differed in their cold-induced dynamics between Col-0 and *chup1*.

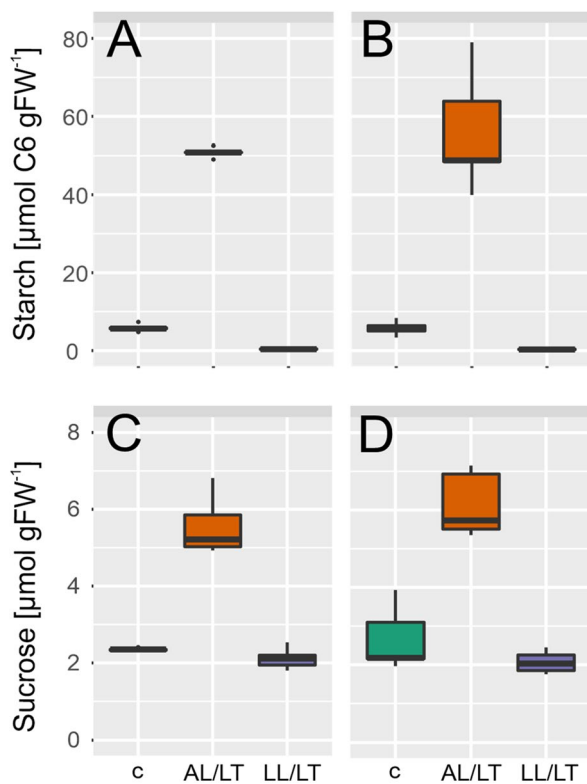


**Fig. 3** Cold-induced dynamics of starch and sucrose. **a** Starch amount in Col-0, **b** Starch amount in *chup1*, **c** Sucrose amount in Col-0 and **d** Sucrose amount in *chup1*. In each panel, left/green: control; middle/orange: AL/LT; right/purple: LL/LT. An overview of significances revealed by ANOVA is provided in the supplements (Supplementary Table III;  $n=5$ )

### Cold-induced dynamics of gluco- and fructokinase activities are significantly reduced in *chup1*

Enzyme activities of the central carbohydrate metabolism were quantified to reveal a potential effect of the *CHUP1* mutation on metabolic regulation (Fig. 5). Dynamics of sucrose phosphate synthase (SPS) activity under AL/LT was reduced in *chup1* (Fig. 5a, b). Most significant effects were observed for gluco- (GlcK) and fructokinase (FrcK) activities under low temperature (Fig. 5c–f). In Col-0, GlcK activity significantly increased ~threefold under AL/LT compared to control conditions while no effect was observed in *chup1* (Fig. 5c, d). Under LL/LT, FrcK activity dropped in both genotypes but only in Col-0 this effect was significant (Fig. 5e). Activities of neutral, acidic and cell wall-associated invertases were reduced significantly under low temperature in both genotypes (see ANOVA results in Supplementary Table III) and this reduction was most pronounced under AL/LT (Fig. 5g–i). Activities of phosphoglucosomerase (PGI) and glucose 6-phosphate dehydrogenase revealed similar cold-induced changes in both genotypes

with an activity increase under AL/LT and no change or only a slight decrease under LL/LT (Supplementary Figure S5).

### Kinetic modelling reveals a shift of reaction rates in *chup1* from hexose phosphorylation into G6P oxidation under low temperature

Metabolite concentrations, net rates of  $\text{CO}_2$  assimilation and enzyme activities were integrated into a mathematical kinetic model. Graphical model structure and identified steady state models for Col-0 and *chup1* under all tested conditions are provided in the supplement (Supplemental Figure S6 and Supplemental Tables IV–VI). For kinetic simulation, a steady state was identified by parameter optimization using temperature-corrected enzyme activities and mean values of quantified metabolites. Particularly under AL/LT, simulations revealed that reaction rates of PGI and G6PDH in Col-0 decreased stronger than in *chup1* (Fig. 6). Vice versa, reaction rates of hexose phosphorylation ('rGLCK' and 'rFRCK') together with sucrose cleavage ('rINV') were lower in *chup1* than in Col-0 AL/LT. Simulated rates of sucrose biosynthesis ('rSPS') decreased to similar values in both genotypes. In summary, kinetic simulations suggest that particularly under AL/LT a higher rate of glucose oxidation, catalysed by G6PDH, in *chup1* leads to reduced rates of hexose phosphorylation when compared to Col-0.

## Discussion

Chloroplast avoidance movement is a protective mechanism by which plants mitigate photodamage. Under high light intensities, chloroplasts typically move to the side walls of cells to minimize the area of potential light absorption. Mutants like *chup1*, which are defective in this avoidance movement, have been shown to be more susceptible to damage in high light than wild type plants which immediately proves the central importance of this mechanism under changing environmental conditions (Kasahara et al. 2002). However, under ambient light, i.e.  $100 \mu\text{mol photons m}^{-2} \text{ s}^{-1}$ , and long day growth conditions neither we (data not shown) nor others observed any effect on biomass accumulation (Kasahara et al. 2002). In contrast, for plants grown under short day conditions the accumulation response, which is also defective in *chup1* mutants, was shown to enhance leaf photosynthesis and plant biomass production (Gotoh et al. 2018). In line with these observations, we found similar rates of net  $\text{CO}_2$  assimilation in Col-0 and *chup1* at growth PAR intensity under ambient and low temperature (see Fig. 2a) while Gotoh and colleagues observed a significantly reduced rate of net  $\text{CO}_2$  assimilation in *chup1* grown under short day. Together with the finding of lowered net  $\text{CO}_2$  assimilation rates in *chup1* under high light intensity,

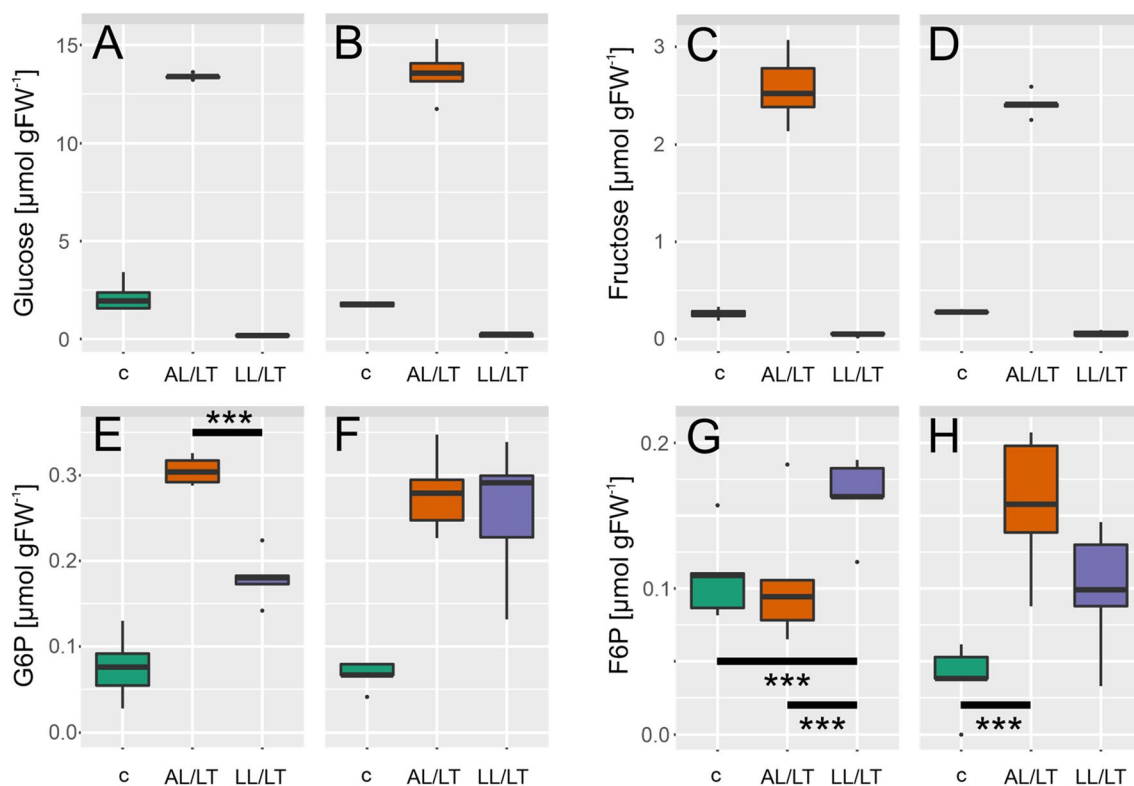


**Fig. 4** Cold-induced dynamics of hexoses and hexose phosphates. **a, c, e, g** amount of substance in Col-0, **b, d, f, h** amount of substance in *chup1*. Boxes in each panel, left/green: control; middle/orange: AL/LT; right/purple: LL/LT. Significances are indicated by asterisks

but only shown where different between Col-0 and *chup1* (ANOVA, \*\*\* $p < 0.001$ ). A complete overview of significances is provided in the supplements (Supplementary Table III;  $n = 5$ )

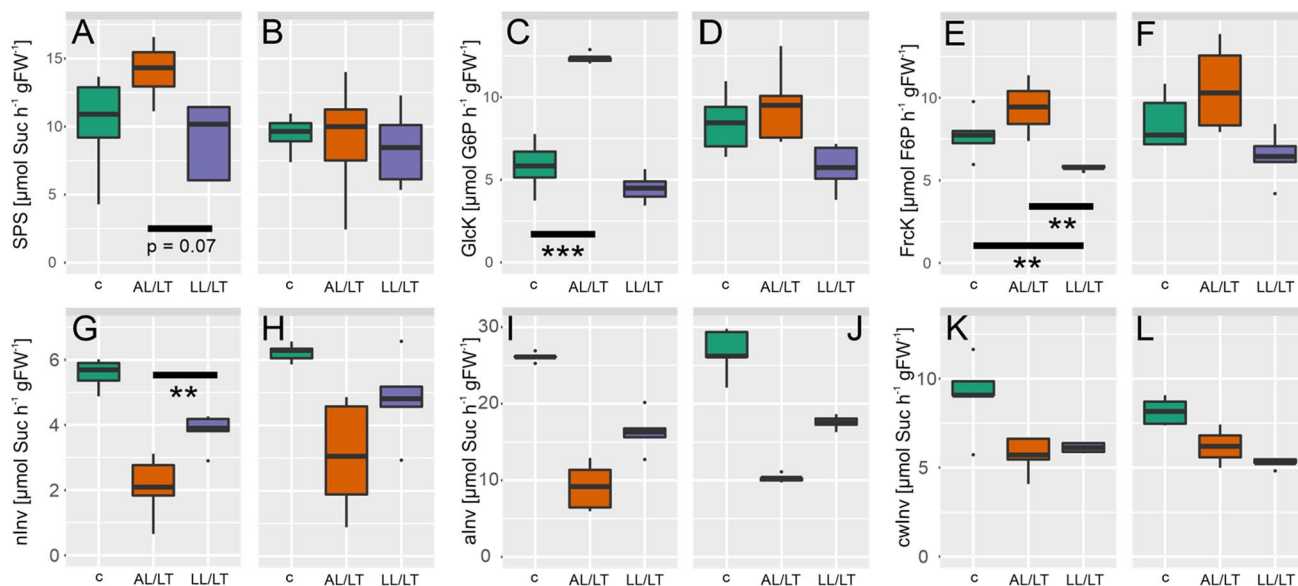


**Fig. 5** Dynamics of enzyme activities of the central carbohydrate metabolism. **a, c, e, g, i, k** enzyme activities in Col-0, **b, d, f, h, j, l** enzyme activities in *chup1*. Boxes in each panel, left/green: control; middle/orange: AL/LT; right/purple: LL/LT. *SPS* Sucrose phosphate synthase, *GlcK* glucokinase, *FrcK* fructokinase, *nlnv* neutral

invertase, *aln* acidic invertase, *cwlInv* cell wall-associated invertase. Significances are indicated by asterisks but only shown where different between Col-0 and *chup1* (ANOVA; \*\* $p < 0.01$ ; \*\*\* $p < 0.001$ ). A complete overview of significances is provided in the supplements (Supplementary Table III;  $n = 5$ )

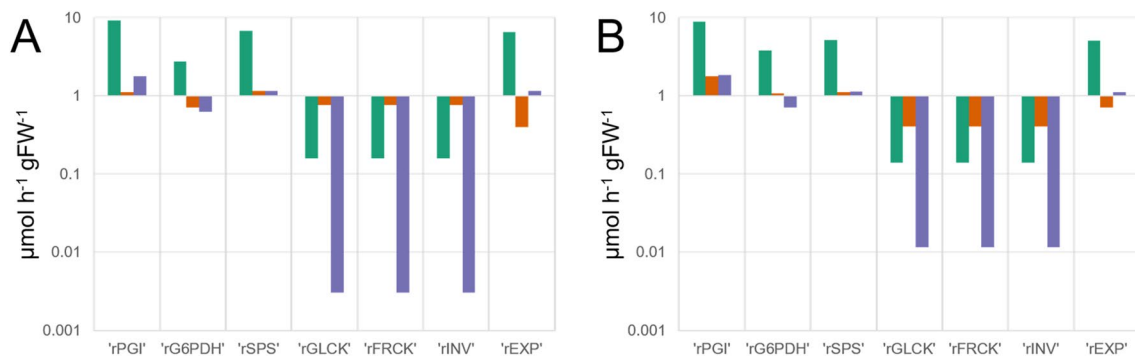


**Fig. 6** Simulated reaction rates before and after cold acclimation in Col-0 and *chup1*. **a** Reaction rates of Col-0 under control, AL/LT and LL/LT. **b** Reaction rates of *chup1* under control, AL/LT and LL/LT. Green bars: control; orange bars: AL/LT; purple bars: LL/LT. Simu-

lations were derived from a kinetic model which is explained in the supplements (Supplementary Figure S6, Supplementary Table IV). Enzyme activities were temperature corrected to 4 °C for AL/LT and LL/LT simulations

i.e. 1200  $\mu\text{mol photons m}^{-2} \text{s}^{-1}$ , these results indicate that *chup1* plants can compensate for effects on photosynthetic  $\text{CO}_2$  uptake rates under long photoperiods.

Under control long day growth conditions, neither of the recorded chlorophyll fluorescence parameters significantly differed between Col-0 and *chup1* which was also observed previously under short day growth conditions (Gotoh et al. 2018). This suggests that potential limitation of  $\text{CO}_2$  net assimilation rates in *chup1* rather arises from biochemistry than photochemistry. Supportively, *chup1* assimilated significantly less  $\text{CO}_2$  than Col-0 under ambient temperature, high light intensity and lowered  $\text{CO}_2$  concentration (200 ppm, Fig. 2b and Supplementary Table II). While under very low  $\text{CO}_2$  concentrations, i.e. 50 ppm, no significant effect was observed this might be due to the very strong overlaying effect of such a condition on all photosynthetic parameters, also in Col-0. Further evidence for a biochemical limitation of photosynthesis in *chup1* is provided by the finding that dynamics of enzyme activities, particularly of SPS, GlcK and Frck, were significantly lowered in *chup1* compared to Col-0 when exposed to 4 °C (see Fig. 5). Previous studies have shown a central role of sucrose biosynthesis for cold acclimation and stabilization of photosynthesis (Nägele et al. 2012; Strand et al. 2003). Yet, although the median SPS activity in Col-0 was ~1.5-fold higher than in *chup1* under AL/LT, neither simulated steady state SPS flux nor Suc amount differed between both genotypes (Figs. 3 and 6). This might be explained by the significantly higher amount of F6P in *chup1* than in Col-0 under AL/LT (see Fig. 4). Together with UDP glucose, F6P is substrate for the SPS reaction and, thus, our data suggest that a higher amount of F6P may compensate for a reduced SPS activity to result in a similar rate of Suc biosynthesis (rSPS) in both genotypes. However, our modelling approach comprised simplifications which need to be discussed and addressed in further studies in order to reveal how far estimated reaction rates reflect

actual in vivo rates. First, in the present study we did not quantify UDP glucose but instead assumed its amount to be ~20% of G6P as reported before (Szecowka et al. 2013). Further, we ignored subcellular distribution of metabolites and, thus, simulated reaction rates might overestimate actual reaction rates due to a higher substrate concentration. For example, approximately one third of F6P amount has previously been reported to be located in the chloroplast of Col-0 and two thirds are located in the cytosol (Szecowka et al. 2013). Future studies on subcellular metabolite distribution might refine the estimated reaction rates and reveal whether compartmentation differs between Col-0 and *chup1*.

While rSPS was similar in both genotypes under all conditions, rates of sucrose cleavage (rINV), fructose phosphorylation (rFRCK) and glucose phosphorylation (rGLCK) were lower in *chup1* than in Col-0 under control and AL/LT conditions (see Fig. 6). Together with rSPS, these reactions describe a cyclic reaction of Suc synthesis and degradation which has been termed as a *futile cycle* due to its seemingly futile consumption of ATP (Geigenberger and Stitt 1991; Nguyen-Quoc and Foyer 2001). However, it has also been discussed earlier that the “waste” of ATP might only comprise 3–5% while, as a benefit, such futile cycles increase sensitivity of metabolic regulation (Geigenberger and Stitt 1991; Hue 1981). Also, in our own previous studies we found evidence for a central role of sucrose cycling in stabilization of photosynthesis during cold exposure (Nägele and Heyer 2013; Weiszmann et al. 2018). Interestingly, while most of the recorded photosynthetic parameters under AL/LT were similar in both genotypes, maximum quantum yield was significantly affected, i.e. lower, in *chup1* and, thus, correlated with the sucrose cycling capacities determined by reaction rates rINV, rGLCK and rFRCK. Conclusively, although *chup1* did not suffer from severe photodamage under AL/LT, our findings provide evidence for an important role of sucrose cycling in precision tuning of photosynthesis

and metabolism under low temperature. This observation emphasizes not only the suitability but also the necessity of mathematical modelling to reveal effects of mutations and/or environmental fluctuation on metabolism. Particularly for the study of metabolic cycles mathematical modelling is the method of choice due to underlying complexity, nested uncertainties and non-intuitive modes of regulation (Henkel et al. 2011; Reznik and Segrè 2010; Schaber et al. 2009).

In addition to activity of hexokinase, oxidation of G6P, catalysed by G6PDH, represents a further important mechanism involved in dynamics of hexose phosphate concentrations under changing environmental conditions. Cold acclimation under AL/LT resulted in a ~ threefold increase of the G6P/F6P ratio in Col-0 and only ~ 1.5-fold in *chup1*. Vice versa, under LL/LT this ratio increased ~ threefold in *chup1* compared to control while in Col-0 concentrations of G6P and F6P increased similarly. A significant increase of the G6P/F6P ratio due to cold acclimation has been reported earlier (Savitch et al. 2001). As suggested by Savitch and colleagues, induction of the ascorbate–glutathione cycle as a ROS defence system might result in an increased supply of NADPH + H<sup>+</sup> by an increased activity of the oxidative pentose phosphate pathway, oxPPP (May et al. 1998; Savitch et al. 2001). In *chup1*, both G6P and F6P amount significantly increased under AL/LT which together with the wild type-like activities of G6PDH and no obvious photodamage might indicate that ROS defence via oxPPP is still functional. Yet, overaccumulation of G6P under LL/LT and higher rG6PDH rates indicate a less tightly regulated balance between photosynthetic light reactions and carbohydrate metabolism in *chup1* which, under high light intensities, would result in lowered CO<sub>2</sub> assimilation rates and photodamage.

## Conclusion

Although cold acclimation of *chup1* did not result in a lowered photosynthetic CO<sub>2</sub> assimilation rate compared to Col-0, the presented findings suggest a central role of CHUP1-mediated chloroplast positioning for tight regulation of photosynthesis and carbohydrate metabolism under low temperature. Future studies might address metabolic effects on the subcellular level, including further mutants affected in chloroplast positioning, e.g. *phototropin* mutants. While the combination of high light intensities and low temperature leads to photoinhibition which prevents the study of metabolic regulation under such conditions, further insights into the effects of chloroplast positioning on metabolic regulation might be gained using other abiotic factors, e.g. heat, high light and a combination of both.

**Acknowledgements** We thank the groups of Plant Evolutionary Cell Biology and Plant Development at LMU München for many fruitful discussions and support.

**Author contributions** AK performed experiments, KS performed microscopy, LF, LS, TS, SF and TN supported experimental analysis. AK and TN analysed data and wrote the manuscript. All authors approved the manuscript.

**Funding** Open Access funding enabled and organized by Projekt DEAL. This work was supported by the LMUexcellent Junior Researcher Fund and by the TRR175, funded by Deutsche Forschungsgemeinschaft (DFG).

## Compliance with ethical standards

**Conflict of interest** The authors declare that they have no conflict of interest.

**Open Access** This article is licensed under a Creative Commons Attribution 4.0 International License, which permits use, sharing, adaptation, distribution and reproduction in any medium or format, as long as you give appropriate credit to the original author(s) and the source, provide a link to the Creative Commons licence, and indicate if changes were made. The images or other third party material in this article are included in the article's Creative Commons licence, unless indicated otherwise in a credit line to the material. If material is not included in the article's Creative Commons licence and your intended use is not permitted by statutory regulation or exceeds the permitted use, you will need to obtain permission directly from the copyright holder. To view a copy of this licence, visit <http://creativecommons.org/licenses/by/4.0/>.

## References

- Aro E-M, Hundal T, Carlberg I, Andersson B (1990) In vitro studies on light-induced inhibition of Photosystem II and D1-protein degradation at low temperatures. *BBA Bioenergetics* 1019:269–275. [https://doi.org/10.1016/0005-2728\(90\)90204-H](https://doi.org/10.1016/0005-2728(90)90204-H)
- Bahrani H et al (2019) Preferential accumulation of glycosylated cyanidins in winter-hardy rye (*Secale cereale* L.) genotypes during cold acclimation. *Environ Exp Bot* 164:203–212. <https://doi.org/10.1016/j.envexpbot.2019.05.006>
- Dreyer A, Dietz K (2018) Reactive oxygen species and the redox-regulatory network in cold stress acclimation. *Antioxidants* 7:169. <https://doi.org/10.3390/antiox7110169>
- Fahrendorf T, Ni B, Shorrosh BS, Dixon RA (1995) Stress responses in alfalfa (*Medicago sativa* L.) XIX. Transcriptional activation of oxidative pentose phosphate pathway genes at the onset of the isoflavonoid phytoalexin response. *Plant Mol Biol* 28(5):885–900
- Fürtauer L, Nägele T (2016) Approximating the stabilization of cellular metabolism by compartmentalization. *Theory Biosci* 135:73–87. <https://doi.org/10.1007/s12064-016-0225-y>
- Fürtauer L, Weiszmann J, Weckwerth W, Nägele T (2019) Dynamics of plant metabolism during cold acclimation. *Int J Mol Sci* 20:5411
- Geigenberger P, Stitt M (1991) A futile cycle of sucrose synthesis and degradation is involved regulating partitioning between sucrose starch and respiration in cotyledons of germinating *ricinus-communis* L. Seedlings when phloem transport is inhibited. *Planta* 185:81–90
- Gibon Y, Vigeolas H, Tiessen A, Geigenberger P, Stitt M (2002) Sensitive and high throughput metabolite assays for inorganic pyrophosphate, ADPGlc, nucleotide phosphates, and glycolytic

- intermediates based on a novel enzymic cycling system. *Plant J* 30:221–235
- Gotoh E et al (2018) Chloroplast accumulation response enhances leaf photosynthesis and plant biomass production. *Plant Physiol* 178:1358–1369. <https://doi.org/10.1104/pp.18.00484>
- Gururani Mayank A, Venkatesh J, Tran LSP (2015) Regulation of photosynthesis during abiotic stress-induced photoinhibition. *Mol Plant* 8:1304–1320. <https://doi.org/10.1016/j.molp.2015.05.005>
- Henkel S, Nägele T, Hörmiller I, Sauter T, Sawodny O, Ederer M, Heyer AG (2011) A systems biology approach to analyse leaf carbohydrate metabolism in *Arabidopsis thaliana*. *EURASIP J Bioinform Syst Biol* 2011:2. <https://doi.org/10.1186/1687-4153-2011-2>
- Herrmann HA, Schwartz JM, Johnson GN (2019) Metabolic acclimation—a key to enhancing photosynthesis in changing environments? *J Exp Bot* 70:3043–3056. <https://doi.org/10.1093/jxb/erz157>
- Hoffmann MH (2002) Biogeography of *Arabidopsis thaliana* (L.) Heynh. (Brassicaceae). *J Biogeogr* 29:125–134. <https://doi.org/10.1046/j.1365-2699.2002.00647.x>
- Hue L (1981) The role of futile cycles in the regulation of carbohydrate metabolism in the liver. In: (Ed.). AM (ed) *Advances in Enzymology and Related Areas of Molecular Biology*. pp 247–331. <https://doi.org/https://doi.org/10.1002/9780470122976.ch4>
- Johnson HS (1972) Dithiothreitol: An inhibitor of glucose-6-phosphate-dehydrogenase activity in leaf extracts and isolated chloroplasts. *Planta* 106:273–277. <https://doi.org/10.1007/BF00388105>
- Kasahara M, Kagawa T, Oikawa K, Suetsugu N, Miyao M, Wada M (2002) Chloroplast avoidance movement reduces photodamage in plants. *Nature* 420:829–832. <https://doi.org/10.1038/nature01213>
- Khanal N, Bray GE, Grisnich A, Moffatt BA, Gray GR (2017) Differential mechanisms of photosynthetic acclimation to light and low temperature in *Arabidopsis* and the extremophile *Eutrema salsugineum*. *Plants* 6:32. <https://doi.org/10.3390/plants6030032>
- Kunz H-H, Zamani-Nour S, Hausler RE, Ludewig K, Schroeder JL, Malinova I, Fettek J, Flugge U-I, Gierth M (2014) Loss of cytosolic phosphoglucose isomerase affects carbohydrate metabolism in leaves and is essential for fertility of *Arabidopsis*. *Plant Physiol* 166(2):753–765
- Levitt J (1980) *Responses of plants to environmental stresses*, 2nd edn. Academic Press, New York
- Liu Y, Dang P, Liu L, He C (2019) Cold acclimation by the CBF-COR pathway in a changing climate: lessons from *Arabidopsis thaliana*. *Plant Cell Rep* 38:511–519. <https://doi.org/10.1007/s00299-019-02376-3>
- May MJ, Vernoux T, Leaver C, Montagu MV, Inze D (1998) Glutathione homeostasis in plants: implications for environmental sensing and plant development. *J Exp Bot* 49:649–667
- Nägele T, Henkel S, Hörmiller I, Sauter T, Sawodny O, Ederer M, Heyer AG (2010) Mathematical modeling of the central carbohydrate metabolism in *Arabidopsis* reveals a substantial regulatory influence of vacuolar invertase on whole plant carbon metabolism. *Plant Physiol* 153:260–272. <https://doi.org/10.1104/pp.110.154443>
- Nägele T, Heyer AG (2013) Approximating subcellular organisation of carbohydrate metabolism during cold acclimation in different natural accessions of *Arabidopsis thaliana*. *New Phytol* 198:777–787. <https://doi.org/10.1111/nph.12201>
- Nägele T, Stutz S, Hörmiller II, Heyer AG (2012) Identification of a metabolic bottleneck for cold acclimation in *Arabidopsis thaliana*. *Plant J* 72:102–114. <https://doi.org/10.1111/j.1365-313X.2012.05064.x>
- Nguyen-Quoc B, Foyer CH (2001) A role for “futile cycles” involving invertase and sucrose synthase in sucrose metabolism of tomato fruit. *J Exp Bot* 52:881–889
- Oikawa K et al (2003) Chloroplast unusual positioning1 is essential for proper chloroplast positioning. *Plant Cell* 15:2805–2815. <https://doi.org/10.1105/tpc.016428>
- Oikawa K et al (2008) Chloroplast outer envelope protein CHUP1 is essential for chloroplast anchorage to the plasma membrane and chloroplast movement. *Plant Physiol* 148:829–842. <https://doi.org/10.1104/pp.108.123075>
- Patzke K et al (2019) The plastidic sugar transporter pSuT influences flowering and affects cold responses. *Plant Physiol* 179:569–587. <https://doi.org/10.1104/pp.18.01036>
- Pons TL (2012) Interaction of temperature and irradiance effects on photosynthetic acclimation in two accessions of *Arabidopsis thaliana*. *Photosynth Res* 113(1–3):207–219
- R Core Team (2019) R: a language and environment for statistical computing. R Foundation for Statistical Computing, Vienna, Austria
- Reyes BA, Pendergast JS, Yamazaki S (2008) Mammalian peripheral circadian oscillators are temperature compensated. *J Biol Rhythms* 23:95–98. <https://doi.org/10.1177/0748730407311855>
- Reznik E, Segrè D (2010) On the stability of metabolic cycles. *J Theor Biol* 266:536–549. <https://doi.org/10.1016/j.jtbi.2010.07.023>
- RStudio Team (2019) RStudio: integrated Development for R. RStudio Inc, Boston, MA
- Ruan YL (2014) Sucrose metabolism: gateway to diverse carbon use and sugar signaling. *Annu Rev Plant Biol* 65:33–67. <https://doi.org/10.1146/annurev-arplant-050213-040251>
- Savitch LV, Barker-Astrom J, Ivanov AG, Hurry V, Oquist G, Huner NP, Gardeström P (2001) Cold acclimation of *Arabidopsis thaliana* results in incomplete recovery of photosynthetic capacity, associated with an increased reduction of the chloroplast stroma. *Planta* 214:295–303
- Schaber J, Liebermeister W, Klipp E (2009) Nested uncertainties in biochemical models. *IET Syst Biol* 3:1–9. <https://doi.org/10.1049/iet-syb:20070042>
- Scharte J, Schön H, Tjaden Z, Weis E, von Schaewen A (2009) Isoenzyme replacement of glucose-6-phosphate dehydrogenase in the cytosol improves stress tolerance in plants. *Proc Natl Acad Sci U S A* 106:8061–8066. <https://doi.org/10.1073/pnas.0812902106>
- Schmidt von Braun S, Schleiff E (2008) The chloroplast outer membrane protein CHUP1 interacts with actin and profilin. *Planta* 227:1151–1159. <https://doi.org/10.1007/s00425-007-0688-7>
- Schnarrenberger C, Oeser A (1974) Two isoenzymes of glucosephosphate isomerase from spinach leaves and their intracellular compartmentation. *Eur J Biochem* 45:77–82. <https://doi.org/10.1111/j.1432-1033.1974.tb03531.x>
- Stitt M, Lunn J, Usadel B (2010) *Arabidopsis* and primary photosynthetic metabolism—more than the icing on the cake. *Plant J* 61:1067–1091. <https://doi.org/10.1111/j.1365-313X.2010.04142.x>
- Strand A, Foyer CH, Gustafsson P, Gardeström P, Hurry V (2003) Altering flux through the sucrose biosynthesis pathway in transgenic *Arabidopsis thaliana* modifies photosynthetic acclimation at low temperatures and the development of freezing tolerance. *Plant Cell Environ* 26:523–535
- Strand A, Zrenner R, Trevanion S, Stitt M, Gustafsson P, Gardeström P (2000) Decreased expression of two key enzymes in the sucrose biosynthesis pathway, cytosolic fructose-1,6-bisphosphatase and sucrose phosphate synthase, has remarkably different consequences for photosynthetic carbon metabolism in transgenic *Arabidopsis thaliana*. *Plant J* 23:759–770. <https://doi.org/10.1046/j.1365-313x.2000.00847.x>
- Szeczowka M et al (2013) Metabolic fluxes in an illuminated *Arabidopsis* rosette. *Plant Cell* 25:694–714. <https://doi.org/10.1105/tpc.112.106989>
- Wada M (2013) Chloroplast movement. *Plant Sci* 210:177–182. <https://doi.org/10.1016/j.plantsci.2013.05.016>
- Wang L et al (2017) The inhibition of protein translation mediated by AtGCN1 is essential for cold tolerance in *Arabidopsis thaliana*. *Plant Cell Environ* 40:56–68. <https://doi.org/10.1111/pce.12826>



- Wanner LA, Junttila O (1999) Cold-induced freezing tolerance in *Arabidopsis*. *Plant Physiol* 120:391–400
- Weiszmann J, Fürtauer L, Weckwerth W, Nägele T (2018) Vacuolar sucrose cleavage prevents limitation of cytosolic carbohydrate metabolism and stabilizes photosynthesis under abiotic stress. *FEBS J* 285:4082–4098. <https://doi.org/10.1111/febs.14656>
- Wiese A et al (1999) Spinach hexokinase I is located in the outer envelope membrane of plastids. *FEBS Lett* 461:13–18
- Xin Z, Browse J (2000) Cold comfort farm: the acclimation of plants to freezing temperatures. *Plant Cell Environ* 23:893–902

**Publisher's Note** Springer Nature remains neutral with regard to jurisdictional claims in published maps and institutional affiliations.







## **9.2 Publication 2: Limitation of sucrose biosynthesis shapes carbon partitioning during plant cold acclimation**

**Kitashova A**, Adler SO, Richter AS, Eberlein S, Dziubek D, Klipp E, Nägele T (2023) Limitation of sucrose biosynthesis shapes carbon partitioning during plant cold acclimation. *Plant, Cell & Environment* 46: 464–478

Supplementary material is available at:

<https://onlinelibrary.wiley.com/doi/abs/10.1111/pce.14483>

# Limitation of sucrose biosynthesis shapes carbon partitioning during plant cold acclimation

Anastasia Kitashova<sup>1</sup>  | Stephan O. Adler<sup>2</sup> | Andreas S. Richter<sup>3</sup>  |  
Svenja Eberlein<sup>1</sup> | Dejan Dziubek<sup>1</sup> | Edda Klipp<sup>2</sup>  | Thomas Nägele<sup>1</sup> 

<sup>1</sup>Plant Evolutionary Cell Biology, Faculty of Biology, Ludwig-Maximilians-Universität München, Planegg-Martinsried, Germany

<sup>2</sup>Theoretical Biophysics, Institute of Biology, Humboldt-Universität zu Berlin, Berlin, Germany

<sup>3</sup>Institute for Biosciences, Physiology of Plant Metabolism, University of Rostock, Rostock, Germany

## Correspondence

Thomas Nägele, Plant Evolutionary Cell Biology, Faculty of Biology, Ludwig-Maximilians-Universität München, Planegg-Martinsried, Germany.  
Email: [thomas.naegele@lmu.de](mailto:thomas.naegele@lmu.de)

## Funding information

Deutsche Forschungsgemeinschaft, Grant/Award Numbers: TR175/C06, TR175/D03

## Abstract

Cold acclimation is a multigenic process by which many plant species increase their freezing tolerance. Stabilization of photosynthesis and carbohydrate metabolism plays a crucial role in cold acclimation. To study regulation of primary and secondary metabolism during cold acclimation of *Arabidopsis thaliana*, metabolic mutants with deficiencies in either starch or flavonoid metabolism were exposed to 4°C. Photosynthesis was determined together with amounts of carbohydrates, anthocyanins, organic acids and enzyme activities of the central carbohydrate metabolism. Starch deficiency was found to significantly delay soluble sugar accumulation during cold acclimation, while starch overaccumulation did not affect accumulation dynamics but resulted in lower total amounts of sucrose and glucose. Anthocyanin amounts were lowered in both starch deficient and overaccumulating mutants. Vice versa, flavonoid deficiency did not result in a changed starch amount, which suggested a unidirectional signalling link between starch and flavonoid metabolism. Mathematical modelling of carbon metabolism indicated kinetics of sucrose biosynthesis to be limiting for carbon partitioning in leaf tissue during cold exposure. Together with cold-induced dynamics of citrate, fumarate and malate amounts, this provided evidence for a central role of sucrose phosphate synthase activity in carbon partitioning between biosynthetic and dissimilatory pathways which stabilizes photosynthesis and metabolism at low temperature.

## KEYWORDS

*Arabidopsis thaliana*, carbon metabolism, cold acclimation, kinetic modelling

## 1 | INTRODUCTION

Exposing plants to a changing temperature regime has an immediate effect on cellular metabolism. If temperature drops or increases severely within a short period, for example, within minutes, a stress response is induced to counteract and prevent irreversible cell and

tissue damage (Kosová et al., 2011). If significant acute damage and death can be prevented, metabolism is adjusted to a new homeostasis within a process termed acclimation. Temperature acclimation, and, more specifically, cold acclimation, is a multigenic process which comprises and affects the expression of thousands of genes (Fowler & Thomashow, 2002; Hannah et al., 2005) and abundance of

This is an open access article under the terms of the Creative Commons Attribution-NonCommercial License, which permits use, distribution and reproduction in any medium, provided the original work is properly cited and is not used for commercial purposes.

© 2022 The Authors. *Plant, Cell & Environment* published by John Wiley & Sons Ltd.

hundreds of metabolites (Cook et al., 2004; Kaplan et al., 2004). Many plant species from temperate regions are able to acclimate to low temperature which results in increased freezing tolerance (Xin & Browse, 2000). For *Arabidopsis thaliana*, it has been shown earlier that low temperature represents an important selective pressure, which indicates the significance of cold acclimation for plant evolution and ecology (Hannah et al., 2006).

Carbohydrates are direct products of photosynthetic CO<sub>2</sub> assimilation and their metabolism needs tight regulation to stabilize photosynthetic efficiency under changing environmental conditions. Primary reactions of photosynthesis are catalysed by photosystems II and I which trap and transform light energy into redox potential energy and a proton gradient. This enables biosynthesis of NADPH and ATP, respectively, being essential for carbon fixation within the Calvin–Benson–Bassham cycle (CBBC). Stabilizing the balance within this reaction network and energy flow is essential for plant cold acclimation (Leonardos et al., 2003). Chilling temperatures between 5°C and 10°C were found to inhibit photosynthetic carbon fixation, for example, due to inactivation of regulatory thioredoxin-activated enzymes of the CBBC (Holaday et al., 1992). Such a reduced CO<sub>2</sub> fixation rate may cause a significant imbalance between light absorption and energy consumption within the CBBC (Huner et al., 1998). To prevent limitations in carbohydrate metabolism, CBBC enzymes and enzymes of the sucrose biosynthesis pathway are tightly regulated on the transcriptional, translational and protein level during cold acclimation (Nägele et al., 2012; Stitt & Hurry, 2002; Strand et al., 2003). This enables plants to significantly accumulate soluble sugars during cold exposure which have been discussed to stabilize metabolism and to have a cryoprotective function (Klotke et al., 2004; Ristic & Ashworth, 1993; Seydel et al., 2022).

In chloroplasts, triose and hexose phosphates are direct CBBC products which serve as substrates for diverse biosynthetic pathways. Starting from fructose-6-phosphate, transient leaf starch is (diurnally) biosynthesised in a sequential reaction catalysed by phosphoglucosyltransferase (PGT), phosphoglucosyltransferase (PGT), ADP-glucose pyrophosphorylase and starch synthase enzymes (Stitt & Zeeman, 2012). During the night, starch is degraded by glucan/water dikinase and phosphoglucan/water dikinase enzymes to yield glucans (Kötting et al., 2005). Glucans are substrate for amylase enzymes yielding maltose moieties. Maltose is exported to the cytosol to supply carbon metabolism (Niittylä et al., 2004; Smith et al., 2005). Previously it was discussed that, during initial cold exposure, starch amount is transiently reduced to stabilize soluble sugar concentrations (Sicher, 2011). Evidence has also been provided for a role of starch degradation in the acquisition of freezing tolerance (Yano et al., 2005). Starch degradation in chloroplasts needs activity of  $\beta$ -amylases. In *Arabidopsis*, nine *BAM* genes have been described, and expression of *BAM3* (*ct-BMY*, *BMY8*, At4g17090) was found to be induced by cold stress (Kaplan & Guy, 2004; Monroe et al., 2014). In addition, relative protein levels of *BAM3* were found to be differentially regulated in freezing

sensitive and -tolerant accessions of *A. thaliana* suggesting a central role in regulation of starch degradation during cold acclimation (Nagler et al., 2015).

Besides biosynthesis and metabolism of carbohydrates, a significant portion of plants' carbon flow may be directed through the shikimate pathway, resulting in diverse metabolic products comprising aromatic amino acids, phytohormones and secondary metabolites. The entry reaction of the shikimate pathway has been shown to be tightly regulated (Yokoyama et al., 2021). Phosphoenolpyruvate and erythrose-4-phosphate from glycolysis and pentose phosphate pathways are interconverted into chorismate which represents the precursor of tryptophan, tyrosine and phenylalanine. Phenylalanine is precursor for flavonoid biosynthesis via the phenylpropanoid pathway which is located to the cytosol. Chalcone synthase (CHS) catalyses the first committed step in flavonoid biosynthesis forming chalcone by intramolecular cyclization and aromatization of a linear phenylpropanoid tetraketide (Austin & Noel, 2003). Plants were estimated to produce several thousands of structurally different flavonoids fulfilling a huge diversity of molecular and physiological functions (Falcone Ferreyra et al., 2012; Ferreyra et al., 2021; Winkel-Shirley, 2001, 2002). The reaction product of CHS, tetrahydroxychalcone, is the substrate for naringenin synthesis, catalysed by chalcone isomerase. Naringenin represents a central precursor for subgroups of flavonoids, which comprise flavones, flavonols, flavandiols, anthocyanins and proanthocyanidins (Winkel-Shirley, 2002). Early steps of anthocyanin biosynthesis comprise the interconversion of naringenin into dihydroflavanol, catalysed by flavanone 3-hydroxylase (F3H) together with flavonoid 3'-hydroxylase (Owens et al., 2008; Shi & Xie, 2014). Enhanced dynamics of flavonoid metabolism have previously been associated with cold and freezing tolerance (Hannah et al., 2006; Korn et al., 2008; Schulz et al., 2015, 2016). Anthocyanins were suggested to have a photoprotective role at chilling temperature (Havaux & Klopstsch, 2001), and by accumulation in the vacuole they were discussed to affect osmotic potential and prevent tissue damage due to freezing (Chalker-Scott, 1999).

While a tightly regulated allocation of photosynthetically fixed carbon between pathways of primary and secondary metabolism seems essential for plant growth, development and stress response (Caretto et al., 2015), underlying metabolic regulation remains elusive. Particularly, under a changing temperature regime, thermodynamic constraints of enzyme activity and metabolic regulation result in a non-linear output of metabolic systems, that is, metabolic regulation, which prevents intuitive interpretation and hypothesis generation of experimental observations. In the present study, kinetics of carbohydrate and anthocyanin accumulation were quantitatively monitored during cold acclimation to reveal regulatory interactions between starch, sucrose and anthocyanin metabolism. Enzyme kinetic modelling was applied to study the effect of low temperature on kinetics of carbon allocation. Finally, analysis of metabolic mutants provided evidence for dynamic carbon partitioning between primary and secondary metabolism during cold acclimation.

## 2 | MATERIALS AND METHODS

### 2.1 | Plant material and growth conditions

Plants of *A. thaliana* accession Col-0 and homozygous T-DNA insertion lines *bam3* (beta-amylase 3, line SALK\_041214, locus AT4G17090), *chs* (line SALK\_020583C, locus AT5G13930), *f3h* (flavanone 3-hydroxylase, line SALK\_113904C, locus AT3G51240), as well as SNP mutant *pgm1* (plastidial PGM, TAIR stock CS3092, locus AT5G51820) were grown on a 1:1 mixture of GS90 soil and vermiculite in a climate chamber under controlled short-day conditions (8 h/16 h light/dark; 90–100  $\mu\text{mol m}^{-2} \text{s}^{-1}$ ; 22°C/16°C; 60% relative humidity). All seeds were harvested from plants grown in one batch, that is, at the same time and under same conditions. After 4 weeks, plants were shifted to a growth cabinet and grown further under long day conditions (16 h/8 h light/dark; 90–100  $\mu\text{mol m}^{-2} \text{s}^{-1}$ ; 22°C/16°C; 60% relative humidity). After 2 weeks, plants were either (i) harvested at midday, that is, 8 h of light (0 days of cold acclimation) or (ii) transferred to a cold room for cold acclimation (16 h/8 h light/dark; 90–100  $\mu\text{mol m}^{-2} \text{s}^{-1}$ ; 4°C/4°C). Cold exposed plants were harvested after 1, 3, 7 or 14 days of acclimation at midday, that is, after 8 h of light. Each sample consisted of nine leaf rosettes which were immediately frozen in liquid nitrogen, ground to a fine powder and lyophilised. The rather low to moderate photosynthetic active radiation (PAR) intensity of 90–100  $\mu\text{mol m}^{-2} \text{s}^{-1}$  was applied to minimize photoinhibition and to prevent mixed effects of cold and light acclimation. Relative proportion of UV radiation in growth chambers was 0.3 – 0.5% of total photon flux density (LICOR LI-180 Spectrometer; [www.licor.com](http://www.licor.com)).

### 2.2 | RNA extraction and qPCR analysis

Whole leaf RNA was extracted as described earlier (Oñate-Sánchez & Vicente-Carbajosa, 2008). Frozen and ground leaf material was resuspended in 300  $\mu\text{l}$  cell lysis buffer (2% [wt/vol] sodium dodecyl sulphate, 68 mM sodium citrate, 132 mM citric acid, 1 mM EDTA), 100  $\mu\text{l}$  DNA/protein precipitation solution were added (4 M NaCl, 16 mM sodium citrate, 32 mM citric acid), and samples were vortexed and incubated on ice for 10 min. Samples were centrifuged at 13 000 rpm (4°C) for 10 min, and 300  $\mu\text{l}$  of the supernatant were used to precipitate the RNA with 300  $\mu\text{l}$  isopropanol. Pellets were washed with 800  $\mu\text{l}$  75% ethanol, centrifuged and dried. The RNA was resuspended in 20–25  $\mu\text{l}$  of H<sub>2</sub>O (RNase free) and stored at –80°C until further use.

For qPCR analysis, 1–2  $\mu\text{g}$  of DNaseI (Thermo Fisher Scientific) treated RNA was transcribed into cDNA using RevertAid reverse transcriptase (Thermo Fisher Scientific) according to the manufacturer protocol. The qPCR analysis was performed in a CFX96-C1000 96-well plate thermocycler (Bio-Rad) and ChamQ Universal SYBR qPCR Master Mix (Absource) in 6  $\mu\text{l}$  reactions containing 1  $\mu\text{l}$  of diluted (1:5) cDNA. Relative gene expression was calculated using the  $2^{-\Delta\Delta\text{Ct}}$  method and SAND (AT2G28390) as the reference gene.

### 2.3 | Net photosynthesis and chlorophyll fluorescence measurements

Rates of net CO<sub>2</sub> assimilation, that is, net photosynthesis (NPS), were recorded for 1 h at midday in 15 min intervals using a WALZ GFS-3000FL system (Heinz Walz GmbH; [www.walz.com](http://www.walz.com)). Maximum quantum yield of PSII ( $F_v/F_m$ ) was determined after 10 min of dark adaptation by supplying a saturating light pulse, which was tested to be suitable for the following experimental setup. Dynamics of quantum efficiency of PSII ( $\Phi(\text{II})$ ), electron transport rate (ETR), photochemical (qP, qL), non-photochemical quenching (qN, NPQ), quantum yield of regulated energy dissipation (Y(NPQ)) and quantum yield of nonregulated energy dissipation (Y(NO)) were determined either (i) within rapid stepwise increase of PAR from 0 to 2400  $\mu\text{mol m}^{-2} \text{s}^{-1}$ ; or (ii) after 10 min of acclimation to ambient light, that is, 100  $\mu\text{mol m}^{-2} \text{s}^{-1}$ , or saturating light, that is, 1200  $\mu\text{mol m}^{-2} \text{s}^{-1}$ , using WALZ JUNIOR-PAM system (Heinz Walz GmbH; [www.walz.com](http://www.walz.com); Figure S1). NPS and chlorophyll fluorescence parameters were recorded at ambient temperature (22°C) for non-acclimated plants (0 days of acclimation) and at 4°C for cold acclimated plant (1, 3, 7 and 14 days of acclimation).

### 2.4 | Quantification of starch, soluble carbohydrates, hexose phosphates and anthocyanins

Transitory starch and soluble carbohydrates amounts were determined as described previously with slight modifications (Atanasov et al., 2020; Nägele et al., 2012). In brief, following extraction with 80% ethanol at 80°C for 30 min and short centrifugation, the supernatant was transferred to a new tube and extraction was repeated. Starch-containing pellets were incubated with 750  $\mu\text{l}$  0.5 N NaOH at 95°C for 60 min before slight acidification with 750  $\mu\text{l}$  1 M CH<sub>3</sub>COOH. Glucose units resulting from digestions with amyloglucosidase were quantified photometrically applying a coupled glucose-oxidase/peroxidase/dianisidine reaction which yielded a reaction product with a specific absorbance maximum at 540 nm.

Dried ethanol extracts were used for quantification of soluble carbohydrates, that is, glucose, fructose and sucrose. Glucose was quantified using a coupled hexokinase/glucose-6-phosphate dehydrogenase (G6PDH) assay, which yielded NADPH + H<sup>+</sup> detectable at 340 nm. For fructose quantification, PGI was added to the reaction mix after glucose amount had been detected. Sucrose concentration was determined using an anthrone reagent composed of 14.6 M H<sub>2</sub>SO<sub>4</sub> and 0.14% (wt/vol) anthrone. Samples were incubated with 30% KOH at 95°C before adding the anthrone reagent, incubating for 30 min at 40°C and detecting absorbance at 620 nm.

Glucose 6-phosphate (G6P) and fructose 6-phosphate (F6P) were quantified as described before (Gibon et al., 2002). G6P and F6P were extracted using trichloroacetic acid (TCA) in diethyl ether (16% wt/vol), washed with 16% (wt/vol) TCA in 5 mM EGTA and neutralised with 5 M KOH/1 M triethanolamine. G6P and F6P

concentration was determined using an enzymatic cycling assay, catalysing interconversion of hexose-phosphates into NADPH + H<sup>+</sup>, which was photometrically determined in a reaction with formazan dye at 570 nm.

Anthocyanins were quantified as described before (Atanasov et al., 2020). In brief, ground plant material was suspended in 1 N HCl and incubated at 25°C for 30 min while shaking. Following short centrifugation, supernatant was transferred to a new tube, and extraction was repeated at 80°C for 30 min. After a second centrifugation, supernatants were pooled and the amount of anthocyanins was quantified photometrically at 540 nm. Total anthocyanin concentration was normalised to pelargonidin standards (C<sub>15</sub>).

## 2.5 | Quantification of enzyme activities

Activities of sucrose phosphate synthase (SPS), glucokinase, fructokinase, invertase and PGI were determined under substrate saturation ( $v_{\max}$ ) at 4°C and 22°C.

Maximal activity of SPS was determined as described earlier (Nägele et al., 2012). Ground plant material was suspended in extraction buffer containing 50 mM HEPES-KOH (pH 7.5), 10 mM MgCl<sub>2</sub>, 1 mM EDTA, 2.5 mM DTT, 10% (vol/vol) glycerine and 0.1% (vol/vol) Triton X-100. After incubation on ice and centrifugation, the supernatant was incubated for 30 min at 22°C or 50 min at 4°C with reaction mixture consisting of 50 mM HEPES-KOH (pH 7.5), 15 mM MgCl<sub>2</sub>, 2.5 mM DTT, 35 mM UDP-glucose, 35 mM F6P and 140 mM G6P. The reaction was stopped by adding 30% KOH and heating samples to 95°C. Sucrose concentration was detected in the anthrone assay as described above.

Neutral (nINV) and acidic (aINV) invertase activities were quantified as described previously with slight modification (Nägele et al., 2012). Ground plant material was suspended in 50 mM HEPES-KOH (pH 7.5), 5 mM MgCl<sub>2</sub>, 2 mM EDTA, 1 mM phenylmethylsulfonylfluoride, 1 mM DTT, 10% (vol/vol) glycerine and 0.1% (vol/vol) Triton X-100 buffer. After incubation on ice and centrifugation, supernatants were desalted using Sephadex G-25 Medium. Activity of nINV was determined using a reaction buffer with pH 7.5 (20 mM HEPES-KOH, 100 mM sucrose), aINV activity was determined at pH 4.7 (20 mM sodium acetate, 100 mM sucrose). After incubation of the reaction mixture at 22°C or 4°C, reaction was stopped by heating to 95°C, and glucose moieties were photometrically determined with a coupled glucoseoxidase/peroxidase/dianisidine reaction to yield a reaction product with specific absorbance maximum at 540 nm.

Activities of gluco- and fructokinase (GLCK, FRCK) were determined as described before with slight modification (Wiese et al., 1999). Following suspension of ground plant material in extraction buffer containing 50 mM Tris-HCl (pH 8.0), 0.5 mM MgCl<sub>2</sub>, 1 mM EDTA, 1 mM DTT and 1% (vol/vol) Triton X-100, samples were incubated on ice and then centrifuged. The supernatant was mixed with reaction mix containing 100 mM HEPES-KOH

(pH 7.5), 10 mM MgCl<sub>2</sub>, 2 mM ATP, 1 mM NADP<sup>+</sup>, 0.5 U G6PDH and either 5 mM glucose for glucokinase measurement or 5 mM fructose for fructokinase measurement. Produced NADPH was recorded photometrically at 340 nm for 20 min for measurements at 22°C, and for 60 min for measurements at 4°C. Activities were derived from slopes of absorbances.

PGI maximal activity was determined as described before (Kitashova et al., 2021). Ground plant material was suspended in extraction buffer containing 50 mM Tris-HCl (pH 8.0), 0.5 mM MgCl<sub>2</sub>, 1 mM EDTA, 1 mM DTT and 1% (vol/vol) Triton X-100. Following incubation on ice and centrifugation, supernatants were mixed with 100 mM HEPES-KOH (pH 7.5), 10 mM MgCl<sub>2</sub>, 1 mM NADP<sup>+</sup> and 0.5 U G6PDH. After addition of 50 mM F6P slopes of NADPH + H<sup>+</sup> were recorded photometrically at 340 nm for 10 min for quantifying  $v_{\max}$  22°C, and for 45 min for quantification at 4°C.

Total amylase (AMY) activity was measured at 22°C following the SIGMA-ALDRICH Amylase Activity Assay Kit protocol, catalogue number MAK009 ([www.sigmaldrich.com](http://www.sigmaldrich.com)). Amylase was extracted with Amylase Assay Buffer on ice and after short centrifugation it was mixed with the Master Reaction Mix. Absorbance at 405 nm was recorded every minute for 15 min.

Activation energy ( $E_a$ ) was determined from the slope ( $-E_a/R$ ;  $R$  is the gas constant) of a linear graph describing natural logarithm of  $v_{\max}$  ( $\ln v_{\max}$ ) as a function of inverse temperature ( $1/T$ ). This was based on a logarithmic conversion of the Arrhenius equation (Arrhenius, 1889), that is,  $\ln v_{\max} = (-E_a/R) \times (1/T) + \ln A$  where the constant  $A$  represents the probability of reaction (Bisswanger, 2008).

## 2.6 | Quantification of organic acids

Organic acids citrate, fumarate and malate were extracted from freeze-dried plant material using hot water and incubating samples at 95°C for 15 min. After short centrifugation, supernatants were used for organic acid amount quantification with SIGMA-ALDRICH Assay Kits (catalogue numbers MAK057, MAK060 and MAK067). Citrate was quantified by incubating the supernatant with Citrate Enzyme Mix, Citrate Developer and Probe Solution in Citrate Assay Buffer in darkness at 22°C for 30 min and recording absorbance at 570 nm. Fumarate concentration was estimated after incubating the supernatant with the Fumarate Enzyme Mix and Fumarate Enzyme Mix in Fumarate Assay Buffer in darkness at 22°C for 30 min and measuring absorbance at 450 nm. Malate amount was detected after incubating the supernatant with the Malate Enzyme Mix and WST Substrate Mix in Malate Assay Buffer in darkness at 37°C for 30 min and measuring absorbance at 450 nm.

## 2.7 | Statistics and mathematical modelling

Statistical data evaluation was done using the free software environment R Version 3.6.2 ([www.r-project.org](http://www.r-project.org)) (R Core Team 2019) and RStudio Version 1.2.5033 ([www.rstudio.com](http://www.rstudio.com)) (RStudio

Team 2019). Mathematical modelling was performed in MATLAB Version 9.10.0.1739362 (R2021a) ([www.mathworks.com](http://www.mathworks.com)) with the toolbox IQM Tools developed by IntiQuan ([www.intiquan.com](http://www.intiquan.com)). Parameter estimation was performed applying a particle swarm pattern search method for bound constrained global optimization (Vaz & Vicente, 2007). The cost function (also: objective function)  $f(z)$  quantified the discrepancy between simulated and experimental metabolite amounts and was minimized within the optimization problem  $\min_{z \in \mathbb{R}^n} f(z)$ ,  $z \in \Omega$ , with  $\Omega = \{z \in \mathbb{R}^n : l \leq z \leq u\}$ .

For model simulations of cold exposed plants,  $v_{\max}$  quantified at 4°C was used. Kinetic parameters not experimentally quantified in the present study, that is,  $K_M$  and  $K_i$  values, were derived from literature, for example, Kitashova et al. (2021), Nägele et al. (2012), Weiszmann et al. (2018).

A graphical illustration of the mathematical model describing the central carbohydrate metabolism is provided (Figure 1), and Figure SII extended this model by an additional F6P consumption pathway, termed  $r_2$ . The model was based on a system of ordinary differential equations which is described in detail in the supplements (Tables SI and SII). Rates of net photosynthesis ( $rNPS$ ) were calculated as the average rate of carbon uptake at midday, that is, after 8 h of light.

Starch was assumed to be synthesised with a constant average rate ( $rSTAsyn$ ) during the first 8 h of light which finally resulted in the quantified amount of non-acclimated plants (0 day). For cold-exposed plants, the net rate of starch biosynthesis was calculated as the difference of starch amount between the day considered and the preceding sampling time point. This revealed the net flux of starch within the system between two sampling time points, that is, for Day 1 at 4°C:  $([starch_{\text{amount},1d} - starch_{\text{amount},0d}]/24 \text{ h})$ , for Day 3 at 4°C:

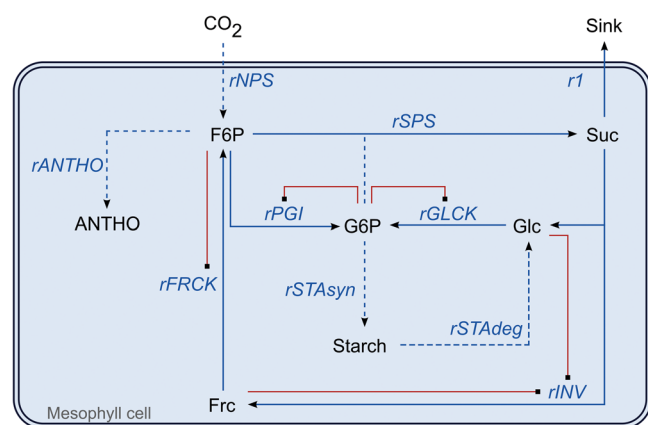


**FIGURE 1** Graphical representation of the central carbohydrate metabolism. Blue arrows represent enzyme reactions, red lines represent inhibition. F6P, fructose-6-phosphate; G6P, glucose-6-phosphate; ANThO, anthocyanins; Glc, glucose; Frc, fructose; Suc, sucrose;  $rNPS$ , rate of net photosynthesis;  $rANThO$ , rate of anthocyanin biosynthesis;  $rSTAsyn$ , rate of starch biosynthesis;  $rSTAdeg$ , rate of starch degradation;  $rSps$ , rate of sucrose phosphate synthase;  $rPgl$ , rate of phosphoglucosomerase;  $rINV$ , rate of invertase;  $rGLCK$ , rate of glucokinase;  $rFRCK$ , rate of fructokinase;  $r_1$ , rate of sucrose export to sinks.

$([starch_{\text{amount},3d} - starch_{\text{amount},1d}]/48 \text{ h})$ , and so on. Also, rates of anthocyanin accumulation ( $rANThO$ ) were calculated as change in net concentration per day.

Models of all genotypes and acclimation time points are provided in SBML format in the supplements (File SBML models). Models with a suffix "exp2" indicate extended model structures comprising a second export rate  $r_2$  (see explanation above).

### 3 | RESULTS

#### 3.1 | Photosynthetic activity during cold acclimation

Chlorophyll fluorescent parameters and  $rNPS$  were quantified to reveal effects of mutation in starch or flavonoid metabolism during cold acclimation (Figures 2 and 3). Generally, cold exposure resulted in a significant reduction of maximum quantum yield of PSII ( $F_v/F_m$ ), ETR, effective PSII yield ( $\Phi(II)$ ) and photochemical quenching ( $qP$ ,  $qL$ ; Figures 2 and SIII; Table SIIIA). Only in the  $f3h$  mutant, a slight decrease of  $F_v/F_m$  was observed from 1 to 3 days of cold acclimation, which recovered again to values higher at 14 days than after 7 days of acclimation (Figure 2). In  $bam3$ ,  $F_v/F_m$  tended to increase during 14 days at 4°C after a significant drop at Day 1, while  $pgm1$  had slightly lower  $F_v/F_m$  during the full acclimation periods compared to all other genotypes.

Rapid light curves were recorded to quantify the effect of rapidly increasing light intensities under low temperature on photosynthetic efficiencies (Figures SIII and SIV). Here, quantum yield of nonregulated energy dissipation ( $Y(NO)$ ), a measure for negative effects of cold on photochemical energy conversion, was significantly increased in all cold-acclimated plants (Figure SIV; Table SIIIA). In addition to rapid light curve measurements, chlorophyll fluorescence was also monitored in steady state conditions after acclimation to ambient and high/saturating light, that is, 100 and 1200  $\mu E$ , respectively (Figure SV; Table SIIIB). Under saturating light, fluctuation of  $qN$ ,  $NPQ$  and  $Y(NPQ)$  was more pronounced in mutants than in Col-0 between 1 and 7 days of cold acclimation (Figure SV). Finally, after

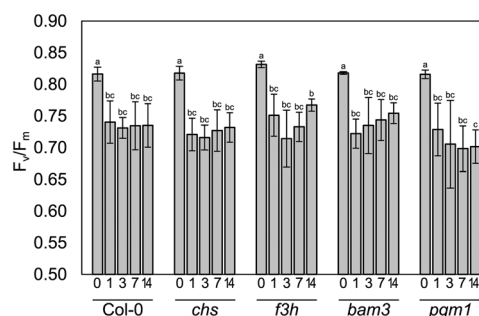


**FIGURE 2** Maximum quantum yield of PSII in Col-0, *chs*, *f3h*, *bam3* and *pgm1* after 0, 1, 3, 7 and 14 days at 4°C. Bars represent means  $\pm$  standard deviation, letters indicate significantly different groups (ANOVA with Tukey HSD,  $p < 0.05$ ;  $n \geq 5$ ).



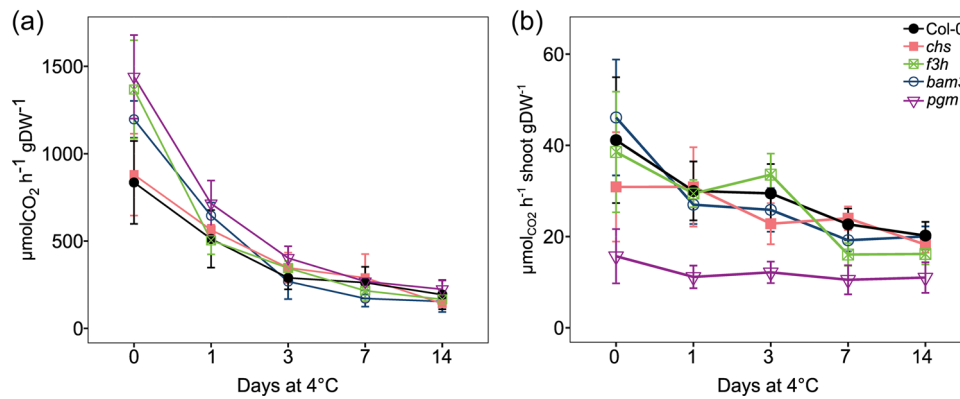


**FIGURE 3** (a) Net CO<sub>2</sub> assimilation rates normalised to 1 g dry weight, and (b) net CO<sub>2</sub> assimilation rates of whole plant shoots in Col-0, *chs*, *f3h*, *bam3* and *pgm1* at 0, 1, 3, 7 and 14 day of cold acclimation. ● (black) represents Col-0; □ (pink): *chs*; × (green): *f3h*; ○ (blue): *bam3*; ▽ (purple): *pgm1*. Vertical bars represent standard deviation,  $n > 3$ . [Color figure can be viewed at [wileyonlinelibrary.com](http://wileyonlinelibrary.com)]

14 days, qN, NPQ and Y(NPQ) reached higher values in Col-0 than in *chs*, *f3h*, *bam3* and *pgm1*.

Rates of net CO<sub>2</sub> fixation normalised to (1 g) dry weight were significantly and immediately decreasing during cold exposure (Figure 3a). Despite differences in non-acclimated plants (Table SIIIA), all mutants had wild-type-like assimilation rates during cold acclimation. Interestingly, when normalised to the dry weight of the whole plant shoot, the cold-induced drop of net CO<sub>2</sub> assimilation rates was less pronounced, or even absent in *chs* (Figure 3b). In *pgm1*, shoot-normalised CO<sub>2</sub> assimilation rates were significantly lower than in Col-0 before and during cold exposure.

Quantifying fresh weight and dry weight of whole plant shoots during the cold acclimation period revealed different growth dynamics of genotypes (Figures SVI and SVII). As expected, dwarf *pgm1* plants had significantly lower shoot fresh and dry weight than all other genotypes but increased its shoot dry weight four- to fivefold within 14 days at 4°C. While fresh and dry weight were significantly positively correlated in Col-0 ( $R = 0.76$ ,  $p = 1.5e-07$ ), flavonoid-deficient mutants *f3h* and *chs* showed even more significant and stronger correlation of fresh and dry weight during cold acclimation (*f3h*:  $R = 0.86$ ,  $p = 1.1e-09$ ; *chs*:  $R = 0.91$ ,  $p = 1.8e-13$ ; Figure SVII).

### 3.2 | Dynamics of central carbohydrates and anthocyanins during cold acclimation

In plants of *f3h* and *chs* mutants, neither anthocyanins nor transcripts of the respective gene were accumulating during cold exposure (Figures 4A and SVIII; Table SIV). In plants of *bam3* and *pgm1*, anthocyanin dynamics were lowered at Days 7 and 14 at 4°C when compared to Col-0 (Figure 4A). Anthocyanin amount in Col-0 increased significantly by almost sixfold between 3 and 7 days at 4°C and dropped again significantly until 14 days of cold exposure. In plants of *bam3*, anthocyanins also increased strongest between 3 and 7 days in the cold but continued accumulating until 14 days at 4°C

reaching a final amount of ~15 μmol pelargonidin g DW<sup>-1</sup>, which was ~75% of the wild-type amount (~20 μmol pelargonidin g DW<sup>-1</sup>). In *pgm1*, anthocyanin amount peaked at Day 7 in the cold to an amount of ~15 μmol pelargonidin g DW<sup>-1</sup>, which was approximately 50% of wild-type amount before it dropped again slightly until 14 days at 4°C.

Starch dynamics during cold exposure were similar across all tested genotypes except for *pgm1*, which was starch deficient (Figure 4b). Following a slight drop during the first day at 4°C, starch of Col-0, *f3h* and *chs* accumulated to three- to fourfold higher amounts until Day 7 in the cold compared to  $t(0)$ , before slightly dropping at Day 14. Plants of *bam3* were observed to continuously accumulate starch during cold exposure and the final amount was about 1.5× higher than in Col-0 (Figure 4b). Sucrose amount significantly increased in all genotypes during the first 3 days at 4°C before it dropped significantly until Day 14 (Figure 4c). In *f3h* and *bam3*, sucrose amount increased slightly between 7 and 14 days in the cold, while it constantly decreased in *pgm1* after peaking at Day 3. While at 22°C (0 day) *pgm1* had almost double amount of sucrose, its cold-induced accumulation was delayed and resulted in a similar amount like in Col-0 after 14 days at 4°C (Figure 4c).

Similar to sucrose, also glucose and fructose amounts strongly increased during the first 3 days of cold exposure before it dropped again significantly until 14 days at 4°C (Figure 5a,b). In *chs* and *pgm1*, accumulation of glucose was delayed and reached its peak amount on day 7 at 4°C, which was, however, significantly lower than in Col-0 (Figure 5a). In *pgm1*, also fructose accumulation was delayed compared to Col-0, reaching a maximum after 7 days in the cold (Figure 5b).

Phosphorylation products of free hexoses, that is, glucose-6-phosphate (G6P) and fructose-6-phosphate (F6P), accumulated during the early phase of cold exposure (1–3 days) and particularly G6P stabilized quickly to a new homeostatic amount (Figure 5c,d). Flavonoid biosynthesis mutants *chs* and *f3h* accumulated slightly higher amounts of G6P at Day 1 in the cold, while *bam3* did not differ significantly from Col-0 (Figure 5c). Starch deficient *pgm1*, however,

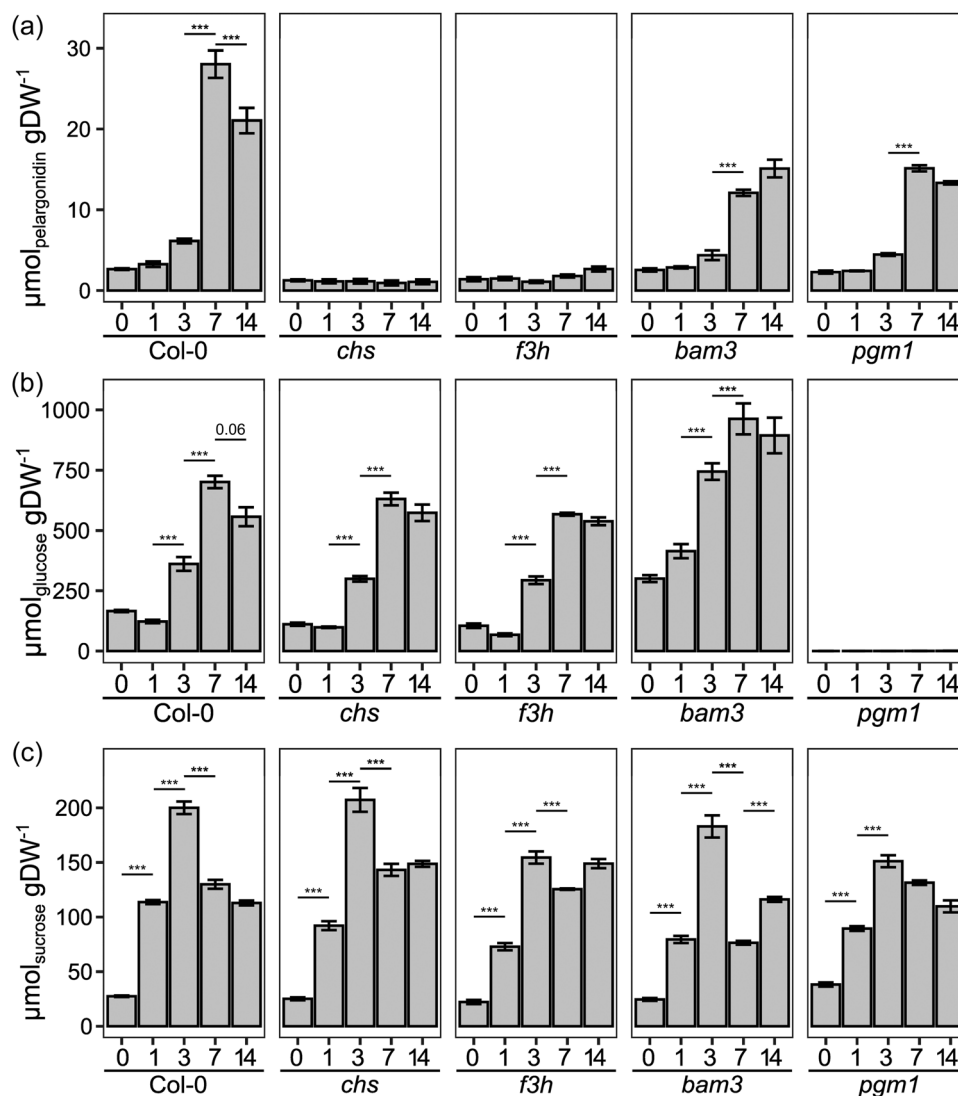


**FIGURE 4** (a) Anthocyanin, (b) starch, and (c) sucrose dynamics in Col-0, *chs*, *f3h*, *bam3* and *pgm1* at 0, 1, 3, 7 and 14 days of cold acclimation. Bars represent means  $\pm$  SD. Asterisks indicate significant difference between consecutive days within one genotype: \*\*\* $p < 0.001$ ; \*\* $p < 0.01$ ; \* $p < 0.05$  (ANOVA with Tukey HSD,  $n \geq 5$ ).

showed the strongest accumulation of both G6P and F6P resulting in a  $\sim 3.5$ -fold increase of G6P and approximately sevenfold increase in F6P after the first day of cold exposure (Figure 5c,d).

### 3.3 | Starch deficiency increases enzyme activities in central carbohydrate metabolism during cold acclimation

Maximum enzyme activity under substrate saturation ( $v_{\text{max}}$ ) was quantified at both 22°C and 4°C to compare (i) regulatory dynamics referencing to ambient temperature (22°C; Figure 6), and (ii) to estimate maximum in vivo flux capacities during cold exposure (4°C; Figure SIX). Both  $v_{\text{max}}$  of glucokinase (GLCK) and fructokinase (FRCK) were found to be increased during cold exposure in Col-0 and *bam3* while remaining constant or even decreasing in *f3h* and *chs*,

respectively (Figure 6a,b). In *pgm1*, GLCK activity remained constant and FRCK activity significantly increased almost twofold after 14 days at 4°C (Figure 6b).

In Col-0 and *pgm1*,  $v_{\text{max}}$  of PGI increased during the first day of cold exposure while it remained constant in all other genotypes (Figure 6c). After 3–7 days at 4°C,  $v_{\text{max}}$  stabilized to a similar value as before cold exposure in all genotypes except for *pgm1* which showed a significant  $\sim 1.6$ -fold increase until 14 days of cold exposure.

Compared to Col-0, all analysed mutants showed a significantly higher  $v_{\text{max}}$  of SPS at ambient growth conditions (0 day 4°C; Figure 6d). Low temperature induced an increase of  $v_{\text{max}}$  in Col-0 and *pgm1*, which resulted in a  $\sim 1.5$ -fold increased SPS capacity after 14 days at 4°C in both genotypes. However, absolute activity in *pgm1* was constantly higher (approximately twofold) than in Col-0. In *bam3*, *chs* and *f3h*, cold induced a decrease in  $v_{\text{max}}$  of SPS, resulting in wild-type-like activity after 7–14 days of cold exposure (Figure 6d).

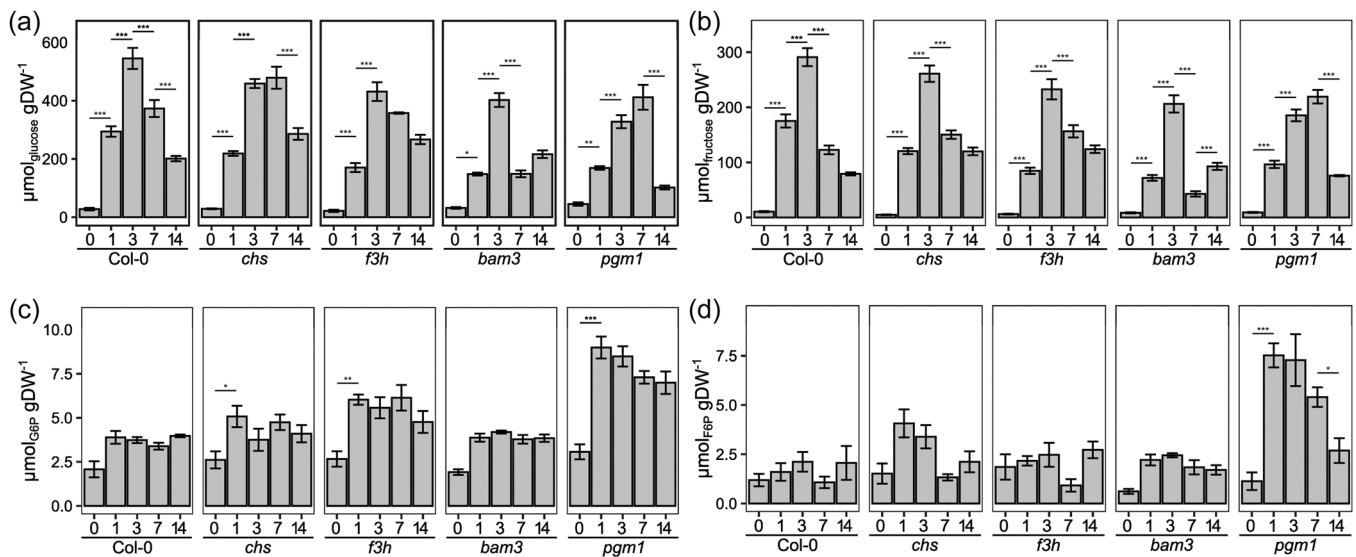


**FIGURE 5** (a) Glucose, (b) fructose, (c) glucose-6-phosphate (G6P) and (d) fructose-6-phosphate (F6P) dynamics in Col-0, *chs*, *f3h*, *bam3* and *pgm1* at 0, 1, 3, 7 and 14 days of cold acclimation. Bars represent means  $\pm$  SD. Asterisks indicate significant difference between consecutive days within one genotype: \*\*\* $p < 0.001$ ; \*\* $p < 0.01$ ; \* $p < 0.05$  (ANOVA with Tukey HSD,  $n \geq 5$ ).

As observed for SPS, also  $v_{\text{max}}$  of acidic (aINV) and neutral (nINV) invertase was found to be higher in metabolic mutants than in Col-0 before and, partially, also during cold exposure (Figure 6e,f). After 14 days at 4°C,  $v_{\text{max}}$  of aINV was similar to Col-0 in all mutants (Figure 6e). For nINV, a similar trend was observed but *pgm1* and *f3h* had higher activities than the other mutants while no strong dynamics was found in Col-0, *chs* and *bam3* (Figure 6f).

Total amylase (AMY) activity quantification showed a fast cold-induced increase in all genotypes except for *bam3*, and the strongest dynamics was observed in Col-0 which reached a peak value already after 1 day at 4°C (Figure 6g). Prolonged cold exposure for 7 days resulted in decreased AMY activity in Col-0, *chs* and *f3h*. Starch deficient *pgm1* displayed a delayed increase of AMY  $v_{\text{max}}$  reaching wild-type-like levels after 7 days. In plants of *bam3*, total AMY activity was found to be significantly lower than in Col-0 before cold acclimation (Table SV) and displayed reduced dynamics in total AMY activity during cold exposure.

Across all genotypes, maximum enzyme activities of PGI, SPS and aINV, quantified at 22°C, positively correlated with activities quantified at 4°C ( $p < 0.05$ , Pearson correlation with Benjamini–Hochberg  $p$  value adjustment; Figure SIX). In contrast, for GLCK, FRCK and nINV measurements at 22°C and 4°C were not observed to correlate, which suggested differential, and enzyme-specific, thermodynamic constraints. To systematically study temperature dependencies of (maximal) reaction rates,  $v_{\text{max}}$  of GLCK, FRCK, PGI, SPS, aINV and nINV were quantified at 4°C, 8°C, 16°C and 22°C (i.e., 277.15, 281.15, 289.15 and 295.15 K) for non-acclimated Col-0 (Figure 7). Applying logarithmic conversion of the Arrhenius equation (see Section 2 for details) revealed activation energies,  $E_a$ , within an overall physiologically feasible range (e.g., for comparison: literature value of  $E_a$  for invertase [unspecific], 40–50 kJ mol $^{-1}$ ; Bisswanger, 2008). Notably, PGI and aINV regression could not

successfully reproduce all experimental observations both over-estimating  $v_{\text{max}}$  at 16°C, that is, 289.15 K (Figure 7c,e).

### 3.4 | Parameter optimization of a kinetic model reveals differential cold-induced metabolic reprogramming

To quantitatively integrate net CO $_2$  assimilation rates, metabolite concentrations and enzyme activities, a kinetic model was developed comprising carbon input and output functions, starch and sugar metabolism as well as carbon export for secondary metabolism, that is, biosynthesis of anthocyanins (see Figure 1; Table SI; Supporting Information SBML model files). For each sampling time point of the experimental setup, models were optimized to simulate steady state metabolite concentrations being constrained by the input function ( $r_{\text{NPS}}$ ), enzyme parameters ( $v_{\text{max}}$ ,  $K_m$ ,  $K_i$ ), rates of starch biosynthesis and degradation ( $r_{\text{STAsyn}}$ ,  $r_{\text{STAdeg}}$ ) as well as net anthocyanin biosynthesis ( $r_{\text{ANTHO}}$ ). Parameter optimization was evaluated by a cost function quantifying the (squared) error between simulated and experimentally quantified metabolite concentrations.

While the model structure could explain steady states in all genotypes before cold exposure (Day 0) with a low-valued cost function ( $< 1 \times 10^{-9}$ ), the first day at 4°C could not be simulated within the experimentally observed standard deviations of both metabolite concentrations and enzyme parameters in neither genotype (cost function value  $> 1 \times 10^5$ ; Figures 8a,b and SX). After 3 days at 4°C, parameter optimization for the *pgm1* model was successful again yielding simulations which reflected metabolite concentrations with a low cost function value (Figure 8b). For all other genotypes, parameter optimization was less successful until 7d (*bam3*) and 14 d (Col-0, *chs*, *f3h*), respectively.

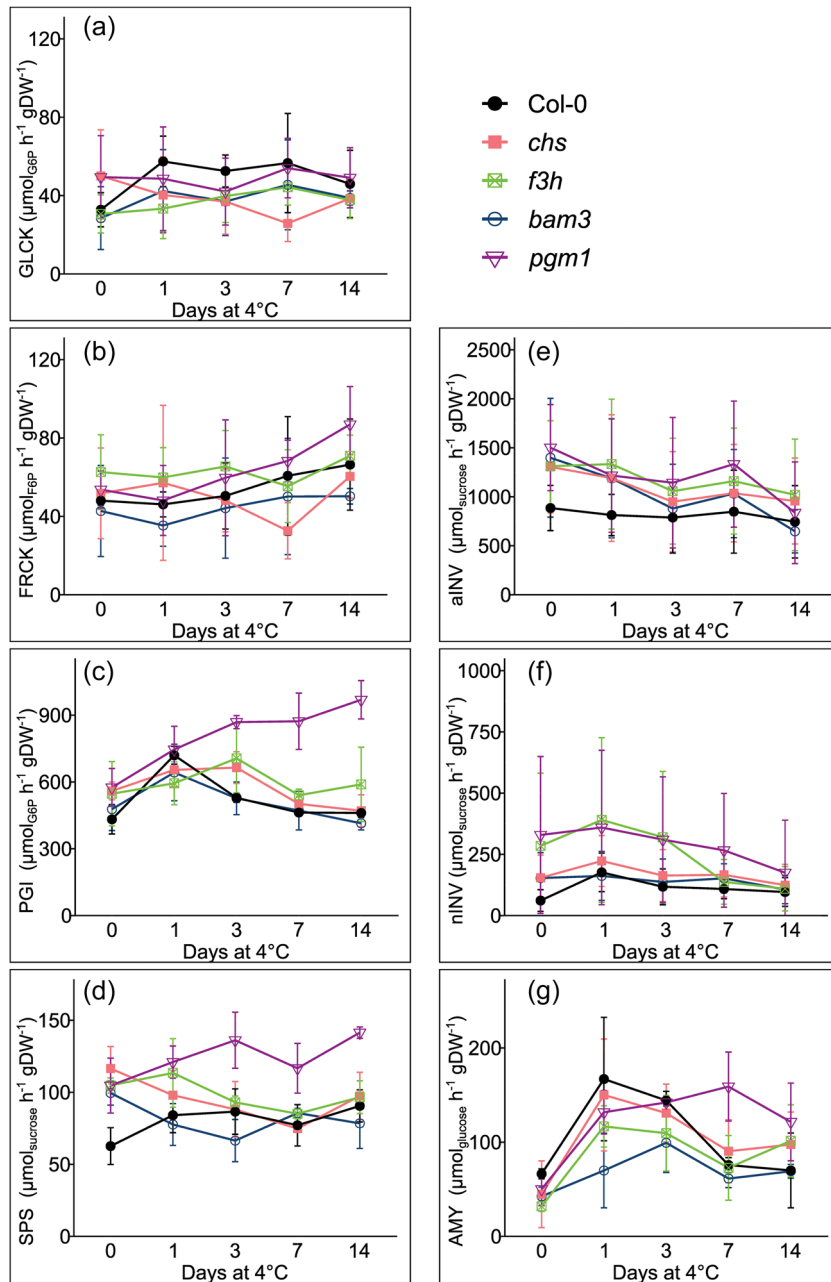


**FIGURE 6** Maximum enzyme activities ( $v_{max}$ ) at ambient temperature (22°C). (a) Glucokinase, GLCK; (b) fructokinase, FRCK; (c) phosphoglucosomerase, PGI; (d) sucrose-phosphate synthase, SPS; (e) acidic invertase, aINV; (f) neutral invertase, nINV; (g) amylase, AMY. ● (black) represents Col-0; ■ (pink): *chs*; ☒ (green): *f3h*; ○ (blue): *bam3*; ▽ (purple): *pgm1*. Vertical bars represent standard deviation,  $n \geq 5$ . [Color figure can be viewed at [wileyonlinelibrary.com](https://onlinelibrary.wiley.com/doi/10.1111/pce.14483)]

Comparison of parameter sets and optimization boundaries indicated a significant limitation of model solutions during cold acclimation by SPS-catalysed sucrose biosynthesis (Table SIV). In model simulations, sucrose amount was significantly lower than levels observed in experiments which suggested an unbalanced sucrose biosynthesis and sucrose cleavage or export to other pathways and/or organs (Figure SX: Days 1, 3 and 7). To overcome this limitation of parameter optimization, an additional (metabolic) sink was introduced representing any flux of F6P consumption which might result in other products than sucrose or starch, for example, organic and amino acids, or might supply respiration (Figure SII; Table SII; Supporting Information SBML model files). This structural change of the model improved model simulations and could successfully recover the simulation quality of experimental data, that is, lower the cost function values (Figure SXI; Table SVII). Based on previous

reports which showed that, under 4°C, organic acids like malate or fumarate significantly accumulate, also during initial hours of cold exposure (Dyson et al., 2016), amounts of citrate, malate and fumarate were determined to indicate whether analysed genotypes possess a similar and plausible range of organic acid concentrations (Figure SXII). While citrate amount fluctuated around the level of non-acclimated plants, fumarate and malate dynamics was affected by low temperature in all genotypes. Malate accumulated in all genotypes until Day 14 of cold acclimation, and most pronounced increase was observed in *f3h*, *bam3* and *pgm1*. In Col-0, the fumarate level under control conditions was higher than in the metabolic mutants, but its amount decreased significantly during cold acclimation. In *chs*, *f3h* and *bam3*, only slight dynamics of fumarate amount was observed during cold acclimation. Related to rates of net  $\text{CO}_2$  assimilation, malate, fumarate and citrate

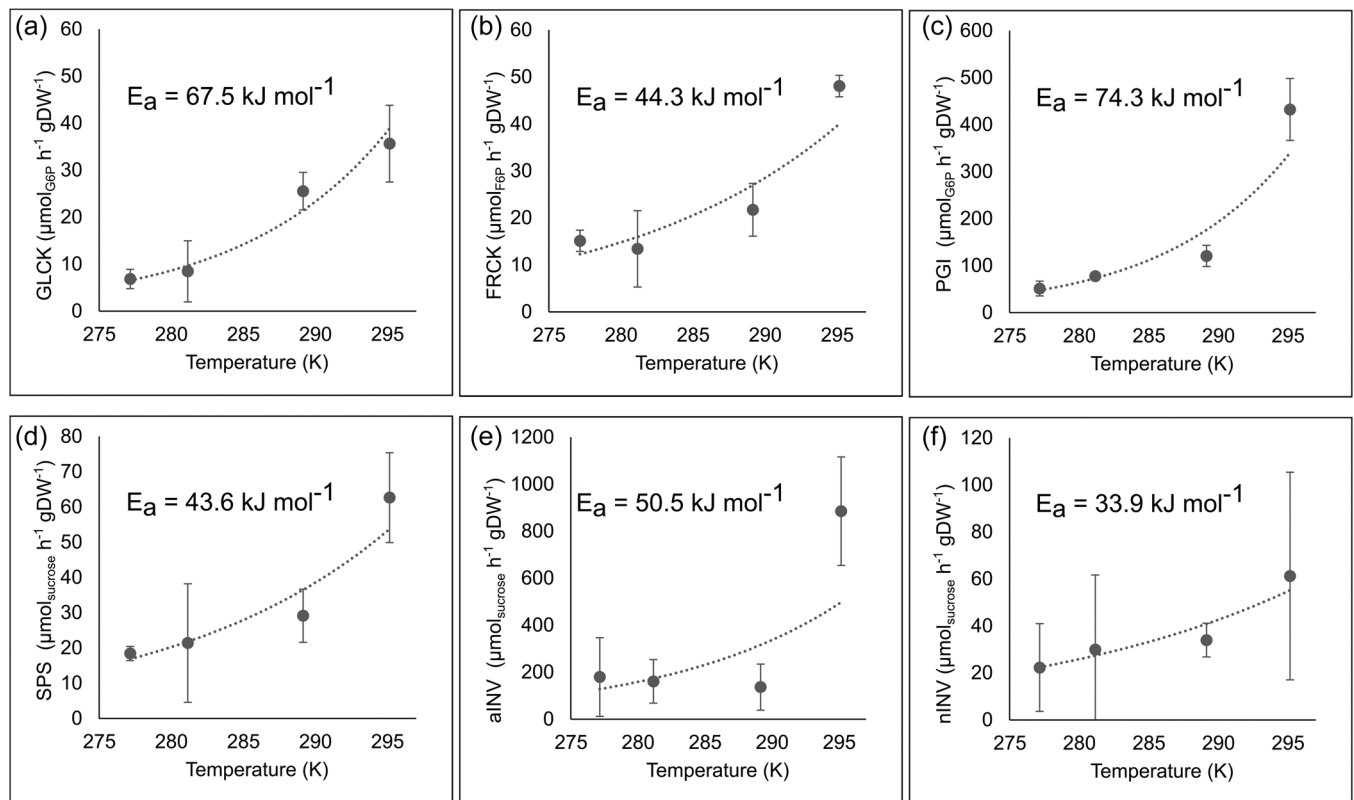


**FIGURE 7** Temperature-dependency of maximum enzyme activities ( $v_{max}$ ). (a) Glucokinase, GLCK; (b) fructokinase, FRCK; (c) phosphoglucoisomerase, PGI; (d) sucrose-phosphate synthase, SPS; (e) acidic invertase, aINV; (f) neutral invertase, nINV. Dashed line: exponential interpolation; vertical bars: standard deviation,  $n \geq 3$ ;  $E_a$ : the activation energy. All measurements were performed with non-cold acclimated plants of Col-0.

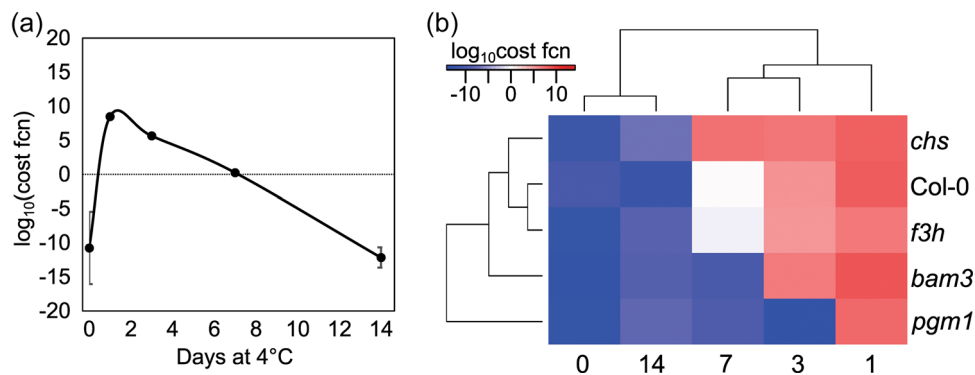


**FIGURE 8** (a) Common logarithm of cost function (cost fcn) of an optimized kinetic model for Col-0 as a function of cold acclimation period. Shown are means  $\pm$  standard deviation ( $n = 15$ ). (b) Hierarchical cluster analysis of mean cost functions (cost fcn) of optimized models (mean values of 15 global optimization runs). The  $\log_{10}$  values of cost functions are displayed in a heatmap and relationships between genotypes and days of acclimation are represented in a dendrogram based on Euclidean distances. [Color figure can be viewed at [wileyonlinelibrary.com](https://onlinelibrary.wiley.com/terms-and-conditions)]

accumulation was more pronounced in these three mutants than in Col-0 (Figure 9). In plants of starch deficient *pgm1* mutants, the fumarate amount increased twofold after 14 days of cold acclimation. In summary, cold-induced dynamics of quantified organic acid amount was found to be heterogeneous across all tested genotypes. The strongest increase of fumarate and malate amount between 0 and 14 days at 4°C was observed for starch deficient *pgm1* plants.

## 4 | DISCUSSION

Exposing plants of *Arabidopsis*, and many other species, to low, but nonfreezing temperature induces a multigenic process termed cold acclimation (Thomashow, 2010). Cold is perceived by sensing and signalling cascades which affect gene expression and metabolic regulation on various levels (Knight & Knight, 2012; Plieth et al., 1999;

Xin & Browse, 2000). Photosynthetic CO<sub>2</sub> uptake and metabolism of carbohydrates are directly affected by low temperature. As previously observed (Savitch et al., 2001), also in the present study cold exposure resulted in a decrease of  $F_v/F_m$  and net CO<sub>2</sub> assimilation rates while only minor differences were observed between analysed metabolic mutants (see Figures 2 and 3). This leads to the conclusion that, under conditions used in this study, neither starch deficiency in *pgm1* nor starch overaccumulation in *bam3* nor deficiency in anthocyanin accumulation (*chs*, *f3h*) have a significant impact on photosynthesis during cold acclimation. While for *pgm1* this is in line with previous findings (Sicher, 2011), such observation may only be valid under similar growth conditions with a low or mediate photosynthetic photon flux density (PPFD) of 100  $\mu\text{mol photons m}^{-2}\text{s}^{-1}$ . Particularly, anthocyanins accumulate only in the cold if

(visible) light intensity or UVB radiation exceeds a certain threshold (Chalker-Scott, 1999). Carbon fixation within the CBBC results in sugar phosphates which are substrate for biosynthetic pathways of primary and secondary metabolism. While cold exposure typically induces both accumulation of carbohydrates and secondary metabolites (Doerfler et al., 2013), it remains unclear how carbon allocation into primary and secondary metabolism is regulated, and to which extend these two carbon flux branches depend on each other. Comparison of starch and anthocyanin amounts across all genotypes revealed a significant impact of both starch deficiency and overaccumulation on the capacity for anthocyanin accumulation, which was lower in both *pgm1* and *bam3* compared to Col-0 after 7 and 14 days of cold acclimation. In contrast, deficiencies in the anthocyanin pathway resulted in wild-type like starch amount (see Figure 4).

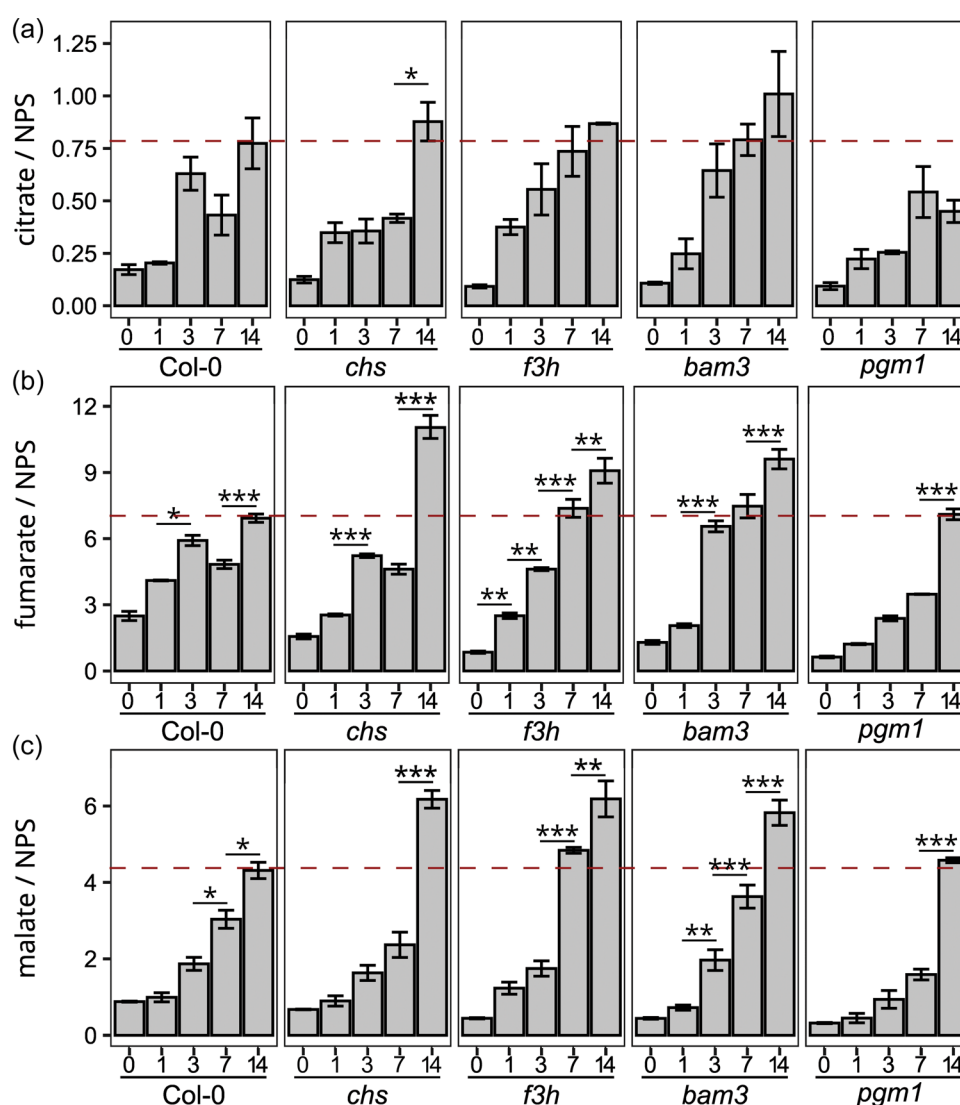


**FIGURE 9** Quantitative ratio of organic acid amounts and net CO<sub>2</sub> uptake rates. (a) Ratio of citrate and NPS (in C<sub>6</sub>/C<sub>6</sub> equivalents), (b) ratio of fumarate and NPS (in C<sub>4</sub>/C<sub>4</sub> equivalents), (c) ratio of malate and NPS (in C<sub>4</sub>/C<sub>4</sub> equivalents). NPS: net CO<sub>2</sub> assimilation. The red dashed line represents the mean maximum ratio in Col-0. Asterisks indicate significant difference between consecutive days within one genotype: \*\*\* $p < 0.001$ ; \*\* $p < 0.01$ ; \* $p < 0.05$  (ANOVA with Tukey HSD,  $n \geq 5$ ). More details about the ANOVA output are provided in Table SVIII. [Color figure can be viewed at [wileyonlinelibrary.com](http://wileyonlinelibrary.com)]

Interestingly, amylase activity was significantly higher in *pgm1* than in Col-0 during the phase of strongest anthocyanin accumulation, that is, between 7 and 14 days (see Figure 6g). This might indicate that starch degradation represents a (metabolic) signal for induction of anthocyanin, or more general, flavonoid biosynthesis. While during the light phase, only a relatively small fraction of transitory leaf starch is degraded (Ishihara et al., 2022), this might be essential to maximise accumulation of flavonoids. Furthermore, it was interesting to observe that the complete flavonoid deficiency in *chs* was accompanied by increased mean growth rates which suggests impact of flavonoid accumulation on biomass accumulation in the cold. In addition, *chs* plants showed the most significant and strongest positive correlation of fresh and dry weight of plant shoot tissue. It remains speculation here but this observation might indicate (i) a role of flavonoids as osmolytes which affect tissue water content during cold acclimation, or (ii) modification of fluxes in metabolism redirecting carbon equivalents from flavonoid into cell wall biosynthesis. Furthermore, flavonoids have previously been suggested to play a central role for cold acclimation output, that is, freezing tolerance, in *A. thaliana* (Schulz et al., 2016). Consequently, reduced anthocyanin amounts of *bam3* and *pgm1* would be expected to result in reduced freezing tolerance. For *pgm1*, this has been shown before by electrolyte leakage assays, quantifying the LT50 of leaf tissue (Hoermiller et al., 2017). In *BMV8 (BAM3) RNAi lines*, freezing temperatures were found to affect  $F_v/F_m$ , that is, PSII integrity (Kaplan & Guy, 2005). In the present study, deficiency of flavonoids (in *chs*) was neither found to significantly affect  $F_v/F_m$  nor net  $\text{CO}_2$  assimilation rates, which might be due to a relatively low/mild PPFD of  $100 \mu\text{mol photons m}^{-2} \text{s}^{-1}$ , which only partially represents in situ conditions, for example, in the shade, of natural habitats (Callahan & Pigliucci, 2002; Nagler et al., 2018). Conclusively, the trade-off between stabilizing primary and energy metabolism and synthesising protective flavonoids in *Arabidopsis* needs to be studied under more challenging environments to quantify physiological effects of deficiencies in secondary metabolism and to validate the impact of starch degradation on flavonoid accumulation.

Amounts of starch and soluble carbohydrates are well known to (strongly) accumulate during cold acclimation despite a significant decrease of photosynthetic  $\text{CO}_2$  uptake (Garcia-Molina et al., 2020; Guy et al., 2008; Hannah et al., 2006; Nägele et al., 2011; Nägele & Heyer, 2013; Savitch et al., 2001). This indicates a significant cold-induced reprogramming of plant metabolism to stabilize a new metabolic homeostasis and to prevent irreversible tissue damage (Kosová et al., 2011). Previous studies have shown that regulation of carbon allocation and flux partitioning between compartments, for example, chloroplasts and cytosol, plays a central role in cold acclimation because it enables compartment-specific accumulation of osmotically active and cryoprotective substances (Fürtauer et al., 2016; Hoermiller et al., 2017; Hoermiller et al., 2022; Lundmark et al., 2006). To reveal if and how deficiencies in starch and flavonoid metabolism may affect carbon partitioning during cold acclimation, substrate saturated enzyme activities, that is,  $v_{\text{max}}$ , of the central carbohydrate metabolism were quantified at different temperatures

ranging from ambient ( $22^\circ\text{C}$ ) to low ( $4^\circ\text{C}$ ) temperature. These experiments enabled a robust estimation of activation energy and kinetic modelling under a changing temperature regime (see Figure 7), except for acidic invertase where the Arrhenius assumption failed to predict experimental observations. This might indicate the necessity of purifying this invertase isoform to robustly estimate its kinetic under low temperature. Still, the estimated activation energy ( $E_a = 50.5 \text{ kJ mol}^{-1}$ ) was similar to a commonly accepted range of many enzymes ( $40\text{--}50 \text{ kJ mol}^{-1}$ ), which still allowed for its application in kinetic models (Bisswanger, 2008). Kinetic simulations of a model comprising carbohydrate and anthocyanin metabolism failed in reproducing experimentally observed metabolite amounts during the initial cold acclimation phase between 1 and 3 days. In more detail, sucrose amount was significantly underestimated by model simulations, which was due to unbalanced sucrose biosynthesis and simulated export rates into other metabolic pathways. Introducing a second carbon efflux leaving the carbohydrate metabolism via the F6P pool could solve this problem across all time points and genotypes. Based on previous findings which showed SPS to catalyse a limiting metabolic step during cold acclimation (Nägele et al., 2012; Strand et al., 2003), simulation output suggested that SPS redirects carbon flux into other branches of primary metabolism, for example, glycolysis, tricarboxylic acid cycle, amino acid biosynthesis or respiration. The estimated carbon flux into the biosynthetic pathway of anthocyanins was of minor importance for solving this problem, which strengthens the hypothesis that flavonoid biosynthesis under growth conditions of the present study was not limited by carbon availability during cold acclimation. This estimation, however, is clearly based on the applied photometric approach for quantification of a  $\text{C}_{15}$  backbone which might underestimate total C of anthocyanins (Saito et al., 2013), and also ignores diverse groups of flavonoids and secondary metabolites.

A plausible metabolic sink to solve the simulation and optimization problem was the pool of organic acids because its regulation has been described earlier to play an important role for cold acclimation (Dyson et al., 2016). Activity of the cytosolic fumarase enzyme FUM2 was found to be responsible for fumarate accumulation (Pracharoenwattana et al., 2010), and its deficiency prevents full acclimation of photosynthesis to low temperature (Dyson et al., 2016). Notably, FUM2 and SPS both are located within the cytosol, which might support the hypothesis that SPS limitation during cold acclimation enforces carbon partitioning in direction of fumarate biosynthesis without being accessible to the TCA cycle. As observed before (Hoermiller et al., 2017), fumarate amount was found to decrease during cold acclimation in Col-0. However, in relation to the total C assimilation flux quantified by NPS (see Figure 3), fumarate amount was increasing from a ratio of  $\sim 2.5$  to  $\sim 7.5$  (see Figure 9). The finding that these ratios reached highest values in *chs* ( $\sim 11$ ), *f3h* ( $\sim 8.5$ ) and *bam3* ( $\sim 9$ ) pointed to a role as alternative carbon sink during cold acclimation if capacities of starch and flavonoid accumulation were limited. Hence, while under ambient temperature ( $22^\circ\text{C}$ ) increased SPS activity in metabolic mutants could compensate for reduced carbon flux into starch and flavonoid pathways, cold-induced

de-regulation of starch and flavonoid metabolism may result in the need for additional alternative sinks, for example, organic acids. Finally, this finding suggests that carbon flux limitation by SPS induces a coordinate channelling during cold acclimation which supplies carbohydrates, organic acids and pathways of secondary metabolism in relation to carbon uptake rates for optimal energy supply under low temperature stress (Talts et al., 2004).

## ACKNOWLEDGEMENTS

The authors thank the members of Plant Evolutionary Cell Biology at LMU Munich for many fruitful discussions. The authors thank AG Leister at LMU for support with spectrometer analysis. The authors also thank the Graduate School Life Science Munich (LSM) for support. This work was funded by Deutsche Forschungsgemeinschaft (DFG), grants TR175/C06 (to Andreas S. Richter) and TR175/D03 (to Thomas Nägele/Edda Klipp). Open Access funding enabled and organized by Projekt DEAL.

## DATA AVAILABILITY STATEMENT

The data that support the findings of this study are available from the corresponding author upon reasonable request.

## ORCID

Anastasia Kitashova  <https://orcid.org/0000-0002-4698-3255>

Andreas S. Richter  <https://orcid.org/0000-0002-2293-7297>

Edda Klipp  <https://orcid.org/0000-0002-0567-7075>

Thomas Nägele  <http://orcid.org/0000-0002-5896-238X>

## REFERENCES

- Arrhenius, S. (1889) Über die Reaktionsgeschwindigkeit bei der Inversion von Rohrzucker durch Säuren. *Zeitschrift für physikalische Chemie*, 4, 226–248.
- Atanasov, V., Fürtauer, L. & Nägele, T. (2020) Indications for a central role of hexokinase activity in natural variation of heat acclimation in *Arabidopsis thaliana*. *Plants*, 9, 819.
- Austin, M.B. & Noel, J.P. (2003) The chalcone synthase superfamily of type III polyketide synthases. *Natural Product Reports*, 20, 79–110.
- Bisswanger, H. (2008) *Enzyme kinetics: principles and methods*. Weinheim: John Wiley & Sons.
- Callahan, H.S. & Pigliucci, M. (2002) Shade-induced plasticity and its ecological significance in wild populations of *Arabidopsis thaliana*. *Ecology*, 83, 1965–1980.
- Caretto, S., Linsalata, V., Colella, G., Mita, G. & Lattanzio, V. (2015) Carbon fluxes between primary metabolism and phenolic pathway in plant tissues under stress. *International Journal of Molecular Sciences*, 16, 26378–26394.
- Chalker-Scott, L. (1999) Environmental significance of anthocyanins in plant stress responses. *Photochemistry and Photobiology*, 70, 1–9.
- Cook, D., Fowler, S., Fiehn, O. & Thomashow, M.F. (2004) A prominent role for the CBF cold response pathway in configuring the low-temperature metabolome of *Arabidopsis*. *Proceedings of the National Academy of Sciences of the United States of America*, 101, 15243–15248.
- Doerfler, H., Lyon, D., Nägele, T., Sun, X., Fragner, L., Hadacek, F. et al. (2013) Granger causality in integrated GC-MS and LC-MS metabolomics data reveals the interface of primary and secondary metabolism. *Metabolomics*, 9, 564–574.
- Dyson, B.C., Miller, M.A.E., Feil, R., Rattray, N., Bowsher, C.G., Goodacre, R. et al. (2016) FUM2, a cytosolic fumarase, is essential for acclimation to low temperature in *Arabidopsis thaliana*. *Plant Physiology*, 172, 118–127.
- Falcone Ferreyra, M.L., Rius, S.P. & Casati, P. (2012) Flavonoids: biosynthesis, biological functions, and biotechnological applications. *Frontiers in Plant Science*, 3, 222.
- Ferreyra, M.L.F., Serra, P. & Casati, P. (2021) Recent advances on the roles of flavonoids as plant protective molecules after UV and high light exposure. *Physiologia Plantarum*, 173, 736–749.
- Fowler, S. & Thomashow, M.F. (2002) *Arabidopsis* transcriptome profiling indicates that multiple regulatory pathways are activated during cold acclimation in addition to the CBF cold response pathway. *The Plant Cell*, 14, 1675–1690.
- Fürtauer, L., Weckwerth, W. & Nägele, T. (2016) A benchtop fractionation procedure for subcellular analysis of the plant metabolome. *Frontiers in Plant Science*, 7, 1912.
- García-Molina, A., Kleine, T., Schneider, K., Mühlhaus, T., Lehmann, M. & Leister, D. (2020) Translational components contribute to acclimation responses to high light, heat, and cold in *Arabidopsis*. *iScience*, 23, 101331.
- Gibon, Y., Vigeolas, H., Tiessen, A., Geigenberger, P. & Stitt, M. (2002) Sensitive and high throughput metabolite assays for inorganic pyrophosphate, ADPGlc, nucleotide phosphates, and glycolytic intermediates based on a novel enzymic cycling system. *The Plant Journal*, 30, 221–235.
- Guy, C., Kaplan, F., Kopka, J., Selbig, J. & Hinch, D.K. (2008) Metabolomics of temperature stress. *Physiologia Plantarum*, 132, 220–235.
- Hannah, M.A., Heyer, A.G. & Hinch, D.K. (2005) A global survey of gene regulation during cold acclimation in *Arabidopsis thaliana*. *PLoS Genetics*, 1, e26.
- Hannah, M.A., Wiese, D., Freund, S., Fiehn, O., Heyer, A.G. & Hinch, D.K. (2006) Natural genetic variation of freezing tolerance in *Arabidopsis*. *Plant Physiology*, 142, 98–112.
- Havaux, M. & Kloppstech, K. (2001) The protective functions of carotenoid and flavonoid pigments against excess visible radiation at chilling temperature investigated in *Arabidopsis npq* and *tt* mutants. *Planta*, 213, 953–966.
- Hoermiller, I.L., Funck, D., Schönewolf, L., May, H. & Heyer, A.G. (2022) Cytosolic proline is required for basal freezing tolerance in *Arabidopsis*. *Plant, Cell & Environment*, 45, 147–155.
- Hoermiller, I.L., Naegle, T., Augustin, H., Stutz, S., Weckwerth, W. & Heyer, A.G. (2017) Subcellular reprogramming of metabolism during cold acclimation in *Arabidopsis thaliana*. *Plant, Cell & Environment*, 40, 602–610.
- Holaday, A.S., Martindale, W., Alred, R., Brooks, A.L. & Leegood, R.C. (1992) Changes in activities of enzymes of carbon metabolism in leaves during exposure of plants to low temperature. *Plant Physiology*, 98, 1105–1114.
- Huner, N.P.A., Öquist, G. & Sarhan, F. (1998) Energy balance and acclimation to light and cold. *Trends in Plant Science*, 3, 224–230.
- Ishihara, H., Alseekh, S., Feil, R., Perera, P., George, G.M., Niedźwiecki, P. et al. (2022) Rising rates of starch degradation during daytime and trehalose 6-phosphate optimize carbon availability. *Plant Physiology*, 189, 1976–2000.
- Kaplan, F. & Guy, C.L. (2004)  $\beta$ -Amylase induction and the protective role of maltose during temperature shock. *Plant Physiology*, 135, 1674–1684.
- Kaplan, F. & Guy, C.L. (2005) RNA interference of *Arabidopsis* beta-amylase8 prevents maltose accumulation upon cold shock and increases sensitivity of PSII photochemical efficiency to freezing stress. *The Plant Journal*, 44, 730–743.



- Kaplan, F., Kopka, J., Haskell, D.W., Zhao, W., Schiller, K.C., Gatzke, N. et al. (2004) Exploring the temperature-stress metabolome of *Arabidopsis*. *Plant Physiology*, 136, 4159–4168.
- Kitashova, A., Schneider, K., Fürtauer, L., Schröder, L., Scheibenbogen, T., Fürtauer, S. et al. (2021) Impaired chloroplast positioning affects photosynthetic capacity and regulation of the central carbohydrate metabolism during cold acclimation. *Photosynthesis Research*, 147, 49–60.
- Klotke, J., Kopka, J., Gatzke, N. & Heyer, A.G. (2004) Impact of soluble sugar concentrations on the acquisition of freezing tolerance in accessions of *Arabidopsis thaliana* with contrasting cold adaptation – evidence for a role of raffinose in cold acclimation. *Plant, Cell & Environment*, 27, 1395–1404.
- Knight, M.R. & Knight, H. (2012) Low-temperature perception leading to gene expression and cold tolerance in higher plants. *New Phytologist*, 195, 737–751.
- Korn, M., Peterek, S., Mock, H.-P., Heyer, A.G. & Hinch, D.K. (2008) Heterosis in the freezing tolerance, and sugar and flavonoid contents of crosses between *Arabidopsis thaliana* accessions of widely varying freezing tolerance. *Plant, Cell & Environment*, 31, 813–827.
- Kosová, K., Vítámvás, P., Prášil, I.T. & Renaut, J. (2011) Plant proteome changes under abiotic stress—contribution of proteomics studies to understanding plant stress response. *Journal of Proteomics*, 74, 1301–1322.
- Kötting, O., Pusch, K., Tiessen, A., Geigenberger, P., Steup, M. & Ritte, G. (2005) Identification of a novel enzyme required for starch metabolism in *Arabidopsis* leaves. The phosphoglucan, water dikinase. *Plant Physiology*, 137, 242–252.
- Leonardos, E.D., Savitch, L.V., Huner, N.P.A., Öquist, G., & Grodzinski, B. (2003) Daily photosynthetic and C-export patterns in winter wheat leaves during cold stress and acclimation. *Physiologia Plantarum*, 117(4), 521–531. <https://doi.org/10.1034/j.1399-3054.2003.00057.x>
- Lundmark, M., Cavaco, A.M., Trevanion, S. & Hurry, V. (2006) Carbon partitioning and export in transgenic *Arabidopsis thaliana* with altered capacity for sucrose synthesis grown at low temperature: a role for metabolite transporters. *Plant, Cell & Environment*, 29, 1703–1714.
- Monroe, J.D., Storm, A.R., Badley, E.M., Lehman, M.D., Platt, S.M., Saunders, L.K. et al. (2014)  $\beta$ -Amylase1 and  $\beta$ -amylase3 are plastidic starch hydrolases in *Arabidopsis* that seem to be adapted for different thermal, pH, and stress conditions. *Plant Physiology*, 166, 1748–1763.
- Nägele, T. & Heyer, A.G. (2013) Approximating subcellular organisation of carbohydrate metabolism during cold acclimation in different natural accessions of *Arabidopsis thaliana*. *New Phytologist*, 198, 777–787.
- Nägele, T., Kandel, B.A., Frana, S., Meißner, M. & Heyer, A.G. (2011) A systems biology approach for the analysis of carbohydrate dynamics during acclimation to low temperature in *Arabidopsis thaliana*. *FEBS Journal*, 278, 506–518.
- Nägele, T., Stutz, S., Hörmiller, I.I. & Heyer, A.G. (2012) Identification of a metabolic bottleneck for cold acclimation in *Arabidopsis thaliana*. *The Plant Journal*, 72, 102–114.
- Nagler, M., Nägele, T., Gilli, C., Fragner, L., Korte, A. & Platzer, A. et al. (2018) Eco-metabolomics and metabolic modeling: making the leap from model systems in the lab to native populations in the field. *Frontiers in Plant Science*, 9, 1556.
- Nagler, M., Nukarinen, E., Weckwerth, W. & Nägele, T. (2015) Integrative molecular profiling indicates a central role of transitory starch breakdown in establishing a stable C/N homeostasis during cold acclimation in two natural accessions of *Arabidopsis thaliana*. *BMC Plant Biology*, 15, 284.
- Niittylä, T., Messlerli, G., Trevisan, M., Chen, J., Smith, A.M. & Zeeman, S.C. (2004) A previously unknown maltose transporter essential for starch degradation in leaves. *Science*, 303, 87–89.
- Oñate-Sánchez, L., & Vicente-Carbajosa, J. (2008). DNA-free RNA isolation protocols for *Arabidopsis thaliana*, including seeds and siliques. *BMC Research Notes*, 1(1), 93. <https://doi.org/10.1186/1756-0500-1-93>
- Owens, D.K., Crosby, K.C., Runac, J., Howard, B.A. & Winkel, B.S.J. (2008) Biochemical and genetic characterization of *Arabidopsis* flavanone 3 $\beta$ -hydroxylase. *Plant Physiology and Biochemistry*, 46, 833–843.
- Plieth, C., Hansen, U.-P., Knight, H. & Knight, M.R. (1999) Temperature sensing by plants: the primary characteristics of signal perception and calcium response. *The Plant Journal*, 18, 491–497.
- Pracharoenwattana, I., Zhou, W., Keech, O., Francisco, P.B., Udomchalothorn, T., Tschoep, H. et al. (2010) *Arabidopsis* has a cytosolic fumarase required for the massive allocation of photosynthate into fumaric acid and for rapid plant growth on high nitrogen. *The Plant Journal*, 62, 785–795.
- Ristic, Z. & Ashworth, E.N. (1993) Changes in leaf ultrastructure and carbohydrates in *Arabidopsis thaliana* L. (Heyn) cv. Columbia during rapid cold acclimation. *Protoplasma*, 172, 111–123.
- Saito, K., Yonekura-Sakakibara, K., Nakabayashi, R., Higashi, Y., Yamazaki, M., Tohge, T. et al. (2013) The flavonoid biosynthetic pathway in *Arabidopsis*: structural and genetic diversity. *Plant Physiology and Biochemistry*, 72, 21–34.
- Savitch, L.V., Barker-Åstrom, J., Ivanov, A.G., Hurry, V., Öquist, G., Huner, N.P. et al. (2001) Cold acclimation of *Arabidopsis thaliana* results in incomplete recovery of photosynthetic capacity, associated with an increased reduction of the chloroplast stroma. *Planta*, 214, 295–303.
- Schulz, E., Tohge, T., Zuther, E., Fernie, A.R. & Hinch, D.K. (2015) Natural variation in flavonol and anthocyanin metabolism during cold acclimation in *Arabidopsis thaliana* accessions. *Plant, Cell & Environment*, 38, 1658–1672.
- Schulz, E., Tohge, T., Zuther, E., Fernie, A.R. & Hinch, D.K. (2016) Flavonoids are determinants of freezing tolerance and cold acclimation in *Arabidopsis thaliana*. *Scientific Reports*, 6, 34027.
- Seydel, C., Kitashova, A., Fürtauer, L. & Nägele, T. (2022) Temperature-induced dynamics of plant carbohydrate metabolism. *Physiologia Plantarum*, 174, e13602.
- Shi, M.-Z. & Xie, D.-Y. (2014) Biosynthesis and metabolic engineering of anthocyanins in *Arabidopsis thaliana*. *Recent Patents on Biotechnology*, 8, 47–60.
- Sicher, R. (2011) Carbon partitioning and the impact of starch deficiency on the initial response of *Arabidopsis* to chilling temperatures. *Plant Science*, 181, 167–176.
- Smith, A.M., Zeeman, S.C. & Smith, S.M. (2005) Starch degradation. *Annual Review of Plant Biology*, 56, 73–98.
- Stitt, M. & Hurry, V. (2002) A plant for all seasons: alterations in photosynthetic carbon metabolism during cold acclimation in *Arabidopsis*. *Current Opinion in Plant Biology*, 5, 199–206.
- Stitt, M. & Zeeman, S.C. (2012) Starch turnover: pathways, regulation and role in growth. *Current Opinion in Plant Biology*, 15, 282–292.
- Strand, Å., Foyer, C.H., Gustafsson, P., Gardeström, P. & Hurry, V. (2003) Altering flux through the sucrose biosynthesis pathway in transgenic *Arabidopsis thaliana* modifies photosynthetic acclimation at low temperatures and the development of freezing tolerance. *Plant, Cell & Environment*, 26, 523–535.
- Talts, P., Pärnik, T., Gardeström, P. & Keerber, O. (2004) Respiratory acclimation in *Arabidopsis thaliana* leaves at low temperature. *Journal of Plant Physiology*, 161, 573–579.
- Thomashow, M.F. (2010) Molecular basis of plant cold acclimation: insights gained from studying the CBF cold response pathway. *Plant Physiology*, 154, 571–577.
- Vaz, A.I.F., & Vicente, L.N. (2007). A particle swarm pattern search method for bound constrained global optimization. *Journal of Global Optimization*, 39(2), 197–219. <https://doi.org/10.1007/s10898-007-9133-5>

- Weizmann, J., Fürtauer, L., Weckwerth, W. & Nägele, T. (2018) Vacuolar sucrose cleavage prevents limitation of cytosolic carbohydrate metabolism and stabilizes photosynthesis under abiotic stress. *FEBS Journal*, 285, 4082–4098.
- Wiese, A., Gröner, F., Sonnewald, U., Deppner, H., Lerchl, J., Hebbeker, U. et al. (1999) Spinach hexokinase I is located in the outer envelope membrane of plastids. *FEBS Letters*, 461, 13–18.
- Winkel-Shirley, B. (2001) Flavonoid biosynthesis. A colorful model for genetics, biochemistry, cell biology, and biotechnology. *Plant Physiology*, 126, 485–493.
- Winkel-Shirley, B. (2002) Biosynthesis of flavonoids and effects of stress. *Current Opinion in Plant Biology*, 5, 218–223.
- Xin, Z. & Browse, J. (2000) Cold comfort farm: the acclimation of plants to freezing temperatures. *Plant, Cell & Environment*, 23, 893–902.
- Yano, R., Nakamura, M., Yoneyama, T. & Nishida, I. (2005) Starch-related  $\alpha$ -glucan/water dikinase is involved in the cold-induced development of freezing tolerance in Arabidopsis. *Plant Physiology*, 138, 837–846.

- Yokoyama, R., de Oliveira, M.V.V., Kleven, B. & Maeda, H.A. (2021) The entry reaction of the plant shikimate pathway is subjected to highly complex metabolite-mediated regulation. *The Plant Cell*, 33, 671–696.

## SUPPORTING INFORMATION

Additional supporting information can be found online in the Supporting Information section at the end of this article.

**How to cite this article:** Kitashova, A., Adler, S.O., Richter, A.S., Eberlein, S., Dziubek, D., Klipp, E., et al. (2023) Limitation of sucrose biosynthesis shapes carbon partitioning during plant cold acclimation. *Plant, Cell & Environment*, 46, 464–478. <https://doi.org/10.1111/pce.14483>

### **9.3 Publication 3: Plant cold acclimation and its impact on sensitivity of carbohydrate metabolism**

Adler SO, **Kitashova A**, Bulović A, Nägele T, Klipp E (2024) Plant cold acclimation and its impact on sensitivity of carbohydrate metabolism. *bioRxiv preprint* 2024.06.04.597423

Supplementary material is available at:

<https://www.biorxiv.org/content/10.1101/2024.06.04.597423v1>

# Plant cold acclimation and its impact on sensitivity of carbohydrate metabolism

Stephan O. Adler<sup>1</sup>, Anastasia Kitashova<sup>2</sup>, Ana Bulović<sup>1</sup>, Thomas Nägele<sup>2</sup>, Edda Klipp<sup>1\*</sup>

<sup>1</sup> Theoretical Biophysics, Institute of Biology, Humboldt-Universität zu Berlin, Berlin, Germany.

<sup>2</sup> Plant Evolutionary Cell Biology, Faculty of Biology, Ludwig-Maximilians-Universität München, Planegg-Martinsried, Germany.

\* Corresponding Author, [edda.klipp@rz.hu-berlin.de](mailto:edda.klipp@rz.hu-berlin.de)

## Abstract

The ability to acclimate to changing environmental conditions is essential for the fitness and survival of plants. Not only are seasonal differences challenging for plants growing in different habitats but, facing climate change, the likelihood of encountering extreme weather events increases. In order to better assess and respond to associated future challenges and risks it is important to understand the processes happening during acclimation. Previous studies of acclimation processes of *Arabidopsis thaliana* to changes in temperature and light conditions have revealed a multigenic trait comprising and affecting multiple layers of molecular organization. Here, a combination of experimental and computational methods was applied to study the effects of changing light intensities during cold acclimation on the central carbon metabolism of *Arabidopsis thaliana* leaves. Mathematical modeling, simulation and sensitivity analysis predicted an important role of hexose phosphate balance for stabilization of photosynthetic CO<sub>2</sub> fixation. Experimental validation revealed a profound effect of temperature on the sensitivity of carbohydrate metabolism.

## 1. Introduction

Dynamic environmental factors affect plant metabolism, growth, and development. Due to their sessile lifestyle, all plants have developed mechanisms to respond to varying magnitudes and time scales of changes in light intensity, temperature, or humidity. The reversible adjustment of metabolism to such factors is termed acclimation and comprises various

responses on a molecular and physiological level (Kleine et al. 2021).

Many plant species, e.g., *Arabidopsis thaliana* (Seydel et al. 2022), *Zea mays* (Kingston-Smith et al. 1999; Pandolfi et al. 2016) and *Nicotiana tabacum* (Vranová et al. 2002), have been studied to reveal insights into the processes happening during acclimation to e.g. cold, heat,

fluctuating or high light. When exposed to temperature changes, besides the need for protection from freezing or adverse heat, all vital chemical processes need to be maintained.

Because the velocity and balance of involved chemical reactions is differently affected by temperature, these processes are likely to become unbalanced. This effect needs to be compensated. The compensation can happen actively, e.g. through changes in gene expression or molecular modifications, or passively, e.g. through the architecture of the reaction network and the physical properties of its components (Rouff et al. 2007). Besides having a compensatory nature, the reaction network can offer potential for regulation (Adler et al. 2020). Taken together, these processes form a complex system of intertwined mechanisms that is difficult to entangle. Following approaches that combine different experimental procedures with mathematical modeling has shown to be a fruitful strategy to address complex problems like this.

During cold acclimation of *Arabidopsis thaliana*, a reprogramming of several metabolic processes has been described. This includes the accumulation of soluble sugars, such as sucrose and raffinose, which potentially act as cryoprotectants and stabilize metabolism (Klotke, 2004; Ristic & Ashworth, 1993; Seydel, 2022). This is accompanied by the induction of *BAM3* expression (Sicher 2011; Kaplan 2004; Monroe 2014), an amylase that is involved in starch breakdown, leading to a decrease of starch amounts during the first hours of acclimation and supporting the accumulation of soluble sugars (Yano et al. 2005). Later during acclimation, starch accumulates (Klotke et al. 2004). Additionally, the activity of TCA cycle enzymes and oxidative respiration is reduced,

resulting in a decrease of respiration and energy production (Fürtauer 2019). The activity of enzymes involved in photosynthesis is inhibited, causing a decrease in carbon fixation and the accumulation of reducing equivalents, such as NADPH, which are used for biosynthetic processes (Hannah 2005; Savitch 2001; Fürtauer 2019). Alongside these processes within the primary metabolism, also secondary metabolism undergoes several rearrangements. Here, the accumulation of anthocyanins has been observed (Korn et al 2008). Anthocyanin synthesis is a downstream branch of flavonoid synthesis which branches from the shikimate pathway (Austin & Noel, 2003). It has been demonstrated that this accumulation process is vital for cold protection (Chalker-Scott 1999; Schulz 2015), but while the full scope of anthocyanin function is not completely clear, there is strong evidence for photoprotection, protection from stress-induced ROS and osmoregulation (Agati 2021; Chalker-Scott 2002; Kaur 2023). Since both, primary and secondary metabolism are differentially regulated during cold acclimation and play vital roles for the plants' survival, there is need for precise regulation of carbon distribution within the different domains of metabolism, that might include regulatory interactions.

Different genotypes of *Arabidopsis thaliana* exhibit different characteristics in their reprogramming of metabolism that are related to their sensitivity to cold. There are, for example, indications for differences of interconversion rates between hexoses and sucrose or of export rates to sink organs (Nägele 2010). Mutants like *bam3*, *pgm1*, *chs* and *f3h* are deficient in processes directly involved in acclimation. The *bam3* mutant is deficient in amylase activity that is upregulated in cold conditions. This leads to insufficient retrieval of

carbon from starch. The *pgm1* mutant, in contrast, is starch deficient because it lacks phosphoglucomutase that catalyzes an initial step of starch synthesis (Stitt & Zeemann 2012). While these mutations are starch related and, therefore, correspond to primary metabolism the *chs* and *f3h* mutations are related to secondary metabolism and are defective in flavonoid biosynthesis. Chalcone synthase (CHS) catalyzes the diversion of phenylpropanoid tetraketide from the shikimate pathway, the initial step of flavonoid biosynthesis. In a later step, F3H and F3'H (flavanone 3-hydroxylase and flavanone 3'-hydroxylase) catalyze the conversion of naringenin, a precursor of a subgroup of flavonols including anthocyanins, into dihydroflavonol (Owens 2008; Shi & Xie 2014).

Despite the numerous successful studies using different experimental and computational approaches, many aspects of the complex and dynamic mechanisms and processes during cold acclimation are still elusive. In an earlier study (Kitashova et al. 2022), the natural accession Columbia-0, together with the mentioned four mutant genotypes *bam3*, *pgm1*, *chs* and *f3h* were used to investigate regulatory interactions between primary and secondary metabolism during acclimation. Data on metabolite levels, enzyme activities and photosynthetic carbon uptake was obtained and used to calibrate a condensed mathematical model, comprising

core elements of the central carbon metabolism of plant leaves. In this way, evidence for dynamic carbon partitioning between starch, sucrose and anthocyanin metabolism, including a unidirectional signaling link between starch and flavonoid metabolism and a central role of sucrose could be identified.

In the present study, we analyzed this model to investigate the effects of variations in light intensity on the five genotypes of *Arabidopsis thaliana* during and after two weeks of cold acclimation. We re-estimated the model parameters with literature-based constraints for coherent enzyme specific values across the different genotypes and investigated the sensitivity towards dynamics of net photosynthetic CO<sub>2</sub> assimilation rates after different periods of high light exposure at 4°C *in vivo* and *in silico*. A comparison of the dynamics showed a good agreement between experiments and simulations. This enabled for broader analysis of these dynamics through further simulations and the introduction of a sensitivity measure (sensitivity score). In combination with the analysis of control coefficients within the system, this approach indicates that temperature has a stronger impact on the overall sensitivity of central carbon metabolism than the different mutations and that there is likely one or more compensation or rescue mechanisms shared by primary and secondary metabolism.

## 2. Methods

### 2.1. The model

#### 2.1.1. Model overview

This work is based on the model presented before (Kitashova et al. 2022). In this study, different genotypes (wild type: Col-0; mutants: *chs*, *f3h*, *bam3*, *pgm1*) of *Arabidopsis thaliana* were exposed to 4°C over the course of 14 days. On days 0, 1, 3, 7 and 14, samples were taken and net photosynthesis (nps), levels of starch, soluble carbohydrates, hexose phosphates, anthocyanins, and organic acids, as well as enzyme activities were quantified. The experimental data was then used to estimate parameters for simulation of the central carbon metabolism and its interface with flavonoid biosynthesis.

The basic model comprises 5 metabolites and 12 reactions and is described by a set of ordinary differential equations (ODEs) given in Tab. 1. A scheme of the model is shown in Figure 1.

In the model, fructose 6-phosphate (F6P) is assumed to be the main product of

photosynthesis available for further processes. It is in an equilibrium with glucose 6-phosphate (G6P), that is defined by phosphoglucosomerase (PGI) activity. F6P and G6P together can be converted into sucrose (Suc) by sucrose phosphate synthase (SPS), while only a fraction of G6P is available for this reaction. Here, UDP-glucose as an intermediate metabolite was omitted for simplification, with the assumption that about 20-50% of G6P are converted before entering the SPS reaction. Suc is then directly exported to sink organs. Additionally, F6P is converted into anthocyanins (ANTHO) and diverted to the second export flux ( $r_2$ ) while G6P is converted into starch in a single process (rSTAsyn) lumping the stepwise synthesis. The invertase reaction (rINV), breaking down Suc into fructose (Frc) and glucose (Glc), together with the fructokinase and glucokinase reactions (rFRCK, rGLCK), phosphorylating Frc and Glc and resulting in the recovery of F6P and G6P, form a central loop that enables responsive balancing of metabolites.

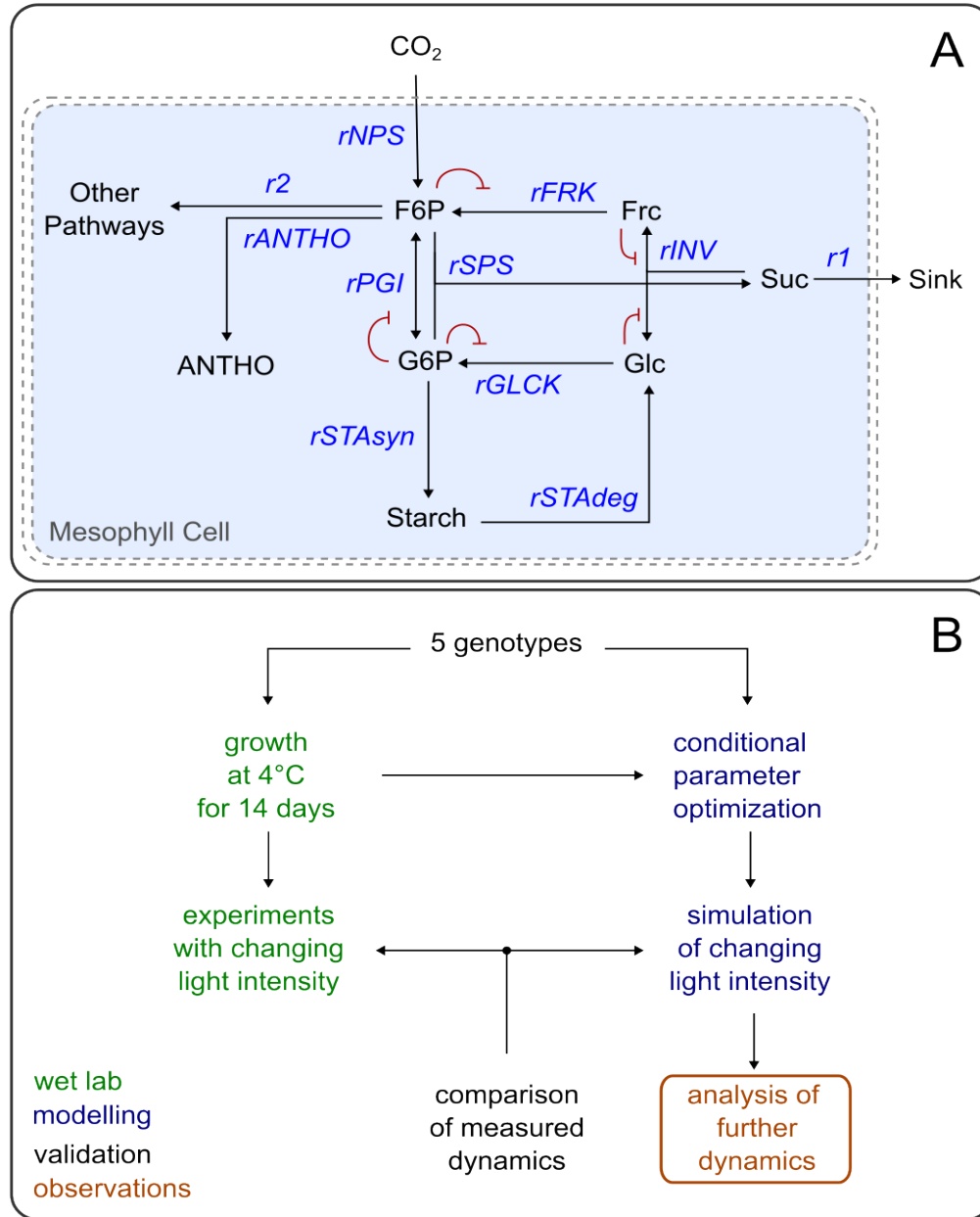


**Figure 1:** Model scheme and workflow. **A:** The model consists of 5 main metabolites: F6P, G6P, Frc, Glc and Suc. These metabolites take part in various enzymatic reactions (*rSPS*, *rPGL*, *rFRCK*, *rGLCK*, *rINV*) or biological processes (*rNPS*, *rSTAsyn*, *rSTAdeg*, *rANTHO*). These are depicted as arrows. There are two export fluxes, *r1* to sink organs and *r2* to other pathways of the central carbon metabolism in the mesophyll cell. The red lines indicate negative feedback regulation by metabolites on reaction fluxes. **B:** This flowchart provides an overview on the workflow and steps in this study. It highlights the experimental (green) and modeling (blue) part and how these are connected. Observations and validation are represented in orange and black, respectively.



## 2.1.2. Model equations

Differential equation system

$$\begin{aligned}\frac{dF6P}{dt} &= rNPS - rSPS - rPGI_1 - rANTHO - r2 + rFRCK \\ \frac{dG6P}{dt} &= rPGI_2 - rSPS - rSTAsyn + rGLCK \\ \frac{dSuc}{dt} &= rSPS - r2 - rINV \\ \frac{dFrc}{dt} &= rINV - rFRCK \\ \frac{dGlc}{dt} &= rINV - rGLCK + rSTAdeg\end{aligned}$$

Rate equations

$$\begin{aligned}rNPS &= \frac{1}{6} \cdot k_{NPS} \\ rSPS &= v_{\max}^{SPS} \cdot F6P \cdot k_{udp} \cdot G6P \\ &\quad \cdot \left( Km_a^{SPS} \cdot F6P + (Km_b^{SPS} + F6P) \cdot k_{udp} \cdot G6P + K_i^{SPS} \cdot Km_a^{SPS} \right)^{-1} \\ rFRCK &= v_{\max}^{FRCK} \cdot \frac{Frc}{(Km^{FRCK} + Frc) \cdot \left(1 + \frac{F6P}{K_i^{FRCK}}\right)} \\ rGLCK &= v_{\max}^{GLCK} \cdot \frac{Glc}{(Km^{GLCK} + Glc) \cdot \left(1 + \frac{G6P}{K_i^{GLCK}}\right)} \\ rINV &= v_{\max}^{INV} \cdot \frac{Suc}{(Km^{INV} \cdot \left(1 + \frac{Frc}{K_i^{INV1}}\right) + Suc) \cdot \left(1 + \frac{Glc}{K_i^{INV2}}\right)} \\ rPGI_1 &= v_{\max}^{PGI} \cdot \frac{F6P}{Km^{PGI} \cdot \left(1 + \frac{G6P}{K_i^{PGI}}\right) + F6P} \cdot f \\ rPGI_2 &= v_{\max}^{PGI} \cdot \frac{G6P}{Km^{PGI} \cdot \left(1 + \frac{F6P}{K_i^{PGI}}\right) + G6P} \cdot (1 - f) \\ r1 &= k_1^{\text{exp}} \cdot Suc \\ r2 &= k_2^{\text{exp}} \cdot F6P \\ rSTAsyn &= k_{STA} \cdot G6P \\ rANTHO &= k_{ANT} \cdot F6P\end{aligned}$$

### 2.1.3. Model refinement and parameter re-estimation

Matching the composition of data presented in Kitashova et al. 2022, the model parameters were optimized to fulfill a steady state assumption for each genotype and time point pair, resulting in 25 conditional model realizations (parameterizations), representing different stages of acclimation for the different genotypes. While keeping the original structure

All corresponding estimated  $K_m$  and  $K_i$  values are within a range of one order of magnitude between each set. It is reasonable to assume the possibility of changes in  $K_m$  values over time, especially during a process of metabolic rearrangement like acclimation due to, for example, post translational modifications such as phosphorylation (Huber and Huber 1996; Ashihara, Crozier, and Komamine 2010; Boex-Fontvieille et al. 2014).

This way, we were able to identify a new refined set of parameters for each combination of genotype and time point, sharing a common, close range of  $K_m$  and  $K_i$  values. In the context of parameterization, it is also important to mention

of the model, here, we applied a different parametrization strategy by restricting all  $K_m$  and  $K_i$  values to common bounds for all genotypes and time points. Additionally, these bounds had to meet conditions derived from literature (Preiser et al. 2020; Dai et al. 1995; Lou et al. 2007; Qi et al. 2007; Xiang et al. 2011):

- $K_{mFRCK} > K_{mGLCK}$
- $K_{mINV}$  similar or close to  $K_{mFRCK}$
- $K_{mFRCK} > K_{mPGI} > K_{mFRCK}$

that, while the model considers starch degradation, the degradation rate was set to 0 for the 25 conditional parameterizations, since they represent steady state conditions during midday and most starch degradation usually happens during the night under ambient temperature / control condition. But, as the starch production rates are estimated in a net balance over several days as described in Kitashova et al. 2022, relative changes of mean starch production and degradation are summarized in the production rate parameter  $k_{STA}$ . The model with the systematically revised parameters was then subjected to a sensitivity analysis.

## 2.2. Simulations and analyses

For all simulations the free software tool Tellurium (version 2.2.7, Choi 2018) was used, utilizing the CVODE integrator to solve the set of ODEs. To perform metabolic control analysis,

methods of libroadrunner (Somogyi et al., 2015; Welsh et al., 2023) within Tellurium were used. The free Matlab software package Data2Dynamics (Raue 2015) was used for parameter estimation.

## 2.3. Experimental procedures

### 2.3.1. Plant material and growth conditions

*Arabidopsis thaliana* accession Col-0 and homozygous T-DNA insertion lines *bam3* (beta amylase 3, line SALK\_041214, locus AT4G17090), *chs* (chalcone synthase, line SALK\_020583C, locus AT5G13930), *f3h* (flavanone 3-hydroxylase, line SALK\_113904C, locus AT3G51240), as well as the SNP mutant *pgm1* (plastidial phosphoglucomutase, TAIR stock CS3092, locus AT5G51820) were grown on a 1:1 mixture of GS90 soil and vermiculite in a climate chamber under controlled conditions (8h/16h day/night;  $100 \mu\text{mol m}^{-2} \text{s}^{-1}$ ;  $22^\circ\text{C}/16^\circ\text{C}$ ; 60% relative humidity). Following two weeks of further growth under long day conditions (16h/8h day/night;  $100 \mu\text{mol m}^{-2} \text{s}^{-1}$ ;  $22^\circ\text{C}/16^\circ\text{C}$ ), plants were shifted to  $4^\circ\text{C}$  (16h/8h day/night;  $90\text{-}100 \mu\text{mol m}^{-2} \text{s}^{-1}$ ;  $4^\circ\text{C}/4^\circ\text{C}$ ). On the 14th day of cold, plants were either (i) sampled

after 3h of ambient light; or (ii) exposed to elevated light ( $240\text{-}270 \mu\text{mol m}^{-2} \text{s}^{-1}$ ;  $4^\circ\text{C}/4^\circ\text{C}$ ) and sampled after 3h and 6h of elevated light. Each sample consisted of 1 leaf rosette which was snap-frozen in liquid nitrogen, ground to a fine powder and freeze-dried.

### 2.3.2. Hexose phosphate quantification

Fructose 6-phosphate (F6P) and glucose 6-phosphate (G6P) amounts were quantified as described before (Gibon et al., 2002). In brief, F6P and G6P were extracted with 16% (w/v) trichloroacetic acid in diethyl ether and washed with 16% (w/v) trichloroacetic acid in 5 mM EGTA. F6P and G6P amounts were determined in a 2-step cycling assay, catalyzing equimolar interconversion of hexose-phosphates into  $\text{NADPH} + \text{H}^+$ , which was photometrically determined in a reaction with thiazolyl blue and phenazine methosulfate at 570 nm.

## 3. Results

In order to investigate the influence of dynamic  $\text{CO}_2$  assimilation rates on the acclimation process of the central carbon metabolism in *Arabidopsis thaliana* leaves, we investigated the presented model in a restricted parameter space. Therefore, we defined a procedure for assessing the dynamic sensitivity to these perturbations and compared its outcome when applied to model simulations or new experimental data. Additionally, we embedded the condensed

model into a large-scale metabolic model and compared the resulting fluxes when constrained accordingly for further validation.

Our presented analysis, together with the evaluation of parameter control coefficients, could reveal an important role of hexose phosphate balance, a rearrangement of sensitivities in response to temperature change and potential common metabolic compensation mechanisms.

### 3.1. Amounts of F6P and G6P are differentially affected by mutations in flavonoid and starch metabolism

Hexose phosphate amounts were quantified in different light conditions after cold acclimation to assess their sensitivity changes in net photosynthesis rates. While the median values of F6P ranged from 2 to 6  $\mu\text{mol gDW}^{-1}$  those of G6P ranged up to 26  $\mu\text{mol gDW}^{-1}$ , the value distributions of the single measurements shared roughly the same range between 0 and 45  $\mu\text{mol gDW}^{-1}$  (Fig. 2). In *chs*, the amount of F6P

increased after 3h of high light while amounts were stabilized in all other genotypes (Fig. 2). Both *pgm1* and *bam3* mutants were significantly affected in G6P metabolism, and *pgm1* accumulated highest amounts across all genotypes. However, between 3h and 6h of high light exposure, G6P amounts decreased again in plants of both *pgm1* and *bam3* which was not observed in Col-0, *chs* and *f3h*.

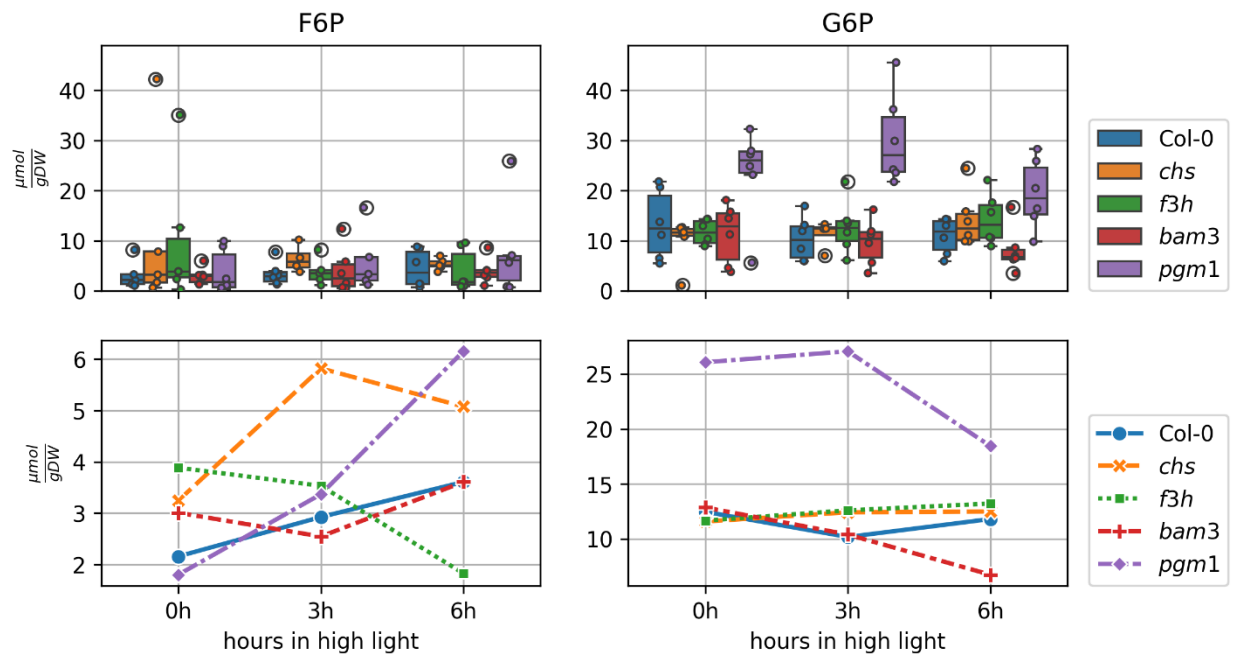


**Figure 2:** Experimental results. The upper panel illustrates the distributions of hexose concentrations, measured after 0, 3 or 6 hours in high light conditions, as boxplots for each genotype. Here, every single measurement is shown by a color filled dot. The lower panel shows the changes of the measured median over time. The 0h time point is actually represented by samples that were subjected to 3 hours of normal light, as described in the methods section, but is put as 0h time point here for better comparison.

## 3.2. Model validation

### 3.2.1. Sensitivity analysis

To further assess the impact of acclimation on central carbon metabolism, the different conditional model realizations were subjected to external perturbations, namely changes in net photosynthesis (nps) rates. Under *in vivo* conditions, variations in nps result from naturally

changing light. Starting from steady states that were derived from the experimental data, the nps rates in the model were increased or decreased by 5 to 30% in 5% increments and 4h time courses were simulated. The resulting changes in metabolite levels and reaction fluxes were then taken together to compute the sensitivity of the respective condition to these perturbations as

$$\gamma_x^{nps} = \sqrt{N \prod_i^N \left| \log_2 \left( \frac{x_i}{x_0} \cdot \frac{r_0^{nps}}{r_i^{nps}} \right) \right|} \quad (\text{eq. 1})$$

where  $\gamma_x^{nps}$  is the sensitivity score of measure  $x$  (metabolite concentration or flux) on perturbations of nps,  $N$  is the number of performed perturbations (increase/decrease, 5%, 10%, ...),  $x_0$  is the initial steady state value of measure  $x$  and  $x_i$  the resulting value after

perturbation  $i$ . The ratio of initial nps rates and rates of perturbation  $i$  are represented by  $r_0^{nps}$  and  $r_i^{nps}$ , respectively. Figure 3 illustrates this procedure and provides a graphic representation of how well the results match those derived from the experimental data.

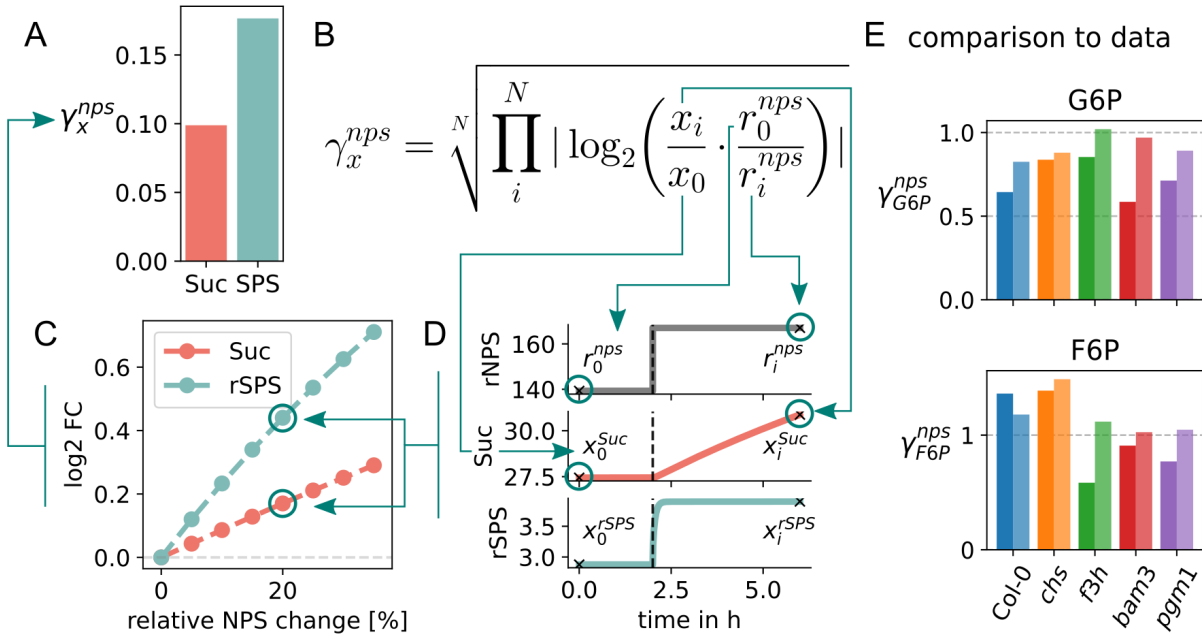


**Figure 3:** Estimation of sensitivity scores  $\gamma_x^{nps}$  and comparison to experimental data. **A:** Sensitivity scores of sucrose concentration (Suc) and the SPS reaction flux (rSPS) of model Col-0 day 0. **B:** Formula for the sensitivity score  $\gamma_x^{nps}$ . **C:** Log<sub>2</sub> fold-changes of Suc and SPS for computed net photosynthesis (nps) increases. **D:** Exemplary time courses of underlying simulations for a change in nps rate (rNPS) of 20%. Shown are the time courses of rNPS, Suc and rSPS. The vertical black lines indicate the time point of rNPS increase (2h). The “x”s mark the corresponding values for the computation of  $\gamma_x^{nps}$ . **E:** Sensitivity scores computed from control experiments (darker bars) are compared to sensitivity scores of simulations (lighter bars).

### 3.2.2. Comparison of model predictions and experimental data

To evaluate the suitability of the described analysis of sensitivity to variations in nps rates, we compared  $\gamma_x^{nps}$  derived from control experiments to values estimated from results of model simulations mimicking the experimental procedure of a newly performed experiment to specifically test the sensitivity *in vivo*. To this end, *Arabidopsis thaliana* plants from all 5 genotypes were grown at 22°C and transferred to 4°C for 14 days, where they could acclimate as described in Kitashova et al. 2022. On day 14, the plants were either exposed to normal light (100μE) and samples were taken after 3h. Or the

plants were transferred to elevated light (240-270μE), which leads to an increase of nps by 20-30%, and samples were taken after 3 and 6h. Concentrations of F6P and G6P were measured for all samples as described in the methods section 2.3.

As a comparison, the model realizations of day 14 were used for each genotype and simulated in the same fashion as the experimental procedure. Here, the shift to high light was simulated as an increase of rNPS by 25%. From the obtained experimental and simulation data  $\gamma_x^{nps}$  values were computed according to eq. 1 with the simple adjustment that, instead of different perturbation intensities,  $x_i$  represent different durations of exposure (3h and 6h). The concentrations obtained under normal light are

the reference values  $x_0$  and  $r_0^{\text{nps}}$ . This comparison is shown in Fig. 3 E. We see a very good agreement between experimentally obtained values and simulation results. For each metabolite there is one genotype (*bam3* for G6P and *f3h* for F6P) where the model predictions deviate more than 50% from the data. In summary, the overall agreement verifies a good suitability of the presented sensitivity assessment.

### 3.2.3. Model fits well into broader metabolic network context

To further validate the model and test its performance, especially considering the degree of condensation, we compared it to a large scale metabolic model.

Because the tackled phenomenon of carbon partitioning into starch and sucrose involves some highly connected metabolites (used in many reactions), we wanted to make sure that our model simplification still fits reasonably well into the broader context of the metabolic network of *A. thaliana*. For this, we compared the flux distribution from the dynamic model

proposed here, and the one obtained through a Flux Balance Analysis (FBA) (Orth, Thiele, and Palsson 2010) simulation of a genome-scale metabolic reconstruction of *A. thaliana* known as AraCore (Arnold and Nikoloski 2014).

All comparisons were done for the Col-0 genotype, as the other strains involve either interruptions in the pathways, used to produce biomass precursors (which make the strains non-viable in FBA context), or reduce the efficiency of a cellular process, a subtlety which cannot be considered in a stoichiometry-based modeling framework such as FBA.

We used a number of fluxes from the dynamic model to constrain the AraCore model. The import reaction to F6P was used to constrain the flux through FBPase (both cytosolic and chloroplastic), the major contributor to synthesis of F6P through the Calvin-Benson-Bassham cycle. Additionally, we used the dynamic model fluxes to constrain the fluxes through S6P synthase (S6PS\_c), G6P isomerase (PGI\_c), and hexokinase (HEXK\_c). The lower and upper bound of those reactions were set to 90 and 110% of the flux values obtained in the dynamic model.

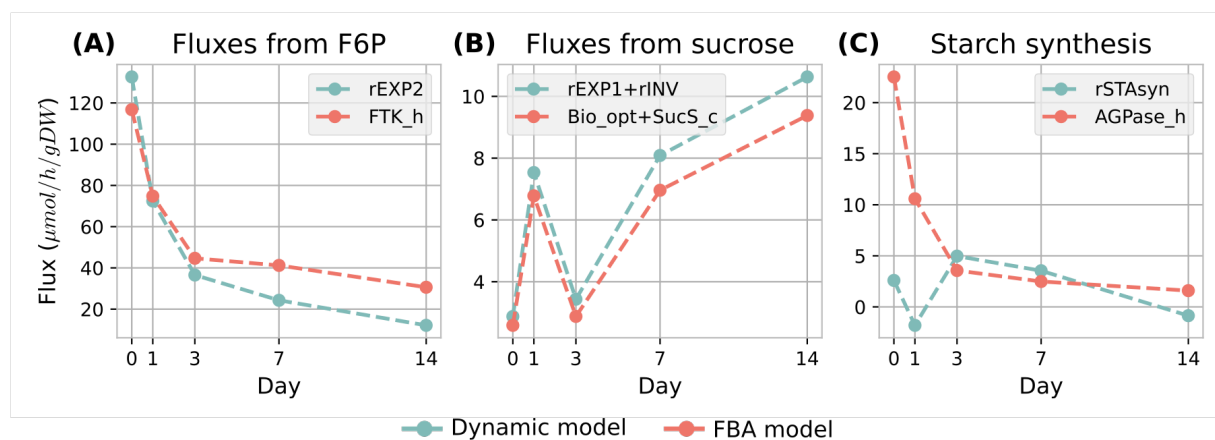


**Figure 4:** Comparison of flux values between the dynamic model and FBA. **A:** Comparison between *r2* dynamic model flux and the flux through FTK reaction in the chloroplast facilitating replenishment of CBC metabolites. **B:** Comparison of outgoing fluxes of sucrose (invertase and export flux *r1*). **C:** Comparison between starch synthesis fluxes.

We then compared (1) the flux  $r_2$  (flux going out from F6P, see Figure 1) to the flux through F6P transketolase which is a major pathway through which F6P is used for replenishing of the Calvin-Benson-Bassham cycle intermediates, (2) the total flux going out of sucrose in both our dynamic model and the FBA model and (3) the total rate of starch synthesis. One outgoing flux from F6P, which we did not compare to the AraCore prediction, is the production of anthocyanins. The reason for this is that anthocyanins are not explicitly modeled in the condensed dynamic model, and their modeled precursor, shikimate, is not exclusively used for anthocyanin synthesis. Due to this discrepancy, we decided that this comparison would not be meaningful.

When analyzing the results in detail, we see that the major flux depleting F6P ( $r_2$  in dynamic model) matches well (in order of magnitude and exact quantitative value) to the one predicted by AraCore (see Fig. 4 A). Since these are some of the fluxes with highest absolute values, this indicates that the major stoichiometric constraints on the network are well represented in the dynamic model, and that it can reliably be used as a proxy for the global metabolic state of the modeled metabolites.

Next, the total fluxes going out of sucrose match almost exactly in both models (see Fig. 4 B). However, we have to point out that the values of two individual fluxes that go out of sucrose in the

dynamic model, i.e. the export flux  $r_1$  and the flux through the invertase, do not match well to their corresponding fluxes in the FBA model. The predicted export flux of sucrose is much smaller in the FBA model due to the fact that it is represented directly by the biomass reaction. Since the biomass reaction requires many metabolites in a particular stoichiometric relation, the flux through it cannot be easily changed, and is determined not only by sucrose, but by the entire state of the metabolic network. The comparison of starch synthesis does not match as well as the other two comparisons, even if the order of magnitude is not far off, especially after day 3 (see Fig. 4 C). We assume this is because of the way in which the starch synthesis rate was initially calculated from starch measurements, by averaging the difference between starch quantity in the morning between consecutive days over 24 hours (net balance).

Overall, we see a good agreement between the fluxes concerning the modeled metabolites in the dynamic and in the FBA model, giving further confidence in the developed model, the measurements used to calibrate it, and the calibration itself. On this basis, we will subject the model to a thorough analysis of parameter sensitivity in order to understand the role of individual parameters in the acclimation ability of the plants.

### 3.3. Observations and Insights

#### 3.3.1. Hexose phosphate balance has a big impact on the overall carbon distribution

After investigating the plausibility of the model and parameters, first by comparing the

sensitivity to variation of nps rates with new *in vivo* data and, second, by comparing the fluxes of our small dynamic model to an established genome-scale FBA model, we also did a classical sensitivity analysis by computing all flux, concentration, and parameter control coefficients to assess the impact of parameter



choices on the model behavior. We used the control coefficients in the definition according to

$$C_p^X = \frac{d \ln(X)}{d \ln(p)} \quad (\text{eq. 2})$$

where  $C_p^X$  is the control coefficient of flux, concentration or parameter  $p$  over measure  $X$  (flux or concentration) (Heinrich & Rapoport 1974; Kacser & Burns 1973). It describes how strong a variation of  $p$  affects the steady state values of  $X$ . In this sense, it differs from the approach described before, because it always considers a relaxed system.

The results of this systematic sensitivity analysis are shown in Figure S2. In general, we see a variable influence of most parameters, depending on the given conditions, while no clear trend is apparent. For some parameters, the control coefficients show 2 modes, representing conditions under which the given parameter has an influence or doesn't have an influence (e.g. due to substrate depletion). The same observations hold for fluxes and concentrations.

Notably, the parameter control coefficient of  $f$ , the parameter that determines the balance between F6P and G6P at the PGI reaction was significantly (4-5 times) larger than all other control coefficients.

An overview of this analysis is provided in supplementary section 1.

To identify critical parameters and conditions, control coefficients with values larger than 1.5 were investigated more closely. This is the point at which the distribution of control coefficients exhibits a clear drop and a relatively wide tail, meaning that most values are smaller, but a few are considerably larger than 1.5. Interestingly, these values could not clearly be attributed to certain days or genotypes during acclimation, but largely to fructose, glucose and reactions

connected to them. This suggests a comparably high sensitivity of this part of central carbon metabolism to perturbations within the system. Since this lack of dependence on genotype or duration of cold exposure was an unexpected result, we decided to investigate whether there might be a sensitivity dependence on temperature instead.

### 3.3.2. Model sensitivities are more temperature than genotype specific

The investigation of high value control coefficients revealed two additional indications. First, when comparing the frequency of these values between genotypes the values increase from *bam3* along the flavonoid mutants to Col-0 arriving at *pgm1* with the highest frequency. Thus, defects in either starch synthesis or degradation seem to have opposing effects on this centralization of increased sensitivities around Frc and Glc. Second, when comparing the frequency of high value control coefficients between days, day 0 significantly stands out, having a much smaller frequency (10 compared to 35-50). This means that the described sensitivities around Frc and Glc are particular to low temperatures, as they clearly become more pronounced during and after acclimation to 4°C. Both of these observations are illustrated in Figure 5 A, B.

To investigate differences in nps variation responses between different genotypes or throughout the course of acclimation, a principal component analysis on  $\gamma_x^{\text{nps}}$  was performed. The two components with the highest contribution make up 46.27% (PC1) and 20.41% (PC2) of the differences between the values of all model realizations. The composition of these two

components is given in Table 2. The analysis did not show any apparent trend when comparing different genotypes, but interestingly, it exposed an observation that goes along with the described investigation of high value control coefficients. When comparing the days, day 0 is significantly shifted along the PC1 axis, compared to all other days, as illustrated in Figure 5 C, D. This means that the variation of nps rates affects the system in a considerably different manner before and during

or after the acclimation process. Since PC1 and PC2, together, account for 66.68% of the variation there are still components PC3 and PC4 adding a considerable amount to the variation with 14.72% and 11.77%, respectively. These components were also investigated, but no clusters or other particularities could be observed. A visualization of these components is provided in the supplementary Fig. S2.

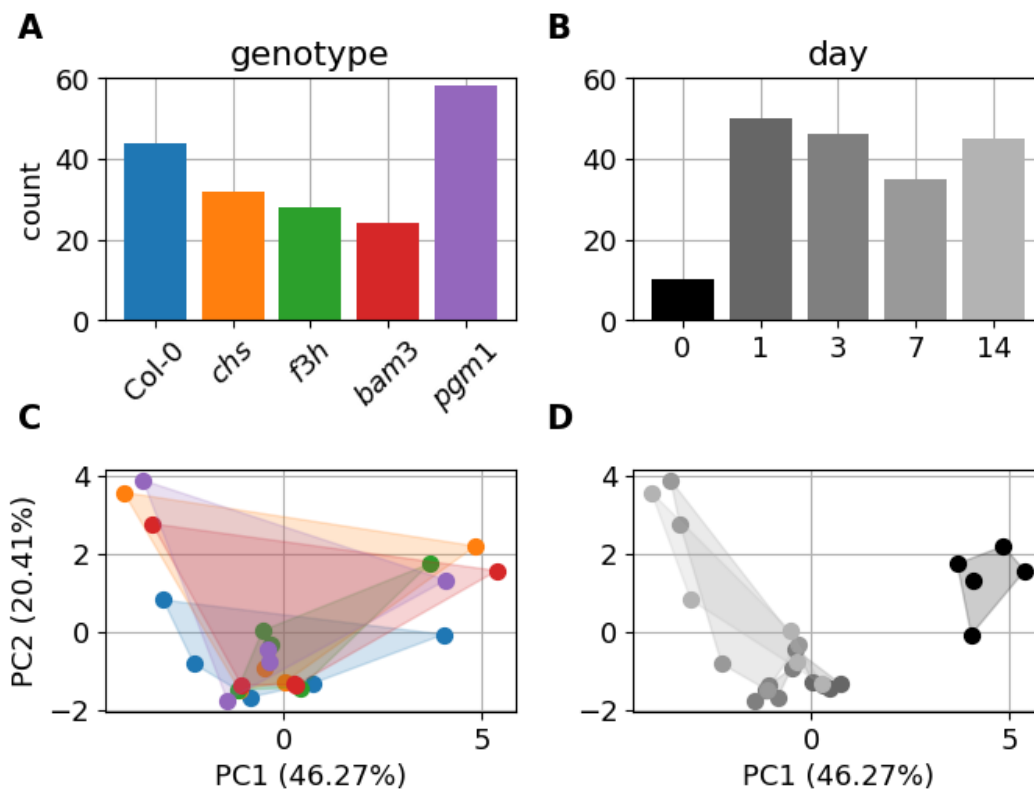


**Figure 5:** Comparison of model features by genotype or day. The upper panel shows the frequency of parameter control coefficients larger than 1.5 for each genotype (A) or day (B). The lower panel shows a two-component PCA for the variations in  $\gamma_x^{nps}$ . The color attribution of the dots in the lower panels correspond to those in the upper panel (A → C, B → D). The shaded areas in the PCA plots serve a better identifiability of related dots.

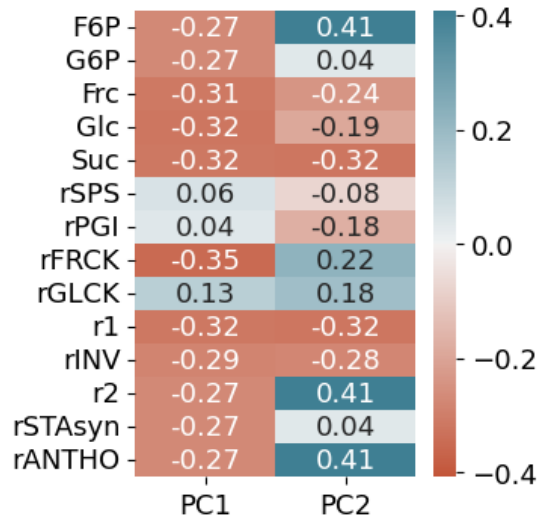


Table 2. PCA component composition

### 3.3.3. Mutants with deficiencies in reactions of the central carbon metabolism exhibit similar deviations from the wild type

An overview of  $\gamma_x^{\text{nps}}$  values for all genotypes and days is given in Figure 6. We see that the rFRCK and rGLCK reactions are particularly sensitive to nps rate variations, and also the concentrations of Frc and Glc have relatively high values over all genotypes. Alongside an increase of rFRCK sensitivity over the course of acclimation, also those of F6P, anthocyanin synthesis and r2 increase. While peaking on day 14 for Col-0 and the flavonoid deficient mutants (*chs* and *f3h*), the peak already occurs on day 7 for the mutants with defects in starch metabolism (*bam3* and *pgm1*). Interestingly, the sensitivities of rFRCK, rGLCK, Frc, Glc are prominent compared to values of other measures, but are in a close range over all genotypes. This becomes evident when looking at the heatmaps in the right part of Fig. 6 depicting the  $\log_2$  fold changes of all  $\gamma_x^{\text{nps}}$  values compared to the corresponding values of

Col-0. The fold changes of rFRCK, rGLCK, Frc, and Glc are always close to zero for all mutants.

Examining the other measures, we see a set of divergence patterns that appear to be conserved over all considered mutants. Clearly, there are apparent quantitative differences, but the qualitative behavior is fairly robust. The fold change for G6P and starch synthesis (rSTAsyn) starts at positive values and constantly declines, switching to negative values around day 3 for all mutants. Values of F6P, anthocyanin synthesis (rANTHO) and r2 start from a low or slightly negative fold change, switch to positive values during acclimation and return to a low or negative value after acclimation or, in the case of *chs*, already at day 7. The reaction fluxes rPGI and rSPS follow a similar pattern but return to low or negative values already at day 7 for all mutants. Here, the flavonoid mutants both show more negative values on day 0 than the starch related mutants. Suc, r1 and rINV start with negative fold changes that vanish during and after acclimation.

When following the mean  $\gamma_x^{\text{nps}}$  values for each genotype over the course of days, as illustrated in the top right corner of Figure 6, one can notice an overall increase of mean absolute sensitivity from day 0 to day 14. Considering Col-0 as the baseline sensitivity, we again see a similar pattern for all mutants, that is comparable to the behavior of PGI and SPS with a stronger decline at the end, due to the contributions of G6P and starch synthesis.

It is difficult to interpret these observations in terms of defined mechanistic insight. However, the emergence of similar divergence patterns from the wild type indicates that common rescue mechanisms might compensate for the deficiencies of these mutants, even if different parts of the central carbon metabolism are affected.

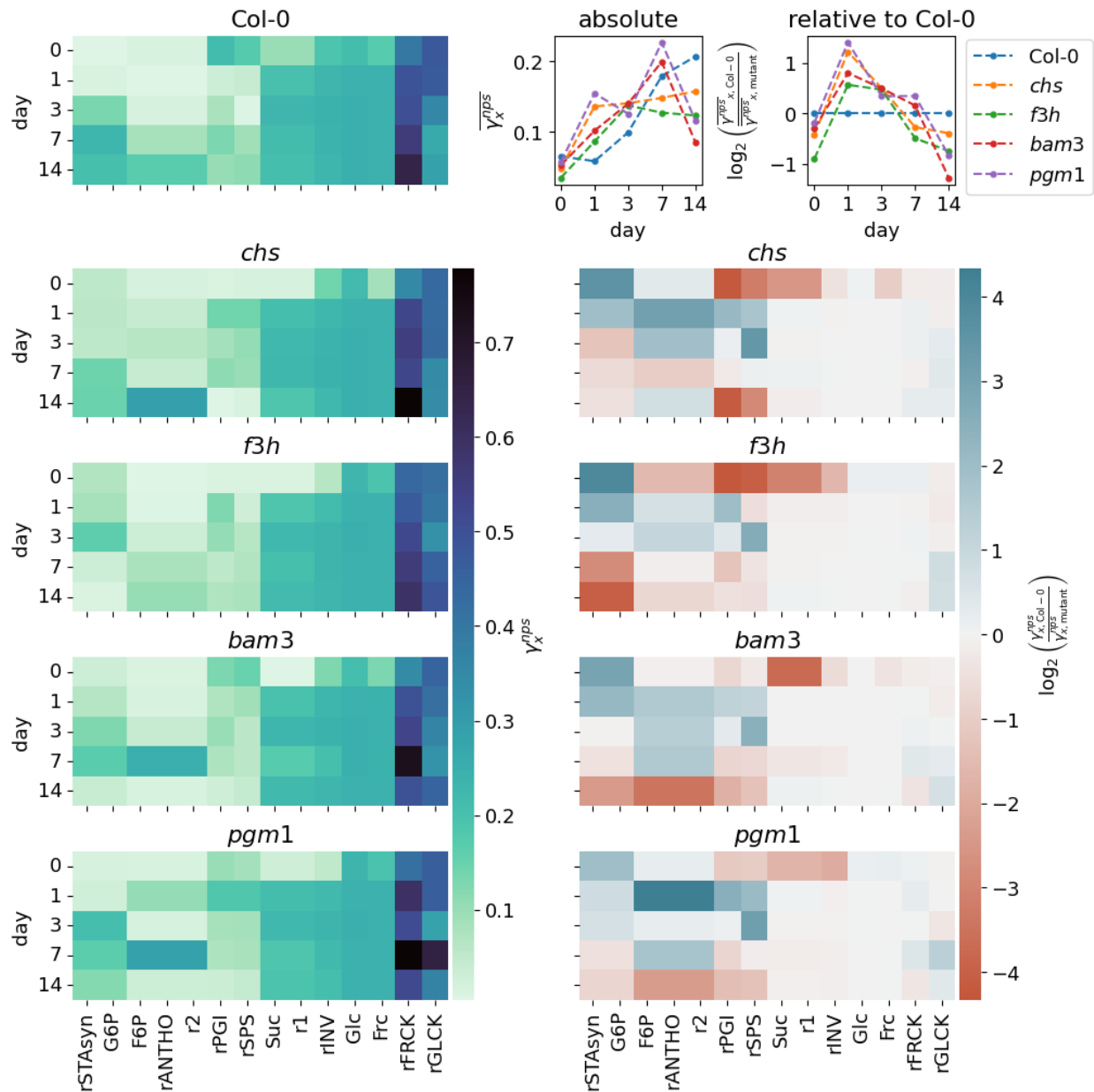


**Figure 6:** Overview of  $\gamma_x^{np5}$  values. The heatmaps on the left side show the  $\gamma_x^{np5}$  values for every model realization. For each genotype the evolution of values can be followed over days from top to bottom. Each column represents a different measure of the model, that is either a metabolite concentration or a flux. They are not ordered by type, but in the sense of related blocks within the model structure. The heatmaps on the right side show  $\log_2$  fold-changes of these values when compared to the corresponding value of Col-0. The panel in the top right corner illustrates the evolution of the geometric mean of all  $\gamma_x^{np5}$  values per day for each genotype. The left panel shows the absolute values, while the right panel, again, shows the  $\log_2$  fold-changes compared to Col-0.

## 4. Discussion

In this study we present an in-depth analysis of a condensed dynamic model of the core central carbon metabolism of *Arabidopsis thaliana* leaves. It is a model that has already been used to identify a role of limitations in sucrose synthesis in carbon partitioning during acclimation (Kitashova et al. 2022). Since it has been shown that light intensity is of great importance for the cold acclimation process of plants and there are complex interactions between cold and light signaling (Szalai et al. 2018), a dynamic sensitivity analysis was defined, and new experiments were performed to assess its applicability. Also, the model has been refined with additional parameter constraints, according to literature (Preiser et al. 2020; Dai et al. 1995; Lou et al. 2007; Qi et al. 2007; Xiang et al. 2011). Certainly, there are different strategies to calibrate dynamic models. We applied a steady state assumption, because we are considering long term changes (days compared to minutes or hours) and there are measures that were estimated as net balance from the experimental data (starch synthesis) for which this assumption is suitable. In terms of parameter estimation, we tried various procedures. These were: (a) finding the best optimization score for each condition individually without further restrictions, (b) for each condition individually with the restrictions explained in the methods section, (c) for conditions sharing the exact same  $K_m/K_i$  values, (d) for each day in a pairwise  $K_m/K_i$  fitting procedure. While (c) did not result in any successful optimization, parameter sets were found for (a), (b) and (d). Their performance in comparison to the experimental data was tested and (b) scored the best. Since it also follows reasonable restrictions for the kinetic

parameters derived from literature, we are confident that it is best suitable and provides the most reliable predictive power for the presented study. Additionally, it has been embedded into a large-scale metabolic network, resulting in flux values that are in good accordance with those derived from dynamic simulations.

Utilizing the presented sensitivity analysis in combination with a classical approach, using control coefficients, revealed several indications: (i) Classical analysis showed a strong influence of the hexose phosphate balance on overall dynamics. (ii) Both, classical and dynamic sensitivity analysis, demonstrate a more pronounced and discernible impact of temperature on the system's sensitivity compared to genotype. Classical analysis shows notable differences between different mutants, by an increase of highly sensitive elements due to a lack of starch, but a decrease due to diminished carbon retrieval from starch or defects in flavonoid synthesis. (iii) The dynamic analysis revealed consistent patterns of response deviation from the wild type among mutants with diverse defects in central carbon metabolism, suggesting shared mechanisms to counteract or compensate for these deficiencies.

When looking at the model structure as shown in Figure 1, at first glance, it seems obvious that  $f$ , the parameter responsible for F6P-G6P balancing in connection to the PGI reaction, can have a strong impact on carbon partitioning, since it defines the fraction of carbon that can flow into the lower right part of the scheme (G6P, Suc, Starch, Glc and Frc) or into the upper left part (F6P, anthocyanins and other pathways), representing primary and secondary

metabolism and carbon recycling, respectively. This does not mean it is used as a main regulator of carbon partitioning *in vivo*, but from a modeling point of view, its value has a strong influence on the overall model behavior. Nevertheless, this relationship needs to be balanced because F6P and G6P are both needed for an adequate flux through the rSPS reaction. Interestingly, when looking at the control coefficients of  $f$  for each system measure, there is a strong positive effect on Glc concentration, but an equally strong negative effect on Frc concentration, which is not immediately obvious by intuition. Here, the negative feedback of G6P plays an important role. Because the F6P/G6P balance emphasizes G6P, but the flux through rSPS is limited, there is an accumulation of G6P, that in turn blocks the activity of glucokinase via a negative feedback, leading to an accumulation of Glc as well. This accumulation of Glc in turn, inhibits invertase activity and consequently leads to a depletion of Frc.

Given the high control coefficients of  $f$ , the rPGI reaction appears to be the most prominent control point for carbon distribution in the system. However, one needs to pay attention to the fact that the presented model is considerably simplified and condensed and the considered rPGI reaction comprises both, plastid and cytosol reactions. Compartmentalization and subcellular organization has been pointed out to play an important role for the central carbon metabolism and in terms of cold acclimation (Hoermiller et al. 2017; Lundmark 2006). It is an appropriate assumption that not only the ratio of hexose phosphates, but also their subcellular proportions are of great importance for the coordination of carbon partitioning. An extension of this study could focus on exploring this aspect. Nonetheless, these observations underline the critical importance of F6P/G6P balancing and a fine-tuned interplay of related

reactions and processes. This notion is in agreement with the indications in Kitashova et al. 2022, as the rSPS reaction directly affects the balance of these hexoses.

Additionally, the new experimental data contains interesting insight connected to F6P/G6P balancing, by revealing that, for starch related mutants, the qualitative changes of F6P concentrations under high light and after acclimation are much closer to those of the wild type, than those of flavonoid related mutants. They increase for longer exposure while those of flavonoid related mutants decrease. With G6P, it is the other way around. For the wild type and flavonoid related mutants G6P concentrations are fairly stable, while those of starch related mutants decrease. Since flavonoid synthesis depends on F6P and starch synthesis depends on G6P, these qualitative deviations from wild type behavior directly indicate the affected parts of central carbon metabolism for each category of mutants.

Although (ii), the more pronounced and discernible impact of temperature, and (iii), the consistent differences to Col-0 in response patterns, are two separate observations, they fit into a coherent picture. Considering a more exposed alteration of the systems sensitivity through a temperature shift compared to the metabolic defects, suggests a successful compensation mechanism for the different mutants and it has been shown that there are mechanisms that can compensate gene knockouts in *Arabidopsis thaliana* (Buzduga 2018). Shared, or partially shared, compensation mechanisms for different deficiencies would be beneficial for the plant, because it would not require a specifically tailored response for all different kinds of limitations, enabling a more economical use of resources. The observed alterations in response patterns hint to a general

or shared mechanism like this because the observed patterns are always of the same quality. If different compensation programs were at play, one would expect more apparent differences between the responses, at least between starch related and flavonoid related mutations, like more pronounced or opposing sensitivity changes for some reactions or metabolites. It has been observed that most metabolic heat shock responses are also responses to cold shock (Kaplan et al. 2004), demonstrating the existence of common stress response mechanisms in the context of central carbon metabolism.

Even though these similarities are remarkable there are noticeable differences. When looking at the temporal evolution of the aggregated sensitivities in Fig. 6, we see that the starch related mutants show the highest deflection and overall deviation from Col-0. Also, the aggregated sensitivity of Col-0 increases up until day 14. While the timecourses of the flavonoid related mutants seem to saturate, the values of the starch related mutants drastically decrease again between day 7 and 14, indicating that this enhanced sensitivity cannot be maintained throughout the acclimation process by these mutants. One can interpret this observation in the sense that defects in the primary metabolism, especially starch might be more severe for successful acclimation, highlighting the central role of starch within this process.

The deviations from the Col-0 sensitivity scores seem not to affect the already sensitive parts of the system around Frc and Glc, even though we see differences in the number of highly sensitive elements between different genotypes. This might be a safety feature of the compensation mechanism, to make sure that these sensitive vital parts are maintained against destabilization. Although, a substantial difference in subcellular reprogramming of

sucrose cleavage by invertase between natural genotypes of *A. thaliana* has been demonstrated with model simulations (Weizmann et al. 2018), this is not necessarily the case between mutant genotypes that are not specialized to grow in different habitats. The high control coefficients for Frc, Glc and neighboring reactions support the concept of a buffering effect of futile cycling against external perturbations (Atanasov et al. 2020; Brauner et al. 2015; Claeysen et al. 2013; Geigenberger & Stitt 1991; Küstner et al. 2019; Nägele et al. 2010; Nägele et al. 2012), since it provides favorable conditions for a fine-tuned and flexible system. The fructokinase and glucokinase reactions also have a high sensitivity to changes in photosynthesis rates. Like this, the system can react fast and reliably to a sudden imbalance of sugars. The multiple feedback inhibitions provide a good backup, preventing overcompensation.

It is worth noticing that on day 0 (before acclimation), there is a significant quantitative difference between the deviations of the flavonol related and the starch related mutants for the rPGI and rSPS reactions. The  $\gamma_x^{nps}$  values of the starch mutants are much closer to Col-0, while the absolute values of the flavonoid mutants are generally lower for these reactions. It might be the case that under normal conditions, these mutants naturally divert less carbon into the secondary pathways, since these are partially defective, so there is more carbon available that can potentially feed primary metabolism, rendering the initial steps less sensitive. This is in accordance with indications from the calibration, where the parameters  $k_{ANT}$  and  $k_{r2}$  have the lowest values for the two flavonol mutants.

Similar compensation programs, as indicated by the similar response patterns, for mutations in different metabolic branches hint to bi- or unidirectional signaling between these

branches. Results from Kitashova et al. 2022 suggest a unidirectional signaling link between starch and flavonoid metabolism. These observations could possibly be connected.

A long-term objective for further investigation is the identification of potential common

compensation mechanisms. It could be part of an already studied stress response. Additionally, the more downstream effects of the investigated mutations in combination with cold stress could be examined to see if and at which level the differences become more specific.

## Funding Information

Deutsche Forschungsgemeinschaft, Grant/Award Numbers: TR175/C06, TR175/D03

## Author Approval and Competing Interests

All authors have read and approved the manuscript.

The manuscript has not been accepted or published elsewhere.

There are no competing interests.

## References (cited)

Adler, S.O., Klipp, E., 2020. Chemical Reaction Networks Possess Intrinsic, Temperature-Dependent Functionality. *Entropy* 22, 117.

Agati, G., Guidi, L., Landi, M., Tattini, M., 2021. Anthocyanins in photoprotection: knowing the actors in play to solve this complex ecophysiological issue. *New Phytol* 232, 2228–2235. <https://doi.org/10.1111/nph.17648>

Arnold, Anne, and Zoran Nikoloski. 2014. “Bottom-up Metabolic Reconstruction of Arabidopsis and Its Application to Determining the Metabolic Costs of Enzyme Production.” *Plant Physiology* 165 (3): 1380–91.

Ashihara, Hiroshi, Alan Crozier, and Atsushi Komamine. 2010. *Plant Metabolism and Biotechnology*. John Wiley & Sons.

Atanasov, V., Fürtauer, L. & Nägele, T. (2020) Indications for a central role of hexokinase activity in natural variation of heat acclimation in *Arabidopsis thaliana*. *Plants*, 9(7), 819.

Austin, M.B., Noel, J.P., 2003. The chalcone synthase superfamily of type III polyketide synthases. *Nat. Prod. Rep.* 20, 79–110. <https://doi.org/10.1039/B100917F>

Boex-Fontvieille, Edouard, Marlène Davanture, Mathieu Jossier, Michel Zivy, Michael Hodges, and Guillaume Tcherkez. 2014. “Photosynthetic Activity Influences Cellulose Biosynthesis and Phosphorylation of Proteins Involved Therein in *Arabidopsis* Leaves.” *Journal of Experimental Botany*



65 (17): 4997–5010.

- Bonente, G., Pippa, S., Castellano, S., Bassi, R., Ballottari, M., 2012. Acclimation of *Chlamydomonas reinhardtii* to different growth irradiances. *J Biol Chem* 287, 5833–5847.
- Brauner, K., Stutz, S., Paul, M. & Heyer, A.G. (2015) Measuring whole plant CO<sub>2</sub> exchange with the environment reveals opposing effects of the *gin2-1* mutation in shoots and roots of *Arabidopsis thaliana*. *Plant Signaling & Behavior*, 10(1), e973822.
- Buzduga, I.M., Volkov, R.A., Panchuk, I.I., 2018. Metabolic compensation in *Arabidopsis thaliana* catalase-deficient mutants. *Cytol. Genet.* 52, 31–39. <https://doi.org/10.3103/S0095452718010036>
- Chalker-Scott, L., 1999. Environmental Significance of Anthocyanins in Plant Stress Responses. *Photochemistry and Photobiology* 70, 1–9. <https://doi.org/10.1111/j.1751-1097.1999.tb01944.x>
- Chalker-Scott, L., 2002. Do anthocyanins function as osmoregulators in leaf tissues?, in: *Advances in Botanical Research*. Academic Press, pp. 103–127. [https://doi.org/10.1016/S0065-2296\(02\)37046-0](https://doi.org/10.1016/S0065-2296(02)37046-0)
- Choi, K., Medley, J.K., König, M., Stocking, K., Smith, L., Gu, S., Sauro, H.M., 2018. Tellurium: An extensible python-based modeling environment for systems and synthetic biology. *Biosystems* 171, 74–79. <https://doi.org/10.1016/j.biosystems.2018.07.006>
- Claeyssen, E., Dorion, S., Clendenning, A., He, J.Z., Wally, O., Chen, J. et al. (2013) The futile cycling of hexose phosphates could account for the fact that hexokinase exerts a high control on glucose phosphorylation but not on glycolytic rate in transgenic potato (*Solanum tuberosum*) roots. *PLoS One*, 8(1), e53898.
- Dai, N., Schaffer, A.A., Petreikov, M., Granot, D., 1995. *Arabidopsis thaliana* hexokinase cDNA isolated by complementation of yeast cells. *Plant Physiol* 108, 879–880. <https://doi.org/10.1104/pp.108.2.879>
- Fürtauer, Lisa, Jakob Weiszmann, Wolfram Weckwerth, and Thomas Nägele. 2019. “Dynamics of Plant Metabolism during Cold Acclimation.” *International Journal of Molecular Sciences* 20 (21). <https://doi.org/10.3390/ijms20215411>.
- Geigenberger, P. & Stitt, M. (1991) A futile cycle of sucrose synthesis and degradation is involved regulating partitioning between sucrose starch and respiration in cotyledons of germinating *ricinus-communis* l. seedlings when phloem transport is inhibited. *Planta*, 185, 81–90.
- Gibon Y, Vigeolas H, Tiessen A, Geigenberger P, Stitt M. 2002. Sensitive and high throughput metabolite assays for inorganic pyrophosphate, ADPGlc, nucleotide phosphates, and glycolytic intermediates based on a novel enzymic cycling system. *The Plant Journal* 30, 221-235.
- Grossman, A., 2000. Acclimation of *Chlamydomonas reinhardtii* to its nutrient environment. *Protist* 151, 201–224.
- Hannah, M.A., Heyer, A.G., Hinch, D.K., 2005. A Global Survey of Gene Regulation during Cold Acclimation in *Arabidopsis thaliana*. *PLOS Genetics* 1, e26. <https://doi.org/10.1371/journal.pgen.0010026>

- Heinrich, R., Rapoport, T.A., 1974. A Linear Steady-State Treatment of Enzymatic Chains. *European Journal of Biochemistry* 42, 89–95. <https://doi.org/10.1111/j.1432-1033.1974.tb03318.x>
- Huber, Steven C., and Joan L. Huber. 1996. "ROLE AND REGULATION OF SUCROSE-PHOSPHATE SYNTHASE IN HIGHER PLANTS." *Annual Review of Plant Physiology and Plant Molecular Biology* 47 (June): 431–44.
- Hoermiller, I.I., Naegle, T., Augustin, H., Stutz, S., Weckwerth, W., Heyer, A.G., 2017. Subcellular reprogramming of metabolism during cold acclimation in *Arabidopsis thaliana*. *Plant, Cell & Environment* 40, 602–610. <https://doi.org/10.1111/pce.12836>
- Kacser, H., Burns, J.A., 1973. The control of flux. *Symp Soc Exp Biol* 27, 65–104.
- Kaplan, F., Kopka, J., Haskell, D.W., Zhao, W., Schiller, K.C., Gatzke, N., Sung, D.Y., Guy, C.L., 2004. Exploring the Temperature-Stress Metabolome of *Arabidopsis*. *Plant Physiol* 136, 4159–4168. <https://doi.org/10.1104/pp.104.052142>
- Kaur, S., Tiwari, V., Kumari, A., Chaudhary, E., Sharma, A., Ali, U., Garg, M., 2023. Protective and defensive role of anthocyanins under plant abiotic and biotic stresses: An emerging application in sustainable agriculture. *Journal of Biotechnology* 361, 12–29. <https://doi.org/10.1016/j.jbiotec.2022.11.009>
- Kingston-Smith, A.H., Harbinson, J., Foyer, C.H., 1999. Acclimation of photosynthesis, H<sub>2</sub>O<sub>2</sub> content and antioxidants in maize (*Zea mays*) grown at sub-optimal temperatures. *Plant, Cell & Environment* 22, 1071–1084. <https://doi.org/10.1046/j.1365-3040.1999.00469.x>
- Kitashova, A., Adler, S.O., Richter, A.S., Eberlein, S., Dziubek, D., Klipp, E., Nägele, T., 2022. Limitation of sucrose biosynthesis shapes carbon partitioning during plant cold acclimation. *Plant, Cell & Environment* 46, 464–478. <https://doi.org/10.1111/pce.14483>
- Kleine, T., Nägele, T., Neuhaus, H.E., Schmitz-Linneweber, C., Fernie, A.R., Geigenberger, P., Grimm, B., Kaufmann, K., Klipp, E., Meurer, J., Möhlmann, T., Mühlhaus, T., Naranjo, B., Nickelsen, J., Richter, A., Ruwe, H., Schroda, M., Schwenkert, S., Trentmann, O., Willmund, F., Zoschke, R., Leister, D., 2021. Acclimation in plants - the Green Hub consortium. *Plant J* 106, 23–40.
- Klotke, J., Kopka, J., Gatzke, N., Heyer, A.G., 2004. Impact of soluble sugar concentrations on the acquisition of freezing tolerance in accessions of *Arabidopsis thaliana* with contrasting cold adaptation – evidence for a role of raffinose in cold acclimation. *Plant, Cell & Environment* 27, 1395–1404. <https://doi.org/10.1111/j.1365-3040.2004.01242.x>
- Korn, M., Peterek, S., Mock, H.-P., Heyer, A.G., Hinch, D.K., 2008. Heterosis in the freezing tolerance, and sugar and flavonoid contents of crosses between *Arabidopsis thaliana* accessions of widely varying freezing tolerance. *Plant Cell Environ* 31, 813–827. <https://doi.org/10.1111/j.1365-3040.2008.01800.x>
- Küstner, L., Nägele, T. & Heyer, A.G. (2019) Mathematical modeling of diurnal patterns of carbon allocation to shoot and root in *Arabidopsis thaliana*. *npj Systems Biology and Applications*, 5(1), 4.
- Lou, Y., Gou, J.-Y., Xue, H.-W., 2007. PIP5K9, an *Arabidopsis* phosphatidylinositol monophosphate kinase,

- interacts with a cytosolic invertase to negatively regulate sugar-mediated root growth. *Plant Cell* 19, 163–181.
- Lundmark, M., Cavaco, A.M., Trevanion, S., Hurry, V., 2006. Carbon partitioning and export in transgenic *Arabidopsis thaliana* with altered capacity for sucrose synthesis grown at low temperature: a role for metabolite transporters. *Plant Cell Environ* 29, 1703–1714. <https://doi.org/10.1111/j.1365-3040.2006.01543.x>
- Monroe, J.D., Storm, A.R., Badley, E.M., Lehman, M.D., Platt, S.M., Saunders, L.K., Schmitz, J.M., Torres, C.E., 2014.  $\beta$ -Amylase1 and  $\beta$ -amylase3 are plastidic starch hydrolases in *Arabidopsis* That Seem to Be Adapted for Different Thermal, pH, and stress conditions. *Plant Physiol* 166, 1748–1763. <https://doi.org/10.1104/pp.114.246421>
- Nägele, T., Henkel, S., Hörmiller, I., Sauter, T., Sawodny, O., Ederer, M., Heyer, A.G., 2010. Mathematical Modeling of the Central Carbohydrate Metabolism in *Arabidopsis* Reveals a Substantial Regulatory Influence of Vacuolar Invertase on Whole Plant Carbon Metabolism. *Plant Physiology* 153, 260–272. <https://doi.org/10.1104/pp.110.154443>
- Nägele, T., Stutz, S., Hörmiller, I. & Heyer, A.G. (2012) Identification of a metabolic bottleneck for cold acclimation in *Arabidopsis thaliana*. *The Plant Journal*, 72(1), 102–114.
- Orth, Jeffrey D., Ines Thiele, and Bernhard Ø. Palsson. 2010. “What Is Flux Balance Analysis?” *Nature Biotechnology* 28 (3): 245–48.
- Owens, D.K., Alerding, A.B., Crosby, K.C., Bandara, A.B., Westwood, J.H., Winkel, B.S.J., 2008. Functional Analysis of a Predicted Flavonol Synthase Gene Family in *Arabidopsis*. *Plant Physiology* 147, 1046–1061. <https://doi.org/10.1104/pp.108.117457>
- Pandolfi, C., Azzarello, E., Mancuso, S., Shabala, S., 2016. Acclimation improves salt stress tolerance in *Zea mays* plants. *J Plant Physiol* 201, 1–8. <https://doi.org/10.1016/j.jplph.2016.06.010>
- Preiser, Alyssa L., Aparajita Banerjee, Nicholas Fisher, and Thomas D. Sharkey. 2018. “Supply and Consumption of Glucose 6-Phosphate in the Chloroplast Stroma.” *bioRxiv*. <https://doi.org/10.1101/442434>.
- Preiser, A.L., Banerjee, A., Weise, S.E., Renna, L., Brandizzi, F., Sharkey, T.D., 2020. Phosphoglucoisomerase Is an Important Regulatory Enzyme in Partitioning Carbon out of the Calvin-Benson Cycle. *Frontiers in Plant Science* 11. <https://doi.org/10.3389/fpls.2020.580726>
- Raue, A., Steiert, B., Schelker, M., Kreutz, C., Maiwald, T., Hass, H., Vanlier, J., Tönsing, C., Adlung, L., Engesser, R., Mader, W., Heinemann, T., Hasenauer, J., Schilling, M., Höfer, T., Klipp, E., Theis, F., Klingmüller, U., Schöberl, B., Timmer, J., 2015. Data2Dynamics: a modeling environment tailored to parameter estimation in dynamical systems. *Bioinformatics* 31, 3558–3560.
- Ristic, Z., Ashworth, E.N., 1993. Changes in leaf ultrastructure and carbohydrates in *Arabidopsis thaliana* L. (Heyn) cv. Columbia during rapid cold acclimation. *Protoplasma* 172, 111–123. <https://doi.org/10.1007/BF01379368>

- Ruoff, P., Zakhartsev, M., Westerhoff, H.V., 2007. Temperature compensation through systems biology: Temperature compensation of fluxes. *The FEBS Journal* 274, 940–950. <https://doi.org/10.1111/j.1742-4658.2007.05641.x>
- Rütgers M, Muranaka LS, Mühlhaus T, Sommer F, Thoms S, Schurig J, Willmund F, Schulz-Raffelt M, Schroda M (2017) Substrates of the chloroplast small heat shock proteins 22E/F point to thermolability as a regulative switch for heat acclimation in *Chlamydomonas reinhardtii*. **Plant Mol Biol** 95: 579-591
- Salon, Christophe, Jean-Christophe Avice, Sophie Colombié, Martine Dieuaide-Noubhani, Karine Gallardo, Christian Jeudy, Alain Ourry, Marion Prudent, Anne-Sophie Voisin, and Dominique Rolin. 2017. “Fluxomics Links Cellular Functional Analyses to Whole-Plant Phenotyping.” *Journal of Experimental Botany* 68 (9): 2083–98.
- Savitch, L.V., Barker-Åstrom, J., Ivanov, A.G., Hurry, V., Öquist, G., Huner, N.P., Gardeström, P., 2001. Cold acclimation of *Arabidopsis thaliana* results in incomplete recovery of photosynthetic capacity, associated with an increased reduction of the chloroplast stroma. *Planta* 214, 295–303. <https://doi.org/10.1007/s004250100622>
- Schulz, E., Tohge, T., Zuther, E., Fernie, A.R., Hinch, D.K., 2015. Natural variation in flavonol and anthocyanin metabolism during cold acclimation in *Arabidopsis thaliana* accessions. *Plant, Cell & Environment* 38, 1658–1672. <https://doi.org/10.1111/pce.12518>
- Seydel, C., Kitashova, A., Fürtauer, L., Nägele, T., 2022. Temperature-induced dynamics of plant carbohydrate metabolism. *Physiologia Plantarum* 174, e13602.
- Sicher, R., 2011. Carbon partitioning and the impact of starch deficiency on the initial response of *Arabidopsis* to chilling temperatures. *Plant Sci* 181, 167–176. <https://doi.org/10.1016/j.plantsci.2011.05.005>
- Shi, M.-Z., Xie, D.-Y., 2014. Biosynthesis and Metabolic Engineering of Anthocyanins in *Arabidopsis thaliana*. *Recent Pat Biotechnol* 8, 47–60. <https://doi.org/10.2174/1872208307666131218123538>
- Somogyi, E.T., Bouteiller, J.-M., Glazier, J.A., König, M., Medley, J.K., Swat, M.H., Sauro, H.M., 2015. libRoadRunner: a high performance SBML simulation and analysis library. *Bioinformatics* 31, 3315–3321. <https://doi.org/10.1093/bioinformatics/btv363>
- Stitt, M., Zeeman, S.C., 2012. Starch turnover: pathways, regulation and role in growth. *Curr Opin Plant Biol* 15, 282–292. <https://doi.org/10.1016/j.pbi.2012.03.016>
- Szalai, G., Majláth, I., Pál, M., Gondor, O.K., Rudnóy, S., Oláh, C., Vanková, R., Kalapos, B., Janda, T., 2018. Janus-Faced Nature of Light in the Cold Acclimation Processes of Maize. *Frontiers in Plant Science* 9.
- Theis J, Lang J, Spaniol B, Ferte S, Niemeyer J, Sommer F, Zimmer D, Venn B, Mehr SF, Mühlhaus T, Wollman FA, Schroda M (2019) The *Chlamydomonas deg1c* mutant accumulates proteins involved in high light acclimation. **Plant Phys** 181: 1480-1497
- Qi, X., Wu, Z., Li, J., Mo, X., Wu, S., Chu, J., Wu, P., 2007. AtCYT-INV1, a neutral invertase, is involved in

- osmotic stress-induced inhibition on lateral root growth in Arabidopsis. *Plant Mol Biol* 64, 575–587.
- Virtanen, O., Khorobrykh, S., Tyystjärvi, E., 2021. Acclimation of *Chlamydomonas reinhardtii* to extremely strong light. *Photosynth Res* 147, 91–106.
- Vranová, E., Atichartpongkul, S., Villarroel, R., Van Montagu, M., Inzé, D., Van Camp, W., 2002. Comprehensive analysis of gene expression in *Nicotiana tabacum* leaves acclimated to oxidative stress. *Proc Natl Acad Sci U S A* 99, 10870–10875. <https://doi.org/10.1073/pnas.152337999>
- Weizmann, J., Fürtauer, L., Weckwerth, W., Nägele, T., 2018. Vacuolar sucrose cleavage prevents limitation of cytosolic carbohydrate metabolism and stabilizes photosynthesis under abiotic stress. *The FEBS Journal* 285, 4082–4098. <https://doi.org/10.1111/febs.14656>
- Welsh, C., Xu, J., Smith, L., König, M., Choi, K., Sauro, H.M., 2023. libRoadRunner 2.0: a high performance SBML simulation and analysis library. *Bioinformatics* 39, btac770. <https://doi.org/10.1093/bioinformatics/btac770>
- Yano, R., Nakamura, M., Yoneyama, T., Nishida, I., 2005. Starch-Related  $\alpha$ -Glucan/Water Dikinase Is Involved in the Cold-Induced Development of Freezing Tolerance in Arabidopsis. *Plant Physiol* 138, 837–846. <https://doi.org/10.1104/pp.104.056374>
- Xiang, L., Le Roy, K., Bolouri-Moghaddam, M.-R., Vanhaecke, M., Lammens, W., Rolland, F., Van den Ende, W., 2011. Exploring the neutral invertase-oxidative stress defence connection in Arabidopsis thaliana. *J Exp Bot* 62, 3849–3862. <https://doi.org/10.1093/jxb/err069>



#### **9.4 Publication 4: Insights into physiological roles of flavonoids in plant cold acclimation**

**Kitashova A**, Lehmann M, Schwenkert S, Leister D, Nägele T (2024) Flavonoid metabolism and its different physiological roles in plant cold acclimation. *The Plant Journal* in print, available online <https://doi.org/10.1111/tpj.17097>

Supplementary material is available at:

<https://onlinelibrary.wiley.com/doi/10.1111/tpj.17097>

## RESOURCE

# Insights into physiological roles of flavonoids in plant cold acclimation

Anastasia Kitashova<sup>1</sup> , Martin Lehmann<sup>2,3</sup> , Serena Schwenkert<sup>2,3</sup> , Maximilian Münch<sup>2,3</sup> , Dario Leister<sup>2,3</sup>  and Thomas Nägele<sup>1,\*</sup> 

<sup>1</sup>Faculty of Biology, Plant Evolutionary Cell Biology, LMU München, Großhaderner Str. 2-4, 82152 Planegg, Germany,

<sup>2</sup>Faculty of Biology, Plant Molecular Biology, LMU München, Großhaderner Str. 2-4, 82152 Planegg, Germany, and

<sup>3</sup>Faculty of Biology, MSBioLMU, LMU München, Großhaderner Str. 2-4, 82152 Planegg, Germany

Received 19 June 2024; revised 7 October 2024; accepted 10 October 2024.

\*For correspondence (e-mail [thomas.naegle@lmu.de](mailto:thomas.naegle@lmu.de)).

## SUMMARY

Flavonoids represent a diverse group of plant specialised metabolites which are also discussed in the context of dietary health and inflammatory response. Numerous studies have revealed that flavonoids play a central role in plant acclimation to abiotic factors like low temperature or high light, but their structural and functional diversity frequently prevents a detailed mechanistic understanding. Further complexity in analysing flavonoid metabolism arises from the different subcellular compartments which are involved in biosynthesis and storage. In the present study, non-aqueous fractionation of *Arabidopsis* leaf tissue was combined with metabolomics and proteomics analysis to reveal the effects of flavonoid deficiencies on subcellular metabolism during cold acclimation. During the first 3 days of a 2-week cold acclimation period, flavonoid deficiency was observed to affect pyruvate, citrate and glutamate metabolism which indicated a role in stabilising C/N metabolism and photosynthesis. Also, tetrahydrofolate metabolism was found to be affected, which had significant effects on the proteome of the photorespiratory pathway. In the late stage of cold acclimation, flavonoid deficiency was found to affect protein stability, folding and proteasomal degradation, which resulted in a significant decrease in total protein amounts in both mutants. In summary, these findings suggest that flavonoid metabolism plays different roles in the early and late stages of plant cold acclimation and significantly contributes to establishing a new protein homeostasis in a changing environment.

**Keywords:** *Arabidopsis thaliana*, plant cold acclimation, photosynthesis, photorespiration, flavonoids.

## INTRODUCTION

Plant metabolism comprises numerous metabolic compounds, belonging to diverse chemical substance classes, which are synthesised, degraded and interconverted enzymatically within comprehensive and highly interconnected metabolic networks. Carbohydrates are direct products of photosynthetic CO<sub>2</sub> fixation and, thus, represent substrates for all further anabolic metabolic pathways. Hence, the metabolism of carbohydrates is tightly linked to carboxylic and amino acids, which altogether represent the building blocks for protein, lipid and nucleotide biosynthesis. Further, they also represent substrates for the biosynthesis of diverse specialised compounds, for example, alkaloids, glucosinolates or flavonoids, which have been shown to protect plants against environmental stressors both biotic

and abiotic, by their specialised functions (Erb & Kliebenstein, 2020).

In many plant species, exposure to low but non-freezing temperatures induces a process termed cold acclimation which increases freezing tolerance. This process has been studied for decades and has revealed numerous molecular and physiological responses that are involved in its regulation (Garcia-Molina et al., 2020; Gilmour et al., 1998; Kaplan et al., 2007; Ristic & Ashworth, 1993; Steponkus, 1984). Adjustment of photosynthesis and carbohydrate metabolism is a central cold acclimation response to prevent or mitigate photoinhibition and unbalanced primary and secondary photosynthetic reactions (Stitt & Hurry, 2002). Sucrose metabolism has been found to play a crucial role in photosynthetic



acclimation (Strand et al., 2003). It has been discussed that adjustment of sucrose phosphate synthase (SPS) activity to low temperature prevents a limitation of triose phosphate/phosphate translocation between cytosol and chloroplasts, which would result in a limitation of photosynthetic ATP biosynthesis (Nägele et al., 2012). Recently, we found evidence for the role of SPS activity in the regulation of carbon fluxes between carbohydrate and flavonoid metabolism during cold acclimation (Kitashova et al., 2023).

While the metabolism of flavonoids is well known to be involved in many plant–environment interactions (Winkel-Shirley, 2002), their physiological role in cold acclimation remains elusive. Flavonoids are phenylpropanoids that are synthesised predominantly from phenylalanine through the shikimic acid pathway. For *Brassica napus*, phenylpropanoid deficiency has been found to result in lowered freezing tolerance and a decreased cold acclimation capacity of photosynthesis (Solecka & Kacperska, 2003). Also, for *Arabidopsis*, a significant impact of flavonoids and their metabolism on cold acclimation capacity and freezing tolerance has been described (Schulz et al., 2015, 2016). Under high light, recent findings suggested flavonoid metabolism to be tightly interconnected with chloroplast carbohydrate metabolism and the SnRK1-related signalling network (Zirngibl et al., 2023). Other studies have provided further evidence for the diverse functional roles of flavonoids, comprising, for example, DNA protection, protection against UV radiation or serving as signalling compounds to affect gene expression (Nakabayashi et al., 2014; Naoumkina & Dixon, 2008; Sarma & Sharma, 1999). These findings, together with observations made in many other studies (for an overview, see Tohge et al., 2018), provide strong evidence for a central role of flavonoids in plant stress response and cold acclimation.

Flavonoid accumulation is typically observed in the vacuole (for an overview, see Pucker & Selmar, 2022). Also, flavonoids have been detected in other compartments, for example, the nucleus and chloroplasts (Agati et al., 2007; Peer et al., 2001). Together with the structural diversity of flavonoids, also the diversity of subcellular localization challenges the analysis of their plant biochemical and physiological functions.

The core pathway of flavonoid biosynthesis is located in the cytosol and comprises activities of chalcone synthase (CHS), chalcone isomerase (CHI), flavanone 3-hydroxylase (F3H), flavonol synthase (FLS), dihydroflavonol 4-reductase (DFR) and anthocyanidin synthase (ANS). Phenylalanine is a precursor of flavonoid biosynthesis and is synthesised in plastids from erythrose 4-phosphate and phosphoenolpyruvate (Rippert et al., 2009). Erythrose 4-phosphate is a product of the Calvin–Benson–Bassham Cycle (CBBC) and, thus, directly links the shikimate pathway and subsequent flavonoid biosynthesis to photosynthetic CO<sub>2</sub> fixation and carbohydrate biosynthesis.

Under changing environmental conditions, for example, low temperature, photosynthetic acclimation prevents unbalanced electron transport, ATP-biosynthesis and enzymatic CO<sub>2</sub> fixation. Photosynthetic acclimation is a comprehensive process that comprises and affects the regulation of redox and ion homeostasis of the chloroplast, protein amounts of photosystems, metabolism and multicompartmental signalling networks (Gjindali & Johnson, 2023). Under low temperature, enzymes of the CBBC have been found to be upregulated to compensate for the decrease in activity due to thermodynamic constraints (Stitt & Hurry, 2002; Strand et al., 1999). Together with the regulation of the central carbohydrate metabolism, for example, the sucrose biosynthesis pathway, these are immediate cold-induced processes, which can be observed during the initial hours and days of a cold acclimation period (Nägele et al., 2011; Savitch et al., 2001). Accumulation of flavonoids and other specialised metabolites typically follows these initial acclimation reactions of primary metabolism, resulting in peak values after several days and up to weeks of cold exposure (Doerfler et al., 2013; Kitashova et al., 2023).

The balance between energy absorbed through photochemistry, photosynthetic electron transport and interconverting metabolic processes, also termed photostasis, plays a critical role in plant–environment interactions in general (Huner et al., 2003). Here, regeneration of NADP<sup>+</sup> as an electron acceptor and ADP as a substrate for the ATP synthase reaction are essential to prevent photoinhibition and generation of reactive oxygen species. The multicompartmental pathway of photorespiration has been discussed to play a central role in balancing ATP and NADPH production and usage (for an overview, see Timm & Hagemann, 2020). Further, photorespiration affects many other pathways due to its role in C1 metabolism, S-metabolism or C/N balance.

To better understand the role of flavonoids during cold acclimation in a pathway-specific context, the present study analysed metabolism in flavonoid-deficient mutants *chs* (also *tt4-11*) and *f3h* (also *tt6-3*) on a compartmental level. While a mutation of the CHS enzyme leads to a general absence of flavonoids, the function of the F3H enzyme can be partially complemented by FLS and ANS (Owens et al., 2008). Here, both mutants were analysed together to reveal traits and effects of plant metabolic cold acclimation, which are due to (i) complete flavonoid deficiency (only in *chs*) or (ii) partial flavonoid deficiency (in *f3h* and *chs*).

## RESULTS

### Flavonoid deficiency affects citrate and glutamate metabolism during cold acclimation

To investigate cold-induced dynamics of the subcellular metabolomes in Col-0, *chs* and *f3h*, leaf tissue was analysed by non-aqueous fractionation coupled with GC–MS

measurements. This methodology revealed plastidial, cytosolic and vacuolar metabolite amounts. An overlap of mitochondrial and plastidial fractions could not be excluded due to technical limitations of compartment separation (see [Materials and methods](#) section). Hence, all results entitled in the following as 'plastidial' might represent an overlap of both compartments. An overview of changes in metabolite abundances on cellular and subcellular levels is provided in the supplements (Figure S6; Table S7). Time series analysis, which compared dynamics of substrate-product relationships in a metabolic network, revealed that particularly citrate and glutamate metabolism (*r23-r25*, see Figure S1) were consistently perturbed in *chs* and *f3h* plants during the full cold acclimation period of 14 days (Figure 1; Figures S2 and S3; Table S1). In Col-0, cytosolic pyruvate, which is the substrate for citrate biosynthesis via the pyruvate dehydrogenase reaction (*r24* in Figure S1), was found to drop significantly during the first 3 days at 4°C and to be stabilised again until 14 days of cold acclimation (Figure S3). In both mutants, the cytosolic pyruvate amounts consistently decreased until 14 days at 4°C. In Col-0 and *chs*, citrate amounts decreased in all compartments until 3 days of cold exposure before they consistently increased again. In *f3h*, cold-induced dynamics of citrate amounts were almost absent. Remarkably, both mutants showed a higher variance of citrate amounts after 14 days at 4°C than Col-0. Furthermore, in *f3h*, a high variance of subcellular citrate amounts was observed across all time points of cold acclimation (Figure 1). Glutamate amounts showed an opposite trend in both mutants compared to Col-0. While cold acclimation resulted in increased glutamate amounts in Col-0 across all compartments, amounts decreased in both mutants at 14 days of 4°C in comparison to non-acclimated plants, and the strongest decrease was observed in the plastidial fraction. Plastidial glutamine amounts in Col-0 decreased after 3 days of cold exposure which was followed by an increase after 14 days. In contrast, *chs* and *f3h* mutants demonstrated opposite trends: both mutants showed an increase in plastidial glutamine after 3 days, with no significant change in *chs* or with a decrease in *f3h* after 14 days at 4°C (Figure 1).

In addition to a perturbed pyruvate and citrate metabolism, also, LC-MS-based proteome analysis revealed that the abundances of pyruvate dehydrogenases (PDHs) and isocitrate dehydrogenases (ICDHs) were affected in *chs* and *f3h* compared to Col-0 (Figure S4). Remarkably, cytosolic ICDH (CICDH, At1G65930) significantly decreased in Col-0 until 3 days at 4°C and stabilised until 14 days. In both mutants, the abundance of CICDH was significantly higher at 3 days and decreased to levels of Col-0 until 14 days. In contrast, mitochondrially located ICDHs showed similar dynamics across all genotypes. Interestingly, in the full data set, that is, comprising all time points and genotypes, CICDH positively correlated with plastidial pyruvate

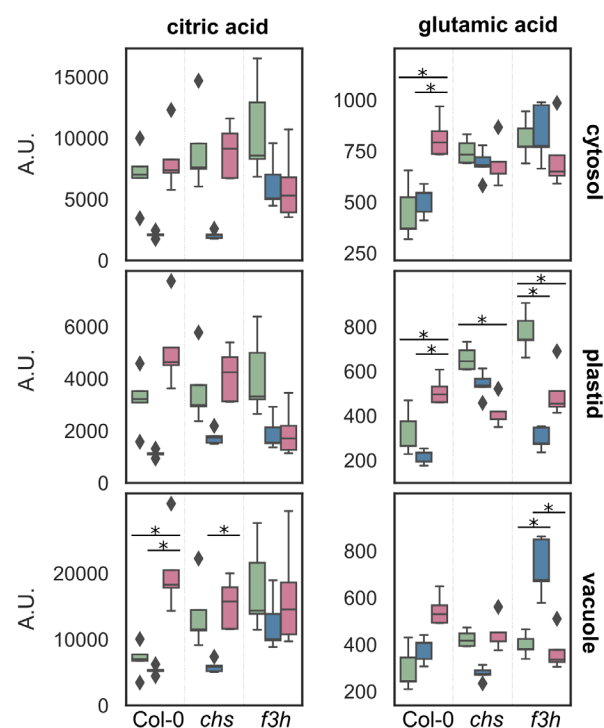


**Figure 1.** Cold-induced subcellular dynamics of citric acid and glutamic acid.

Dynamics of citric acid and glutamic acid in Col-0, *chs* and *f3h* after 0, 3 and 14 days of cold acclimation. A.U., arbitrary units, that is, peak areas normalised to the internal standard and sample dry weight. Green colour represents 0 day; blue: 3 days; magenta: 14 days of cold acclimation; diamonds represent outliers;  $n = 5$ . Asterisks indicate significant difference between time points within genotypes (ANOVA with Tukey HSD,  $P$ -value  $< 0.05$ ). The full list of significance levels is provided in Table S2B.

dehydrogenase (AT1G01090) while it correlated negatively with the mitochondrial IDH2 (AT2G17130) and the mitochondrial PDH component subunit alpha-1 (AT1G59900; Figure 2).

#### Flavonoid deficiency modulates photorespiration, dynamics of amino acid metabolism and tetrahydrofolate-related C1 metabolism

Primary metabolites and lipids were quantified via chromatography coupled with mass spectrometry to reveal the effects of flavonoid deficiencies on metabolism during cold acclimation. Dimensionality reduction by principal component analysis (PCA) showed a general effect of cold acclimation on metabolomes and lipidomes (Figure 3), separating non-acclimated from cold-acclimated samples along PC1, while 3 and 14 days of cold acclimation were separated along PC2. Loadings with the highest contribution to separation along PC1 were carbohydrates (sucrose, maltose, glucose, fructose and raffinose), shikimic acid and glyceric acid. Along PC2, *O*-acetylserine, phosphoglyceric acid, malic acid, quinic acid, xylitol and galactonic acid contributed strongest to the separation (see Table S3).

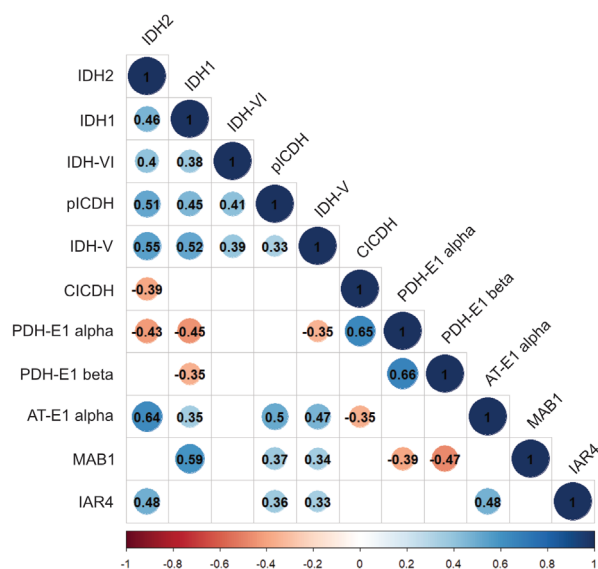


**Figure 2.** Pearson correlation of pyruvate dehydrogenases and isocitrate dehydrogenases.

Numbers show Pearson correlation coefficients; blank fields were not significant ( $P < 0.05$ ). Blue: positive correlation; red: negative correlation. AT2G17130: mitochondrial isocitrate dehydrogenase 2 (IDH2); AT4G35260: mitochondrial IDH1; AT3G09810: mitochondrial IDH-VI; AT5G14590: plastidial isocitrate dehydrogenase (pICDH); AT5G03290: mitochondrial IDH-V; AT1G65930: cytosolic isocitrate dehydrogenase (CICDH); AT1G01090: plastidial pyruvate dehydrogenase component subunit alpha-3 (PDH-E1 alpha); AT1G30120: plastidial PDH component subunit beta-3 (PDH-E1 beta); AT1G59900: mitochondrial PDH component subunit alpha-1 (AT-E1 alpha); AT5G50850: mitochondrial PDH component subunit beta-1 (MAB1); AT1G24180: mitochondrial PDH component subunit alpha-2 (IAR4).

Although the low-temperature exposure had a dominant effect on sample separation (PC1), there was a subtle separation of Col-0 samples from *chs* and *f3h* after 3 days of cold. Thus, the absence of cytosolic flavonoid biosynthesis affected metabolic cold acclimation of primary metabolism, and this effect was most pronounced during the early cold exposure period. An overview of growth phenotypes and PCA loadings, representing the contribution of individual metabolites and lipids to the observed separation, along with the components, is provided in the supplements (Figure S5; Table S3).

As subcellular compartments contribute differently to metabolic cold acclimation (Nägele & Heyer, 2013), subcellular metabolic effects of flavonoid deficiency on primary metabolism were analysed by combining NAF of leaf tissue with GC-MS analysis. Comparing subcellular amounts of metabolites before and after cold exposure (0–3 and 3–14 days) revealed that the strongest effects of flavonoid deficiency on cold-induced metabolic reprogramming, which were conserved across *chs* and *f3h* mutants, were located in the plastid and occurred during the early acclimation period, that is, between 0 and 3 days at 4°C (Figure 4a; Figure S6a,b). The metabolites that contributed most to the separation of the *chs* and *f3h* cluster from

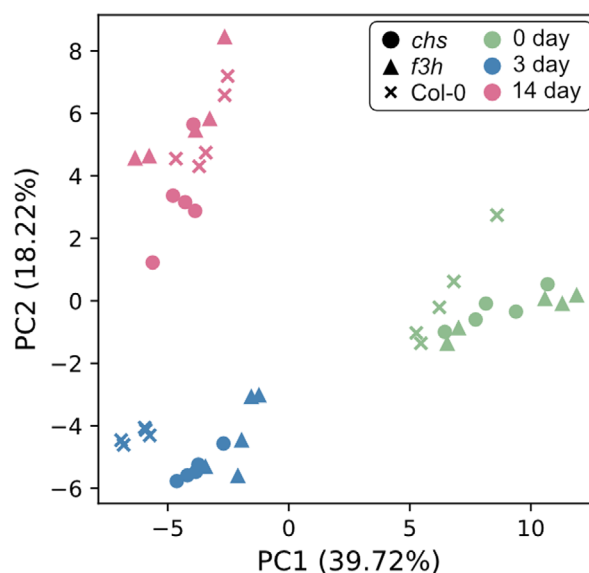


**Figure 3.** Principal component analysis of the cellular metabolome comprising all considered genotypes and time points of cold acclimation.

Circles: *chs*; triangles: *f3h*; crosses: Col-0. Green colour represents 0 days; blue: 3 days; magenta: 14 days of cold acclimation. Detailed information about loadings and components are provided in the supplements (Table S3).

Col-0 at this time point included proline, glycine, serine, fumaric acid, aspartic acid and malic acid. Due to their central role in photorespiration, the observed accumulation of glycine and a decrease in serine amounts suggested an effect in the regulation of photorespiration in both mutants (Figure 4b). Moreover, glutamine and fumaric acid were found to increase in both mutants while amounts decreased in Col-0 (Figure 4a). Additionally, *chs* plants were found to accumulate plastidial carbohydrates more than Col-0. These were glucose, fructose, raffinose, glucose 6-phosphate, trehalose and sucrose after 3 days of cold exposure (Figure 4a).

After 3 days of cold exposure, both mutants showed significantly higher amounts of amino acids than Col-0 in all three analysed compartments (Figure S7). In the cytosol and vacuole, there were notable differences between the *chs* and *f3h* mutants. The *f3h* mutant formed a distinct cluster and showed a stronger accumulation of amino acids than *chs*. While serine levels did not change significantly in these compartments, glycine peaked after 3 days, especially in the vacuole of both *chs* and *f3h* mutants. Interestingly, both *chs* and *f3h* showed stronger accumulation of cytosolic raffinose (Figure S6a).

Given the pronounced effect on amino acids, changes in the proteome were quantified with functional relation to amino acid biosynthesis (Figure 4c; Table S4). Also, in the proteome, a similar hierarchical clustering of *chs* and *f3h* mutants became evident after 3 days of cold exposure. The

proteins contributing most to this clustering were 5'-adenylsulfate reductase 3 (APR3), 4-hydroxy-tetrahydrodipicolinate reductase 1 (DAPB1), bifunctional aspartate aminotransferase and glutamate/aspartate-

prephenate aminotransferase (PAT), phosphoserine phosphatase (PSP), serine O-acetyltransferase 3 (SAT3) and TSK-associating protein 1 (TSA1; Figure 4c). APR3, PAT, PSP and SAT3 are involved in serine metabolism, which

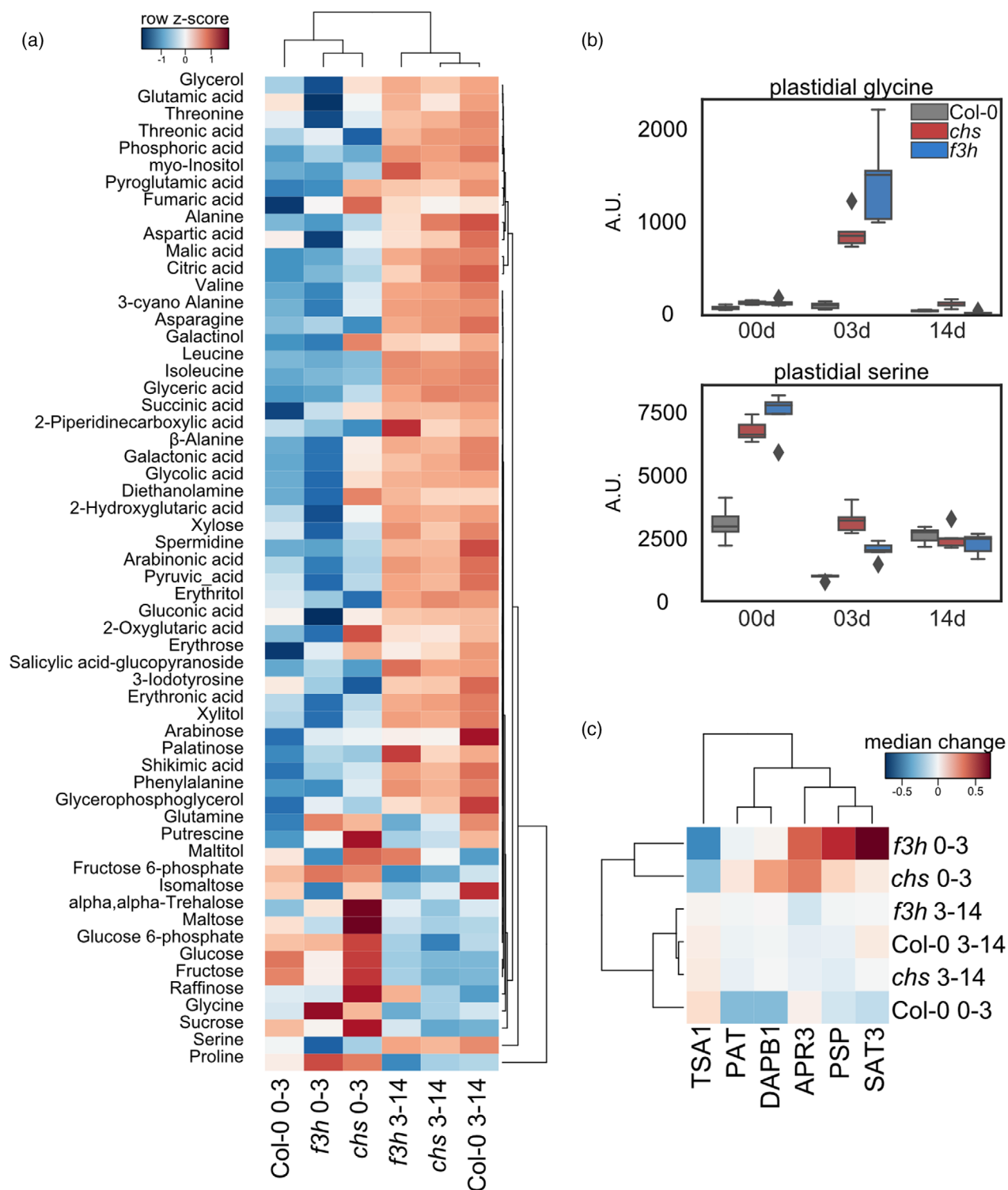


**Figure 4.** Plastidial metabolic cold acclimation.

(a) Hierarchical cluster analysis of the subcellular metabolite abundance change rate in plastid between Col-0 and flavonoid mutants. Rates were calculated between 0 and 3 (0–3) and 3 and 14 (3–14) days of cold acclimation (e.g.,  $\text{rate} = [\text{median}_{3 \text{ day}} - \text{median}_{0 \text{ day}}]/3$ ) in Col-0, *chs* and *f3h*. Results are displayed in a dendrogram and a heatmap indicating relationships between metabolites and samples based on Euclidean distance and complete-linkage clustering. The values were column-wise standardised using the z-score method.

(b) Plastidial glycine and serine dynamics in Col-0, *chs* and *f3h* after 0, 3 and 14 days of cold acclimation. A.U., intensities normalised to the internal standard and sample dry weight. Grey: Col-0; red: *chs*; blue: *f3h*;  $n = 5$ . The list of significance levels (ANOVA with Tukey HSD) is provided in Table S2B.

(c) Hierarchical cluster analysis of the top 6 amino acid biosynthesis pathway-associated protein abundances contributing to the separation of *chs* and *f3h* mutants and Col-0 after 3 days of cold acclimation. Complete information about Euclidean distances in the cluster analysis of the amino acid biosynthesis-related protein dynamics can be found in Table S4. Protein abbreviations: APR3, 5'-adenylylsulfate reductase 3; DAPB1, 4-hydroxy-tetrahydrodipicolinate reductase 1; PAT, bifunctional aspartate aminotransferase and glutamate/aspartate-prephenate aminotransferase; PSP, phosphoserine phosphatase; SAT3, serine O-acetyltransferase 3; TSA1, TSK-associating protein 1.

further suggests a differential regulation of the photorespiratory pathway in flavonoid mutants.

Based on the observed differential response of metabolic mutants in amino acids and enzymes related to serine metabolism, protein dynamics in the photorespiratory pathway with its connection to nitrogen, tetrahydrofolate-related C1, sulphur and methionine metabolism were analysed (Figure 5). The most significant effects in the flavonoid mutants were observed in photorespiration reactions following the serine-hydroxymethyltransferase 1 (SHM1) reaction. In contrast to Col-0 and *f3h*, the *chs* mutant was not significantly affected in SHM1. Simultaneously, the levels of serine:glyoxylate aminotransferase (SGAT), glycinate kinase (GLYK) and plastid glycolate glycerate transporter 1 (PLGG1) decreased in *chs* during the initial 3 days at 4°C. Additionally, ferredoxin-dependent glutamine:oxoglutarate aminotransferase (Fd-GOGAT) and the exchange of glutamic acid and 2-oxoglutaric acid across the plastid membrane were downregulated in *chs* plants. Notably, the *chs* mutant showed higher abundances of SHM1 and serine O-acetyltransferase 3 (SAT3), along with slightly elevated abundances of O-acetylserine (thiol) lyase C (OASC). Consequently, dynamics were observed in tetrahydrofolate-related (THF-related) C1 metabolism. 5-formyl-THF acts as a (potential) inhibitor of SHM1, and an increased abundance of 5-formyltetrahydrofolate cyclo-ligase (5-FCL), that interconverts 5-formyl-THF into 5,10-methenyl-THF, in *chs* could possibly indicate a feedback regulation of glycine/serine ratio in mitochondria. The *chs* mutant showed an upregulated phosphorylated pathway of serine biosynthesis, which is a possible response in the plastid to alternations in serine-consuming pathways in the mitochondria. THF-related C1 metabolism connects photorespiration with methionine metabolism in the cytosol, and S-adenosylmethionine synthase (SAM1) abundance showed a stronger reduction in Col-0 than in *chs* and *f3h* mutants after 3 days of cold exposure (Figure 5). To validate if the deficiency of flavonoids leads to changes in photorespiration, net CO<sub>2</sub> assimilation rates were quantified as functions of light intensities and CO<sub>2</sub> concentrations. From these measurements, CO<sub>2</sub> compensation

points, that is, the CO<sub>2</sub> concentrations at which NPS became 0, were calculated (Figure S8). Both flavonoid mutants showed higher CO<sub>2</sub> compensation points than Col-0 after 3 days of cold acclimation, with the highest difference between *chs* and Col-0 of 17.6 μmol mol<sup>-1</sup> (Figure S8c). This suggested higher rates of photorespiration in *chs* and *f3h*. Since no major differences were observed in glycine decarboxylase (GDC) abundance between the three genotypes, the increase of abundance of formate dehydrogenase (FDH) in *chs* and *f3h* indicated higher activity of this enzyme. This increase in FDH activity could contribute to a higher rate of CO<sub>2</sub> release, affecting the overall balance between photosynthesis and photorespiration (Figure 5). In summary, flavonoid metabolism appears to affect photorespiration and, consequently, plastidial amino acid metabolism after 3 days of cold exposure.

Two mitochondrial proteins involved in THF-related C1 metabolism, 5-formyltetrahydrofolate cyclo-ligase (5-FCL) and FDH, were detected and quantified by the LC-MS/MS proteomics approach in the present study, and the deficiency of flavonoids had an impact on both of them (Figure 5). The THF-related C1 metabolism is connected to the flavonoid biosynthesis pathway through the shikimate pathway, chorismate and the biosynthesis of para-aminobenzoic acid (Kotlon et al., 2022). Although shotgun proteomics applied in the present study could not detect or quantify all proteins of THF metabolism, similar dynamics in aminodeoxychorismate lyase abundance in *chs* and Col-0 suggested that flavonoids might interact with THF-related C1 metabolism not only by influencing precursor availability but also by direct interactions with central enzymes of this pathway. Evidence from a study on mice suggested a possible direct interaction between isoquercetin and cytosolic C-1-THF synthase (C1TC), a homologue of the bifunctional 5,10-methylene-THF dehydrogenase/5,10-methenyl-THF cyclohydrolase (FOLD1, 2, 3 and 4) proteins in Arabidopsis (Manzoor et al., 2022). The mitochondrial FOLD1 protein and its homologues in plants, yeast, mice and humans are evolutionarily related (Figure 6a). The structural alignment between the mitochondrial FOLD1 protein of Arabidopsis



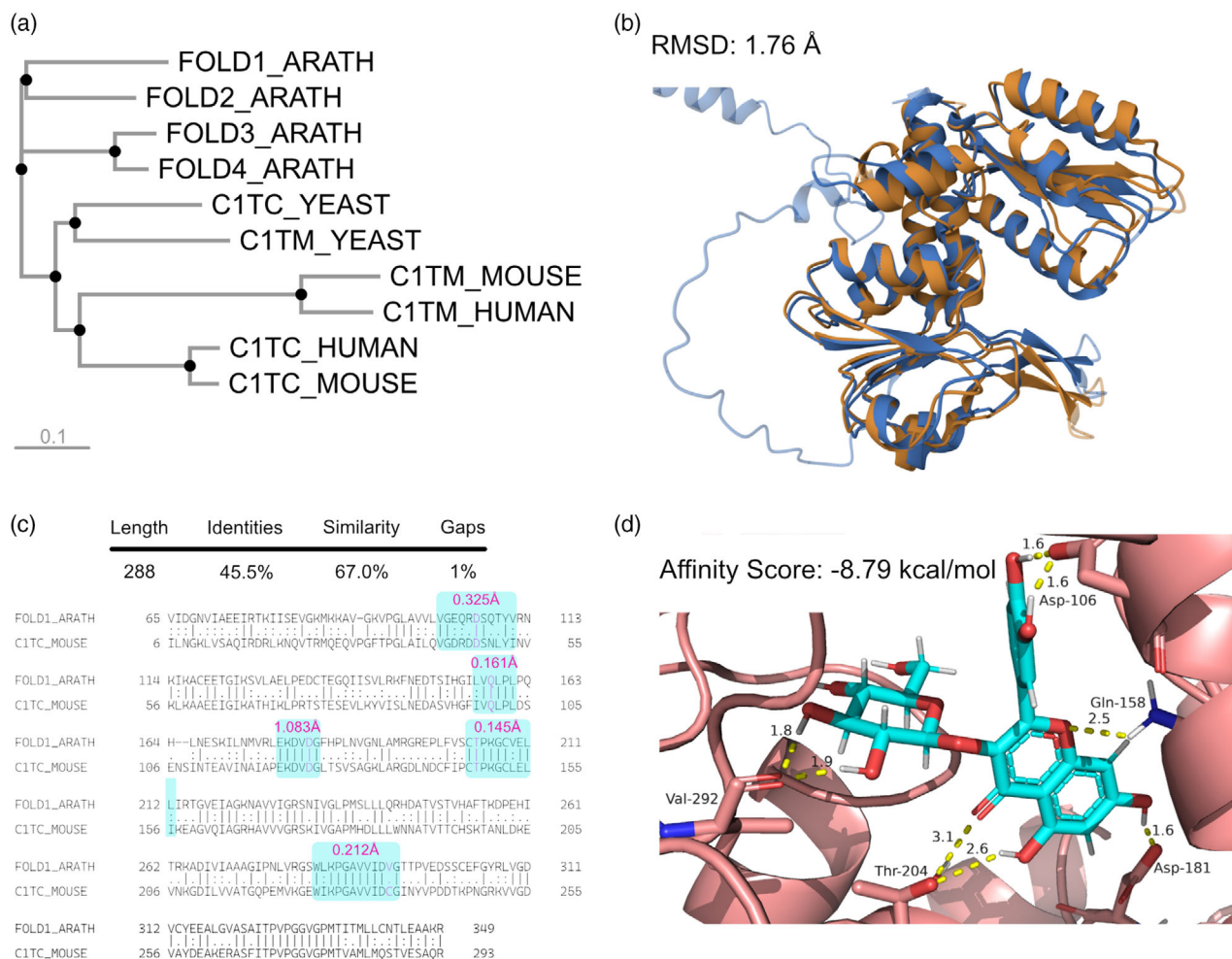


**Figure 6.** Bifunctional 5,10-methylene-THF dehydrogenase/5,10-methenyl-THF cyclohydrolase (FOLD1) protein analysis.

(a) Phylogenetic tree of FOLD1 and its homologues with the Neighbour-Joining method demonstrating common ancestry of these proteins. The branch length represents the number of substitutions per site. C1TC, cytosolic enzyme of yeast, mouse and human; FOLD2/3/4, plastidial enzymes of Arabidopsis; FOLD1, cytosolic enzyme of Arabidopsis.

(b) Pairwise protein structure alignment of Arabidopsis FOLD1 (blue) and dehydrogenase/cyclohydrolase functional domain of cytosolic mouse C1-THF-synthase protein (orange) with root mean square deviation (RMSD) of 1.76 Å.

(c) Pairwise amino acid sequence alignment of Arabidopsis FOLD1 and dehydrogenase/cyclohydrolase functional domain of cytosolic mouse C1-THF-synthase protein. Turquoise colour indicates highly conservative regions of the protein that potentially interact with isoquercetin. Pink colour indicates interacting with isoquercetin amino acid residues; pink text indicates alignment RMSD of the highlighted regions.

(d) 3D interaction between the FOLD1 and isoquercetin after molecular docking analysis. Cyan colour: carbon backbone of isoquercetin molecule; salmon: carbon backbone of FOLD1; red: oxygen; grey: hydrogen; blue: nitrogen atoms. Yellow dashed lines represent polar contacts within 5 Å of the isoquercetin, numbers represent the distance in Å between the interacting atoms of isoquercetin and amino acid residues. The 3D model is provided in Supplementary File S1 and the molecular docking energy information is provided in Table S5.

supported a possible intermolecular interaction (Table S5). These findings suggest that flavonoids and their precursors affect THF-related C1 metabolism, and consequently, photorespiration.

Four amino acids involved in the interaction of isoquercetin and FOLD1 (Asp-106, Gln-158, Asp-181 and Thr-204) were identical between Arabidopsis and mouse (Figure 6c). A molecular docking experiment on the mouse C1TC protein revealed a binding pocket similar to that in Arabidopsis, with an affinity score of

-8.075 kcal mol<sup>-1</sup> (Supplementary File S2). This interaction in the C1TC protein involved four amino acids, three of which were identical to Asp-106, Gln-158 and Asp-181 in Arabidopsis. Alignment of the individual regions of FOLD1 and C1TC proteins that contain interacting amino acid residues revealed similar 3D structures, with an RMSD varying between 0.145 and 1.083 Å. The evolutionary conservation profile of the FOLD1 protein revealed these interacting amino acids to be highly conserved and exposed functional residues (Figure S9), further supporting the

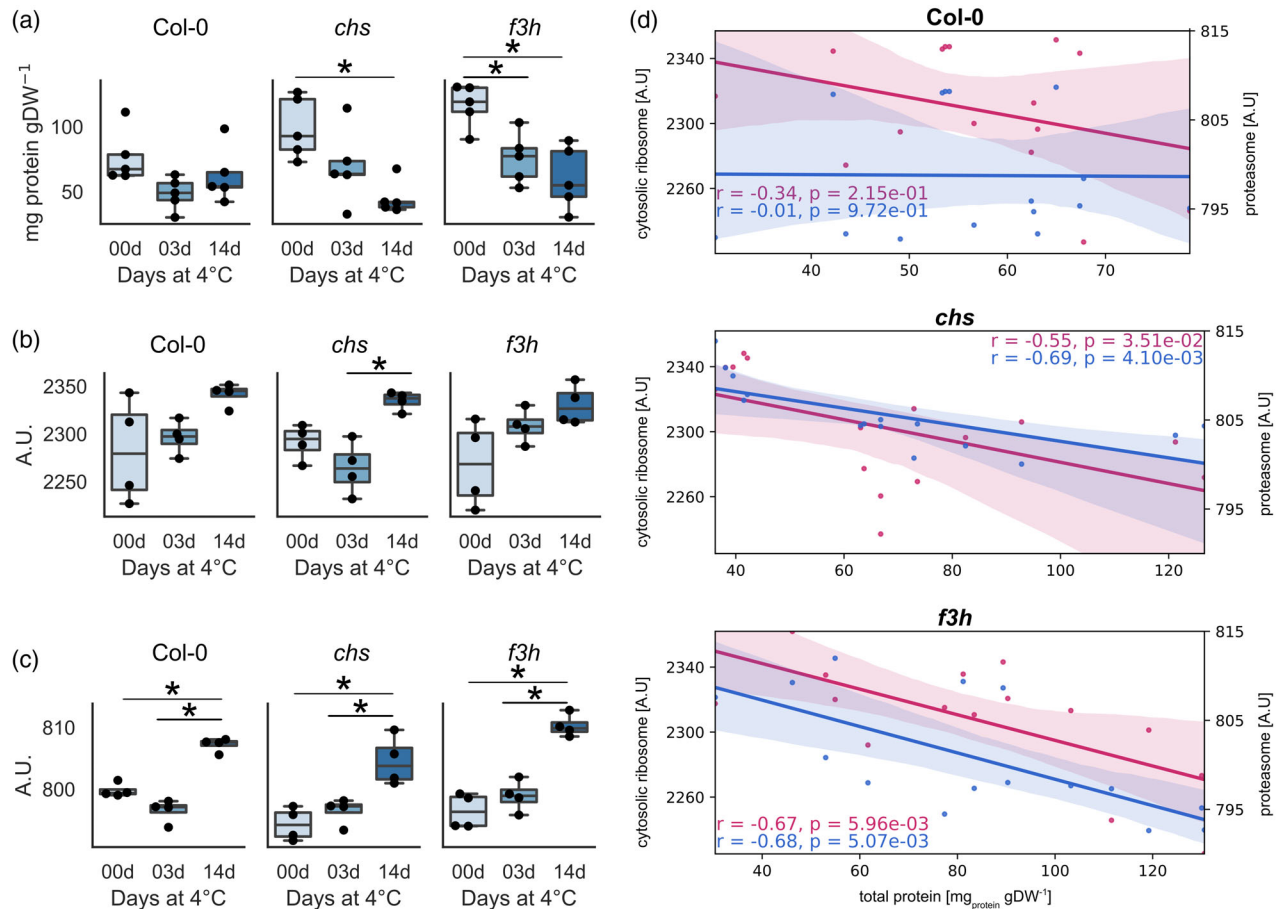


**Figure 7.** Total protein amounts during cold acclimation.

(a) Total protein amount; (b) cytosolic ribosome and (c) proteasome-associated protein abundance in *Col-0*, *chs* and *f3h* before (0 day) and after (3 or 14 days) of cold acclimation. A.U., log<sub>2</sub> transformation of LFQ intensities. Points represent biological replicates ( $n \geq 4$ ), asterisks represent significant differences (ANOVA with Tukey HSD,  $P$ -value < 0.05), and the full list of significance levels is provided in Table S2A.

(d) Pearson correlation analysis between total protein amount (x-axis) and cytosolic ribosome-associated protein abundance (primary y-axis, pink), and between total protein amount (x-axis) and proteasome-associated protein abundance (secondary y-axis, blue) in *Col-0*, *chs* and *f3h* across 0, 3 and 14 days of cold acclimation. Points represent independent replicates,  $n = 5$ ; the solid line represents linear regression and the shaded area represents the confidence interval of the linear regression.

hypothesis of a conserved interaction mechanism between flavonoids and FOLD1 and its homologues.

### Flavonoid deficiency affects total protein amounts and proteasomal compounds

Flavonoid deficiencies were found to affect amino acid metabolism (Figures 1, 4, and 5). To determine whether these dynamics in amino acid metabolism might also have an impact on protein homeostasis, the total protein amount was quantified photometrically in a Bradford assay and normalised to dry weight (Figure 7a). During the first 3 days of cold acclimation, total protein amounts decreased across all genotypes, with the *chs* and *f3h* mutants showing a more pronounced decrease than *Col-0*. Additionally, between 3 and 14 days, protein amounts in both mutants were found to further decline, while *Col-0*

stabilised its protein homeostasis. Overall, between 0 and 14 days, the *chs* mutant showed the most significant reduction in total protein level, with a median decrease of more than 2-fold. In contrast, *Col-0* showed a stabilised protein content after 14 days of cold acclimation, with only a 1.2-fold decrease (Figure 7a). After 3 days of cold, both *chs* and *f3h* mutants exhibited similar or higher levels of amino acids in the plastid, cytosol and vacuole compared to *Col-0* (Figure S7). After 14 days, both mutants showed reduced amino acid levels in the cytosol, although *chs* still had more than after 3 days. Only in *f3h*, amino acid levels in the cytosol significantly decreased after 14 days, indicating that the protein decrease in *chs* and *f3h* was not generally due to a general lack of substrates for protein biosynthesis, but rather due to alterations in the regulation of protein biosynthesis and/or degradation.



During early (0–3 days) and later (3–14 days) stages of cold acclimation, genotypes could be distinguished by dynamics of abundances of (cytosolic) ribosomal and proteasomal proteins (Figure 7). During the first 3 days of cold, compounds of the cytosolic ribosome showed an insignificant differential trend in *chs* plants, with ribosome abundance slightly decreasing during the first 3 days at low temperature (Figure 7b). In contrast, Col-0 and *f3h* medians increased in this period. On the other hand, during the same period, protein abundance of proteasomal compounds decreased in Col-0 but increased in both flavonoid mutants, potentially contributing to the initial decline in protein content (Figure 7c). During the later cold acclimation period, that is, after 14 days, both mutants displayed a wild-type-like increase in the cytosolic ribosome and proteasome abundance (Figure 7b,c). Pearson correlation analysis between total protein amount and either cytosolic ribosome abundance or proteasome abundance revealed a strong significant negative correlation throughout the whole period of cold acclimation in *chs* and *f3h*, but not in Col-0 (Figure 7d). This finding suggests a complex interaction between ribosome and proteasome machinery and flavonoid accumulation during the later stages of cold acclimation.

Differential protein abundance GO enrichment analysis on the whole proteome dynamics in the *chs* mutant after 14 days of cold revealed an increase of proteins related to cytoplasmic translation, proteasomal protein catabolic process and ribosome assembly (Table S6). Moreover, unlike Col-0, both *chs* and *f3h* did not show an upregulation of ‘protein folding’. In summary, these results suggest an effect (direct or indirect) of flavonoids on protein biosynthesis, degradation and folding.

## DISCUSSION

### Flavonoid deficiency affects the C/N interface during cold acclimation

Metabolic acclimation of plants during cold exposure has been described in many studies to comprise and affect a large array of enzymatic reactions and transport processes across intracellular membrane systems which ultimately results in adjustment of metabolite concentrations (see Garcia-Molina et al., 2020; Hannah et al., 2006; Hoermiller et al., 2017; Korn et al., 2008; Koster & Lynch, 1992). Although many of these metabolic adjustments are strong and significant, frequently, their physiological function remains elusive. This might be due to the high number of enzymes involved in biosynthesis, degradation and compartmental sequestration which contribute to the physiological function. For example, the accumulation of soluble carbohydrates, for example, sucrose, hexoses and raffinose oligosaccharides is a well-known cold response of diverse plant species (Alberdi et al., 1993; Kaplan

et al., 2004; Klotke et al., 2004; Koster & Lynch, 1992). Although biophysical studies provided evidence for the protective functions of carbohydrates during cold and freezing *in vitro* (Hincha et al., 2003), the *in vivo* function can hardly be predicted without subcellular localization (Knaupp et al., 2011; Zuther et al., 2004).

Based on such observations, in the present study, plant metabolism was resolved to a subcellular and compartment-specific level to reduce the ambiguity of functional interpretation of metabolite dynamics. Time series analysis of GC–MS derived metabolomics data unravelled a cold-induced perturbation of citrate and glutamate metabolism in *chs* and *f3h* mutants (see Figure 1; Figure S2). Subcellular proteomics suggested a shift of ICDH activity from mitochondria to the cytosol due to flavonoid deficiency (see Figure 2; Figure S4). Such a cytosolic bypass was discussed earlier in the context of C/N balance and interconversion of citrate storage outside the mitochondria (Sweetlove et al., 2010). Even more, for illuminated leaves, such non-cyclic TCA cycle flux modes were shown to reduce PDH-catalysed decarboxylation rates by up to 75% (Tcherkez et al., 2009). Carbon skeletons of such fluxes are then substrates for glutamate and glutamine biosynthesis. Due to the finding that both metabolites over-accumulated in the cytosol and plastids of *chs* and *f3h* during the first 3 days of cold acclimation, this suggests that flavonoid deficiency affects, or maybe even co-regulates, the C/N balance during cold exposure. Also, previous work suggested that a high C/N ratio under low nitrogen availability increases flavonoid content (Li et al., 2023). Further, flavonoid pathway activators *PAP1* and *PAP2* were found to strongly respond to low temperature and low nitrogen (Olsen et al., 2009). Together with the data of the present study, this suggests that C/N balance and flavonoid metabolism are mutually regulated. This is also supported by the finding that in *chs*, both GOGAT enzymes and plastidial dicarboxylate transporters were significantly downregulated during the initial cold acclimation period. Hence, during the early phase of cold acclimation, flavonoid biosynthesis may stabilise plastidial C/N metabolism and, indirectly, photosynthesis by consuming carbon skeletons in the cytosol which originate from citrate metabolism. Finally, this might connect mitochondrial, cytosolic and plastidial redox and energy balance under environmental fluctuation.

Flavonoid biosynthesis results from a combination of the phenylpropanoid pathway and the acetate pathway (Perez de Souza et al., 2020). Acetyl-CoA plays a central role in multiple pathways, including citrate metabolism. Based on the observation that CICDH positively correlated with PDH-E1 alpha (see Figure 2), this suggests that flavonoid deficiency could affect the metabolic flux through the acetate pathway in a feedback manner. This, in turn, would increase the availability of acetyl-CoA for other pathways,

such as fatty acid and lipid biosynthesis. Indeed, flavonoid deficiency was associated with a significant increase in triacylglycerols under cold (Tables S3 and S7 and S7), further suggesting a potential role of flavonoids in the regulation of associated pathways.

### Flavonoid metabolism interacts with photorespiration and amino acid metabolism

The analysis of primary metabolism revealed a strong and significant effect of flavonoid deficiency on amino acid metabolism, and this effect was most pronounced in plastids (see Figure 4). While it may not be surprising that the metabolism of aromatic amino acids, which are precursors for flavonoid biosynthesis, are affected in *chs* and *f3h* mutants, it is even more interesting to see emphasised effects in the photorespiratory intermediates glycine and serine. Due to experimental limitations of the NAF protocol, in which separation of plastidial and mitochondrial metabolomes remains difficult (Fürtauer et al., 2019), the presented data cannot be exclusively interpreted as plastidial or mitochondrial metabolite concentrations. However, due to the accumulation of the substrate glycine and the depletion of the product serine of the mitochondrial SHM1-catalysed reaction, it appears plausible that the observed metabolic phenotype is due to affected photorespiratory regulation. Further, quantified protein dynamics suggested that deficiencies in the flavonoid biosynthesis pathway resulted in upregulated plastidial serine biosynthesis (see Figure 5). This might be a consequence of a depleted mitochondrial serine pool which limits its availability for cellular functions and might be compensated for by this plastidial bypass. Plastidial proteins PGDH, PSP and SHM3 were found to be upregulated in both *chs* and *f3h* plants. Simultaneously, cysteine biosynthesis via *O*-acetylserine was upregulated during the first 3 days of cold acclimation in these mutants which further indicates that mitochondrial deficiencies in serine biosynthesis may have been compensated for in the plastids. Additionally, the alternations in photorespiration caused by mutations in the flavonoid biosynthesis pathway led to a shift in CO<sub>2</sub> compensation points in *chs* and *f3h* after 3 days of cold acclimation, potentially due to increased activity of FDH.

In mitochondria, SHM1 catalyses the interconversion of glycine to serine which comprises a methylene transfer from 5,10-methylene-THF (Shi & Bloom, 2021). Alternatively, 5,10-methylene-THF might be interconverted into 5,10-methenyl-THF, catalysed by FOLD1 (AT2G38660), which represents a bifunctional 5,10-methylene-THF dehydrogenase/5,10-methenyl-THF cyclohydrolase being localised to mitochondria (Collakova et al., 2008; Groth et al., 2016). The competitive inhibitor of SHM1 and other folate-dependent enzymes, 5-formyl-THF, is synthesised by SHM1 in the presence of glycine (Stover & Schirch, 1990). In *chs* plants, a significant and strong upregulation of

5-FCL during the first 3 days at 4°C was observed which metabolises 5-formyl-THF (Roje et al., 2002). Even though 5-FCL was also upregulated in Col-0, the upregulation was stronger in both flavonoid mutants and only significant in *chs* (Figure 5). Although so far not described in plants, quercetin uptake by mitochondria was reported for human cells (Fiorani et al., 2010). Thus, a potential explanation for the upregulation of 5-FCL in *chs* might be that metabolic compounds or pathways that are affected by the *chs* mutation represent potential inhibitors of 5-formyl-THF biosynthesis. Indeed, the FOLD1-homologue in mice, C1TC, was observed to be inhibited by isoquercetin, which is produced downstream of CHS (Manzoor et al., 2022). Isoquercetin and quercetin were shown to interact with FOLD1 *in silico* (see Figure 6). However, isoquercetin, due to its glucoside moiety, formed more connections and had a slightly lower affinity score than quercetin (−8.79 vs. −8.02 kcal mol<sup>−1</sup>; see Table S5), potentially establishing a more stable complex. Such a possible regulatory role of isoquercetin was further supported by the finding that it significantly accumulated in Col-0 after 3 days of cold, which was observed neither in *f3h* nor in *chs* (Figure S10; Table S2C). Together with the observation that, until 3 days at 4°C, anthocyanin amounts, that is, late products of the flavonoid pathway, did not significantly increase (Kitashova et al., 2023), this further suggests that early intermediates of flavonoid biosynthesis clearly differ in their function from end products of the same pathway. While early intermediates of the flavonoid biosynthesis pathway seem to play a crucial role in metabolic acclimation, late products, such as anthocyanins, might rather have a function as light or UV protectants (Li et al., 1993; Zhang et al., 2017; Zirngibl et al., 2023). In *f3h* plants, quercetin and isoquercetin were still found to accumulate as already reported before (Owens et al., 2008). However, under low temperature, these amounts were very small compared to Col-0 (Figure S10). Still, this needs to be considered when the potential conserved effects of flavonoids on metabolism and its regulation are discussed.

### Changes in protein homeostasis due to flavonoid deficiency during cold acclimation

Cold acclimation resulted in a decrease of protein amounts normalised to sample dry mass (see Figure 7). While Col-0 was found to successfully stabilise its protein amount on a slightly lower level than at 22°C, both *f3h* and *chs* mutants showed a significant decrease over the full cold acclimation period. Proteomics data revealed that in both flavonoid mutants proteasomal complexes were upregulated during the initial phase of cold acclimation, that is, during 3 days at 4°C, while a negative trend was observed for Col-0. This resulted in significantly negative correlations of proteasome and protein amounts in *f3h* and *chs* while no significant correlation was observed in Col-0. This points

towards a function of flavonoids and/or intermediates of flavonoid biosynthesis in stabilisation of the protein homeostasis at low temperature. Interestingly, in a GO term enrichment analysis, 'protein folding' was significantly over-represented in *chs* between 0 and 3 days at 4°C while no significance was detected in Col-0 and *f3h* (Table S6). The functional category 'protein refolding' was decreased in this period in Col-0 while it remained constant in both mutants. While, to the best of our knowledge, up to today there is no direct experimental proof for flavonoid-based stabilisation of proteins during plant cold acclimation, such interaction has been shown in other systems. For example, an *in vitro* study in mice showed that flavonoids, for example, quercetin or myricetin, enhanced the stability and folding of the visual G protein-coupled receptor rhodopsin, which is expressed in the rod photoreceptors of the bovine eye (Ortega et al., 2019). It was observed that flavonoids modulate the protein's conformation by direct interaction and stabilise it, probably by introducing structural rigidity. Hence, deficiencies of flavonoids might lead to misfolded proteins which subsequently undergo refolding or proteasomal degradation. Another study showed that flavonoids inhibited proteasome 26S activity in pig red blood cells (Chang, 2009), further supporting the role of flavonoids in inhibiting proteasomal compounds and, thereby, regulating protein degradation rates.

Although the effect on ribosomes in *chs* and *f3h* was less pronounced than on the proteasome, it still became significant in the correlation with protein amounts (see Figure 7d). Previous work has highlighted the important role of ribosomes and translational regulation during cold acclimation (Garcia-Molina et al., 2020). Moreover, flavonoids were shown to interact with isolated tRNA (Kanakis et al., 2006). In line with this, data from the present study suggests that flavonoids influence protein homeostasis during cold exposure, maybe through their direct interactions with ribosomes or tRNA. In summary, although it remains speculation from experimental data of the present study, it seems plausible that also in plants, such interactions between flavonoids and proteins as well as the proteasome, ribosomes and/or tRNAs might occur and contribute to a stable protein homeostasis at low temperature.

## CONCLUSION

The findings of the present study indicate that flavonoids play different physiological roles during a 2-week cold acclimation period. During the initial cold response, flavonoids were found to affect, and maybe even regulate, photorespiration and stabilisation of the C/N balance between plastids, cytosol and mitochondria. During the late cold acclimation period, flavonoids affect protein stability and folding which has dramatic effects on a plant's energy

homeostasis. While the experimental design of the present study does not allow discrimination between direct and secondary effects of flavonoid deficiency on cold acclimation, we have observed a robust photosynthetic acclimation in *f3h* and *chs* in a previous study (Kitashova et al., 2023). This might support the assumption of direct effects on acclimation capacity, but it remains speculation at this point. It remains to be elucidated whether such functional diversity can also be observed under different flavonoid-stimulating conditions, such as high light or excess UV. Finally, however, the physiological function of flavonoids and involved pathways clearly goes beyond the accumulation of pigments for the dissipation of electromagnetic radiation energy.

## MATERIALS AND METHODS

### Plant material and growth conditions

Plants of *Arabidopsis thaliana* accession Col-0 and homozygous T-DNA insertion lines *chs* (chalcone synthase, line SALK\_020583C, locus AT5G13930, allele *tt4-11*), and *f3h* (flavanone 3-hydroxylase, line SALK\_113904C, locus AT3G51240, allele *tt6-3*) were grown as described before (Kitashova et al., 2023). In summary, plants were grown on a 1:1 mixture of GS90 soil and vermiculite in a climate chamber under controlled short-day conditions (8 h/16 h light/dark; 100  $\mu\text{mol m}^{-2} \text{sec}^{-1}$ ; 22°C/16°C; 60% relative humidity). After 4 weeks, plants were shifted to a growth cabinet and grown further under long day conditions (16 h/8 h light/dark; 100  $\mu\text{mol m}^{-2} \text{sec}^{-1}$ ; 22°C/16°C; 60% relative humidity). After 2 weeks, plants were either (i) harvested at midday, that is, 8 h of light (0 days of cold acclimation) or (ii) transferred to a cold room for cold acclimation (16 h/8 h light/dark; 90–100  $\mu\text{mol m}^{-2} \text{sec}^{-1}$ ; 4°C/4°C). Cold exposed plants were harvested after 3 or 14 days of acclimation at midday, that is, after 8 h of light. Each sample consisted of nine leaf rosettes which were immediately frozen in liquid nitrogen, ground to a fine powder and lyophilised.

### Net CO<sub>2</sub> assimilation rate measurements

Rates of net photosynthetic CO<sub>2</sub> uptake (NPS) were recorded using a WALZ® GFS-3000FL system with Standard Measuring Head 3010-S (Heinz Walz GmbH, www.walz.com). NPS was determined within two response curves: (i) light curves where photosynthetically active radiation (PAR) increased stepwise from 0 to 1200  $\mu\text{mol m}^{-2} \text{sec}^{-1}$  in 5 min intervals under constant CO<sub>2</sub> concentration of 450 ppm, and (ii) CO<sub>2</sub> curves where CO<sub>2</sub> concentration increased stepwise from 50 to 1200 ppm in 5 min intervals under constant PAR intensity of 1200  $\mu\text{mol m}^{-2} \text{sec}^{-1}$ . The CO<sub>2</sub> compensation point, that is, the CO<sub>2</sub> concentration at which NPS was 0, was calculated using a linear interpolation of NPS between 50 and 450 ppm CO<sub>2</sub>.

### Non-aqueous subcellular fractionation

Non-aqueous subcellular fractionation (NAF) was performed as described before with slight modifications (Fürtauer et al., 2016). In brief, approximately 10 mg of lyophilised plant material were homogenised in tetrachloroethylene ( $\rho = 1.60 \text{ g cm}^{-3}$ ) with an ultrasonic homogeniser (Hielscher Ultrasonics UP200St, www.hielscher.com). After centrifugation with 20 000g, the supernatant was transferred to another tube, and its density was reduced with

heptane ( $\rho = 0.68 \text{ g cm}^{-3}$ ). The pellet was then resuspended in tetrachloroethylene. Sonication of the supernatant with the adjusted density, centrifugation, separation of pellet and density adjustment of the supernatant were repeated several times until a gradient of 5–7 densities was obtained. Each of the resulting resuspended pellets was split into 2 sub-fractions and dried in a desiccator. These fractions were used for (i) marker enzyme quantification and (ii) primary metabolite quantification using GC–MS. Activities of marker enzymes, that is, plastidial pyrophosphatase, cytosolic uridine 5'diphosphoglucose pyrophosphorylase and vacuolar acidic phosphatase, were determined photometrically and correlated with metabolite amounts (Fürtauer et al., 2016). Based on observations about the distribution of marker proteins made in a previous study, it was assumed that the plastidial fraction included both plastidial and mitochondrial metabolites due to limitations in separating both compartments (Fürtauer et al., 2019). Therefore, assumptions regarding the separation of plastidial and mitochondrial metabolomes were made carefully, aligning them with the observed dynamics of the subcellular proteome.

### Extraction of lipids and primary metabolites for mass spectrometry

Lipids and non-polar metabolites were extracted following the method described by (Hummel et al., 2011). In summary, approximately 5 mg of freeze-dried leaf material or NAF fractionation pellets were subjected to extraction using 1 mL of a pre-cooled ( $-20^\circ\text{C}$ ) mixture of methanol and methyl tert-butyl ether in a ratio of 3:1. This extraction solution included 10  $\mu\text{L}$  corticosterone, 5  $\mu\text{L}$  chloramphenicol, 1.25  $\mu\text{L}$  ampicillin, 2.5  $\mu\text{L}$  sorbitol- $^{13}\text{C}$  and 5  $\mu\text{L}$  ribitol, each at a concentration of 0.2  $\text{mg mL}^{-1}$ , serving as internal standards. The mixture was vigorously mixed until the tissue was fully suspended and then shaken for 10 min at  $4^\circ\text{C}$ , followed by 10 min of sonication on ice. Phase separation was initiated by adding 500  $\mu\text{L}$  of water:methanol (3:1) solution, followed by vigorous mixing and centrifugation at maximum speed using a Centrifuge 5417R (Eppendorf, [www.eppendorf.com](http://www.eppendorf.com)). For lipid analysis, 600–700  $\mu\text{L}$  of the upper phase was collected, while 400–500  $\mu\text{L}$  of the lower phase was divided into equal aliquots for GC–TOF–MS analysis (sample dependent). All samples were dried using a vacuum concentrator (Concentrator 5301; [www.eppendorf.com](http://www.eppendorf.com)) and subsequently stored at  $-80^\circ\text{C}$  until further analysis. To prevent oxidation, argon was added during storage.

### GC–MS: Primary metabolite analysis

For the derivatization process, the pellet was suspended in 10  $\mu\text{L}$  of methoxyamine hydrochloride solution (20  $\text{mg mL}^{-1}$  in pyridine) and incubated for 90 min at  $40^\circ\text{C}$ . Following this, 20  $\mu\text{L}$  of BSTFA (*N,O*-Bis[trimethylsilyl]trifluoroacetamide) containing 2.5  $\mu\text{L}$  of a retention time standard mixture comprising linear alkanes (*n*-decane, *n*-dodecane, *n*-pentadecane, *n*-nonadecane, *n*-docosane, *n*-octacosane and *n*-dotriacontane) was added, and the mixture was further incubated at  $40^\circ\text{C}$  for 45 min. Subsequently, 1 and 2  $\mu\text{L}$  of each sample was injected into a GC–TOF–MS system (Pegasus HT, Leco, [www.leco.com](http://www.leco.com)) utilising splitless injection as well as split ratios of 10, 30 and 50 (metabolite dependent). Sample injection and processing were automated using an autosampler system (Combi PAL, CTC Analytics AG, [www.ctc.ch](http://www.ctc.ch)). Helium was employed as the carrier gas at a constant flow rate of 0.6  $\text{mL min}^{-1}$ . Gas chromatographic separation was conducted on an Agilent GC (7890A, Agilent, [www.agilent.com](http://www.agilent.com)) equipped with a 30 m VF-5 ms column coupled with a 10 m EZ-Guard column. The temperature of the split/splitless injector, transfer line and ion

source was maintained at  $250^\circ\text{C}$ . The initial oven temperature was set at  $70^\circ\text{C}$  and ramped up to  $350^\circ\text{C}$  at a rate of  $9^\circ\text{C min}^{-1}$ . Metabolites were fractionated and ionised by a 70 eV ion pulse. Mass spectra were acquired at a rate of 20 scans per second within an *m/z* range of 50–600. Chromatograms and mass spectra were analysed using ChromaTOF 4.72 and TagFinder 4.1 software (Luedemann et al., 2008). Raw values were normalised by internal standard and dry weight.

### LC–MS: Lipid analysis

For LC–MS analysis, the Dionex Ultimate 3000 UHPLC (Thermo Fisher Scientific, [www.thermofisher.com](http://www.thermofisher.com)) in combination with a timsTOF (Bruker, [www.bruker.com](http://www.bruker.com)) was used. The dry extract was resolved in acetonitrile:isopropanol (7:3) and injected on a C8 reversed-phase column (Ultra C8 100  $\times$  2.1 mm; Restek, [www.restek.com](http://www.restek.com)) with 300  $\mu\text{L min}^{-1}$  flow at  $60^\circ\text{C}$ . The solvents used are (A) water and (B) acetonitrile:isopropanol (7:3), both including 1% (v/v) ammonium acetate and 0.1% (v/v) acetic acid. The 26 min gradient started at 55% B, followed by a ramp to 99% B within 15 min. After a 5-min washing step at 99% B, the gradient was returned to 55% B and kept constant for 5 min equilibration.

MS detection was performed using an electrospray ionisation (ESI) source, operating in positive mode. Nitrogen served as the dry gas, at 8  $\text{L min}^{-1}$ , 8 bar and  $200^\circ\text{C}$ . The timsTOF mass spectra were recorded in MS and MSMS mode from 50 to 1300 *m/z* with 40 000 resolution, 1 Hz scan speed and 0.3 ppm mass accuracy. Compounds were annotated in a targeted approach using the specific mass (*m/z*) at retention time and the isotopic pattern. All data were acquired by Compass HyStar 4.1 and otofControl 6.2. The evaluation was performed by DataAnalysis 5.1 and MetaboScape 2021. All software tools were provided by Bruker. Raw values were normalised by internal standard and gram dry weight.

### Extraction and quantification of flavonoids

The extraction of flavonoids was performed as described previously with some modifications (Likić et al., 2014). In brief, 15 mg of dry plant material was treated with 1 mL of a 1:1 (v/v) mixture of methanol and 1.2 M hydrochloric acid containing 2  $\mu\text{g mL}^{-1}$  of corticosterone as an internal standard. The mixture was thoroughly vortexed and incubated at  $80^\circ\text{C}$  with shaking at 1000 rpm for 30 min, supplemented by a 30 sec ultrasonication period (Hielscher UP200St). Following ultrasonication, the samples were centrifuged at  $8^\circ\text{C}$  for 15 min at maximum speed to clarify the supernatant, which was transferred into a clean tube. This process was repeated to ensure the complete removal of plant debris. Chromatographic separation was achieved using a Dionex Ultimate 3000 UHPLC system coupled to a timsTOF mass spectrometer (Bruker). An aliquot of 60  $\mu\text{L}$  of each extract was introduced onto a C18 reversed-phase column (Ultra AQ C18 3  $\mu\text{m}$  100  $\times$  2.1 mm) maintained at  $30^\circ\text{C}$ , employing a mobile phase of (A) water and (B) acetonitrile, each containing 0.1% (v/v) formic acid, at a flow rate of 400  $\mu\text{L min}^{-1}$ . The gradient program started with 95% aqueous phase (A) for 2 min, transitioning to 95% organic phase (B) over 20 min, followed by a 3-min organic wash and a 5-min re-equilibration to initial conditions.

Mass spectrometric detection was performed using an electrospray ionisation source (ESI) operating in positive ion mode. The parameters set included a dry gas flow of 8  $\text{L min}^{-1}$ , a nebuliser pressure of 8 bar, and a source temperature of  $200^\circ\text{C}$ . Mass spectra were collected from 50 to 1300 *m/z* with a resolution of 40 000, Scan speed of 1 Hz, and mass accuracy of 0.3 ppm. Identification of compounds based on exact mass, true isotopic patterns

and retention time confirmed by commercial standards. Data acquisition and processing were conducted using otofControl 6.2, DataAnalysis 5.3 and MetaboScape 2021, with further analysis in Microsoft Excel.

### Protein extraction and analysis by LC–MS/MS

Protein extraction and preparation for the LC–MS/MS quantification was done as previously described with minor adjustments (Marino et al., 2019). In summary, proteins were extracted using 6 M guanidine-chlorine in 10 mM HEPES pH 7.8, supplemented with 1 tablet of protease inhibitor cocktail per 10 mL buffer (cOmplete™ Proteasehemmer-Cocktail, ©Roche) with an ultrasonic homogeniser (Hielscher Ultrasonics UP200St, [www.hielscher.com](http://www.hielscher.com)). Then, the proteins were precipitated with methanol/chloroform in water, washed with methanol and the supernatant was discarded, leaving protein-containing pellets. Dried pellets were resuspended in 6 M urea/2 M thiourea in 50 mM HEPES pH 7.8 buffer at 37°C. Total protein content was quantified using the Pierce™ 660 nm Protein Assay Kit (©Thermo Scientific™). Following quantification, 80 µg of protein was aliquoted, reduced with 10 mM DTT and alkylated with 50 mM iodoacetamide. The proteins were subsequently digested overnight with trypsin at 37°C. Acidified with formic acid samples were purified using home-made C18 stage tips with 80% acetonitrile and 0.5% formic acid solution. Finally, 1 µg of purified protein extract was used for the LC–MS/MS analysis.

LC–MS/MS analysis was conducted as previously described with minor modifications, involving peptide separation over a 90 min linear gradient ranging from 5 to 80% (v/v) acetonitrile (ACN) (Espinoza-Corral et al., 2023). Raw data files were processed using MaxQuant software version 2.2.0.0 (Cox & Mann, 2008), with peak lists searched against the Arabidopsis reference proteome from Uniprot ([www.uniprot.org](http://www.uniprot.org)), employing default settings with ‘match-between-runs’ enabled. Protein quantification was achieved utilising the label-free quantification algorithm (LFQ) (Cox et al., 2014). Subsequent analysis was conducted using Perseus version 2.0.9.0 (Tyanova et al., 2016). To refine the dataset, potential contaminants, proteins identified solely through site modification and reverse hits were excluded. Only protein groups quantifiable by the LFQ algorithm in at least three out of four replicates under at least one condition were retained. LFQ intensities underwent log<sub>2</sub> transformation, and missing values were imputed from a normal distribution within Perseus using standard settings.

### Statistics and data analysis

Dynamics of the subcellular metabolomes were analysed in MATLAB® ([www.themathworks.com](http://www.themathworks.com)) using a method for time series analysis in the context of biochemical network information (Nägele et al., 2016). In brief, sigmoidal Gompertz functions (Equation 1) were fitted to experimental data (0–3 days at 4°C, 3–14 days at 4°C).

$$h(x) = d + (a - d)e^{-e^{-b(x-c)}} \quad (1)$$

Gompertz functions describe growth rates with the slowest growth at the beginning of the period, that is, reflecting the moment of cold exposure and thermodynamically affected enzymatic reaction rates. Derivatives of Gompertz functions represented metabolic functions, that is, the summed rates of biosynthesis and degradation for each metabolite pool. Dynamics of metabolic functions were then compared to the dynamics of substrate concentrations of each enzymatic reaction described by a metabolic network of subcellular carbohydrate metabolism,

carboxylic acids and amino acids (Figure S1). Dynamics were indicated by  $\omega$ -functions (Equation 2):

$$\omega(M_i \rightarrow M_j, t) = \frac{\frac{d}{dt} f_{M_j}(\mathbf{M}, \mathbf{p}, t)}{f_{M_i}(\mathbf{M}, \mathbf{p}, t)} \quad (2)$$

Here,  $M_i$  denotes the substrate concentration of an enzymatic reaction and  $M_j$  represents the product concentration. Metabolic functions of both substrate and product pools,  $f_{M_i}$  and  $f_{M_j}$ , were derived from Gompertz functions as described before. To identify metabolic deregulation in both mutants, ratios of z-scaled omega values were built (Figure S2; Table S1).

Statistical analysis and figure preparation was performed with free software R version 4.2.2 ([www.r-project.org](http://www.r-project.org)) (R Core Team 2019) and RStudio version 2023.9.1.494 ([www.rstudio.com](http://www.rstudio.com)), Python version 3.8.8 ([www.python.org](http://www.python.org)), Jupyter Notebook version 6.3.0 (<https://jupyter.org>) and MATLAB® ([www.themathworks.com](http://www.themathworks.com)). The protein phylogeny analysis was performed using MUSCLE Multiple Sequence Alignment version 3.8, and pairwise sequence alignment was conducted using the EMBOSS Water tool (<https://www.ebi.ac.uk>). Pairwise protein structure alignment of proteins was performed using AlphaFold structures (<https://www.rcsb.org>). Ligand docking simulation was performed using the free software DockThor version 2.0 (<https://dockthor.incc.br/v2>). The results from ligand docking were visualised using PyMOL version 2.5.7 (<https://pymol.org>). The evolutionary conservation profile of the FOLD1 protein was performed using the free software ConSurf (<https://consurf.tau.ac.il>). Differentially abundant proteins (DAP) were identified according to the ANOVA significance test with Tukey HSD (Table S2A). DAP GO term enrichment analysis (Biological Process) was performed using the R ‘org.At.tair.db’ package version 3.16.0 and ‘clusterProfiler’ package version 4.6.2. GO terms were checked for redundancies with the most significant terms being kept.

### AUTHOR CONTRIBUTIONS

AK performed fractionation experiments, statistical analysis and data evaluation, and wrote the paper. ML performed metabolomics analyses, MM performed quantification of flavonoids, SS and DL performed, supervised and conceived proteomics analyses, and TN conceived the study, performed statistics and data evaluation and wrote the paper.

### ACKNOWLEDGEMENTS

We thank the members of Plant Evolutionary Cell Biology at LMU München and the members of TRR175 for constructive discussions and advice. Further, we thank the team of MSBioLMU as well as the Graduate School Life Science Munich (LSM) for their support. We thank Timo Mühlhaus, David Zimmer and the DataPLANT consortium for supporting data archiving following the FAIR data principles (<https://www.nfdi4plants.de/>). This work was funded by Deutsche Forschungsgemeinschaft (DFG), TRR175/D03 and TRR175/Z1.

### CONFLICT OF INTEREST STATEMENT

The authors declare no conflict of interest.

### DATA AVAILABILITY STATEMENT

Proteomics and metabolomics data acquired in this study are accessible via the DataPLANT platform, which is part

of NFDI: [https://git.nfdi4plants.org/thomas.naegele/2024\\_Kitashova\\_et\\_al\\_subcellular](https://git.nfdi4plants.org/thomas.naegele/2024_Kitashova_et_al_subcellular).

## SUPPORTING INFORMATION

Additional Supporting Information may be found in the online version of this article.

**Figure S1.** Graphical representation of the metabolic network of subcellular carbohydrate metabolism, carboxylic acids and amino acids used for the analysis of the dynamics of subcellular metabolomes.

**Figure S2.** Ratios of omega functions revealed by time series analysis.

**Figure S3.** Cold-induced dynamics of the subcellular metabolome.

**Figure S4.** Dynamics of isocitrate dehydrogenases and pyruvate dehydrogenases in Col-0, *chs* and *f3h* after 0, 3 and 14 days of cold acclimation.

**Figure S5.** Growth phenotypes of Col-0, *chs* and *f3h* after 0, 3 and 14 days of cold acclimation.

**Figure S6.** Hierarchical cluster analysis of the subcellular metabolite abundance change rate.

**Figure S7.** Dynamics of main amino acid pool in Col-0, *chs* and *f3h* in cytosol, plastid and vacuole after 0, 3 and 14 days of cold acclimation.

**Figure S8.** Net CO<sub>2</sub> assimilation rates.

**Figure S9.** Evolutionary conservation profile of FOLD1 protein.

**Figure S10.** Cold-induced dynamics of flavonoids.

**Table S1.** Ratios of scaled time series omega functions. Interpolated Gompertz functions were used to calculate omega functions (see [Materials and methods](#) section). Functions were scaled (z-scale, i.e., zero mean—unit variance) before ratios of function values were built for (A) *chs*/Col-0 (0–3 days), (B) *f3h*/Col-0 (0–3 days), (C) *chs*/Col-0 (3–14 days) and (D) *f3h*/Col-0 (3–14 days).

**Table S2.** ANOVA with Tukey HSD results. Significance levels for (A) proteome level; (B) subcellular metabolomics; (C) cellular metabolomics and (D) comparison of CO<sub>2</sub> compensation points; *P*-values below 0.05 are highlighted in green.

**Table S3.** Principal component analysis (PCA) loadings and component scores for metabolites quantified.

**Table S4.** Cluster analysis results for proteins involved in amino acid biosynthesis. (A) List of proteins involved in amino acid biosynthesis; (B) row-wise and (C) column-wise calculated Euclidean distances.

**Table S5.** Summary of molecular docking results for isoquercetin and quercetin with bifunctional 5,10-methylene-THF dehydrogenase/5,10-methenyl-THF cyclohydrolase (FOLD1) protein.

**Table S6.** GO term enrichment analysis. Differentially abundant proteins in *chs* and *f3h* were identified based on ANOVA with Tukey HSD results between 0 and 3 days, and 3 and 14 days of cold acclimation (Table S2A). Only GO terms related to biological processes are included in the analysis.

**Table S7.** Cold-induced dynamics of metabolome in Col-0, *chs* and *f3h* after 0, 3 and 14 days of cold acclimation. Mean values and standard deviations are provided for (A) subcellular and (B) cellular metabolite amounts.

**Supplementary File 1.** 3D structure of isoquercetin and bifunctional 5,10-methylene-THF dehydrogenase/5,10-methenyl-THF cyclohydrolase (FOLD1) protein of Arabidopsis interaction.

**Supplementary File 2.** 3D structure of isoquercetin and C-1-THF synthase protein of mouse interaction.

**Supplementary File 3.** 3D structure of quercetin and bifunctional 5,10-methylene-THF dehydrogenase/5,10-methenyl-THF cyclohydrolase (FOLD1) protein of Arabidopsis interaction.

## REFERENCES

- Agati, G., Matteini, P., Goti, A. & Tattini, M. (2007) Chloroplast-located flavonoids can scavenge singlet oxygen. *New Phytologist*, **174**(1), 77–89. Available from: <https://doi.org/10.1111/j.1469-8137.2007.01986.x>
- Alberdi, M., Corcuera, L.J., Maldonado, C., Barrientos, M., Fernandez, J. & Henriquez, O. (1993) Cold-acclimation in cultivars of *Avena sativa*. *Phytochemistry*, **33**(1), 57–60. Available from: [https://doi.org/10.1016/0031-9422\(93\)85396-9](https://doi.org/10.1016/0031-9422(93)85396-9)
- Chang, T.-L. (2009) Inhibitory effect of flavonoids on 26S proteasome activity. *Journal of Agricultural and Food Chemistry*, **57**(20), 9706–9715. Available from: <https://doi.org/10.1021/jf9017492>
- Collakova, E., Goyer, A., Naponelli, V., Krassovskaya, I., Gregory, J.F., III, Hanson, A.D. et al. (2008) Arabidopsis 10-formyl tetrahydrofolate deformylases are essential for photorespiration. *The Plant Cell*, **20**(7), 1818–1832. Available from: <https://doi.org/10.1105/tpc.108.058701>
- Cox, J., Hein, M.Y., Luber, C.A., Paron, I., Nagaraj, N. & Mann, M. (2014) Accurate proteome-wide label-free quantification by delayed normalization and maximal peptide ratio extraction, termed MaxLFQ\*. *Molecular & Cellular Proteomics*, **13**(9), 2513–2526. Available from: <https://doi.org/10.1074/mcp.M113.031591>
- Cox, J. & Mann, M. (2008) Maxquant enables high peptide identification rates, individualized P.P.B.-range mass accuracies and proteome-wide protein quantification. *Nature Biotechnology*, **26**(12), 1367–1372. Available from: <https://doi.org/10.1038/nbt.1511>
- Doerfler, H., Lyon, D., Nägele, T., Sun, X.L., Fragner, L., Hadacek, F. et al. (2013) Granger causality in integrated GC-MS and LC-MS metabolomics data reveals the interface of primary and secondary metabolism. *Metabolomics*, **9**(3), 564–574. Available from: <https://doi.org/10.1007/s11306-012-0470-0>
- Erb, M. & Kliebenstein, D.J. (2020) Plant secondary metabolites as defenses, regulators, and primary metabolites: the blurred functional trichotomy. *Plant Physiology*, **184**(1), 39–52. Available from: <https://doi.org/10.1104/pp.20.00433>
- Espinoza-Corral, R., Schwenkert, S. & Schneider, A. (2023) Characterization of the preferred cation cofactors of chloroplast protein kinases in *Arabidopsis thaliana*. *FEBS Open Bio*, **13**(3), 511–518. Available from: <https://doi.org/10.1002/2211-5463.13563>
- Fiorani, M., Guidarelli, A., Blasa, M., Azzolini, C., Candiracci, M., Piatti, E. et al. (2010) Mitochondria accumulate large amounts of quercetin: prevention of mitochondrial damage and release upon oxidation of the extramitochondrial fraction of the flavonoid. *The Journal of Nutritional Biochemistry*, **21**(5), 397–404. Available from: <https://doi.org/10.1016/j.jnutbio.2009.01.014>
- Fürtauer, L., Küstner, L., Weckwerth, W., Heyer, A.G. & Nägele, T. (2019) Resolving subcellular plant metabolism. *The Plant Journal*, **100**(3), 438–455. Available from: <https://doi.org/10.1111/tpj.14472>
- Fürtauer, L., Weckwerth, W. & Nägele, T. (2016) A benchtop fractionation procedure for subcellular analysis of the plant metabolome. *Frontiers in Plant Science*, **7**, 1912. Available from: <https://doi.org/10.3389/fpls.2016.01912>
- Garcia-Molina, A., Kleine, T., Schneider, K., Mühlhaus, T., Lehmann, M. & Leister, D. (2020) Translational components contribute to acclimation responses to high light, heat, and cold in Arabidopsis. *iScience*, **23**(7), 101331. Available from: <https://doi.org/10.1016/j.isci.2020.101331>
- Gilmour, S.J., Zarka, D.G., Stockinger, E.J., Salazar, M.P., Houghton, J.M. & Thomashow, M.F. (1998) Low temperature regulation of the Arabidopsis CBF family of AP2 transcriptional activators as an early step in cold-induced COR gene expression. *The Plant Journal*, **16**(4), 433–442. Available from: <https://doi.org/10.1046/j.1365-3113x.1998.00310.x>
- Gjindali, A. & Johnson, G.N. (2023) Photosynthetic acclimation to changing environments. *Biochemical Society Transactions*, **51**(2), 473–486. Available from: <https://doi.org/10.1042/BST20211245>
- Groth, M., Moissiard, G., Wirtz, M., Wang, H., Garcia-Salinas, C., Ramos-Parra, P.A. et al. (2016) MTHFD1 controls DNA methylation in Arabidopsis. *Nature Communications*, **7**(1), 11640. Available from: <https://doi.org/10.1038/ncomms11640>

- Guntero, V.A., Gutierrez, L., Kneeteman, M.N. & Ferretti, C.A. (2021) In silico study of the interaction between casein with tocopherols: preliminary evaluation of lipophilic substrate inclusion on proteic matrix. *Chemistry Proceedings*, 3(1), 49. Available from: <https://doi.org/10.3390/ecsoc-24-08345>
- Hannah, M.A., Wiese, D., Freund, S., Fiehn, O., Heyer, A.G. & Hinch, D.K. (2006) Natural genetic variation of freezing tolerance in *Arabidopsis*. *Plant Physiology*, 142(1), 98–112. Available from: <https://doi.org/10.1104/pp.106.081141>
- Hinch, D.K., Zuther, E. & Heyer, A.G. (2003) The preservation of liposomes by raffinose family oligosaccharides during drying is mediated by effects on fusion and lipid phase transitions. *Biochimica et Biophysica Acta (BBA)—Biomembranes*, 1612, 172–177. Available from: [https://doi.org/10.1016/S0005-2736\(03\)00116-0](https://doi.org/10.1016/S0005-2736(03)00116-0)
- Hoermiller, I.I., Naegle, T., Augustin, H., Stutz, S., Weckwerth, W. & Heyer, A.G. (2017) Subcellular reprogramming of metabolism during cold acclimation in *Arabidopsis thaliana*. *Plant, Cell & Environment*, 40(5), 602–610. Available from: <https://doi.org/10.1111/pce.12836>
- Hummel, J., Segu, S., Li, Y., Irgang, S., Jueppner, J. & Giavalisco, P. (2011) Ultra performance liquid chromatography and high resolution mass spectrometry for the analysis of plant lipids. *Frontiers in Plant Science*, 2, 54. Available from: <https://doi.org/10.3389/fpls.2011.00054>
- Huner, N.P.A., Öquist, G. & Melis, A. (2003) Photostasis in plants, green algae and cyanobacteria: the role of light harvesting antenna complexes. In: Green, B.R. & Parson, W.W. (Eds.) *Light-harvesting antennas in photosynthesis. Advances in photosynthesis and respiration*, Vol. 13. Berlin: Springer, pp. 401–421. Available from: [https://doi.org/10.1007/978-94-017-2087-8\\_14](https://doi.org/10.1007/978-94-017-2087-8_14)
- Kanakis, C.D., Tarantilis, P.A., Polissiou, M.G. & Tajmir-Riahi, H.-A. (2006) Interaction of antioxidant flavonoids with tRNA: intercalation or external binding and comparison with Flavonoid-DNA adducts. *DNA and Cell Biology*, 25(2), 116–123. Available from: <https://doi.org/10.1089/dna.2006.25.116>
- Kaplan, F., Kopka, J., Haskell, D.W., Zhao, W., Schiller, K.C., Gatzke, N. et al. (2004) Exploring the temperature-stress metabolome of *Arabidopsis*. *Plant Physiology*, 136(4), 4159–4168. Available from: <https://doi.org/10.1104/pp.104.052142>
- Kaplan, F., Kopka, J., Sung, D.Y., Zhao, W., Popp, M., Porat, R. et al. (2007) Transcript and metabolite profiling during cold acclimation of *Arabidopsis* reveals an intricate relationship of cold-regulated gene expression with modifications in metabolite content. *The Plant Journal*, 50(6), 967–981. Available from: <https://doi.org/10.1111/j.1365-313X.2007.03100.x>
- Kitashova, A., Adler, S.O., Richter, A.S., Eberlein, S., Dziubek, D., Klipp, E. et al. (2023) Limitation of sucrose biosynthesis shapes carbon partitioning during plant cold acclimation. *Plant, Cell & Environment*, 46(2), 464–478. Available from: <https://doi.org/10.1111/pce.14483>
- Klotke, J., Kopka, J., Gatzke, N. & Heyer, A.G. (2004) Impact of soluble sugar concentrations on the acquisition of freezing tolerance in accessions of *Arabidopsis thaliana* with contrasting cold adaptation—evidence for a role of raffinose in cold acclimation. *Plant, Cell & Environment*, 27(11), 1395–1404. Available from: <https://doi.org/10.1111/j.1365-3040.2004.01242.x>
- Knaupp, M., Mishra, K.B., Nedbal, L. & Heyer, A.G. (2011) Evidence for a role of raffinose in stabilizing photosystem II during freeze–thaw cycles. *Planta*, 234(3), 477–486. Available from: <https://doi.org/10.1007/s00425-011-1413-0>
- Kotton, A., Dlugosz-Grochowska, O., Wojciechowska, R. & Czaja, M. (2022) Biosynthesis regulation of folates and phenols in plants. *Scientia Horticulturae*, 291, 110561. Available from: <https://doi.org/10.1016/j.scienta.2021.110561>
- Korn, M., Peterek, S., Mock, H.P., Heyer, A.G. & Hinch, D.K. (2008) Heterosis in the freezing tolerance, and sugar and flavonoid contents of crosses between *Arabidopsis thaliana* accessions of widely varying freezing tolerance. *Plant, Cell & Environment*, 31(6), 813–827. Available from: <https://doi.org/10.1111/j.1365-3040.2008.01800.x>
- Koster, K.L. & Lynch, D.V. (1992) Solute accumulation and compartmentation during the cold acclimation of puma rye. *Plant Physiology*, 98(1), 108–113. Available from: <https://doi.org/10.1104/pp.98.1.108>
- Li, J., Ou-Lee, T.M., Raba, R., Amundson, R.G. & Last, R.L. (1993) *Arabidopsis* flavonoid mutants are hypersensitive to UV-B irradiation. *The Plant Cell*, 5(2), 171–179. Available from: <https://doi.org/10.1105/tpc.5.2.171>
- Li, Z., Jiang, H., Jiang, X., Zhang, L. & Qin, Y. (2023) Integrated physiological, transcriptomic, and metabolomic analyses reveal that low-nitrogen conditions improve the accumulation of flavonoids in snow chrysanthemum. *Industrial Crops and Products*, 197, 116574. Available from: <https://doi.org/10.1016/j.indcrop.2023.116574>
- Likić, S., Šola, I., Ludwig-Müller, J. & Rusak, G. (2014) Involvement of kaempferol in the defence response of virus infected *Arabidopsis thaliana*. *European Journal of Plant Pathology*, 138(2), 257–271. Available from: <https://doi.org/10.1007/s10658-013-0326-0>
- Luedemann, A., Strassburg, K., Erban, A. & Kopka, J. (2008) TagFinder for the quantitative analysis of gas chromatography–mass spectrometry (GC-MS)-based metabolite profiling experiments. *Bioinformatics*, 24, 732–737. Available from: <https://doi.org/10.1093/bioinformatics/btn023>
- Manzoor, M., Muroi, M., Ogawa, N., Kobayashi, H., Nishimura, H., Chen, D. et al. (2022) Isoquercitrin from *Apocynum venetum* L. produces an anti-obesity effect on obese mice by targeting C-1-tetrahydrofolate synthase, carbonyl reductase, and glutathione S-transferase P and modification of the AMPK/SREBP-1c/FAS/CD36 signaling pathway in mice *in vivo*. *Food & Function*, 13(21), 10923–10936. Available from: <https://doi.org/10.1039/D2FO02438A>
- Marino, G., Naranjo, B., Wang, J., Penzler, J.-F., Kleine, T. & Leister, D. (2019) Relationship of GUN1 to FUG1 in chloroplast protein homeostasis. *The Plant Journal*, 99(3), 521–535. Available from: <https://doi.org/10.1111/tpj.14342>
- Nägele, T., Fürtauer, L., Nagler, M., Weiszmann, J. & Weckwerth, W. (2016) A strategy for functional interpretation of metabolomic time series data in context of metabolic network information. *Frontiers in Molecular Biosciences*, 3, 6. Available from: <https://doi.org/10.3389/fmolb.2016.00006>
- Nägele, T. & Heyer, A.G. (2013) Approximating subcellular organisation of carbohydrate metabolism during cold acclimation in different natural accessions of *Arabidopsis thaliana*. *New Phytologist*, 198(3), 777–787. Available from: <https://doi.org/10.1111/nph.12201>
- Nägele, T., Kandel, B.A., Frana, S., Meißner, M. & Heyer, A.G. (2011) A systems biology approach for the analysis of carbohydrate dynamics during acclimation to low temperature in *Arabidopsis thaliana*. *The FEBS Journal*, 278(3), 506–518. Available from: <https://doi.org/10.1111/j.1742-4658.2010.07971.x>
- Nägele, T., Stutz, S., Hörmiller, I.I. & Heyer, A.G. (2012) Identification of a metabolic bottleneck for cold acclimation in *Arabidopsis thaliana*. *The Plant Journal*, 72(1), 102–114. Available from: <https://doi.org/10.1111/j.1365-313X.2012.05064.x>
- Nakabayashi, R., Yonekura-Sakakibara, K., Urano, K., Suzuki, M., Yamada, Y., Nishizawa, T. et al. (2014) Enhancement of oxidative and drought tolerance in *Arabidopsis* by overaccumulation of antioxidant flavonoids. *The Plant Journal*, 77(3), 367–379. Available from: <https://doi.org/10.1111/tpj.12388>
- Naoumkina, M. & Dixon, R.A. (2008) Subcellular localization of flavonoid natural products: a signaling function? *Plant Signaling & Behavior*, 3(8), 573–575. Available from: <https://doi.org/10.4161/psb.3.8.5731>
- Olsen, K.M., Slimestad, R., Lea, U.S., Brede, C., Løvdal, T., Ruoff, P. et al. (2009) Temperature and nitrogen effects on regulators and products of the flavonoid pathway: experimental and kinetic model studies. *Plant, Cell & Environment*, 32(3), 286–299. Available from: <https://doi.org/10.1111/j.1365-3040.2008.01920.x>
- Ortega, J.T., Parmar, T. & Jastrzebska, B. (2019) Flavonoids enhance rod opsin stability, folding, and self-association by directly binding to ligand-free opsin and modulating its conformation. *Journal of Biological Chemistry*, 294(20), 8101–8122. Available from: <https://doi.org/10.1074/jbc.RA119.007808>
- Owens, D.K., Crosby, K.C., Runac, J., Howard, B.A. & Winkel, B.S. (2008) Biochemical and genetic characterization of *Arabidopsis* flavanone 3β-hydroxylase. *Plant Physiology and Biochemistry*, 46(10), 833–843. Available from: <https://doi.org/10.1016/j.plaphy.2008.06.004>
- Peer, W.A., Brown, D.E., Tague, B.W., Muday, G.K., Taiz, L. & Murphy, A.S. (2001) Flavonoid accumulation patterns of transparent testa mutants of *Arabidopsis*. *Plant Physiology*, 126(2), 536–548. Available from: <https://doi.org/10.1104/pp.126.2.536>
- Perez de Souza, L., Garbowicz, K., Brotman, Y., Tohge, T. & Fernie, A.R. (2020) The acetate pathway supports flavonoid and lipid biosynthesis in *Arabidopsis*. *Plant Physiology*, 182(2), 857–869. Available from: <https://doi.org/10.1104/pp.19.00683>

- Pucker, B. & Selmar, D. (2022) Biochemistry and molecular basis of intracellular flavonoid transport in plants. *Plants*, **11**(7), 963. Available from: <https://doi.org/10.3390/plants11070963>
- Rippert, P., Puyaubert, J., Grisolle, D., Derrier, L. & Matringe, M. (2009) Tyrosine and phenylalanine are synthesized within the plastids in *Arabidopsis*. *Plant Physiology*, **149**(3), 1251–1260. Available from: <https://doi.org/10.1104/pp.108.130070>
- Ristic, Z. & Ashworth, E.N. (1993) Changes in leaf ultrastructure and carbohydrates in *Arabidopsis thaliana* L (Heyn) cv Columbia during rapid cold-acclimation. *Protoplasma*, **172**(2–4), 111–123. Available from: <https://doi.org/10.1007/Bf01379368>
- Roje, S., Janave, M.T., Ziemak, M.J. & Hanson, A.D. (2002) Cloning and characterization of mitochondrial 5-formyltetrahydrofolate cycloligase from higher plants. *Journal of Biological Chemistry*, **277**(45), 42748–42754. Available from: <https://doi.org/10.1074/jbc.M205632200>
- Sarma, A.D. & Sharma, R. (1999) Anthocyanin-DNA copigmentation complex: mutual protection against oxidative damage. *Phytochemistry*, **52**(7), 1313–1318. Available from: [https://doi.org/10.1016/S0031-9422\(99\)00427-6](https://doi.org/10.1016/S0031-9422(99)00427-6)
- Savitch, L.V., Barker-Astrom, J., Ivanov, A.G., Hurry, V., Oquist, G., Huner, N.P. *et al.* (2001) Cold acclimation of *Arabidopsis thaliana* results in incomplete recovery of photosynthetic capacity, associated with an increased reduction of the chloroplast stroma. *Planta*, **214**(2), 295–303. Available from: <https://doi.org/10.1007/s004250100622>
- Schulz, E., Tohge, T., Zuther, E., Fernie, A.R. & Hinch, D.K. (2015) Natural variation in flavonol and anthocyanin metabolism during cold acclimation in *Arabidopsis thaliana* accessions. *Plant, Cell & Environment*, **38**(8), 1658–1672. Available from: <https://doi.org/10.1111/pce.12518>
- Schulz, E., Tohge, T., Zuther, E., Fernie, A.R. & Hinch, D.K. (2016) Flavonoids are determinants of freezing tolerance and cold acclimation in *Arabidopsis thaliana*. *Scientific Reports*, **6**, 34027. Available from: <https://doi.org/10.1038/srep34027>
- Sefika Feyza, M., Selin, S. & Saliha Ece, A. (2022) Chapter 2: Fundamentals of molecular docking and comparative analysis of protein–small-molecule docking approaches. In: Erman Salih, I. (Ed.) *Molecular docking*. London: IntechOpen. Available from: <https://doi.org/10.5772/intechopen.105815>
- Shi, X. & Bloom, A. (2021) Photorespiration: the futile cycle? *Plants*, **10**(5), 908. Available from: <https://doi.org/10.3390/plants10050908>
- Solecka, D. & Kacperska, A. (2003) Phenylpropanoid deficiency affects the course of plant acclimation to cold. *Physiologia Plantarum*, **119**(2), 253–262. Available from: <https://doi.org/10.1034/j.1399-3054.2003.00181.x>
- Steponkus, P.L. (1984) Role of the plasma membrane in freezing injury and cold acclimation. *Annual Review of Plant Physiology*, **35**(1), 543–584. Available from: <https://doi.org/10.1146/annurev.pp.35.060184.002551>
- Stitt, M. & Hurry, V. (2002) A plant for all seasons: alterations in photosynthetic carbon metabolism during cold acclimation in *Arabidopsis*. *Current Opinion in Plant Biology*, **5**(3), 199–206. Available from: [https://doi.org/10.1016/S1369-5266\(02\)00258-3](https://doi.org/10.1016/S1369-5266(02)00258-3)
- Stover, P. & Schirch, V. (1990) Serine hydroxymethyltransferase catalyzes the hydrolysis of 5,10-methylenetetrahydrofolate to 5-formyltetrahydrofolate. *Journal of Biological Chemistry*, **265**(24), 14227–14233. Available from: [https://doi.org/10.1016/S0021-9258\(18\)77290-6](https://doi.org/10.1016/S0021-9258(18)77290-6)
- Strand, A., Foyer, C.H., Gustafsson, P., Gardeström, P. & Hurry, V. (2003) Altering flux through the sucrose biosynthesis pathway in transgenic *Arabidopsis thaliana* modifies photosynthetic acclimation at low temperatures and the development of freezing tolerance. *Plant, Cell & Environment*, **26**(4), 523–535. Available from: <https://doi.org/10.1046/j.1365-3040.2003.00983.x>
- Strand, A., Hurry, V., Henkes, S., Huner, N., Gustafsson, P., Gardeström, P. *et al.* (1999) Acclimation of *Arabidopsis* leaves developing at low temperatures. Increasing cytoplasmic volume accompanies increased activities of enzymes in the Calvin Cycle and in the sucrose-biosynthesis pathway. *Plant Physiology*, **119**, 1387–1397. Available from: <https://doi.org/10.1104/pp.119.4.1387>
- Sweetlove, L.J., Beard, K.F.M., Nunes-Nesi, A., Fernie, A.R. & Ratcliffe, R.G. (2010) Not just a circle: flux modes in the plant TCA cycle. *Trends in Plant Science*, **15**(8), 462–470. Available from: <https://doi.org/10.1016/j.tplants.2010.05.006>
- Tcherkez, G., Mahé, A., Gauthier, P., Mauve, C., Gout, E., Bligny, R. *et al.* (2009) In folio respiratory fluxomics revealed by <sup>13</sup>C isotopic labeling and h/d isotope effects highlight the noncyclic nature of the tricarboxylic acid “cycle” in illuminated leaves. *Plant Physiology*, **151**(2), 620–630. Available from: <https://doi.org/10.1104/pp.109.142976>
- Timm, S. & Hagemann, M. (2020) Photorespiration—how is it regulated and how does it regulate overall plant metabolism? *Journal of Experimental Botany*, **71**(14), 3955–3965. Available from: <https://doi.org/10.1093/jxb/eraa183>
- Tohge, T., Perez de Souza, L. & Fernie, A.R. (2018) On the natural diversity of phenylacetylated-flavonoid and their in planta function under conditions of stress. *Phytochemistry Reviews*, **17**(2), 279–290. Available from: <https://doi.org/10.1007/s11101-017-9531-3>
- Tyanova, S., Temu, T., Sinitcyn, P., Carlson, A., Hein, M.Y., Geiger, T. *et al.* (2016) The Perseus computational platform for comprehensive analysis of (prote)omics data. *Nature Methods*, **13**(9), 731–740. Available from: <https://doi.org/10.1038/nmeth.3901>
- Winkel-Shirley, B. (2002) Biosynthesis of flavonoids and effects of stress. *Current Opinion in Plant Biology*, **5**(3), 218–223. Available from: [https://doi.org/10.1016/s1369-5266\(02\)00256-x](https://doi.org/10.1016/s1369-5266(02)00256-x)
- Zhang, Q., Liu, M. & Ruan, J. (2017) Metabolomics analysis reveals the metabolic and functional roles of flavonoids in light-sensitive tea leaves. *BMC Plant Biology*, **17**(1), 64. Available from: <https://doi.org/10.1186/s12870-017-1012-8>
- Zirngibl, M.E., Araguirang, G.E., Kitashova, A., Jahnke, K., Rolka, T., Kühn, C. *et al.* (2023) Triose phosphate export from chloroplasts and cellular sugar content regulate anthocyanin biosynthesis during high light acclimation. *Plant Communications*, **4**(1), 100423. Available from: <https://doi.org/10.1016/j.xplc.2022.100423>
- Zuther, E., Buchel, K., Hundertmark, M., Stitt, M., Hinch, D.K. & Heyer, A.G. (2004) The role of raffinose in the cold acclimation response of *Arabidopsis thaliana*. *FEBS Letters*, **576**(1–2), 169–173. Available from: <https://doi.org/10.1016/j.febslet.2004.09.006>



## 10 Discussion

In many plant species, the multigenic process of cold acclimation is induced due to exposure of plants to low but non-freezing temperatures. It involves reprogramming of multiple signalling pathways and regulatory cascades, which finally results in an increased freezing tolerance (Xin and Browse 2000; Thomashow 2010; Knight and Knight 2012; Seydel et al. 2022). Reprogramming of photosynthetic CO<sub>2</sub> uptake, carbohydrate and specialised metabolism needs a tight regulation for efficient cold acclimation.

### 10.1 Plasticity of sucrose metabolism buffers the effects of chloroplast positioning during cold acclimation

Chloroplast positioning is an adaptive mechanism that ensures most efficient photosynthesis under different light conditions (Wada 2013). This implies that chloroplast positioning is also crucial for cold acclimation, which is sensitive to excessive light yet requires sufficient light for protective metabolite production (Wanner and Juntila 1999). To investigate the role of chloroplast positioning in metabolic cold acclimation, a mutant deficient in chloroplast positioning, *chup1*, was studied under cold and ambient light and cold and low light conditions (Kitashova et al. 2021). Previously, it was observed that despite similar maximum quantum yield of photosystem II efficiency ( $F_v/F_m$ ) values in both wild type *Arabidopsis* Col-0 and *chup1* mutant, *chup1* demonstrated reduced CO<sub>2</sub> assimilation under short day conditions, i.e., 8 hours of light in a diurnal cycle (Gotoh et al. 2018). Tholen and colleagues suggested that the reduced photosynthesis in *chup1* was due to smaller intercellular airspaces and reduced internal conductance (Tholen et al. 2008). However, in our study, under long day conditions (16 hours of light), both Col-0 and *chup1* showed similar CO<sub>2</sub> assimilation rates at growth light intensities, indicating the presence of compensatory mechanisms in *chup1* under long days. Notably, *chup1* displayed a lower net CO<sub>2</sub> assimilation rate at higher light intensity under control temperature, although  $F_v/F_m$  did not differ significantly (Kitashova et al. 2021). This finding along with findings by (Gotoh et al. 2018) suggests that the limitation of CO<sub>2</sub> assimilation at higher light intensities is due to underlying biochemical reactions rather than photochemical limitations, linking chloroplast positioning to primary carbohydrate metabolism.

This connection became more evident in cold conditions, where *chup1* showed reduced cold-induced dynamics of enzyme in the central carbohydrate metabolism, under both ambient and low light. Kinetic modelling revealed lower reaction rates catalysed by invertase, glucokinase (GLCK), and fructokinase (FRCK) under cold and ambient light. Previous studies on spinach and *Arabidopsis* indicated that increased CO<sub>2</sub> assimilation in cold is associated with increased SPS activity suggesting the involvement of cyclic sucrose synthesis and breakdown in photosynthetic stabilisation under low temperature (Guy et al. 1992; Holaday et al. 1992; Strand et al. 2003; Nägele and Heyer 2013; Weiszmann et al. 2018). Additionally,  $F_v/F_m$  was lower in *chup1* under cold and ambient light which positively correlated with reaction rates of the sucrose cycle. Nevertheless, *chup1* exhibited similar rates of photosynthetic CO<sub>2</sub> assimilation and amounts of sucrose under cold, which suggested that, during cold acclimation, the sucrose cycle significantly buffers the effects of altered chloroplast positioning to maintain a metabolic homeostasis and photosynthetic stabilisation comparable to Col-0.

Another notable finding was a higher G6PDH-mediated G6P oxidation rate in *chup1*. Typically, the G6P/F6P ratio increases in cold (Savitch et al. 2001). However, this increase was markedly reduced in *chup1* compared to Col-0 under cold and ambient light. Conversely, under cold and low light, the G6P/F6P ratio was higher in *chup1* than in Col-0, potentially indicating a compensatory mechanism to produce additional reducing power. Together with the absence of major photodamage in *chup1*, this suggests a differential regulatory strategy in *chup1* to mitigate ROS and photoinhibition. Nonetheless, an imbalance in hexose phosphate metabolism regulation could result in limited CO<sub>2</sub> assimilation under high light and altered other pathways, such as those mediated by the protein kinase sucrose non-fermenting related kinase 1 (SnRK1). SnRK1 is a key regulator of energy homeostasis and is a central player of a complex stress signalling network that integrates metabolic signals, allowing plants to adapt to fluctuating environmental conditions (Crepin and Rolland 2019). It is involved in the phosphorylation of various substrates that modulate metabolic pathways, including both SPS and CHUP1, which suggests underlying coregulatory mechanisms (Nukarinen et al. 2016).

### 10.2 Sucrose biosynthesis orchestrated carbon partitioning during cold acclimation

While specialised metabolites, such as flavonoids, were found to significantly affect cold acclimation capacities and freezing tolerance in *Arabidopsis* (Schulz et al. 2016), their physiological function co-regulation with carbohydrate metabolism remain unclear. Previously, sugar-induced flavonoid biosynthesis was reported, indicating an interconnectedness between carbohydrate and specialised metabolism (Teng et al. 2005; Lv et al. 2022). In *Arabidopsis*, a mutant deficient in AGPase, which is involved in starch biosynthesis, showed higher expression of anthocyanin biosynthesis related genes under highlight, suggesting a co-regulatory mechanism between flavonoid and starch metabolism (Zirngibl et al. 2023).

To investigate this interplay, *Arabidopsis* wild type plants (accession Col-0) were studied together with mutants deficient in starch biosynthesis (*pgm1*), starch degradation (*bam3*), and flavonoid metabolism (*chs* and *f3h*) during cold acclimation (Kitashova et al. 2023). Statistical analysis revealed that starch deficiency and overaccumulation significantly affect anthocyanin accumulation, with both *pgm1* and *bam3* showing lower anthocyanin amounts compared to Col-0. Notably, amylase activity was higher in *pgm1* during maximal anthocyanin accumulation, suggesting that the reaction of starch degradation may signal anthocyanin or flavonoid biosynthesis. Although reduced flavonoid amounts could indicate impaired cold tolerance and photosynthesis in both starch and flavonoid mutants (Kaplan and Guy 2005; Schulz et al. 2016; Hoermiller et al. 2017), similar CO<sub>2</sub> assimilation rate and F<sub>v</sub>/F<sub>m</sub> were observed in all genotypes, indicating a minor effect of starch or flavonoid metabolism on photosynthetic acclimation under ambient light during cold exposure.

Metabolism of soluble sugars is well-known to be significantly involved in plant cold acclimation (Sasaki et al. 1996; Wanner and Junttila 1999; Nägele and Heyer 2013). To explore this further, a kinetic model of the central carbohydrate metabolism was developed to study the effects of carbon partitioning between starch, soluble sugars, and anthocyanins by computational simulations. Activation energies for enzymes in central carbohydrate metabolism were experimentally quantified to estimate metabolic fluxes at 4°C. Consistent with previous studies, kinetic simulations revealed that SPS is a limiting metabolic step,

regulating carbon distribution between metabolic pathways such as glycolysis, TCA cycle, and amino acid biosynthesis (Nägele et al. 2012). While SPS was a limiting reaction, additional carbon flux towards other metabolic pathways was necessary to solve the kinetic model, especially in the flavonoid mutants. Here, organic acids were identified to represent essential metabolic sinks. Fumarate, which can be synthesised by cytosolic fumarase FUM2, plays an important role in cold acclimation and photosynthetic stabilisation at low temperatures (Dyson et al. 2016; Herrmann et al. 2021). Furthermore, the *fum2* mutant demonstrated a weaker increase in CHS abundance in cold compared to Col-0, supporting a regulatory link between flavonoid and carboxylic acid metabolism (Herrmann et al. 2021). The limitation in carbon flux through sucrose biosynthesis plays a critical role in the delicate coordination of carbon allocation among carbohydrates, organic acids, and specialised metabolites. When one of these metabolic pathways cannot effectively accommodate carbon flow – such as in the case of *chs* and *f3h* mutants – the rate of sucrose biosynthesis redirects carbon allocation toward alternate pathways. In flavonoid mutants, this redirection of carbon flux leads to an increased assimilation of organic acid. These findings indicate the role of sucrose biosynthesis as a master regulator, enabling successful cold acclimation through facilitating efficient distribution of energy resources.

### **10.3 Sensitivity analysis reveals key metabolic adjustments in hexose phosphate metabolism upon cold exposure**

Mathematical modelling of metabolic networks has been proven to support the analysis and interpretation of complex and non-intuitive patterns of metabolic regulation. For example, a kinetic model incorporating CBBC and triose phosphate transport across the chloroplast membrane showed that the reaction rate within the CBBC is primarily regulated by the contestation of the orthophosphate in the cytosol (Pettersson and Ryde-Pettersson 1988). Ordinary differential equations (ODEs) based kinetic modelling is a typical approach to estimate time-dependent dynamics of metabolism. In such a model, dynamics of metabolite concentrations, i.e., model states, are quantified by the sum of synthesising (input) and interconverting (output) reaction rates. Simulation, which is the numerical integration of an ODE system, then allows for the estimation of metabolite concentrations. In this thesis, such an approach helped to identify the central role of sucrose metabolism in buffering the effects

of chloroplast positioning and modulating carbon distribution between primary and specialised metabolism (Kitashova et al. 2021, 2023).

In a step further, flux balance analysis (FBA) was applied to expand the kinetic model analysis to a broad genome-scale metabolic network which was capable of integrating a higher number of reactions and metabolite pools (Adler et al. 2024). Sensitivity analysis revealed that fructose and glucose metabolism, specifically the FRCK and GLCK reactions, were most sensitive to exposure to low temperature. This, in turn, had a strong influence on hexose phosphate balance. Hexose phosphates, i.e., F6P and G6P, are products of the CBBC and serve as branching points in metabolism. To quantify hexose phosphate dynamics and assess the sensitivity of central carbohydrate metabolism in Col-0, starch metabolism mutants *pgm1* and *bam3*, and flavonoid mutants *chs* and *f3h*, fluctuations in net CO<sub>2</sub> assimilation rates were introduced by varying light intensity after 14 days of cold exposure. Flavonoid mutants showed stronger fluctuations in median F6P amounts. The decrease in F6P in flavonoid mutants suggests its consumption by pathways such as glycolysis and TCA cycle, which is in line with our previous findings (Kitashova et al. 2023). Interestingly, *chs* was the only genotype with increased sensitivity in F6P amount, F6P to anthocyanin flux, and F6P to organic acid flux after 14 days of cold exposure. This might indicate that flavonoids play a stabilising role in carbon metabolism, helping to regulate the flow of carbon through various metabolic pathways during cold acclimation.

### **10.4 Flavonoid biosynthesis stabilises photorespiration, amino acid metabolism and protein homeostasis during cold acclimation**

Previous studies have highlighted the importance of specialised metabolism for cold acclimation in plants (Schulz et al. 2015, 2016). However, the specific mechanism by which flavonoids contribute to this process remains poorly understood. The main reason is the use of whole-cell analysis, which heavily limits the insights into the flavonoid roles due to the high compartmentalisation within plants cells (Lunn 2007). Flavonoid precursors are synthesised in plastids, when flavonoids themselves are produced in the cytosol through a highly interconnected enzymatic network (Burbulis and Winkel-Shirley 1999; Rippert et al. 2009). Following their synthesis, flavonoids are transported across several cellular compartments, including the chloroplast and nucleus, and are predominantly stored in the vacuole (Pucker

and Selmar 2022). Hence, to truly elucidate the role of flavonoids in cold acclimation, it is vital to resolve plant metabolism at the subcellular level. Fortunately, recent advances in the non-aqueous fractionation made this very accessible (Fürtauer et al. 2016). In this thesis, the method was combined with gas chromatography-mass spectrometry (GC-MS)-based metabolomics analysis to investigate subcellular metabolic reprogramming in Col-0 and flavonoid mutants, *chs* and *f3h*, during cold acclimation.

Both *chs* and *f3h* plants exhibited perturbations in cold-induced subcellular dynamics in citrate and glutamate amounts. This was further supported by a shift in isocitrate dehydrogenase activity from mitochondria to the cytosol, indicating a cytosolic bypass of the TCA cycle (Sweetlove et al. 2010). This bypass involves the production of glutamate in the cytosol, thereby affecting nitrogen metabolism. Additionally, in *chs* plants, both ferredoxin-dependent glutamine:oxoglutarate aminotransferase enzyme and plastidial dicarboxylate transporters were significantly downregulated during cold acclimation. Previous studies have demonstrated that low nitrogen conditions lead to upregulation of the flavonoid biosynthesis pathway (Liu et al. 2021; Li et al. 2023), further suggesting a cross-talk between flavonoids and nitrogen metabolism.

Indeed, both *chs* and *f3h* mutants showed significant overaccumulation of amino acids in plastids, further supporting a stabilising role of flavonoids in C/N metabolism. The most pronounced effects were observed in glycine and serine, which, due to limitations of the fractioning method that cannot definitively separate chloroplast and mitochondria, indicate differential regulation of photorespiration. Consequently, upregulation of plastidial serine biosynthesis could be due to impaired serine-hydroxymethyltransferase (SHM1) mediated serine biosynthesis in mitochondria. In *chs* plants, a stronger accumulation of 5-formyltetrahydrofolate cycloligase, which consumes the potential inhibitor of SHM1, 5-formyltetrahydrofolate (Goyer et al. 2005), may indicate a response mechanism to the imbalance between photorespiration and tetrahydrofolate (THF) related metabolism. This aligns with previous studies suggesting that photorespiration and THF-related metabolism are co-dependent and require co-regulatory mechanisms (Collakova et al. 2008; Rosa-Téllez et al. 2024).

The absence of flavonoid compounds in the *chs* could potentially lead to the deregulation of THF-related metabolic enzymes, resulting in disruptions within the interconnected THF-

related metabolic pathways, amino acid biosynthesis and photorespiration. The differential dynamics of 5,10-methylene-tetrahydrofolate, a substrate for both SHM1 and the bifunctional 5,10-methylene-THF dehydrogenase/5,10-methenyl-THF cyclohydrolase (FOLD1) protein, could influence glycine to serine interconversion (Eisenhut et al. 2019). The interaction of isoquercetin, one of the early products of the flavonoid biosynthesis pathway, and FOLD1 *in silico* indicates a potential direct role of flavonoids in stabilising protein function. Evidence shows that its mouse homologue, C-1-THF synthase, interacts with isoquercetin *in vivo* (Manzoor et al. 2022), further supporting a stabilising role of flavonoids in THF-related metabolism. The most significant effects on photorespiratory regulation in flavonoid mutants were observed after 3 days of cold exposure, when flavonoid biosynthesis was just initiated, suggesting a temporal separation of flavonoid roles during cold acclimation.

Another interesting observation was that cold exposure led to an initial decrease in protein amounts in all genotypes but, unlike the wild type, protein amounts continuously declined in both *chs* and *f3h* mutants throughout the full period of cold acclimation. Proteomics data revealed a negative correlation between proteasome proteins and total protein amounts in both flavonoid mutants, suggesting an inhibitory role of flavonoids on the proteasome activity. This inhibitory effect was observed before for isolated proteasome 26S activity in pig red blood cells (Chang 2009). Additionally, a similar effect was observed in cytosolic ribosomal proteins where flavonoids were discussed to interact directly with ribosomes or tRNAs, influencing translational regulation during cold exposure (Kanakis et al., 2006). Finally, the amounts of proteins belonging to the GO term 'protein folding' stayed constant in both *chs* and *f3h*, while they decreased in Col-0, further suggesting a stabilising role of flavonoids in protein metabolism. These results highlight that flavonoids play a critical stabilising role in carbon and nitrogen metabolism, photorespiration, and protein homeostasis during cold acclimation.





### **11 Conclusion and outlook**

This dissertation provides novel insights into the subcellular regulation of plant metabolic acclimation to low temperature. It demonstrates a direct regulatory interaction between sucrose metabolism and chloroplast positioning, explores the sensitivity of hexose phosphate metabolism to changing environment and establishes the stabilising role of flavonoids in photorespiration, nitrogen metabolism, and protein homeostasis. Furthermore, a computational framework will support future studies focusing on simulating plant metabolism in a changing temperature regime, aiding in identifying promising targets for modifying and optimising plant yield and performance. Additionally, new evidence suggests a previously unexplored role of flavonoids in early metabolic cold acclimation, which requires further validation and functional characterisation.

Future research could focus on the mechanisms by which flavonoids accumulation and chloroplast relocation adapt to light and temperature changes. Phototropins and cryptochromes appear central in this process, influencing both chloroplast positioning and flavonoids biosynthesis (Jenkins et al. 2001; Brelford et al. 2019; Sugita et al. 2024). Preliminary findings on chloroplast positioning effects on flavonoid accumulation raise questions regarding the coordination between structural proteins and enzymes like CHUP1 and CHS. SnRK1-mediated sugar signalling could play a role in integrating light perception with sugar metabolism to optimise photosynthesis, balancing light absorption and photoprotection in response to low temperature.

Overall, this work provides a foundation for further advancing our understanding of plant metabolic acclimation, with implications for improving resilience and productivity in changing environments.



## 12 References

- Adler SO, Kitashova A, Bulović A, Nägele T, Klipp E** (2024) Plant Cold Acclimation and Its Impact on Sensitivity of Carbohydrate Metabolism. *bioRxiv preprint* 2024.06.04.597423
- Agati G, Azzarello E, Pollastri S, Tattini M** (2012) Flavonoids as Antioxidants in Plants: Location and Functional Significance. *Plant Science* 196: 67–76
- Agati G, Brunetti C, Di Ferdinando M, Ferrini F, Pollastri S, Tattini M** (2013) Functional Roles of Flavonoids in Photoprotection: New Evidence, Lessons from The Past. *Plant Physiology and Biochemistry* 72: 35–45
- Aguilera-Alvarado GP, Sánchez-Nieto S** (2017) Plant Hexokinases are Multifaceted Proteins. *Plant and Cell Physiology* 58: 1151–1160
- Banaś AK, Gabryś H** (2007) Influence of Sugars on Blue Light-Induced Chloroplast Relocations. *Plant Signaling & Behavior* 2: 221–230
- Austin BM, Noel PJ** (2003) The Chalcone Synthase Superfamily of Type III Polyketide Synthases. *Natural Product Reports* 20: 79–110
- Bittner A, van Buer J, Baier M** (2020) Cold Priming Uncouples Light and Cold-Regulation of Gene Expression in *Arabidopsis thaliana*. *BMC Plant Biology* 20: 281
- Brelsford CC, Morales LO, Nezval J, Kotilainen TK, Hartikainen SM, Aphalo PJ, Robson TM** (2019) Do UV-A Radiation and Blue Light During Growth Prime Leaves to Cope with Acute High Light in Photoreceptor Mutants of *Arabidopsis thaliana*? *Physiologia Plantarum* 165: 537–554
- Burbulis IE, Winkel-Shirley B** (1999) Interactions Among Enzymes of the Arabidopsis Flavonoid Biosynthetic Pathway. *Proceedings of the National Academy of Sciences* 96: 12929–12934
- Chalker-Scott L** (1999) Environmental Significance of Anthocyanins in Plant Stress Responses. *Photochemistry and Photobiology* 70: 1–9
- Chang TL** (2009) Inhibitory Effect of Flavonoids on 26S Proteasome Activity. *Journal of Agricultural and Food Chemistry* 57: 9706–9715

## 12. References

---

- Chinnusamy V, Zhu J, Zhu JK** (2006) Gene Regulation During Cold Acclimation in Plants. *Physiologia Plantarum* 126: 52–61
- Collakova E, Goyer A, Naponelli V, Krassovskaya I, Gregory JF III, Hanson AD, Shachar-Hill Y** (2008) Arabidopsis 10-Formyl Tetrahydrofolate Deformylases Are Essential for Photorespiration. *The Plant Cell* 20: 1818–1832
- Crepin N, Rolland F** (2019) SnRK1 Activation, Signaling, and Networking for Energy Homeostasis. *Current Opinion in Plant Biology* 51: 29–36
- Crosby KC, Pietraszewska-Bogiel A, Gadella TWJ, Winkel BSJ** (2011) Förster Resonance Energy Transfer Demonstrates a Flavonoid Metabolon in Living Plant Cells That Displays Competitive Interactions Between Enzymes. *FEBS Letters* 585: 2193–2198
- Di Ferdinando M, Brunetti C, Fini A, Tattini M** (2012) Flavonoids as Antioxidants in Plants Under Abiotic Stresses. *Abiotic Stress Responses in Plants: Metabolism, Productivity and Sustainability*, Springer pp. 159–179
- Dyson BC, Miller MAE, Feil R, Rattray N, Bowsher CG, Goodacre R, Lunn JE, Johnson GN** (2016) FUM2, a Cytosolic Fumarase, Is Essential for Acclimation to Low Temperature in *Arabidopsis thaliana*. *Plant Physiology* 172: 118–127
- Eisenhut M, Roell M-S, Weber APM** (2019) Mechanistic Understanding of Photorespiration Paves the Way to A New Green Revolution. *New Phytologist* 223: 1762–1769
- Endler A, Meyer S, Schelbert S, Schneider T, Weschke W, Peters SW, Keller F, Baginsky S, Martinoia E, Schmidt UG** (2006) Identification of A Vacuolar Sucrose Transporter in Barley and Arabidopsis Mesophyll Cells By A Tonoplast Proteomic Approach. *Plant Physiology* 141: 196–207
- Erb M, Kliebenstein DJ** (2020) Plant Secondary Metabolites as Defenses, Regulators, and Primary Metabolites: The Blurred Functional Trichotomy. *Plant Physiology* 184: 39–52
- Flügge UI, Heldt HW** (1984) The Phosphate-Triose Phosphate-Phosphoglycerate Translocator of The Chloroplast. *Trends in Biochemical Sciences* 9: 530–533
- Flügge UI, Westhoff P, Leister D** (2016) Recent Advances in Understanding Photosynthesis. *F1000Research* 5: 2890

- Fürtauer L, Nägele T** (2016) Approximating the Stabilization of Cellular Metabolism by Compartmentalization. *Theory in Biosciences* 135: 73–87
- Fürtauer L, Weckwerth W, Nägele T** (2016) A Benchtop Fractionation Procedure for Subcellular Analysis of the Plant Metabolome. *Frontiers in Plant Science* 7: 1912
- Fürtauer L, Weiszmann J, Weckwerth W, Nägele T** (2019) Dynamics of Plant Metabolism During Cold Acclimation. *International Journal of Molecular Sciences* 20: 5411
- Garcia-Molina A, Kleine T, Schneider K, Mühlhaus T, Lehmann M, Leister D** (2020) Translational Components Contribute to Acclimation Responses to High Light, Heat, and Cold in Arabidopsis. *iScience* 23:
- Geigenberger P, Stitt M** (1991) A “Futile” Cycle of Sucrose Synthesis and Degradation Is Involved in Regulating Partitioning Between Sucrose, Starch and Respiration in Cotyledons of Germinating *Ricinus communis* L. Seedlings When Phloem Transport Is Inhibited. *Planta* 185: 81–90
- Gonzali S, Pistelli L, De Bellis L, Alpi A** (2001) Characterization of Two *Arabidopsis thaliana* Fructokinases. *Plant Science* 160: 1107–1114
- Gorelova V, Bastien O, De Clerck O, Lespinats S, Rébeillé F, Van Der Straeten D** (2019) Evolution of Folate Biosynthesis and Metabolism Across Algae and Land Plant Lineages. *Scientific Reports* 9: 5731
- Gotoh E, Suetsugu N, Yamori W, Ishishita K, Kiyabu R, Fukuda M, Higa T, Shirouchi B, Wada M** (2018) Chloroplast Accumulation Response Enhances Leaf Photosynthesis and Plant Biomass Production. *Plant Physiology* 178: 1358–1369
- Goyer A, Collakova E, de la Garza RD, Quinlivan EP, Williamson J, Gregory JF, Shachar-Hill Y, Hanson AD** (2005) 5-Formyltetrahydrofolate Is an Inhibitory but Well Tolerated Metabolite in Arabidopsis Leaves. *Journal of Biological Chemistry* 280: 26137–26142
- Guo Z, Ou W, Lu S, Zhong Q** (2006) Differential Responses of Antioxidative System to Chilling and Drought in Four Rice Cultivars Differing in Sensitivity. *Plant Physiology and Biochemistry* 44: 828–836

## 12. References

---

- Guy C, Kaplan F, Kopka J, Selbig J, Hinch DK** (2008) Metabolomics of Temperature Stress. *Physiologia Plantarum* 132: 220–235
- Guy CL, Huber JLA, Huber SC** (1992) Sucrose Phosphate Synthase and Sucrose Accumulation at Low Temperature. *Plant Physiology* 100: 502–508
- Herrmann HA, Dyson BC, Miller MAE, Schwartz JM, Johnson GN** (2021) Metabolic Flux from The Chloroplast Provides Signals Controlling Photosynthetic Acclimation to Cold In *Arabidopsis thaliana*. *Plant, Cell & Environment* 44: 171–185
- Herrmann KM, Weaver LM** (1999) The Shikimate Pathway. *Annual Review of Plant Biology* 50: 473–503
- Hildebrandt TM** (2018) Synthesis Versus Degradation: Directions of Amino Acid Metabolism During Arabidopsis Abiotic Stress Response. *Plant Molecular Biology* 98: 121–135
- Hoermiller II, Funck D, Schönewolf L, May H, Heyer AG** (2022) Cytosolic Proline Is Required for Basal Freezing Tolerance in Arabidopsis. *Plant, Cell & Environment* 45: 147–155
- Hoermiller II, Naegele T, Augustin H, Stutz S, Weckwerth W, Heyer AG** (2017) Subcellular Reprogramming of Metabolism During Cold Acclimation in *Arabidopsis thaliana*. *Plant, Cell & Environment* 40: 602–610
- van't Hoff MJH** (1884) Etudes de Dynamique Chimique. *Recueil des Travaux Chimiques des Pays-Bas* 3: 333–336
- Holaday AS, Martindale W, Alred R, Brooks AL, Leegood RC** (1992) Changes in Activities of Enzymes of Carbon Metabolism in Leaves during Exposure of Plants to Low Temperature. *Plant Physiology* 98: 1105–1114
- Huber SC, Huber JL** (1996) Role and Regulation of Sucrose-Phosphate Synthase in Higher Plants. *Annual Review of Plant Physiology and Plant Molecular Biology* 47: 431–444
- Huner NPA, Öquist G, Sarhan F** (1998) Energy Balance and Acclimation to Light and Cold. *Trends in Plant Science* 3: 224–230

- Igarashi D, Tsuchida H, Miyao M, Ohsumi C** (2006) Glutamate:Glyoxylate Aminotransferase Modulates Amino Acid Content during Photorespiration. *Plant Physiology* 142: 901–910
- Janská A, Maršík P, Zelenková S, Ovesná J** (2010) Cold Stress and Acclimation – What Is Important for Metabolic Adjustment? *Plant Biology* 12: 395–405
- Jenkins GI, Long JC, Wade HK, Shenton MR, Bibikova TN** (2001) UV and Blue Light Signalling: Pathways Regulating Chalcone Synthase Gene Expression in Arabidopsis. *New Phytologist* 151: 121–131
- Johnson NC, Xie S-P, Kosaka Y, Li X** (2018) Increasing Occurrence of Cold and Warm Extremes During the Recent Global Warming Slowdown. *Nature Communications* 9: 1724
- Kaplan F, Guy CL** (2005) RNA Interference of Arabidopsis Beta-Amylase8 Prevents Maltose Accumulation Upon Cold Shock and Increases Sensitivity of PSII Photochemical Efficiency to Freezing Stress. *The Plant Journal* 44: 730–743
- Kaplan F, Kopka J, Haskell DW, Zhao W, Schiller KC, Gatzke N, Sung DY, Guy CL** (2004) Exploring the Temperature-Stress Metabolome of Arabidopsis. *Plant Physiology* 136: 4159–4168
- Kasahara M, Kagawa T, Oikawa K, Suetsugu N, Miyao M, Wada M** (2002) Chloroplast Avoidance Movement Reduces Photodamage in Plants. *Nature* 420: 829–832
- Kitashova A, Adler SO, Richter AS, Eberlein S, Dziubek D, Klipp E, Nägele T** (2023) Limitation of Sucrose Biosynthesis Shapes Carbon Partitioning During Plant Cold Acclimation. *Plant, Cell & Environment* 46: 464–478
- Kitashova A, Schneider K, Fürtauer L, Schröder L, Scheibenbogen T, Fürtauer S, Nägele T** (2021) Impaired Chloroplast Positioning Affects Photosynthetic Capacity and Regulation of The Central Carbohydrate Metabolism During Cold Acclimation. *Photosynthesis Research* 147: 49–60
- Klotke J, Kopka J, Gatzke N, Heyer AG** (2004) Impact of Soluble Sugar Concentrations on The Acquisition of Freezing Tolerance in Accessions of Arabidopsis Thaliana with

## 12. References

---

Contrasting Cold Adaptation – Evidence for A Role of Raffinose In Cold Acclimation. *Plant, Cell & Environment* 27: 1395–1404

**Knaupp M, Mishra KB, Nedbal L, Heyer AG** (2011) Evidence for A Role of Raffinose In Stabilizing Photosystem II During Freeze–Thaw Cycles. *Planta* 234: 477–486

**Knight MR, Knight H** (2012) Low-Temperature Perception Leading to Gene Expression and Cold Tolerance in Higher Plants. *New Phytologist* 195: 737–751

**Kodama Y, Tsuboi H, Kagawa T, Wada M** (2008) Low Temperature-Induced Chloroplast Relocation Mediated by A Blue Light Receptor, Phototropin 2, in Fern Gametophytes. *Journal of Plant Research* 121: 441–448

**Kong SG, Yamazaki Y, Shimada A, Kijima ST, Hirose K, Katoh K, Ahn J, Song HG, Han JW, Higa T, Takano A, Nakamura Y, Suetsugu N, Kohda D, Uyeda TQP, Wada M** (2024) CHLOROPLAST UNUSUAL POSITIONING 1 Is A Plant-Specific Actin Polymerization Factor Regulating Chloroplast Movement. *The Plant Cell* 36: 1159–1181

**Korn M, Peterek S, Mock H-P, Heyer AG, Hinch DK** (2008) Heterosis In the Freezing Tolerance, And Sugar and Flavonoid Contents of Crosses Between Arabidopsis Thaliana Accessions of Widely Varying Freezing Tolerance. *Plant, Cell & Environment* 31: 813–827

**Landi S, Capasso G, Esposito S** (2021) Different G6PDH Isoforms Show Specific Roles in Acclimation to Cold Stress at Various Growth Stages of Barley (*Hordeum vulgare*) and *Arabidopsis thaliana*. *Plant Physiology and Biochemistry* 169: 190–202

**Lee HS, Sturm A** (1996) Purification and Characterization of Neutral and Alkaline Invertase from Carrot. *Plant Physiology* 112: 1513–1522

**Li Z, Jiang H, Jiang X, Zhang L, Qin Y** (2023) Integrated Physiological, Transcriptomic, And Metabolomic Analyses Reveal That Low-Nitrogen Conditions Improve the Accumulation Of Flavonoids In Snow Chrysanthemum. *Industrial Crops and Products* 197: 116574

**Liu J, Liu M, Fang H, Zhang Q, Ruan J** (2021) Accumulation of Amino Acids and Flavonoids in Young Tea Shoots Is Highly Correlated with Carbon and Nitrogen Metabolism in Roots and Mature Leaves. *Frontiers in Plant Science* 12:



- Liu J, Wang X, Guan Z, Wu M, Wang X, Fan R, Zhang F, Yan J, Liu Y, Zhang D, Yin P, Yan J** (2024) The LIKE SEX FOUR 1–Malate Dehydrogenase Complex Functions as A Scaffold to Recruit B-Amylase to Promote Starch Degradation. *The Plant Cell* 36: 194–212
- Lunn JE** (2007) Compartmentation in Plant Metabolism. *Journal of Experimental Botany* 58: 35–47
- Lv YQ, Li D, Wu LY, Zhu YM, Ye Y, Zheng XQ, Lu JL, Liang YR, Li QS, Ye JH** (2022) Sugar Signal Mediates Flavonoid Biosynthesis in Tea Leaves. *Horticulture Research* 9: uhac049
- Maai E, Nishimura K, Takisawa R, Nakazaki T** (2020) Light Stress-Induced Chloroplast Movement and Midday Depression of Photosynthesis in Sorghum Leaves. *Plant Production Science* 23: 172–181
- Maeda H, Dudareva N** (2012) The Shikimate Pathway and Aromatic Amino Acid Biosynthesis in Plants. *Annual Review of Plant Biology* 63: 73–105
- Manzoor M, Muroi M, Ogawa N, Kobayashi H, Nishimura H, Chen D, B. Fasina O, Wang J, Osada H, Yoshida M, Xiang L, Qi J** (2022) Isoquercitrin from *Apocynum venetum* L. Produces an Anti-Obesity Effect on Obese Mice by Targeting C-1-Tetrahydrofolate Synthase, Carbonyl Reductase, And Glutathione S -Transferase P and Modification of The AMPK/SREBP-1c/FAS/CD36 Signaling Pathway in Mice *in vivo*. *Food & Function* 13: 10923–10936
- Monroe JD, Storm AR, Badley EM, Lehman MD, Platt SM, Saunders LK, Schmitz JM, Torres CE** (2014)  $\beta$ -Amylase1 and  $\beta$ -Amylase3 Are Plastidic Starch Hydrolases in Arabidopsis That Seem to Be Adapted for Different Thermal, pH, and Stress Conditions. *Plant Physiology* 166: 1748–1763
- Moreno JI, Martín R, Castresana C** (2005) Arabidopsis SHMT1, a Serine Hydroxymethyltransferase That Functions in The Photorespiratory Pathway Influences Resistance to Biotic and Abiotic Stress. *The Plant Journal* 41: 451–463
- Nägele T** (2022) Metabolic Regulation of Subcellular Sucrose Cleavage Inferred from Quantitative Analysis of Metabolic Functions. *Quantitative Plant Biology* 3: e10

## 12. References

---

- Nägele T, Heyer AG** (2013) Approximating Subcellular Organisation of Carbohydrate Metabolism During Cold Acclimation in Different Natural Accessions of *Arabidopsis thaliana*. *New Phytologist* 198: 777–787
- Nägele T, Stutz S, Hörmiller II, Heyer AG** (2012) Identification of A Metabolic Bottleneck for Cold Acclimation in *Arabidopsis thaliana*. *The Plant Journal* 72: 102–114
- Nagler M, Nukarinen E, Weckwerth W, Nägele T** (2015) Integrative Molecular Profiling Indicates A Central Role of Transitory Starch Breakdown in Establishing A Stable C/N Homeostasis During Cold Acclimation in Two Natural Accessions of *Arabidopsis thaliana*. *BMC Plant Biol* 15: 284
- Nukarinen E, Nägele T, Pedrotti L, Wurzinger B, Mair A, Landgraf R, Börnke F, Hanson J, Teige M, Baena-Gonzalez E, Dröge-Laser W, Weckwerth W** (2016) Quantitative Phosphoproteomics Reveals the Role of The AMPK Plant Ortholog Snrk1 As A Metabolic Master Regulator Under Energy Deprivation. *Scientific Reports* 6: 31697
- Ogasawara Y, Ishizaki K, Kohchi T, Kodama Y** (2013) Cold-Induced Organelle Relocation in The Liverwort *Marchantia polymorpha* L. *Plant, Cell & Environment* 36: 1520–1528
- Owens DK, Crosby KC, Runac J, Howard BA, Winkel BSJ** (2008) Biochemical and Genetic Characterization Of Arabidopsis Flavanone 3 $\beta$ -hydroxylase. *Plant Physiology and Biochemistry* 46: 833–843
- Patzke K, Prananingrum P, Klemens PAW, Trentmann O, Rodrigues CM, Keller I, Fernie AR, Geigenberger P, Bölder B, Lehmann M, Schmitz-Esser S, Pommerrenig B, Haferkamp I, Neuhaus HE** (2019) The Plastidic Sugar Transporter pSuT Influences Flowering and Affects Cold Responses. *Plant Physiology* 179: 569–587
- Pettersson G, Ryde-Pettersson U** (1988) A Mathematical Model of The Calvin Photosynthesis Cycle. *European Journal of Biochemistry* 175: 661–672
- Pucker B, Selmar D** (2022) Biochemistry and Molecular Basis of Intracellular Flavonoid Transport in Plants. *Plants* 11: 963

- Rippert P, Puyaubert J, Grisolle D, Derrier L, Matringe M** (2009) Tyrosine and Phenylalanine Are Synthesized within the Plastids in *Arabidopsis*. *Plant Physiology* 149: 1251–1260
- Rosa-Téllez S, Alcántara-Enguíanos A, Martínez-Seidel F, Casatejada-Anchel R, Saeheng S, Bailes CL, Erban A, Barbosa-Medeiros D, Alepúz P, Matus JT, Kopka J, Muñoz-Bertomeu J, Krueger S, Roje S, Fernie AR, Ros R** (2024) The Serine–Glycine–One-Carbon Metabolic Network Orchestrates Changes in Nitrogen and Sulfur Metabolism and Shapes Plant Development. *The Plant Cell* 36: 404–426
- Ruan YL** (2014) Sucrose Metabolism: Gateway to Diverse Carbon Use and Sugar Signaling. *Annual Review of Plant Biology* 65: 33–67
- Sasaki H, Ichimura K, Oda M** (1996) Changes in Sugar Content during Cold Acclimation and Deacclimation of Cabbage Seedlings. *Annals of Botany* 78: 365–369
- Savitch LV, Barker-Åstrom J, Ivanov AG, Hurry V, Öquist G, Huner NP, Gardeström P** (2001) Cold Acclimation of *Arabidopsis thaliana* Results in Incomplete Recovery of Photosynthetic Capacity, Associated with An Increased Reduction of The Chloroplast Stroma. *Planta* 214: 295–303
- Savitch LV, Gray GR, Huner NPA** (1997) Feedback-Limited Photosynthesis and Regulation of Sucrose–Starch Accumulation During Cold Acclimation and Low-Temperature Stress In A Spring And Winter Wheat. *Planta* 201: 18–26
- Schilbert HM, Busche M, Sáez V, Angeli A, Weisshaar B, Martens S, Stracke R** (2024) Generation and Characterisation of An *Arabidopsis thaliana* F3h/F1s1/Ans Triple Mutant That Accumulates Eriodictyol Derivatives. *BMC Plant Biology* 24: 99
- Schmidt von Braun S, Schleiff E** (2008) The Chloroplast Outer Membrane Protein CHUP1 Interacts with Actin and Profilin. *Planta* 227: 1151–1159
- Schulz E, Tohge T, Zuther E, Fernie AR, Hinch DK** (2015) Natural Variation in Flavonol And Anthocyanin Metabolism During Cold Acclimation in *Arabidopsis thaliana* Accessions. *Plant, Cell & Environment* 38: 1658–1672

- Schulz E, Tohge T, Zuther E, Fernie AR, Hinch DK** (2016) Flavonoids Are Determinants of Freezing Tolerance and Cold Acclimation in *Arabidopsis thaliana*. *Scientific Reports* 6: 34027
- Seydel C, Kitashova A, Fürtauer L, Nägele T** (2022) Temperature-Induced Dynamics of Plant Carbohydrate Metabolism. *Physiologia Plantarum* 174: e13602
- Sherson SM, Alford HL, Forbes SM, Wallace G, Smith SM** (2003) Roles of Cell-Wall Invertases and Monosaccharide Transporters in The Growth and Development of Arabidopsis. *Journal of Experimental Botany* 54: 525–531
- Sicher R** (2011) Carbon Partitioning and The Impact of Starch Deficiency on The Initial Response of Arabidopsis To Chilling Temperatures. *Plant Science* 181: 167–176
- Smith AM** (2012) Starch in the Arabidopsis Plant. *Starch - Stärke* 64: 421–434
- Stitt M, Lunn J, Usadel B** (2010) Arabidopsis And Primary Photosynthetic Metabolism – More Than the Icing on The Cake. *The Plant Journal* 61: 1067–1091
- Strand Å, Foyer CH, Gustafsson P, Gardeström P, Hurry V** (2003) Altering Flux Through the Sucrose Biosynthesis Pathway in Transgenic Arabidopsis Thaliana Modifies Photosynthetic Acclimation at Low Temperatures and The Development of Freezing Tolerance. *Plant, Cell & Environment* 26: 523–535
- Strand Å, Hurry V, Henkes S, Huner N, Gustafsson P, Gardeström P, Stitt M** (1999) Acclimation of Arabidopsis Leaves Developing at Low Temperatures. Increasing Cytoplasmic Volume Accompanies Increased Activities of Enzymes in the Calvin Cycle and in the Sucrose-Biosynthesis Pathway<sup>1</sup>. *Plant Physiology* 119: 1387–1398
- Sturm A** (1999) Invertases. Primary Structures, Functions, and Roles in Plant Development and Sucrose Partitioning. *Plant Physiology* 121: 1–8
- Suetsugu N, Wada M** (2020) Signalling Mechanism of Phototropin-Mediated Chloroplast Movement in Arabidopsis. *Journal of Plant Biochemistry and Biotechnology* 29: 580–589
- Sugita K, Takahashi S, Uemura M, Kawamura Y** (2024) Freezing Treatment Under Light Conditions Leads to A Dramatic Enhancement of Freezing Tolerance in Cold-Acclimated Arabidopsis. *Plant, Cell & Environment* 1:

- Sweetlove LJ, Beard KFM, Nunes-Nesi A, Fernie AR, Ratcliffe RG** (2010) Not Just A Circle: Flux Modes in The Plant TCA Cycle. *Trends in Plant Science* 15: 462–470
- Teng S, Keurentjes J, Bentsink L, Koornneef M, Smeekens S** (2005) Sucrose-Specific Induction of Anthocyanin Biosynthesis in Arabidopsis Requires the MYB75/PAP1 Gene. *Plant Physiology* 139: 1840–1852
- Tholen D, Boom C, Noguchi K, Ueda S, Katase T, Terashima I** (2008) The Chloroplast Avoidance Response Decreases Internal Conductance to CO<sub>2</sub> Diffusion in Arabidopsis Thaliana Leaves. *Plant, Cell & Environment* 31: 1688–1700
- Thomashow MF** (2001) So What's New in the Field of Plant Cold Acclimation? Lots! *Plant Physiology* 125: 89–93
- Thomashow MF** (2010) Molecular Basis of Plant Cold Acclimation: Insights Gained from Studying the CBF Cold Response Pathway. *Plant Physiology* 154: 571–577
- Tohge T, R. Fernie A** (2017) An Overview of Compounds Derived from the Shikimate and Phenylpropanoid Pathways and Their Medicinal Importance. *Mini Reviews in Medicinal Chemistry* 17: 1013–1027
- Voss I, Sunil B, Scheibe R, Raghavendra AS** (2013) Emerging Concept for The Role of Photorespiration as An Important Part of Abiotic Stress Response. *Plant Biology* 15: 713–722
- Wada M** (2013) Chloroplast Movement. *Plant Science* 210: 177–182
- Wahid A, Gelani S, Ashraf M, Foolad MR** (2007) Heat Tolerance in Plants: An Overview. *Environmental and Experimental Botany* 61: 199–223
- Wang B, Zhao X, Zhao Y, Shanklin J, Zhao Q, Liu CJ** (2021) Arabidopsis Snrk1 Negatively Regulates Phenylpropanoid Metabolism Via Kelch Domain-Containing F-Box Proteins. *New Phytologist* 229: 3345–3359
- Wang XC, Wu J, Guan ML, Zhao C-H, Geng P, Zhao Q** (2020) Arabidopsis MYB4 Plays Dual Roles in Flavonoid Biosynthesis. *The Plant Journal* 101: 637–652
- Wanner LA, Junttila O** (1999) Cold-Induced Freezing Tolerance in Arabidopsis. *Plant Physiol* 120: 391–400

## 12. References

---

- Weizmann J, Fürtauer L, Weckwerth W, Nägele T** (2018) Vacuolar Sucrose Cleavage Prevents Limitation of Cytosolic Carbohydrate Metabolism and Stabilizes Photosynthesis Under Abiotic Stress. *The FEBS Journal* 285: 4082–4098
- Xiang L, Le Roy K, Bolouri-Moghaddam M-R, Vanhaecke M, Lammens W, Rolland F, Van den Ende W** (2011) Exploring the Neutral Invertase–Oxidative Stress Defence Connection in *Arabidopsis thaliana*. *Journal of Experimental Botany* 62: 3849–3862
- Xiang L, Van den Ende W** (2013) Trafficking of Plant Vacuolar Invertases: From a Membrane-Anchored to a Soluble Status. Understanding Sorting Information in Their Complex N-Terminal Motifs. *Plant and Cell Physiology* 54: 1263–1277
- Xin Z, Browse J** (2000) Cold Comfort Farm: The Acclimation of Plants to Freezing Temperatures. *Plant, Cell & Environment* 23: 893–902
- Yano R, Nakamura M, Yoneyama T, Nishida I** (2005) Starch-Related  $\alpha$ -Glucan/Water Dikinase Is Involved in the Cold-Induced Development of Freezing Tolerance in Arabidopsis. *Plant Physiology* 138: 837–846
- Yuan N, Mendu L, Ghose K, Witte CS, Frugoli J, Mendu V** (2023) FKF1 Interacts with CHUP1 and Regulates Chloroplast Movement in Arabidopsis. *Plants* 12: 542
- Zhang X, Abraham C, Colquhoun TA, Liu CJ** (2017) A Proteolytic Regulator Controlling Chalcone Synthase Stability and Flavonoid Biosynthesis in Arabidopsis. *The Plant Cell* 29: 1157–1174
- Zirngibl ME, Araguirang GE, Kitashova A, Jahnke K, Rolka T, Kühn C, Nägele T, Richter AS** (2023) Triose Phosphate Export from Chloroplasts and Cellular Sugar Content Regulate Anthocyanin Biosynthesis During High Light Acclimation. *Plant Communications* 4: 100423

### 13 Acknowledgements

As I am writing these acknowledgments, I am astonished how many people come to mind. Although I consider myself a relatively resilient person, I would never be able to make it through this journey without the kindness and support from everyone. Even a little gesture could make a huge difference, so I am thankful to everyone. Below I would like to express my gratitude to people contributed most to me getting to where I am now 😊

First and foremost, I would like to express my deepest gratitude to my supervisor **Professor Doctor Thomas Nägele**. I have been incredibly fortunate to have a supervisor who is an exceptional scientist *and* a leader with unlimited kindness. His belief in people, limitless patience, and his constant support have left a significant impact on me, both personally and professionally. Thomas offered me more than just academic guidance—he provided life wisdom. In his always opened office, I could seek advice, share ideas, or simply be. His authentic leadership created an environment where I felt safe to be myself, and felt encouraged to grow and learn, not only as a researcher but as a person. He taught me the value of good laboratory practice and data analysis, while also helping me fight unhealthy levels of perfectionism. His constructive feedback and motivation pushed me to improve and made a significance difference in my work. I am equally grateful for the get-togethers, post-work discussions over a beer, the invaluable mentorship and genuine care for my well-being. The standards that Thomas set will be definitely carried by me throughout my career.

I am grateful to the examination committee **Hans-Henning Kunz, Christof Osman, Laura Busse, Annika Guse** and **Herwig Stibor** for taking their time to review my work. I am especially grateful to Henning, who was also a part of my thesis advisory committee and offered many insights and encouragement during these 4 years. I am very grateful to the SFB TRR175 consortium, especially **Dario Leister, Edda Klipp, Andreas Richter, Ekkehard Neuhaus**, and **Stephan Adler**, whose support and contributions have been important part of my research. I also want to extend my thanks to **Martin Lehmann** for his patience and dedication in processing thousands of samples, insightful questions and support. I am deeply thankful to **Serena Schwenkert** for her support, and enthusiasm in working on my samples. A special thanks goes to **Ute Thomas** for being amazing support in navigating the bureaucratic matters.

### 13. Acknowledgements

---

I am incredibly grateful to **my parents** for encouraging me to learn, to move forward, and to pursue this step in life – thanks to them I got to know pretty early in my life that doctoral studies exist and, although tough, it's absolutely special. I am grateful for their constant support throughout this journey – celebrating with me when my papers were accepted, listening to my stories about science and university life. I am very thankful to my mom for being an emergency contact, always positive and kind, understanding and reassuring during difficult times. I am deeply appreciative for the financial support, which made it easier for me to focus on my work, too.

I am very grateful that **Vasil Atanasov** and I reconnected during our doctoral studies. First as a coffee-klatsch buddy, then as a PhD buddy and a good friend Vasil helped me navigating life not only at university, but in Germany in general. He provided not only encouragement, opinions and lots of support, but also lots of fun and memes. I am very happy that I met **Sabrina Walz**, who became a dear friend. Both Vasil and Sabrina celebrated my happy moments and listened and supported me during harder times. Especially thanks to them, I got the feeling of “not being alone” during doctoral studies. To **Nikita Orlov** and **Lena Volynchikova**, I owe my deepest gratitude. Knowing that my oldest friends were going through the same doctoral journey, despite us living in three different countries, was a great comfort. Their friendship helped me navigate difficult times and celebrate every small victory. Lena motivated me to take care of my mental and physical health. Nikita, with his endless patience and kindness, was always there to talk me through the hard times. I would also like to thank **Katja Schneider** for being a constant source of friendship and wisdom. Her advice and insights have not only helped me personally but have also influenced how I engage with my own students. I am grateful for all the fun times, and for always being there to listen. I am deeply grateful for **Lisa Fürtauer's** friendship. Having the opportunity to work alongside her already before beginning my doctoral studies was a life-changing/saving experience that prepared me for the challenges ahead. Lisa introduced me to the world of high-throughput sample handling and efficient workspace. Even when separated by kilometres, Lisa continued to be a source of kindness, guidance and support, being always there to offer advice, and help me in the moments of frustration. I am also grateful to **Vika Cheredeeva** and **Masha Goldberg** for their friendship, support, and the much-needed hangouts that provided a break from the intense university life.



### 13. Acknowledgements

---

I was lucky to be surrounded by a friendly community of LSM graduate school students. Thanks to them I became a better person and a better team player. Special thanks go to **Nupur Sharma** for her empowering energy, our numerous meet-ups have a special place in my heart. I am grateful to **Wing Tung (Michi) Lo** for nice talks, advice, treats and hangouts. **Victoria Holzer** always supported me with a good talk, treats and absolutely fantastic Austrian schnapps, for all of which I am grateful. Extra thanks go also to **David González Campo** for being always supportive, and especially for all the hangouts at conferences and retreats. Lots of gratitude go also to an absolutely invaluable member of the LSM **Nadine Hamze**. Her guidance, support, kindness and understanding contributed to the smoothness of my doctoral journey.

I am grateful to my students **Svenja Eberlein, Beyza Özmen, Chun Kwan Yip, and Sophia Bagshaw** for their huge support, for being curious and being helpful, for being patient, for helping me to become a better supervisor, and for all the great data that has been collected. I am especially thankful to Beyza and Sophia for their friendship, support and shared fun times. My thanks also go to the rest of the group for their help and support. I am thankful to the **IT team** for helping me with my computer problems. I am also grateful to the **gardeners**, who took care of my plants during all these years. I am grateful to the whole **second floor** for being nice to me and helping me out, especially to **Oğuz Top, Beate Minov, Jennifer Lindstadt, Stephan Kirchner, and Cordelia Bolle**.

---

It's a dangerous business, going out your door...  
There's no knowing where you might be swept off to.  
— J.R.R. Tolkien, *The Lord of the Rings*

---



## 14 Curriculum vitae

### Personal details

First name: Anastasia  
Last name: Kitashova  
Date of birth: 25.02.1996

### Education

- 2020-2024** **Doctoral Studies in the Plant Systems Biology** at LMU München, Germany, Plant Evolutionary Cell Biology
- 2017-2020** **Master of Science in Biology** at LMU München, Germany, Plant Evolutionary Cell Biology (grade 1.4, 1 is maximum)
- 2013-2017** **Bachelor of Science in Biology** at Lomonosov Moscow State University, Russia, Genetics (grade 4.75, 5 is maximum)
- 2002-2013** **High School** studies at State Educational Institution № 1948 with intensive study of English and Chinese

### Fellowships and Awards

- 2022** Top Downloaded Article in 2021 in Physiologia Plantarum
- 2022** Gender Equality Funds gained for a mini-project within the SFB TR175
- 2017** DAAD “Deutscher Akademischer Austauschdienst” Scholarship

### Academic duties and extra curriculum activities

- 2021-2024** Supervising the practical course “Systems Biology”  
Supervising the students during their research courses and master thesis  
President of student council at “Life Science Munich” Graduate School  
Co-editor of “Chlorocast” podcast of the SFB TR175 collaboration hub

### Conference contributions

- 2023** “A quantitative model of carbon partitioning during plant cold acclimation”, **ICAR 2023** [The 33rd International Conference on Arabidopsis Research]. Chiba, Japan, June 2023 (**talk**)
- 2022** “Cold-induced dynamics of carbon partitioning”, **TR 175 International Conference** [Chloroplast: From Genes to Systems]. Kloster Irsee, Germany, August 2022 (**poster**)
- 2020** “Impaired chloroplast positioning affects photosynthetic capacity and regulation of the central carbohydrate metabolism during cold acclimation”, **Horizons in Molecular Biology Symposium**. MPIBPC, online due to COVID-19, September 2020 (**poster**)

### **Contribution to the scientific society**

**Kitashova A**, Lehmann M, Schwenkert S, Leister D, Nägele T (2024) Flavonoid metabolism and its different physiological roles in plant cold acclimation. *The Plant Journal* in print, available online <https://doi.org/10.1111/tpj.17097>

Adler SO, **Kitashova A**, Bulović A, Nägele T, Klipp E (2024) Plant cold acclimation and its impact on sensitivity of carbohydrate metabolism. *bioRxiv preprint* 2024.06.04.597423

Hernandez JS, Dziubek D, Schröder L, Seydel C, **Kitashova A**, Brodsky V, Nägele T (2023) Natural variation of temperature acclimation of *Arabidopsis thaliana*. *Physiologia Plantarum* 175: e14106

**Kitashova A\***, Brodsky V\*, Chaturvedi P\*, Pierides I, Ghatak A, Weckwerth W, Nägele T (2023) Quantifying the impact of dynamic plant-environment interactions on metabolic regulation. *Journal of Plant Physiology* 290: 154116 (\*authors contributed equally)

Valifard M, Fernie AR, **Kitashova A**, Nägele T, Schröder R, Meinert M, Pommerrenig B, Mehner-Breitfeld D, Witte C-P, Brüser T, Keller I, Neuhaus HE (2023) The novel chloroplast glucose transporter pGlcT2 affects adaptation to extended light periods. *Journal of Biological Chemistry* 299: 104741

**Kitashova A**, Adler SO, Richter AS, Eberlein S, Dziubek D, Klipp E, Nägele T (2023) Limitation of sucrose biosynthesis shapes carbon partitioning during plant cold acclimation. *Plant, Cell & Environment* 46: 464–478

Khan A, Cheng J, **Kitashova A**, Fürtauer L, Nägele T, Picco C, Scholz-Starke J, Keller I, Neuhaus HE, Pommerrenig B (2023) Vacuolar sugar transporter EARLY RESPONSE TO DEHYDRATION6-LIKE4 affects fructose signaling and plant growth. *Plant Physiology* 193: 2141–2163

Zirngibl M-E, Araguirang GE, **Kitashova A**, Jahnke K, Rolka T, Kühn C, Nägele T, Richter AS (2023) Triose phosphate export from chloroplasts and cellular sugar content regulate anthocyanin biosynthesis during high light acclimation. *Plant Communications* 4: 100423

Seydel C\*, **Kitashova A\***, Fürtauer L, Nägele T (2022) Temperature-induced dynamics of plant carbohydrate metabolism. *Physiologia Plantarum* 174: e13602 (\*authors contributed equally)

Krantz M, Zimmer D, Adler SO, **Kitashova A**, Klipp E, Mühlhaus T, Nägele T (2021) Data Management and Modeling in Plant Biology. *Frontiers in Plant Science* 12: 717958

**Kitashova A**, Schneider K, Fürtauer L, Schröder L, Scheibenbogen T, Fürtauer S, Nägele T (2021) Impaired chloroplast positioning affects photosynthetic capacity and regulation of the central carbohydrate metabolism during cold acclimation. *Photosynthesis Research* 147: 49–60